The Role of miRNAs from the 14q32 Region in Acquired Resistance to Lapatinib

Submitted in partial fulfilment of the requirements of the Degree of Doctor of Philosophy

Juliette Thérèse Marguerite Marie Chupin

July 2018

Statement of Originality

I, Juliette Thérèse Marguerite Marie Chupin, confirm that the research included within this thesis is my own work or that where it has been carried out in collaboration with, or supported by others, that this is duly acknowledged below and my contribution indicated. Previously published material is also acknowledged below.

Immunofluorescence staining - supported by Sophie Adams.

miRNA arrays - data generated by previous Schmid lab members. I analysed the data.

Methylation re-sequencing - the experiment was carried out by Darren Korbie on samples I generated. The raw data was analysed by Ai Nagano who also generated the heatmaps. I interpreted the data.

Gene expression array - data generated by previous Schmid lab members and data from GSE16179 (*1*) were used. Ai Nagano and Natasha Saghal analysed the data and generated the heatmaps. I interpreted the data.

NeoALTTO - data from the clinical trial was generated by Pusztia Lajos, Christos Hatzis and their group. mRNA expression was analysed for the selected targets by Weiwei Shi and Ryan Powles. I interpreted the data.

I attest that I have exercised reasonable care to ensure that the work is original, and does not to the best of my knowledge break any UK law, infringe any third party's copyright or other Intellectual Property Right, or contain any confidential material.

I accept that the College has the right to use plagiarism detection software to check the electronic version of the thesis.

I confirm that this thesis has not been previously submitted for the award of a degree by this or any other university.

Signature: Juliette Thérèse Marguerite Marie Chupin
Date: 15th July 2018

Abstract

HER2 is over-expressed in 20-25 % of breast cancers. Due to the increase in proliferation and survival signalling resulting from HER2 over-expression, this sub-type is associated with more aggressive tumour progression and poor prognosis. HER2 targeted-therapy has significantly improved patient prognosis, however, despite all progress only a subgroup derives optimal benefit, whereas others have refractory disease or develop resistance. It is therefore necessary to identify new targets to improve patient outcome. A group of non-coding RNAs, miRNAs, are often aberrantly expressed in tumours and miRNA expression profiles have been seen to evolve over the course of treatment implicating them in therapeutic resistance.

Using the lapatinib sensitive, BT-474, and resistant, BT-474/L, HER2 expressing cells, 44 miRNAs were found to be upregulated. The region with the highest number of differentially expressed miRNAs is the 14q32 region. RT-qPCR confirmed upregulation of 14q32 miRNAs in the BT-474/L compared to BT-474 as well as 2 other pairs (HCC1954, HCC1954/L, and SKBR-3, SKBR-3/L) linking increased miRNA expression with acquired resistance to lapatinib.

As the 14q32 region is regulated by DNA imprinting, we explored epigenetic changes between the sensitive and resistant lines. Global methylation reversal cased upregulation of all three miRNAs in the sensitive cells. This suggests loss of methylation is a key in controlling 14q32 miRNA expression.

Since miRNAs are not suitable therapeutic targets, differential gene expression analysis combined with *in silico* analysis was used to identify targets of the miRNAs. Silencing of five target genes seemed to decrease sensitivity of the cells to HER2-targeted treatment. Analysis of the NeoALTTO clinical trial data suggests high expression of four of these genes, SOCS2, BASP1, NEDD4L, and SH3BGRL could be linked to better prognosis.

These results suggest upregulation of 14q32 miRNAs caused by loss of epigenetic regulation leads to decreased expression of SOCS2, BASP1, NEDD4L, and SH3BGRL. This loss could contribute to HER2-targeted therapy resistance. Therefore expression levels of 14q32 miRNAs could be used as a prognostic biomarker to identify patients likely to relapse.

Acknowledgements

I would like to start by thanking my funders, Breast Cancer Now, for making this project possible. Thank you to the BCI and Molecular Oncology.

I also have to thank Peter Schmid for his supervision and guidance throughout my PhD. I would also like to acknowledge all the members of the group, especially Alice Shia for all the time she dedicated to my project and to shaping me into the scientist I am today. Additionally I would like to thank all my ex-labmates, in particular, Katia for being my western blot mentor, John for his support, as well as Cathy and Jasmin for putting up with me and my silly questions. I would also like to thank previous members of the Schmid group for generating both the miRNA Array data and the Gene Expression Array.

I want to thank my second supervisor Tyson Sharp for all his guidance in the field or miRNAs and his post-doc Kunnal, aka Special K, for helping me in all my miRNA related crises.

A big thank you to Claude Chelala and her group, Ai Nagano and Natasha Saghal in particular, for all their help with analysis of the gene expression array and the methylation re-sequencing data. Thank you to Darren Korbie for his work on the methylation re-sequencing, to Sophie Adams from Susana Godhino's group for help with immunofluorescence staining and microscopy, and to the NeoALTTO team for sharing their data and analysis.

Thank you to the Imaging crew for helping me out these past few months, and to Roxana for sharing her PhD stories. I want to give a shout out to my office friends, those from the 'original office' for their moral support and the occasional science related conversation; and my buddies Sophie and Ramsay for enduring my cloning litanies and being up for coffee and cake at any time, but, most importantly, for always being there.

Finally I would like to thank my family and friends and recognise the role they have had in keeping me sane. To my parents and siblings, thank you for your unconditional love and support throughout these years. Thank you for understanding that there are some questions you just do not ask a PhD student: What is it that you actually do? Have you cured cancer yet? How' s the writing going?...

So thank you all for supporting me to the finish.

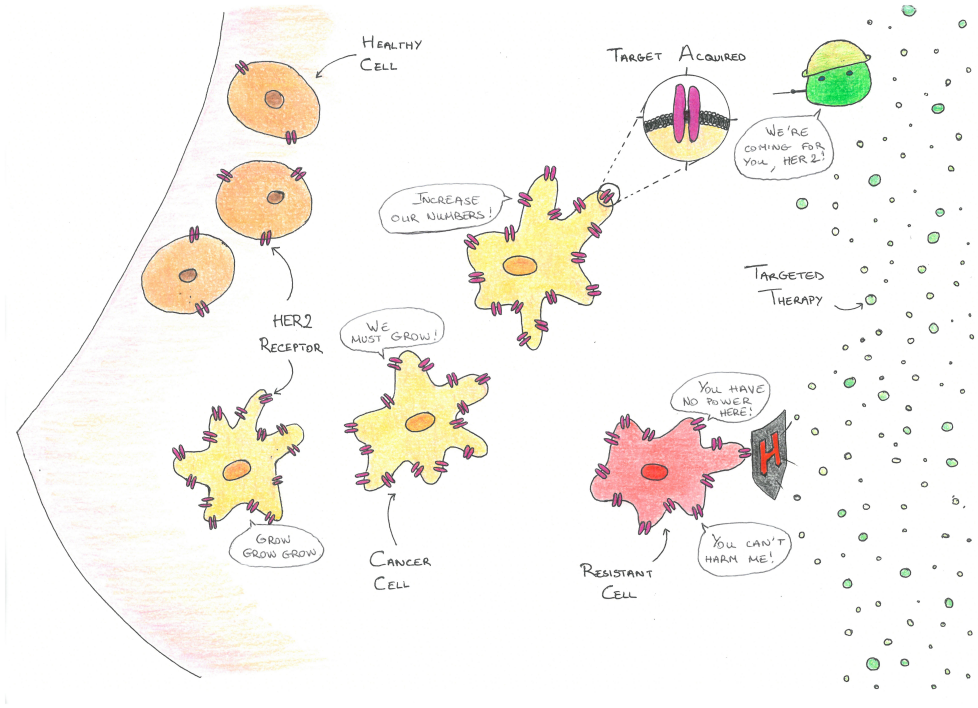

Three Minute Thesis Presentation Slide: HER2+ Breast Cancer and Targeted Therapy. In the case of HER2+ breast cancer, normal breast tissue becomes cancerous with overexpression of the HER2 receptor. Overexpression of the receptor can then be used for a targeted therapy approach as healthy cells do not display as many HER2 receptors. However the cancer cells can adapt and accumulate mutations so that they are no longer vulnerable to the treatment.

Contents

List of Figures

List of Tables

List of Abbreviations

A	Adenine
ABCG2	ATP Binding Cassette Subfamily G Member 2 (Junior Blood Group)
Acetyl-CoA	Acetyl Coenzyme A
Ago2	Argonaute 2
AHNAK	AHNAK Nucleoprotein
AKT	Akt serine/threonine kinase
AKT1	AKT Serine/Threonine Kinase 1
ANOVA	Analysis of variance
AR	Androgen Receptor
AS	Angelman syndrome
ATP	Adenosine triphosphate
ATP8B2	ATPase, Aminophospholipid Transporter, Class I, Type 8B, Member 2
Aza	5-aza-2′-deoxycytidine
BAD	BCL2 Associated Agonist of Cell Death
BASP1	Brain Abundant, Membrane Attached Signal Protein 1
BAX	BCL2 Associated X, Apoptosis Regulator
BCL2	B-Cell chronic lymphocytic leukaemia/Lymphoma 2
BCL2L1	BCL2 Like 1
BCL6	B-Cell chronic lymphocytic leukaemia/Lymphoma 6
BrdU	5-bromo-2′-deoxyuridine
BSA	Bovine serum albumin
C	Cytosine
CA12	Carbonic Anhydrase XII
CARD11	Caspase Recruitment Domain Family Member 11
CASP3	Caspase 3, Apoptosis-Related Cysteine Peptidase
CCND	Cyclin D
CCND1	Cyclin D1
CDH1	Cadherin 1
CDK6	Cyclin Dependent Kinase 6
CDKN1B	Cyclin Dependent Kinase Inhibitor 1B
CDKN1A	Cyclin Dependent Kinase Inhibitor 1A

CG	Cytosine-guanine dinucleotide
CH3	Methyl group
ChIP	Chromatin immunoprecipitation
CI	Confidence interval
CLL	Chronic lymphocytic leukemia
COCH3	Acetyl group
CpG	5′-cytosine-phosphate-guanine-3′
Ct	Threshold cycle
CTCF	CCCTC-binding factor
CXCL1	C-X-C Motif Chemokine Ligand 1
CXCL8	C-X-C Motif Chemokine Ligand 8
CXCR4	C-X-C Motif Chemokine Receptor 4
DCIS	Ductal carcinoma in situ
DCLK1	Doublecortin Like Kinase 1
DDP	Cisplatin
DGCR8	DiGeorge Syndrome Critical Region 8
DIXDC1	DIX Domain Containing 1
DLK1	Delta, drosophila like homologue 1
DMR	Differentially methylated region
DMSO	Dimethyl sulphoxide
DNA MTase	DNA Methyltransferases
DNMT1	DNA (Cytosine-5)-Methyltransferase 1
DNMT3A	DNA (Cytosine-5)-Methyltransferase 3A
DNMT3B	DNA (Cytosine-5)-Methyltransferase 3B
DUSP2	Dual Specificity Phosphatase 2
ECL	Enhanced chemiluminescence
EDTA	2,2′,2″,2‴-(ethane-1,2-diyldinitrilo)tetraacetic acid
EGFR	Epidermal Growth Factor Receptor
EMP1	Epithelial Membrane Protein 1
EMT	Epithelial to mesanchymal transistion
ER	Œstrogn Receptor
ERBB2	Human Epidermal Growth Factor Receptor 2
ERCC1	Excision Repair Cross-Complementing 1, Endonuclease Non-Catalytic Subunit
ERK	Extracellular Signal-Regulated Kinase
F11R	F11 Receptor
FADS1	Fatty Acid Desaturase 1
FBS	Fœtal bovine serum
FEC	Fluorouracil, epirubicin, and cyclophosphamide
FOXO	Forkhead Box Protein O

FOXO1	Forkhead Box O1
FOXO3A	Forkhead Box Protein O3
G	Guanine
GAB1	GRB2 Associated Binding Protein 1
GATA3	GATA Binding Protein 3
GDP	Guanosine diphosphate
GEF	Guanine exchange factor
GRB2	Growth Factor Receptor-Bound Protein 2
GRCh37	Genome Reference Consortium Human Build 37
GSK3	Glycogen Synthase Kinase 3
GTP	Guanosine triphosphate
H1	Histone 1
H2A	Histone 2A
H2B	Histone 2B
H3	Histone 3
H3K27me3	H3 lysine 27 trimethylation
H3K4me3	H3 lysine 4 trimethylation
H3K9me3	H3 lysine 9 trimethylation
H4	Histone 4
HAT	Histone acetyl transferase
HDAC	Histone deacetylase
HER1	Epidermal Growth Factor Receptor
HER2	Human Epidermal Growth Factor Receptor 2
HER2−	HER2 negative
HER2+	HER2 positive
HER3	Human Epidermal Growth Factor Receptor 3
HER4	Human Epidermal Growth Factor Receptor 4
HIF1A	Hypoxia Inducible Factor 1 Subunit Alpha
HITS-CLIP	High-throughput sequencing of RNA isolated by crosslinking immunoprecipitation
HR	Hormone Receptor
HRG	Heregulin
IC_{50}	50 % inhibitory concentration
IG-DMR	Intergenic-differentially methylated region
IGF1R	Insulin Like Growth Factor 1 Receptor
IHC	Immunohistochemistry
IKK	Inhibitor Of Nuclear Factor Kappa B Kinase
IL8	C-X-C Motif Chemokine Ligand 8
INHBB	Inhibin Beta B
ITCH	Itchy E3 Ubiquitin Protein Ligase

ITGB4	Integrin Subunit β4
JAK	Janus Kinase
K	Lysine
KLF9	Kruppel Like Factor 9
KRAS	KRAS Proto-Oncogene, GTPase
L-15	Leibovitz-15
LAMA4	Laminin Subunit Alpha 4
Lap	Lapatinib
LCIS	Lobular carcinoma in situ
lnRNA	Long non-coding RNA
m^5C	5-methylcytosine
MACC1	Metastasis-Associated In Colon Cancer Protein 1
MAPK	Mitogen-Activated Protein Kinase
MBD	Methyl-CpG binding domain
MEG	Maternally expressed gene
MEG3	Maternally Expressed Gene 3
MEG8	Maternally Expressed Gene 8
MET	Mesenchymal Epithelial Transition Proto-Oncogene, Receptor Tyrosine Kinase
MITF	Melanocyte Inducing Transcription Factor
miR	microRNA
miR127	hsa-miR-127-3p
miR409	hsa-miR-409-3p
miR411	hsa-miR-411-5p
miR433	hsa-miR-433-3p
miR495	hsa-miR-495-3p
miR539	hsa-miR-539-5p
miRNA	microRNA
MLL	Mixed lineage leukaemia
MMP9	Matrix Metallopeptidase 9
MMP14	Matrix Metallopeptidase 14
MNAT1	Menage A Trois Cyclin Dependent Kinase-Activating Kinase Assembly Factor 1
mRNA	Messenger RNA
MSI2	Mushashi RNA-Binding Protein 2
MTA3	Metastasis Associated 1 Family Member 3
mTOR	Mechanistic Target of Rapamycin Kinase
MTT	Thiazolyl blue tetrazolium bromide
MX2	MX Dynamin-Like GTPase 2
MYC	Avian Myelocytomatosis Viral Oncogene Homolog

MYT1	Myelin Transcription Factor 1
NAD	Nicotinamide adenine dinucleotide
NEDD4L	Neural Precursor Cell Expressed, Developmentally Down-Regulated 4-Like
NF-$\varkappa$B	Nuclear Factor Kappa B Subunit
NR3C1	Nuclear Receptor Subfamily 3 Group C Member 1
NRCAM	Neuronal Cell Adhesion Molecule
NSCLC	Non-small cell lung carcinoma
OR	Odds ratio
$p21^{Cip1}$	Cyclin Dependent Kinase Inhibitor 1A
$p27^{Kip1}$	Cyclin Dependent Kinase Inhibitor 1B
p38	MAPK p38
PAAF1	Proteosomal ATPase-Associated Factor 1
Pac	Paclitaxel
PAR-CLIP	Photoactivatable-ribonucleoside-enhanced crosslinking and immunoprecipitation
PBS	Phosphate buffered saline
PCR	Polymerase chain reaction
pCR	Pathological complete response
PDPK1	3-Phosphoinositide Dependent Protein Kinase 1
PEG	Paternally expressed gene
PGR	Progesterone Receptor
PHD	Plant homeodomain
PHF10	PHD Finger Protein 10
PI3K	Phosphoinositide-3-Kinase
PIP2	Phosphatidylinositol (4,5)-Bisphosphate
PIP3	Phosphatidylinositol (3,4,5)-Trisphosphate
PKIA	Protein Kinase (cAMP-Dependant, Catalytic) Inhibitor Alpha
poly(A)	Polyadenylation
PQLC3	PQ Loop Repeat Containing 3
PR	Progesterone Receptor
pre-miRNA	Precursor miRNA
PREX1	Phosphatidylinositol-3,4,5-Triphosphate-Dependant Rac Exchange Factor 1
pri-miRNA	primary miRNA
PTB	Phosphotyrosine-binding
PTEN	Phosphate and Tensin Homolog
PTP4A3	Protein Tyrosine Phosphatase Type IVA, Member 3
PWS	Praeder-Willi syndrome
R	Arginine

Rac	RAS-Related C3 Botulinum Toxin Substrate
RAC1	Rac Family Small GTPase 1
RAS	Rat Sarcoma Viral Oncoprotein
RB1CC1	RB1 Inducible Coiled-Coil 1
RDX	Radixin
RIPA	Radioimmunoprecipitation assay
RISC	RNA Induced Silencer Complex
RNA	Ribonucleic acid
RNAi	RNA interference
RNU44	Small Nucleolar RNA, C/D Box 44
RPLP0	Ribosomal Protein Lateral Stalk Subunit P0
RPMI	Roswell Park Memorial Institute
RSU1	RAS Suppressor Protein 1
RTL1	Retrotransposon Like Gene 1
RT-qPCR	Real time quantitative polymerase chain reaction
RUNX2	Runt Related Transcription Factor 2
scb	Scramble negative control
SH2	Src Homology 2
SH3BGRL	SH3 Domain Binding Glutamate-Rich Protein Like
siRNA	Small interfering RNA
SIRT	Silent Information Regulators Type
SMAD	Sma- and Mad-Related Protein
SNAI1	Snail Family Transcriptional Repressor 1
SNAI2	Snail Family Transcriptional Repressor 2
SOCS2	Suppressor of Cytokine Signalling 2
SOS1	Son of Sevenless Homologue 1 (Drosophila)
SOX4	SRY (Sex Determining Region Y)-Box 4
SP1	Specificity Protein 1
SPAG5	Sperm Associated Antigen 5
SPRY4	Sprouty Receptor Tyrosine Kinase Signalling Antagonist 4
Src	Proto-oncogene SRC, Rous Sarcoma
SRY	Sex Determining Region Y
STAT	Signal Transducer
STC2	Stanniocalcin
T	Thymine
TACSTD2	Tumor-Associated Calcium Signal Transducer 2
TGFB1	Transforming Growth Factor Beta 1
TGF-	Transforming Growth Factor Beta
TPM1	Tropomyosin 1
Tras	Trastuzumab

TRBP	Transactivation-Responsive RNA-Binding Protein
TSA	Trichostatin A
TXNIP	Thioredoxin Interacting Protein
U	Uracil
UPD	Uniparental disomie
UQCC	Ubiquinol-Cytochrome C Reductase Complex Chaperone
UV	Ultraviolet
VDR	Vitamin D Receptor
VIM	Vimentin
Wnt	Wingless-Type MMTV Integration Site
XPO5	Exportin 5
ZBTB10	Zinc Finger And BTB Domain Containing 10
ZEB1	Zinc Finger E-Box Binding Homeobox 1
3′UTR	3′ untranslated region
5′UTR	5′ untranslated region
-ve	Non-targeting control siRNA

1 Introduction

1.1 Breast Cancer

Breast cancer is the most commonly diagnosed female cancer (*2*). Overall mortality rates for this tumour type have been decreasing since the end of the XX^{th} century, when mass screening was phased in, as this allowed earlier detection and treatment of the disease (*3*). Age is still the biggest risk factor associated with the disease (*4*). Women under 40 have less than 0.5 % chance of developing breast cancer but this increases with age; so women over 70 have a 1 in 8 chance of being diagnosed with breast cancer (*5*).

1.1.1 Breast Cancer Development

Normal breast tissue is made of an intricate network of ducts (Figure 1.1), set in adipose tissue, that connect lobes of lactiferous glands to the nipple. The lobes consist of multiple lobules each composed of acini; each lobule, along with its associated ducts, form the terminal ductal lobular units (*6*, *7*). These are the secretory units of the mammary gland. Both ducts and lobules are formed by a single layer of polarised luminal epithelial cells surrounding a central lumen. This complex is encircled by a single layer of basal, or myoepithelial, cells (Figure 1.1). This structure is contained in a layer of collagen and laminin, called the basement membrane, which prevents secretions from entering the surrounding stromal tissue (*8*).

Generally breast cancers initiate as benign epithelial lesions which have atypical ductal or lobular structure. If this progresses, abnormal proliferation will generate an extra layer of cells in the lumen, this stage is called atypical hyperplasia and is considered a precancerous lesion (*10*, *11*). With further cell growth this can then become an *in situ* carcinoma, either ductal (DCIS) or lobular

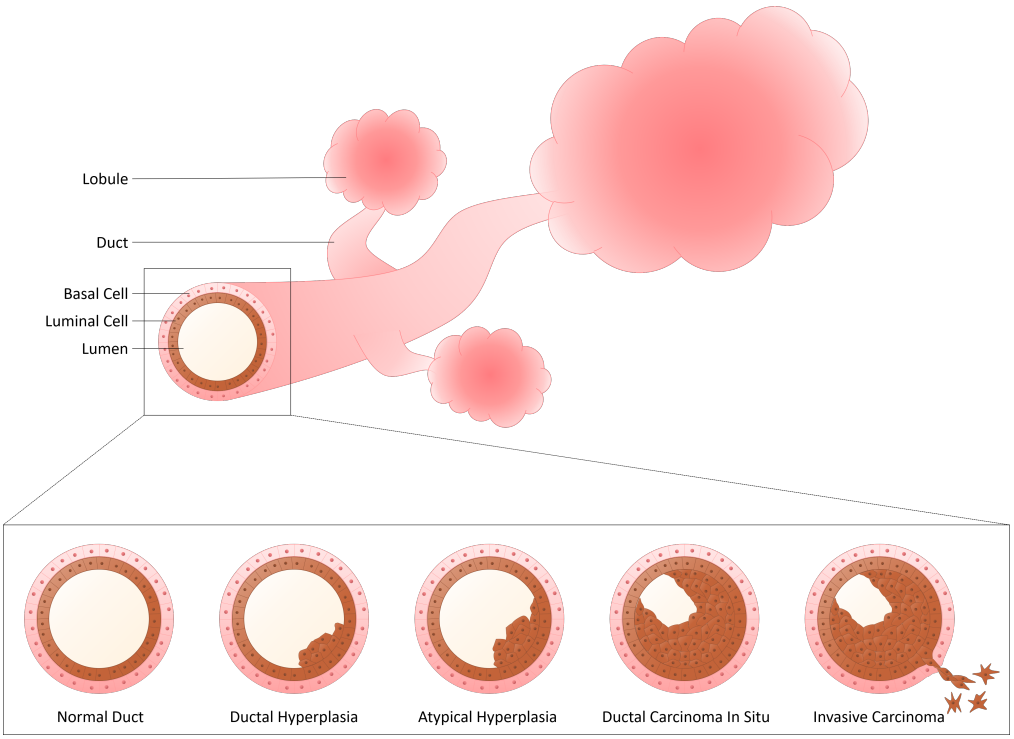

Figure 1.1: Schematic Representation of Breast Structure and Cancer Development. Breast tissue is formed of ducts connecting secretory units, called lobules, to the nipple. Each is formed of a single layer of luminal epithelial cells surrounded by a single layer of basal epithelial or myoepithelial cells. Most breast cancer arise from the epithelial layer and are thought to follow a specific series of steps starting from a benign epithelial lesion, called ductal hyperplasia. With atypical proliferation this evolves into atypical hyperplasia which is considered a precancerous entity. Ductal Carcinoma In Situ (DCIS) and its lobular equivalent Lobular Carcinoma In Situ (LCIS) are non invasive lesions as they do not infiltrate the surrounding tissue. Over time the tumours can become invasive and lead to metastasis (*9*).

(LCIS), depending on the origin of the tumour. These are typically confined to the lumen and are non invasive as they do not infiltrate the surrounding tissue, however, over time the cells can undergo epithelial to mesenchymal transition (EMT) and become invasive (*12*, *13*) which can lead to metastatic spread (Figure 1.1).

Over 90 % of breast cancers originate from luminal epithelial cells as cell renewal and proliferation generally occur in this layer. Breast cancers can either arise in the ducts or in the lobules (*14*). As the disease progresses, loss of the basal epithelial cell layer can occur which leads to a loss of structure in the tissue (*6*, *15*).

Breast cancer is a heterogeneous disease which leads to very different responses to therapy depending on tumour transcriptome, therefore, breast cancer cannot be treated as a single malignancy (*16*).

1.1.2 In Situ Breast Cancer Classification

There are multiple classifications used to subdivide and classify breast cancers. These are based on diverse histopathological and biological features expressed by tumours. This stratification is used to assess prognosis and guide treatment strategies as they will vary in clinical outcome and response to therapy (*17*).

Cancer can be attributed a stage to describe its size and spread from its site of origin, in this classification *in situ* carcinomas will be stage 0 as, although DCIS and LCIS have uncontrolled cell proliferation, they do not invade the surrounding tissue.

These lesions are also graded using a histological classification based on the level of differentiation of the cells. A lower grade is attributed to tumours with highly differentiated cells that still resemble their cells of origin and a higher grade is given to poorly differentiated tumours. The tumour stage will progress as the cancer invades the surrounding tissue (*18*).

1.1.3 Invasive Breast Cancer Classification

Invasive breast cancers are very heterogeneous and can be characterised by stage or grade. They can also be classified using expression profiles of several

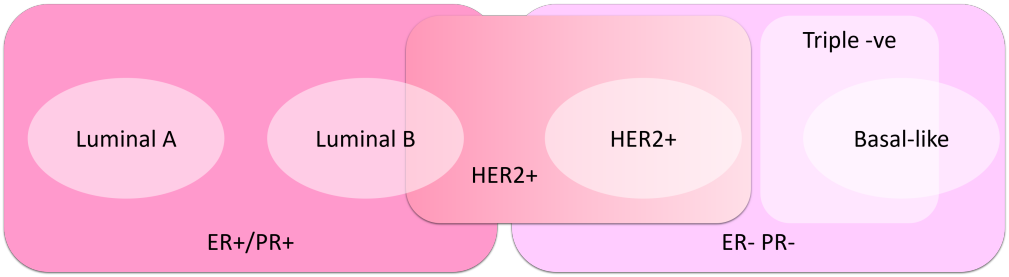

Figure 1.2: Schematic Representation of the Molecular Subtypes of Breast Cancer. Breast cancers are separated into groups based on the presence or absence of several biomarkers. ER: Œstrogen Receptor, PR: Progesterone Receptor, HER2: Human Epidermal Growth Factor Receptor 2. Figure adapted from Chivukula (*21*).

molecular biomarkers. The three main subtypes are based on expression, or lack thereof, of the Œstrogen Receptor (ER), the Progesterone Receptor (PR), and the Human Epidermal Growth Factor Receptor 2 (HER2) (*19*). Accordingly, breast cancers are classified into: hormone receptor positive, which is ER and/or PR positive; HER2 driven, characterised by an amplification of the *HER2* oncogene; and triple negative (*20*), which is neither hormone nor HER2 expressing (Figure 1.2).

Extensive gene expression profiling of both cell lines and patient data has enabled further break-down of the classification into 4 groups with prognostic relevance (*22*–*25*): Luminal A and Luminal B, basal like, and HER2 enriched (Figure 1.2). The luminal subtypes are ER and/or PR positive and, overall, have better survival rates than the other groups. Luminal A represents about 40 % of breast cancers and has high ER signalling with low HER2 expression (*26*); luminal B accounts for 20 % of breast cancers. This subtype generally has lower ER regulation, decreased PR, along with more proliferation than luminal A cancers. Luminal B tumours can be either HER2 positive (HER2+) or HER2 negative (HER2−). Cross-talk occurs between the HER2 and ER pathways which can lead to resistance to hormonal therapies. The absence of HER2 in luminal B tumours has been found to be predictive of better outcome (*27*). Luminal B cancers have been correlated to aggressive clinical behaviour and a higher probability of relapse in patients (*28*, *29*). Basal-like cancers are 15 % of breast tumours, this classification is similar to the triple negative subtype as the tumours do not have any ER, PR, or HER2 expression (*30*, *31*). The HER2 enriched group, has an overexpression of HER2 and underexpression of luminal

associated genes (*32*).

Differences in response to therapy and clinical outcome still occur between tumours that display similar clinical and pathological characteristics. Thus, with the continual progress of sequencing technology, new breast cancer classifications are emerging to attempt to address this issue. A new classification is based on genomic amplifications and duplications found in tumours. This subdivides breast cancers into ten different groups, or integrative clusters, which have been associated with distinct clinical outcomes (*33*). The different molecular subtypes are divided between the various clusters. HER2+ cancers correlate more strongly with clusters 5 and 10 and luminal B with cluster.

Another classification looks at predicting outcome based on the similarities in phenotype of the tumour to that of normal cells. This classification uses the expression status of three hormone receptors (HR): ER, Androgen Receptor (AR), and Vitamin D Receptor (VDR). Expression of these receptors leads to the classification in groups HR0 to HR3 depending on how many of these receptors are expressed (*34*). Thus, tumours expressing one of the receptors, irrespective of which one, will be classified as HR1, tumours expressing all three, will be HR3. Approximately 45 % of HER2+ breast cancers are HR2, 25 % are HR1, another 25 % are HR3, and 5 % are in the HR0 group (*35*). This classification highlights the heterogeneity observed within the different molecular subtypes as they are distributed across the various HR groups.

These new classifications can be used in order to refine the more traditional breast cancer subtypes and stratify patients more accurately. Here, we will be using the wider HER2+ classification based on amplification of the oncogene irrespective of the ER and PR status to study resistance to HER2 therapies more broadly.

1.2 HER2 Positive Breast Cancer

1.2.1 HER2 Signalling

HER2, also called neu in mice or ERBB2, is part of the human epidermal growth factor receptor family. This receptor tyrosine kinase family comprises three other members, the epidermal growth factor receptor (EGFR, HER1),

HER3, and HER4. These three other transmembrane receptors require ligand binding for dimerisation whereas HER2 does not (*36*). Therefore, in HER2+ breast cancer, the increased number of HER2 receptors present on the plasma membrane of tumour cells leads to ligand independent dimerisation of the receptors. The HER receptors homo- or hetero- dimerise allowing for autophosphorylation of the intracellular domains (*37*) leading to the activation of downstream effectors and to signalling through the Rat Sarcoma Viral Oncoprotein (RAS), Rac and the phosphoinositide-3-kinase (PI3K)-Akt serine/threonine kinase (AKT) pathways (*38*) which results in increased cell growth and survival signals (Figure 1.3).

After dimerisation of the HER partners, tyrosine residues in the C-terminal region of the receptors are phosphorylated (*39*). These phosphotyrosines act as docking sites for many signalling molecules containing phosphotyrosine-binding (PTB) domains and Src Homology 2 (SH2) domains, allowing the activation of numerous downstream effectors. The Growth factor receptor-bound protein 2 (GRB2) contains an SH2 domain and docks onto the phosphotyrosine site on the receptor where it will act as an adaptor protein (*38*). It can then recruit the RAS-guanine exchange factor (GEF), Son of Sevenless Homologue 1 (Drosophila) (SOS1), which exchanges guanosine diphosphate (GDP) bound to inactive RAS for guanosine triphosphate (GTP); this activates RAS which, in turn, activates the MAP Kinase pathway (*40*).

The PI3K regulatory subunit, p85, also contains an SH2 domain and is therefore recruited to a phosphotyrosine on the receptor (*41*, *42*). Once it is localised at the membrane, PI3K will phosphorylate Phosphatidylinositol (4,5)-bisphosphate (PIP2) to Phosphatidylinositol (3,4,5)-trisphosphate (PIP3) (*43*). 3-Phosphoinositide Dependent Protein Kinase 1 (PDPK1) and AKT proteins will both bind to PIP3 leading to the phosphorylation of AKT by active PDPK1 and Mechanistic Target Of Rapamycin Kinase (mTOR) (*44*), phosphorylated AKT then dissociates from PIP3 and phosphorylates BCL2 Associated Agonist of Cell Death (BAD).

Phosphorylated BAD can then separate from the inactive apoptosis inhibitory protein it was previously bound to and is inactivated by binding the 14-3-3 protein. The apoptosis inhibitory protein, no longer bound to BAD, is thus activated leading to inhibition of apoptosis (*45–47*). AKT also inhibits other proteins, such as Cyclin Dependent Kinase Inhibitor 1B (CDKN1B or $p27^{Kip1}$)

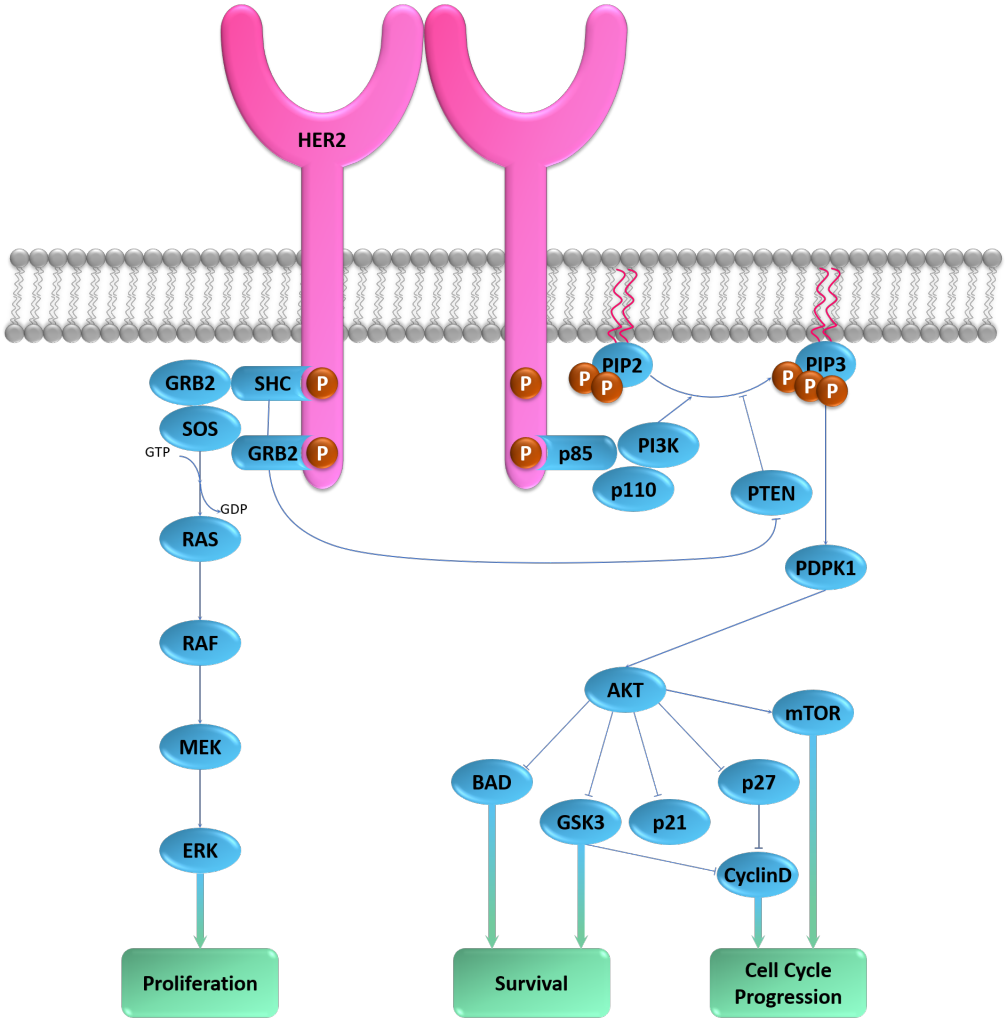

Figure 1.3: Overview of the HER2 Signalling Pathway. After ligand independent dimerisation of the receptors, auto-phosphorylation of C-terminal tyrosine residues occurs. These will act as docking sites for proteins containing phosphotyrosine-binding (PTB) domains and Src Homology 2 (SH2) domains. This will lead to the activation of downstream effectors, resulting in increased proliferation, survival, and cell cycle progression signalling.

and Glycogen Synthase Kinase 3 (GSK3), lifting their inhibition of Cyclin D (CCND) and allowing cell cycle progression.

Therefore, increased levels of HER2 in breast cancers lead to more aggressive tumours as signalling through this pathway leads to proliferation, cell survival, and anti-apoptotic signalling.

1.2.2 Identification in Patients

Identifying the HER2 status of a patient is essential to determine the potential responsiveness of their tumour to therapies targeting HER2. In the clinic, different tests are used to identify HER2+ breast cancers in patients. Generally, HER2 overexpression is graded by immunohistochemistry (IHC) which asses levels of HER2 protein (*48*, *49*); it is graded on a scale where 0 to 1 is considered HER2 negative and 3+ is HER2+. HER2 staining is considered 3+ when more than 30 % of the invasive cells display a uniform and intense membrane staining (*50*). If the score is 2+, the tumour is considered borderline and further testing is required.

If the IHC results are equivocal, amplification of *HER2* can be identified by fluorescence *in situ* hybridisation (FISH), this is used to check for an increase in copy number of the gene. If there are more than six copies of the HER2 gene per cell nucleus, or the ratio of HER2 to the chromosome 17 control probe is greater than 2, the tumour is considered HER2+ (*50*, *51*). If there are less than 4 HER2 gene copies per nucleus, or a FISH ratio lower than 2, the results require further validation. If it has not been done previously, then IHC can be performed. Otherwise the FISH results should be reassessed by an individual blinded to the previous analysis. If this recount still doesn't conclude that the tumour is HER2+, then the diagnosis will be HER2− (*49*).

HER2 overexpression occurs in approximately 20-25 % of breast cancers, and is more common in younger patients who develop the disease. Untreated, this tumour subtype is characterised by a poor prognosis compared to the other subtypes (Figure 1.4). The 5 year survival rate of patients with HER2+ disease compared to HER2 negative tumours is, respectively, 19.70 % and 24.50 % (*52*). The use of targeted therapy has significantly improved the prognosis of patients with HER2+ breast cancer.

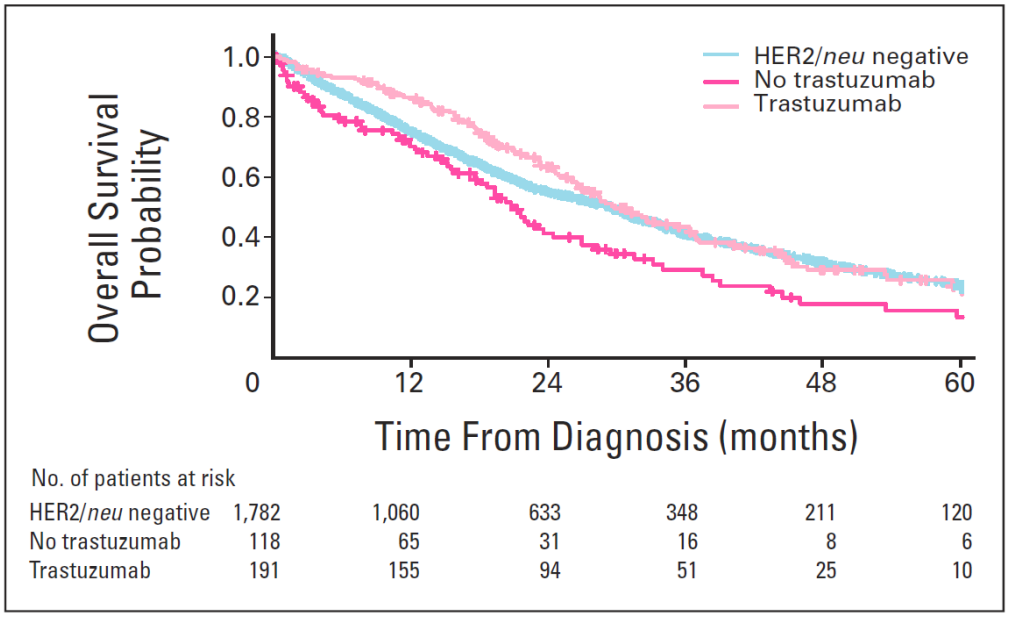

Figure 1.4: Overall Survival by HER2 Status and Treatment, from Dawood *et al.* (*52*).

1.2.3 Treatment with HER2-Targeting Therapy

HER2-targeting therapies are used for the treatment of HER2+ breast cancers, they can be specific or target multiple members of the ERBB protein family (Table 1.1). The HER2-targeting monoclonal antibody trastuzumab (Herceptin) (*53*) is currently the first line therapy used to treat early stage HER2+ breast cancer, however, many trials have been looking at treating these tumours with a combination of trastuzumab and lapatinib (with chemotherapy) and are finding the combination to be more beneficial than the single agent treatment (*54–56*). Additionally, about half of HER2+ tumours also have expression of hormone receptors, ER or PR, and therefore, in certain cases, can benefit from the combination of both a HER2-targeting agent and endocrine therapy (*57*)

Lapatinib is a small molecule inhibitor that targets EGFR and HER2. It binds the adenosine triphosphate (ATP) binding pocket of the receptor, thus preventing autophosphorylation of the intracellular domain of the receptors. Thus inhibiting signalling through the Mitogen-Activated Protein Kinase (MAPK) and PI3K/AKT pathways (*72*). This also leads to decreased phosphorylation of downstream effector proteins, such as Extracellular Signal-Regulated Kinase (ERK), RAF, and AKT. An increase in MAPK p38 (p38), a stress induced

Therapy		Target	Mode of Action	References
Human Monoclonal Antibody	Trastuzumab	HER2	Targets the extracellular domain causing internalisation and degradation of the receptors, leading to antibody-dependant cellular cytotoxicity.	(*58*) (*59*)
	Pertuzumab	HER2	Dimerisation inhibitor, binds to the extracellular domain, at a different epitope than trastuzumab, preventing dimerisation of the receptors.	(*60*) (*61*)
Antibody-Drug Conjugate	Trastuzumab Emtasine	HER2	T-DM1 Trastuzumab directs drug to HER2 and helps delivery of DM1 to cancer cells, only works if high HER2	(*62*) (*63*)
Small Molecule Tyrosine Kinase Inhibitor	Lapatinib	EGFR HER2	Reversible inhibitor that targets the ATP-binding pocket and prevents auto-phosphorylation of the intracellular domains.	(*64*) (*65*)
	Neratinib	Pan-HER	Irreversibly binds the ATP-binding pocket of the receptor preventing auto-phosphorylation of the intracellular domain.	(*66*) (*67*)
	Dacomitinib	Pan-HER	Targets the catalytic domain of the receptors causing covalent modifications to cysteine residues stopping auto-phosphorylation.	(*68*) (*69*)
	Gefitinib	EGFR	Binds the ATP-binding pocket of the receptor and blocks auto-phosphorylation of the intracellular domains.	(*70*) (*71*)

Table 1.1: HER Targeting Agents and their Mode of Action

tumour suppressive protein (*73*), is also achieved. p38 can in turn cause an increase in expression of the cell cycle inhibitors, Cyclin Dependent Kinase Inhibitor 1A (CDKN1A or $p21^{Cip1}$) and CDKN1B (*74*). These proteins cause cell cycle inhibition and senescence eventually causing cell cycle arrest in the G1 phase and apoptosis (*75*).

For metastatic disease, the monoclonal antibodies pertuzumab and trastuzumab emtasine (*62*, *63*) are the current standards in the clinic (*76*). Lapatinib was previously use to treat patients with cancers progressing on trastuzumab.

Yet, despite all progress in HER2-directed therapy only a subgroup of patients derives the optimal benefit, whereas other patients have refractory disease or develop resistance (*50*, *77*). It is therefore necessary to identify new targets to improve patient outcome.

1.2.4 Resistance to HER2-Targeting Therapies

Resistance to therapy is a widely occurring issue in cancer treatment and this is very true for HER2 directed therapy. Many patients who present the disease are intrinsically resistant to the HER2-targeted therapies, or develop resistance over the course of treatment. A multitude of mechanisms have been reported for acquired resistance to trastuzumab and lapatinib.

With most targeted therapies, the most common mechanisms of resistance involve the mutation of the therapeutic target. Here, for both lapatinib and trastuzumab, this results in mutations in the HER2 receptor preventing inhib-

ition by the drug (*78*, *79*). The cell can also downregulate expression of the target, thus escaping inhibition (*80*, *81*) and rely on other pro-survival pathways, such as PI3K/AKT signalling (*82–84*) or the activation of other RTKs like HER3 (*85*, *86*) or Insulin Like Growth Factor 1 Receptor (IGF1R) (*87–89*). Trastuzumab resistance can also be caused by increased EGFR signalling (*90*, *91*), which can be overcome by lapatinib as it targets both EGFR and HER2 (*92*, *93*). Increased levels of Heregulin (HRG), a HER3 ligand, can lead to lapatinib resistance by inducing the formation of HER3-EGFR dimers promoting downstream signalling through PI3K and bypassing HER2 (*94*). Additionally, whilst trastuzumab can cause mutation or loss of Phosphatase And Tensin Homolog (PTEN) (*95*) which leads to resistance, lapatinib functions in a a PTEN independent manner (*96*) meaning it can help surmount trastuzumab resistance.

Autophagy has been linked to trastuzumab resistance in breast cancer (*97*). Additionally, increased autophagosome formation has been observed in lapatinib resistant cell lines, and treatment with autophagy inhibitors restoring sensitivity to lapatinib (*98*). Hypoxia can promote lapatinib resistance through increased Hypoxia Inducible Factor 1 Subunit Alpha (HIF1A) levels by reducing expression of Dual Specificity Phosphatase 2 (DUSP2) leading to activation of the ERK signalling pathway (*99*).

1.3 miRNAs and their Role in Cancer

microRNAs (miRNAs) are small non-coding RNAs, 20 to 22 nucleotides long (*100*). They are involved in the RNA interference (RNAi) machinery responsible for post-transcriptional gene regulation through mRNA repression (*101*). miRNAs have been increasingly identified as having important roles in development and disease.

1.3.1 miRNA Processing

In the canonical maturation pathway, the miRNA is transcribed by RNA polymerase II or III in the nucleus as a primary miRNA transcript (pri-miRNA) that ranges from hundreds to thousand of nucleotides in length. It has a fold-back RNA precursor structure with imperfect base pairing, a 5' cap, and a 3'

poly(A) tail (Figure 1.5). The pri-miRNA is then cleaved by the microprocessor complex made of the ribonuclease III enzyme, Drosha, and the dsRNA specific ribonuclease, DiGeorge Syndrome Critical Region 8 (DGCR8 or Pasha) giving the precursor hairpin structure (pre-miRNA) which is 60 to 70 nucleotides long (*101*). The pre-miRNA is exported to the cytoplasm by Exportin 5 (XPO5)-Ran-GTP. There, it is further processed by the dsRNase type III, Dicer complex (*102*) and the double-stranded RNA-binding protein, Transactivation-responsive RNA-binding protein (TRBP). This generates the mature duplex miRNA, which is composed of a guide and passenger strand (*103*).

To obtain the single stranded mature miRNA, the passenger strand will be unwound and degraded (*104*). The mature miRNA is incorporated into the RNA induced silencer complex (RISC) which contains the Argonaute (Ago2) and Dicer1 proteins (Figure 1.5). Non-canonical processing pathways for miRNAs also exist without ribonuclease III enzymes, however, miRNAs from these pathways are of low abundance and are generally poorly conserved (*105*, *106*).

The mature miRNA is used to guide the RISC complex to post-transcriptionally regulate genes in a sequence specific manner (*107*) by partial sequence complementarity, usually to the 3' untranslated region (3′UTR) of a target messenger RNA (mRNA) (*108*, *109*), however, certain miRNA also target the 5′UTR and certain gene coding regions. The region involved in recognition of the 3′UTR consists of nucleotides 2 to 7 from the 5' end of the miRNA and is called the miRNA seed site. Nucleotides that are downstream of this region are less relevant to the pairing of the miRNA and the 3′UTR, however, the can also contribute to the base pairing (*110*). The degree of complementarity between the miRNA and the mRNA will determine whether the gene is silenced by deadenylation or translational repression (*111*). As only partial complementarity is required, miRNAs have many targets, and are estimated to be in the hundreds or thousands for a single miRNA (*112*). Computational predications have found that over 60 % of human protein coding genes have at least one conserved miRNA seed site (*113*), suggesting that miRNAs are important regulators of gene expression.

miRNA expression patterns have been found to be highly tissue-specific. Since miRNAs regulate many aspects of biological processes, aberrations in the expression of individual or subsets of miRNAs has been implicated in many diseases, including cancers. Additionally their expression profiles continues to evolve over

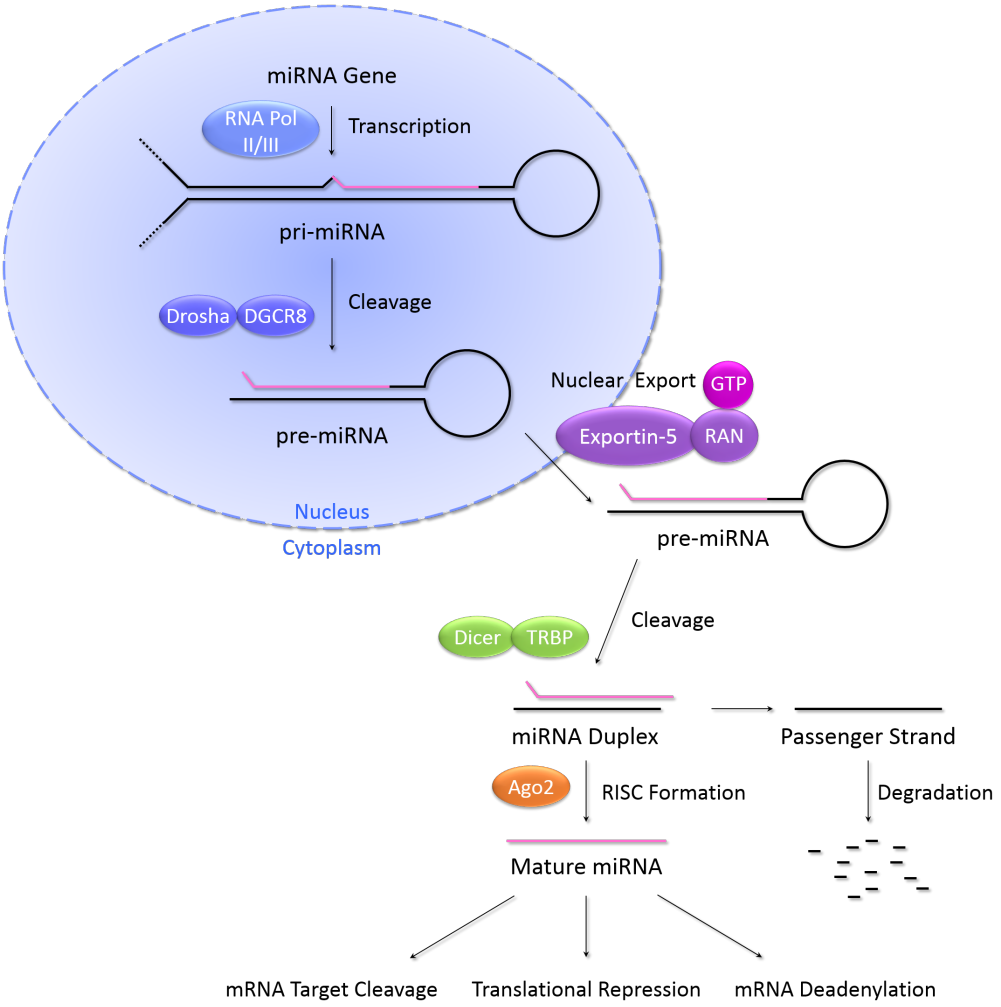

Figure 1.5: Canonical miRNA Processing. miRNAs are transcribed in the nucleus as primary miRNA transcripts (pri-miRNA) and are then processed by the Drosha-DGCR8 complex making the precursor miRNA (pre-miRNA). Drosha is a ribonuclease III enzyme and DGCR8 is a dsRNA specific ribonuclease. The pre-miRNA is exported to the cytoplasm by Exportin 5 (XPO5)-Ran-GTP where it is then processed by the DICER complex. Next, the mature miRNA along with Argonaute 2 (Ago2) is loaded onto the RNA induced silencer complex (RISC). The passenger strand will be degraded and the miR-RISC will bind and target miRNAs for repression and cleavage.

the course of the disease (*114*).

1.3.2 miRNAs in Cancer

As miRNAs are expressed in a time- and tissue-specific manner they can be spatially and temporally aberrantly expressed in cancer. For instance, in breast cancer, miR205 expression was found to be decreased in tumour compared to healthy cells, however, it was also found to be upregulated in cancer initiating cells (*115*). Thus its role promoting or inibiting cancer progression is modulated by the cell type where the miRNA is expressed or not. In tumours miRNAs are often deregulated (*116*, *117*) affecting tumour proliferation and survival. Indeed the bulk of miRNA genes has been found to be in cancer associated genomic break points (*118*). These are fragile sites that are prone to genomic amplifications and deletions as well as chromosomal translocations. The resulting miRNAs can in turn lead to more instability through promoting cell cycle defects, mitosis, and DNA damage repair (*119*).

In many cancers, miRNA signatures have been found to be predictive of clinical outcome (*120*) and can be used to discriminate between cancer subtypes (*121*, *122*). This is the case for breast cancers, where miRNA expression is often deregulated in tumours compared to healthy tissue (*123*). miRNA patterns can be correlated to certain clinicopathological features, such as ER or PR expression, as well as the tumour stage (*124*). miRNAs have been suggested to be used as biomarkers to identify these clinic-pathological features. The histological grade of a tumour can be identified based on levels of miR21, miR126, miR155, and miR199a (*125*). Poor survival can also be predicted from expression levels of miR20b-5p, miR93-5p, miR126-5p, miR195-5p, miR454-3p, miR1274b, miR1825 (*126*, *127*). In HER2+ breast cancer, expression of miR10b, miR107, miR126, miR154, miR195, let7f, and let7g has been identified as specific to the subtype (*128*).

The miRNAs that are deregulated in cancers can be categorised as tumour suppressors or oncogenes depending on their target genes and the context (*129*–*133*). Both oncogenic (*134*) and tumour suppressive (*135*, *136*) miRNAs are present in breast cancers. miR21 and miR27a, for instance, have been identified as oncogenes as they promote tumour growth by targeting tumour suppressor genes such as Tropomyosin 1 (TPM1) (*137*) and G2-M checkpoint regulators

Zinc Finger And BTB Domain Containing 10 (ZBTB10) and Myelin Transcription Factor 1 (MYT1) (*138*). miR125a and miR125b have been labelled as tumour suppressors and are downregulated in HER2+ disease. Indeed, the HER2 and HER3 3′UTR regions contain seed sites for the miRNAs (*139*). let-7 on the other hand has been found to be a tumour suppressive miRNA as it is involved in regulation of self-renewal and its expression is reduced in breast cancer stem cells (*140*). miR200, an inhibitor of angiogenesis, also acts as a tumour suppressor as it prevents C-X-C Motif Chemokine Ligand 8 (IL8, CXCL8) and C-X-C Motif Chemokine Ligand 1 (CXCL1) signalling which leads to an overall decrease in tumour size (*141*). miR143 and miR145 are also decreased in breast cancers are this loss correlates with an increase in HER3, KRAS Proto-Oncogene, GTPase (KRAS), Vimentin (VIM), C-X-C Motif Chemokine Receptor 4 (CXCR4), Matrix Metallopeptidase 9 (MMP9), and Cadherin 1 (E-Cadherin, CDH1) expression which positively correlate to increased tumour size, high histological grade, metastasis, and recurrence (*142*).

As miRNA function is context dependant, some miRNAs can have ambivalent roles. miR221 and miR222 have been labelled as tumour suppressors in high grade luminal carcinomas where their decreased expression correlates to high expression of Integrin Subunit β4 (ITGB4), disintegrins, and Matrix Metallopeptidase 14 (MMP14), essential to an invasive phenotype (*143*). Increased expression of miR221 and miR222, however, has been reported to promote metastasis and the EMT phenotype by causing the downregulation of CDH1 (*144*). Thus the function of these two miRNAs will depend on the cell type as well as time in the tumour's progression where they are expressed.

miRNAs can also contribute to metastasis by promoting migration and invasion of tumour cells (*145*, *146*). It has even been suggested that circulating miRNAs could be used to monitor metastasis progression as the metastasis secretes a different miRNA profile to the primary tumour (*147*). This highlights the potential applications of miRNAs as biomarkers since their expression is very varied between healthy tissue and different tumour stages (*148*). miR210, a hypoxia responsive miRNA, has been proposed as a prognostic marker for breast cancer. As it is upregulated in patients with poor prognosis (*149*). The presence of metastases can be determined from expression levels of miR10b, miR21, miR34a, and miR373 (*150*). Other miRNAs, miR155, miR195, and let-7a, detected in patients with distant metastases have been suggested as markers of

invasiveness (*151–153*). miRNAs of the miR200 family are hypermethylated in certain tumours, which leads to a decrease in expression of the miRNAs. This is commonly seen in cancers where EMT has occurred suggesting methylation levels along with miRNA expression could be used to asses EMT occurrence (*154*).

Over time miRNA profiles have been seen to evolve, especially when tumours are subjected to treatment. Importantly miRNAs have been implicated in therapeutic resistance (*155–158*). Resistance to chemotherapy can be determined based on expression patterns of miR7, miR17, miR21, miR34, miR125b, miR205, miR221, miR210, miR340, and let-7a (*159–161*). In HER2+ breast cancer, trastuzumab resistance has been associated with expression of various miRNAs, such as miR221 (*162*). Plasma levels of miR210 have been found to correlate with sensitivity to this treatment (*163*). High expression of miR21 has also been shown to lead to trastuzumab resistance (*164*). For lapatinib, loss of miR630 has been found to lead to resistance (*165*). One of the most common mechanisms altering miRNA expression in cancer is epigenetic regulation (*166*).

Due to the increasingly important role miRNAs are being attributed in cancer development and progression, miRNAs are being investigated as therapies. These anticancer treatments function by antagonising upregulated oncogenic miRNAs or by enhancing tumour suppressive miRNAs (*167*). Oligonucleotides can be generated to be the antisense pair of an oncogenic miRNA preventing the interaction of the miRNA with its target. miRNA mimics function as replacements for the downregulated tumour suppressor miRNA. Various delivery systems are being developed for these miRNA based therapies using viral vectors, liposomes, nanoparticles, and nanocells (*168*).

1.4 Epigenetics

Epigenetic modifications lead to changes in gene expression without altering the DNA sequence itself. These can be caused by chemical modification on the DNA, DNA methylation, or to DNA associated proteins, histone modifications (Figure 1.6). Non-coding RNAs have also been suggested to be epigenetic regulators due to their role in regulating gene expression (*169*).

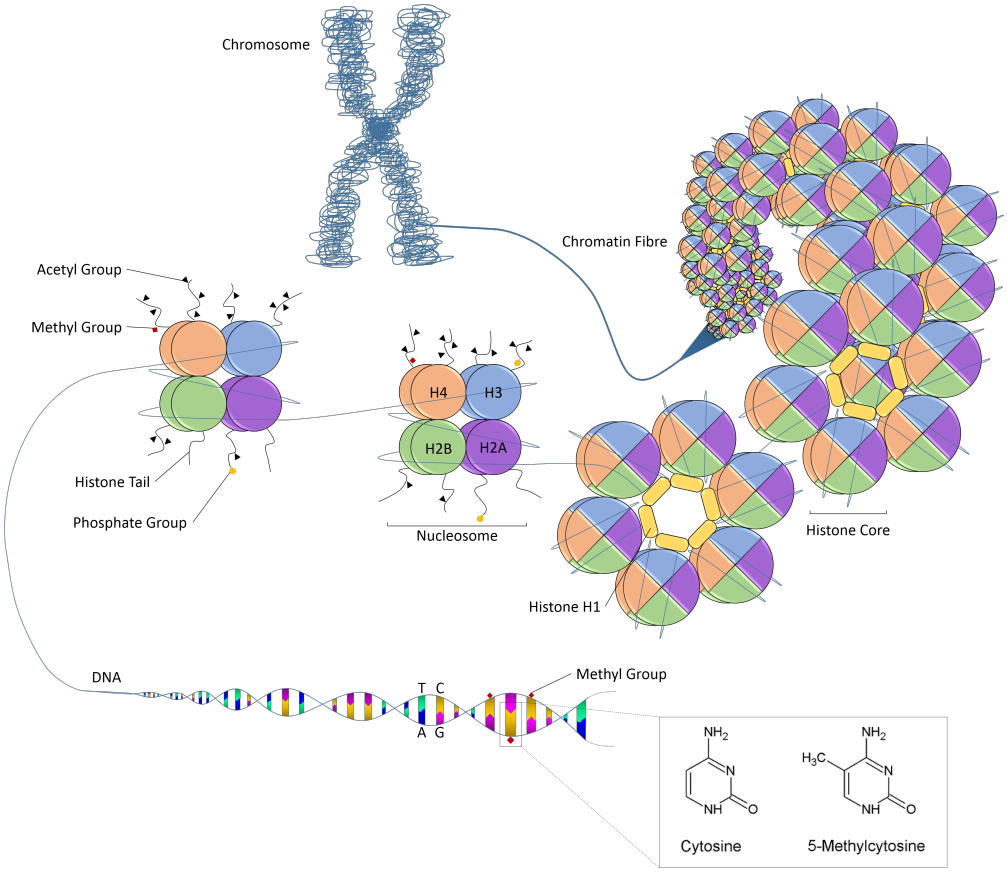

Figure 1.6: Schematic Overview of Different Epigenetic Modifications. Epigenetic alterations affect gene expression without changing the primary nucleotide structure. The DNA double helix is wrapped around the histone core forming a nucleosome. This is formed of the H3-H4 tetramer and two H2A-H2B dimers. Each of these histones has an N-terminal tail which can be post-translationally modified by, for instance, phosphorylation, methylation, and acetylation. The latter plays a key role in regulating the strength of the DNA-histone interaction and in activating gene transcription as acetylation of the histone tails which leads to a decrease in the overall positive charge of the protein and weakens its interaction with the negatively charged DNA molecule, affecting the tightness of DNA packing into chromosomes. Nucleosomes are held together by a histone H1 linker protein. These complexes come together to form chromatin, which coils to form chromatin fibres that are packed into chromosomes. The DNA itself can undergo epigenetic modification by the addition of methyl groups to cytosine residues. This will affect gene expression as the CH_3 will stick out into the major groove of the DNA, preventing transcription factors docking in the promoter region.

1.4.1 DNA Methylation

DNA methylation is one system of epigenetic regulation of gene expression. In eukaryotes, cytosine residues (C) in DNA can be methylated by DNA methyltransferases, this leads to the addition of a methyl group (CH_3) at position 5 of the cytosine ring (Figure 1.6) generating 5-methylcytosine (m^5C) (*170*, *171*). Methylation of cytosine occurs at cytosine-guanine (CG) dinucleotides found in palindromic sequences (*172*, *173*). However, in vertebrates, the CG dinucleotide is only found at one fifth of its randomly expected frequency. Yet in some regions upstream of genes, CG dinucleotides can be found at their expected rate of occurrence (*174*); these regions are called 5′-cytosine-phosphate-guanine-3′ (CpG) islands. Methylation of C residues in these regions has been found to repress expression of the downstream transcribed gene (*173*).

The methylation reaction is initiated by the nucleophilic attack of a Cys thiolate group to the C6 position of the aromatic ring of the pyrimidine. This leads to the activation of the C5 atom acting as a resonance-stabilised carbanion. This leads to the C5 nucleophilic attack on the methyl group of S-adenosylmethionine (SAM), acting as methyl donor in this reaction (*175*). This covalent intermediate is then decomposed to give 5-methylcytosine (m^5C) (Figure 1.6). For this reaction to occur the base is flipped out of the double helix structure allowing DNA methyltransferases (DNA MTase) to start the nucleophilic attack, which, due to the aromatic configuration of the base, is only possible from above or below the carbon ring. The methyl group added projects into the major groove of the DNA double helix allowing DNA binding proteins, which contain a conserved methyl-CpG binding domain (MBD), to interact with it, without disturbing the double helical structure of the DNA (*176*). These MBD containing proteins inhibit transcription of the promoter methylated genes they are bound to by recruiting protein complexes that alter the structure of the chromatin and prevent transcription of genes in the region (*177*). Thus DNA methylation in the promoter region will lead to silencing of the downstream transcribed gene, therefore the promoter region of housekeeping genes will generally be unmethylated (*178*).

As mentioned previously, methylated C residues in CG dinucleotides are usually found in palindromic sequences. During cell division and DNA synthesis, this allows the methylation pattern on the parental strand to guide methylation

on the daughter strand so that methylation is conserved. This is called maintenance methylation, there is therefore inheritance of methylation patterns in daughter cells allowing them to have the same differentiated phenotype as the parental cell (*179*). This type of methylation is mediated by DNA (cytosine-5)-methyltransferase 1 (DNMT1), indeed, this protein preferentially methylates hemimethylated substrate DNA (*180*). This maintenance methylation is essential for cell differentiation and survival as shown by the death at early embryonic stage of DNMT1 knock-out in mice (*181*).

Mature gametes, however, lose their DNA methylation after fertilisation due to epigenetic reprogramming (*182*). By the time the blastocyst is formed, almost all methylation marks are lost. Over time, they reappear throughout the embryo, until the gastrula stage where adult levels of methylation are achieved, these will be perpetuated in all future daughter cells (*183*, *184*). This *de novo* methylation is mainly mediated by DNA (cytosine-5)-methyltransferase 3A (DNMT3A) and DNA (cytosine-5)-methyltransferase 3B (DNMT3B) (*185*).

Nevertheless, some sections of DNA are resistant to this demethylation wave as well as to the *de novo* methylation that follows; these are imprinted genes. Genomic imprinting is the phenomenon by which mammals express certain genes only from the paternally or maternally supplied chromosome (*186*, *187*). This selective gene expression is achieved through differential DNA methylation of specific regions on both chromosomes (*188*). During gametogenesis, the genes will be methylated differently in the two parents and will be passed on as such to the next generation (*189*). This leads to differential expression of genes depending on which chromosome they are located on. Hence inappropriate imprinting of these regions will lead to disease. For instance Praeder-Willi syndrome (PWS) is caused by deletions in the paternally inherited chromosome 15, as this region is imprinted, the maternal chromosome will not express the same genes as the paternal one since genes usually expressed on the paternal chromosome are repressed (*190*, *191*). Angelman syndrome (AS) on the other hand is caused by a deletion in the same region but on the maternally inherited chromosome (*192*). These syndromes can also arise in individuals who inherit two paternal chromosomes for PWS and two maternal ones for AS (*193*).

One of the most prevalent mutations in cancer is deamination of the m^5C to a thymine (T) with the associated guanine (G) becoming an adenine (A) on the complementary strand (*194*). This leads to the loss of a methylation mark and

is usually involved in the transformation of a proto-oncogene to an oncogene or in the inactivation of a tumour suppressor gene. Similarly, altered methylation patterns are often found in cancers, for instance hypomethylation of an oncogene leading to its expression and hypermethylation of a gene encoding for a tumour suppressor causing its repression are common (*172*). Thus, correct methylation patterns are essential for proper development and alterations in these motifs can lead to disease.

1.4.2 Histone Modifications

Another form of epigenetic regulation involves histone modifications. Histones are proteins used to package DNA into its compact chromatin structure (*195*). Due to their important role in cells, these proteins are highly conserved over eukaryotes, one of these characteristics is a sequence of approximately 70 residues near the C-terminus of the sequence that folds into a central α-helix flanked by a loop and a shorter α-helix on both sides. This secondary structure forms the central histone fold found in Histone 2A (H2A), Histone 2B (H2B), Histone 3 (H3), and Histone 4 (H4) (*196*), and is the dimerisation motif used by these proteins to form a histone core around which approximately 200 bp of DNA is wrapped to form the nucleosomes (Figure 1.6). Each nucleosome is held together by a Histone 1 (H1) linker protein, these nucleosome filaments coil into 30 nm thick chromatin fibres (*197*), containing about six nucleosome cores per turn, which are packed into the condensed chromosomes that appear at metaphase (*198*). When DNA is replicated in cell division, the process is also accompanied by its packing into chromatin. During this process the parental histone cores are distributed randomly between the daughter duplexes resulting in the conservation of epigenetic marks associated with the histone cores.

Throughout interphase and the rest of the cell cycle, the chromatin is highly dispersed and the individual chromosomes can't be distinguished. There are two types of dispersed chromatin; euchromatin, which is less dense and transcriptionally expressed or with the potential to be activated, and heterochromatin which is more densely packed and transcriptionally inert (*199*). The latter can be separated into two distinct types: facultative and constitutive heterochromatin (*200*). Facultative heterochromatin varies in a tissue specific manner and is generally located in regions coding for genes that are expressed differentially

throughout development and differentiation. The condensation of facultative heterochromatin transcriptionally inactivates large chromosomal blocks making the DNA inaccessible to transcription mediating proteins (*201*). Facultative heterochromatin is found in the inactivation of stem cell maintenance genes which are permanently switched off in terminally differentiated cells. This is also found in X chromosome inactivation that occurs in female mammalian cells, and is associated with trimethylation of lysine 27 on H3 (H3K27me3) (*202*). Constitutive heterochromatin, on the other hand, is found in gene poor and highly repetitive regions such as telomeres and centromeres, which is permanently condensed and silenced through trimethylation of lysine 9 on H3 (H3K9me3) (*203*). Hence specific histone modifications are associated with the different chromatin states.

Therefore DNA methylation and histone modification regulate gene expression in a coordinated fashion. Unmethylated genes with an euchromatic histone pattern are ready to be expressed, methylated genes with an euchromatic histone pattern are poised to be silenced, and finally, methylated genes with a heterochromatic histone pattern are silenced.

The nucleosome core is a histone octamer (Figure 1.6) composed of two H2A-H2B dimers and an H3-H4 tetramer (*204*). There is no sequence specificity for the histone-DNA binding as the histones bind to the inner face of DNA principally through the sugar-phosphate backbone with hydrogen bonds, hydrophobic interactions, salt bridges, and helix dipoles (*205*). This ionic interaction occurs as histone proteins contain a high proportion of positively charged residues such as lysine (K) and arginine (R) which provide a positive surface charge to the histone complex, allowing for interaction with the negatively charged phosphate groups of DNA. The strength of this interaction determines how tightly packed the DNA will be (*206*).

A flexible N-terminal tail protrudes from the core of each histone, this is a very positively charged polypeptide which makes up around 25 % of the histone mass (*207*). This tail extends out of the nucleosome core and past the coiled DNA, it can interact with linker DNA and the modulation of this interaction by post-translational modification is involved in the regulation of chromatin unfolding and the availability of DNA for transcription, replication, recombination, and repair (*208*). Post-translational modifications include acetylation, methylation, phosphorylation, ubiquitination (Figure 1.6), on specific K, R, and serine (S) side chains (*201*). Most of these modifications are reversible and, apart from

methylation, reduce the overall positive charge of the histone, altering the DNA-histone electrostatic interaction. Indeed, transcriptionally active chromatin is associated with the acetylation of H3 K9, K14, and H4 K5, as well as the methylation of H3 K4 and H4 R3. Inactive chromatin is associated with acetylation of H4 K12, and depending on the type of heterochromatin, methylation of H3 K9 or K27. Acetylation is of particular interest to us as it affects packaging of DNA around the histones and therefore alters gene expression (*209*, *210*).

There are five families of Histone acetyl transferases (HAT) that function as transcriptional coactivators or silencers. The HAT proteins function in large multi-subunit complexes of which the composition will determine the specificities of the histone target sites (*211*). They use Acetyl coenzyme A (Acetyl-CoA) as a cofactor for the acetylation of K residues in core histone tails (*212*). The transfer of a COCH3 group to a positively charged lysine, neutralises its charge thus weakening the DNA-histone interaction. This prevents tight packing of DNA into chromatin by H1 resulting in a more open chromatin configuration which generally leads to transcription of genes in that region (*213*). Acetylation occurs predominantly on H3 and H4 histone tails and is largely targeted to promoter regions (promoter localised acetylation). However, low levels of global acetylation are found throughout transcribed genes (*214*).

Histone deacetylase (HDAC) enzymes are mainly transcriptional repressors as they remove acetyl groups from lysine amino acids leading to DNA condensation and gene silencing (*215*). There are three classes of HDACs, Class I HDACs, HDAC 1 to 3, and 8, generally form the catalytic core of multi-subunit complexes whilst Class II, HDAC 4 to 7, 9, and 10, tend not to be part of complexes (*216*). Both families function as transcriptional corepressors (*217*). Class III HDACs are the sirtuins; silent information regulators type (SIRT) SIRT 1 to 7. These contain a nicotinamide adenine dinucleotide (NAD^+) cofactor, therefore, after hydrolysing the amide bond linking the acetyl group to the K, they transfer it to NAD^+ producing *O*-acetyl-ADP-ribose (*218*, *219*).

Histone acetylation is tightly regulated in cells and disruption of acetylation homeostasis has been linked to disease and cancer (*220*, *221*). Overexpression of HDAC enzymes has been found to be associated with poor prognosis in cancer (*215*) and aberrant HDAC recruitment can lead to tumour development (*222*, *223*) by silencing tumour suppressor genes (*224*, *225*), and cancer progression and metastasis (*226*). Loss of histone acetylation has even been suggested to be

a common hallmark of cancer (*227*) suggesting HDAC inhibitors could have a therapeutic use in certain cancer settings (*228*).

1.4.3 Epigenetic Regulation of miRNAs

As previously described, miRNA expression is under tight spatial and temporal regulation. miRNAs can be characterised as intragenic or intergenic depending on whether or not they are located within a gene transcription region (*229*). The promoter region of intergenic miRNAs and those intragenic but going in the inverse direction of the coded gene is still unclear.

Intragenic miRNAs are generally controlled with the same promoter as the gene but they can also have a different promoter located in the intron in which the miRNA is located. Their expression can be regulated by histone modification and DNA methylation levels (*114*, *230*). This creates a feedback loop as certain miRNAs can regulate epigenetic modulator genes such as those involved in methylation (*231*). These in turn affect miRNA expression through modification of the epigenetic pattern by DNA methylation or histone modifications (*166*). CpG methylation of DNA leads to silencing of the miRNA, however histone modifications can induce or suppress miRNA expression (*232*).

1.5 Summary

As HER2+ breast cancer is one of the more aggressive breast cancer subtypes and a high number of patients develop resistance and have refractory disease using the current HER2-targeting therapies, this highlights the necessity to identify new therapeutic targets to overcome resistance. miRNAs are often deregulated in tumours and their expression has been found to vary with therapeutic resistance, therefore these small non-coding RNAs appear to be key components in resistance. miRNAs however, are not suitable therapeutic targets therefore investigating their downstream effectors could identify new therapeutic options.

1.6 Aims

This PhD project aims to identify miRNAs involved in lapatinib resistance and investigate their epigenetic regulation. In addition to validating putative targets of the miRNAs and assessing their role in clinical breast cancers and their potential as therapeutic targets.

1.6.1 Identification of miRNAs Involved in Resistance to HER2-Targeted Therapy

miRNAs are likely to be deregulated in cancer and their expression patterns to be altered in resistance. Therefore we will study the miRNA expression profile of lapatinib resistant breast cancer cells by miRNA array in order to identify and validate miRNAs common to different cell lines by RT-qPCR. This will help to understand the miRNA driven mechanism of resistance to lapatinib.

1.6.2 Regulation of the miRNAs Involved in Resistance

Once miRNAs altered in lapatinib resistance have been identified, we will investigate the epigenetic mechanism controlling their upregulation in resistance. Firstly by miRNA array of untreated cancer cells and demethylated ones. Then we will investigate the response of our target miRNAs to demethylation and inhibition of deacetylation. This will be followed by methylation resequencing experiments in order to establish the methylome of the selected region.

1.6.3 Identification of Downstream Effectors of the miRNAs and their Potential as Therapeutic Targets

As miRNAs are poor therapeutic targets we aim to identify miRNA gene targets by gene expression array and study their effect on resistance through knock-down assays. As well as assessing the role of these putative targets in clinical breast cancers using data from patients on neoadjuvant HER2-targeting based treatments from the NeoALTTO trial.

2 Materials and Methods

2.1 Cell Culture Assays

2.1.1 Cell Culture

The cell lines are cultured in the appropriate medium, either in Roswell Park Memorial Institute (RPMI)-1640 medium (Sigma-Aldrich, St Louis, MO, USA), L-15 (Leibovitz) medium (Sigma-Aldrich), or McCoy's 5A Modified medium (Sigma-Aldrich). The medium is supplemented with 2 mM L-glutamine, 1 % penicillin-streptomycin (Sigma-Aldrich), and fœtal bovine serum (FBS) (Gibco, Carlsbad, CA, USA) as detailed in Table 2.1. All the cell lines used are derived from HER2+ breast cancers and grow in an adherent monolayer. The cells are cultured at 37 °C with 5 % CO_2 and 95 % air in a humidified incubator. Cells with acquired resistance to lapatinib (Selleck Chemicals, Munich, Germany) are maintained in presence of 2 µM of the drug, twice the resistance threshold.

The cells are passaged by trypsinisation using 1x trypsin-2,2′,2″,2‴-(etane-1,2-diyldinitrilo)tetraacetic acid (EDTA) (Sigma-Aldrich). Once the cells have detached from the plastic, FBS enriched medium is added to a minimum of

Cell Line	**Medium**	**FBS** (%)	**Lapatinib** (µM)	**Trastuzumab** ($mg \cdot L^{-1}$)
BT-474	RPMI 1640	10	-	-
BT-474/L	RPMI 1640	10	2.0	-
BT-474/T	RPMI 1640	10	-	40.0
HCC1954	RPMI 1640	10	-	-
HCC1954/L	RPMI 1640	10	2.0	-
SKBR-3	McCoy's 5A	10	-	-
SKBR-3/L	McCoy's 5A	10	2.0	-
JIMT-1	RPMI 1640	10	-	-
MDA-MB-361	L-15 (Leibovitz)	20	-	-

Table 2.1: Cell Culture Conditions.

three times the volume of trypsin. The suspension is then centrifuged in the Eppendorf 5415D centrifuge (Eppendorf, Hamburg, Germany) at 12000 RCF for five minutes, the supernatant is removed and the cell pellet is re-suspended in the appropriate culture medium. Where necessary cells are counted in presence of trypan blue (Sigma-Aldrich) using the TC20 Automated Cell Counter (Bio-Rad Laboratories, Hercules, CA, USA).

2.1.2 Generation of Resistant Lines

The lapatinib resistant BT-474/L cells were obtained from Liu *et al.* (*1*) as BT-474 J4 clone. The trastuzumab resistant BT-474/T were obtained from Anthony Kong's laboratory (Institute of Cancer and Genomic Sciences, University of Birmingham).

SKBR-3 and HCC1954 cells were cultured in increasing concentrations of lapatinib, starting approximately from the IC_{50} value, respectively 77 nM and 165 nM, as determined by dose-response studies. Through continuous exposure to the drug, the lapatinib sensitive cells die and the live cells are cultured until they outgrow the lapatinib dose. The dose is increased and the process is repeated until the cells are able to grow in 2 µM of lapatinib, a concentration equal to twice the resistance threshold. The resistant cells and their isogenic sensitive cell line are listed in Table 2.2.

Parental Line	**Resistant Line**	
	Lapatinib	**Trastuzumab**
BT-474	BT-474/L	BT-474/T
HCC1954	HCC1954/L	
SKBR-3	SKBR-3/L	

Table 2.2: Parental Cell Line and Derived Acquired Resistant Line.

2.1.3 Cytotoxicity Assay

Thiazolyl blue tetrazolium bromide or MTT (Alfa Aesar, Ward Hill, MA, USA) powder is dissolved in FBS supplemented medium to a stock concentration of 2 $g{\cdot}L^{-1}$ and added to each well in a 1:3 dilution, for a final concentration of 0.67 $g{\cdot}L^{-1}$. After 1 hour 30 minutes to 3 hours incubation at 37 °C the medium

is removed, the cell culture plate can be stored at -20 °C or used immediately.

The MTT crystals are dissolved in dimethyl sulphoxide (DMSO) (Thermo Fisher Scientific, Waltham, MA, USA) and absorbency is acquired on the VICTOR3 Multilabel Counter (PerkinElmer, Waltham, MA, USA) at 560 nm for 0.1 seconds and corrected for background at 630 nm.

2.1.4 Baseline 50 % Inhibitory Concentration Assay (IC_{50})

The cells are plated in 96 well plates as detailled in Table 2.3, and are left to adhere for 24 hours after which the medium is replaced with fresh medium containing a serial dilution of the drug used for the IC_{50}, as detailed in Table 2.4.

Cell Line	**Density** ($cells \cdot mL^{-1}$)
BT-474	$6.0 \cdot 10^4$
BT-474/L	$6.0 \cdot 10^4$
HCC1954	$6.0 \cdot 10^4$
HCC1954/L	$4.0 \cdot 10^4$
SKBR-3	$4.8 \cdot 10^4$
SKBR-3/L	$4.0 \cdot 10^4$
JIMT-1	$6.0 \cdot 10^4$
MDA-MB-361	$8.0 \cdot 10^4$

Table 2.3: Baseline IC_{50} Plating Densities used for the Different Cell Lines.

Drug	Units	**Doses**
Lapatinib Gefitinib Dacomitinib	nM	0.1, 1.0, 10.0, 50.0, 100.0, 500.0, 1000.0, 5000.0, 10000.0
Trastuzumab	$mg \cdot L^{-1}$	0.1, 10.0, 25.0, 50.0, 100.0
Neratinib	nM	0.01, 0.1, 1.0, 10.0, 100.0, 500.0, 1000.0, 5000.0, 10000.0

Table 2.4: Drug Range used for all the IC_{50} Experiments.

2.1.5 Population Doubling Assay

$5.0{\cdot}10^5$ cells are plated in 5 mL in a T25 flask. Every three days, the cells are detached with 1 mL trypsin and diluted in 3 mL of medium and counted with the TC20 Automated Cell Counter in the presence of trypan blue. $5.0{\cdot}10^5$ cells are then plated again in 5 mL in a T25 flask. The process is repeated until day 15.

2.1.6 Immunofluorescence Assay

Cells are plated onto coverslips (Warner Instruments, Hamden, CT, USA) in 6 well plates in FBS free media. After 1 hour 10 % FBS is added to the culture medium. Resistant cells are grown without the addition of lapatinib. When cells are 70 % confluent the coverslips are fixed in methanol for 20 minutes at -20 °C. Cells are permeabilised with 0.2 % Triton-X 100 in PBS and blocked for 30 minutes in a solution of 5 % bovine serum albumin (BSA), 0.1 % Triton-X 100 in PBS. F-actin is stained with Alexa Fluor 568 Phalloidin (LifeTechnologies) at a 1 in 250 dilution in blocking buffer for 1 hour. DNA is then stained with Hoechst (Invitrogen) for 5 minutes at a 1 in 5000 dilution in PBS. Coverslips are mounted using ProLong Gold antifade (Invitrogen).

2.1.7 siRNA Reverse Transfection

The small interfering RNAs (siRNAs) (Qiagen, Hilden, Germany) used are listed below (Table 2.5) and will be referred to as siRNA 1 and siRNA 2 for each gene throughout this document . The siRNA-lipid solution is composed of 50 nM siRNA or negative control (-ve) (AllStars Negative Control, Qiagen) with 1 % Lipofectamine RNAiMAX transfection reagent (Invitrogen by Life-Technologies) in FBS free medium. The siRNA-lipid solution is incubated at room temperature for 5 minutes to allow complexes to form. The mixture is added to each well at 20 % of the final volume of the well, in a 96 well plate, this is equal to 20 µL. Therefore each well has a final concentration of 10 nM siRNA with 0.2 % lipofectamine.

Cells are seeded on top at a density of $4.0{\cdot}10^4$ cells$\cdot$mL^{-1}, in a 96 well plate, 80 µL of cell suspension are added per well. The medium is changed after 24

Gene	siRNA 1		siRNA 2	
	Assay Name	Sequence	Assay Name	Sequence
BASP1	Hs_BASP1_5	TACAGGATGTTGTCCCATCAA	Hs_BASP1_6	CACATGGATCTCAATGCCAAT
KLF9	Hs_KLF9_4	CAAGAGTTATGTAGAAGGAAA	Hs_KLF9_6	AACCAGCATTCTAATTAGATT
NEDD4L	Hs_NEDD4L_3	TAGGCCGAACTTACTATGTCA	Hs_NEDD4L_9	CTCATCCGAGAAATTACTTAA
PKIA	Hs_PKIA_9	ATGATTATCATTAGAAGCTAA	Hs_PKIA_10	TCACTTGATCATATGACGAAA
PREX1	Hs_PREX1_8	AAGGGCCTTCTTCCTCTTCGA	Hs_PREX1_9	CACGGCGTGGTGTATGAGTAT
SH3BGRL	Hs_SH3BGRL_6	TTCACACTACCTTATTACCAA	Hs_SH3BGRL_9	CTCTGGCTCTACAGCGATTAA
SOCS2	Hs_SOCS2_2	CCAACTAATCTTCGAATCGAA	Hs_SOCS2_8	TTGTCTAACCATGGACATAAA

Table 2.5: siRNA Sequences used for Functional Validation of Putative miRNA Gene Targets. In further experiments the siRNAs have been renamed siRNA 1 and siRNA 2 for each gene as detailed above.

hours and the cells can be used for IC_{50} assays using the previously described protocol, or the transfected cells are cultured until the appropriate time point when they are washed in phosphate buffered saline (PBS) (Sigma-Aldrich) and collected for RNA and protein studies.

2.1.8 miRNA Mimic or Inhibitor Reverse Transfection

The miRNA mimics (mirVana miRNA mimic, Thermo Fisher Scientific) and miRNA inhibitors (mirVana miRNA inhibitor, Thermo Fisher Scientific), detailed in Table 2.6, are used in the miRNA-lipid transfection solution. This is composed of a given mimic, inhibitor, or scramble negative control (scramble, scb) with 0.75 % Lipofectamine RNAiMAX transfection reagent in FBS free medium. Mimic and scb or inhibitor and scb are added at the same concentration in each experiment, however, the concentration varies across different experiments. The mimic-lipid solution is incubated at room temperature for 5 minutes to allow complexes to form. The mixture is added to each well at 20 % of the final volume of the well, in a 96 well plate, this is equal to 20 µL.

miRNA	Mimic Assay	Inhibitor Assay
Negative control #1	4464058	4464076
hsa-miR-127-3p	MC10400	MH10400
hsa-miR-409-3p	MC12446	MH12446
hsa-miR-495-3p	MC11526	MH11526

Table 2.6: mirVana miRNA Mimic and Inhibitor Assays Used for Transfections.

Cells are seeded on top, in a 96 well plate, 80 µL of cell suspension are added per well. The medium is changed after 24 hours and the cells can be drugged

for IC_{50} assays using the previously described protocol, or the transfected cells are cultured until the appropriate time point when they are washed in PBS and collected for RNA and protein studies.

2.2 RNA Studies

2.2.1 RNA Samples for mRNA Study

Cells to be used for mRNA extractions are washed in PBS before being stored at -20 °C until total RNA is extracted using a phenol based extraction protocol. The cells are lysed in TRI Reagent (Sigma-Aldrich) and 1-bromo-3-chloropropane (Sigma-Aldrich) is added to each sample at a 1:10 ratio. This solution is vortexed for 10 seconds and centrifuged at 12000 RPM for 10 minutes at 4 °C. The upper aqueous phase is transferred to a new tube whilst the organic phase is discarded. One volume of propan-2-ol is added to the aqueous phase to precipitate the RNA. This solution is vortexed for 10 seconds and incubated at room temperature for 10 minutes before being centrifuged at 12000 RPM for 5 minutes. The supernatant is removed without dislodging the RNA pellet and impurities are cleared with a 75 % ethanol wash centrifuged at 7500 RPM for 5 minutes. The supernatant is removed and the pellet is air dried prior to being re-suspended in RNase free H_2O. The RNA is then quantified using either the NanoDrop 1000 or NanoDrop 2000 spectrophotometer (Thermo Fisher Scientific).

The High-Capacity cDNA Reverse Transcription Kit (Applied Biosystems by Thermo Fisher Scientific) containing random primers is used according to the manufacturer's instructions. 100 ng of RNA is added to each reaction as detailed in Table 2.7, and is incubated in the Veriti Thermal Cycler (Applied Biosystems) with the steps detailed in Table 2.8.

2.2.2 Sybr Green Real Time Quantitative Polymerase Chain Reaction (RT-qPCR) and Quantification

Primers for each of the target genes are designed using Primer3web (*233*, *234*) to be compatible with Sybr green technologies and are detailed in Table

Reagent	Volume (µL)
10x RT Buffer	2.0
25x dNTP Mix (100 mM)	0.8
10x RT Random Primers	2.0
MultiScribe RT	1.0
RNase Free H_2O	4.2
RNA ($10\ ng \cdot \mu L^{-1}$)	10.0
Total Reaction Volume	20.0

Table 2.7: cDNA Reverse Transcription Reaction for mRNA using the High-Capacity cDNA Reverse Transcription Kit.

Step	Temperature (°C)	Time (minutes)
1	25	10
2	37	120
3	85	5
4	4	∞

Table 2.8: cDNA Reverse Transcription Thermal Cycler Conditions for mRNA using the High-Capacity cDNA Reverse Transcription Kit.

2.9. Previously generated cDNA diluted to 1 $ng \cdot \mu L^{-1}$ is used as template in the RT-qPCR reactions. The SYBR green PCR master mix (Applied Biosystems) is used in 10 µL reactions as detailed in Table 2.10 and optimal primer concentrations are determined according to the Applied Biosystems guidelines; selected concentrations are listed in Table 2.11. Default SYBR green setting are used on the ABi 7500 thermal cycler or on the QuantStudio 5 (Applied Biosystems) (Table 2.12) and the PCR cycles are followed by melt curve acquisition. Primer efficiency was determined from standard curves generated for each primer pair. The efficiency (E) is calculated as follows:

$$E = 10^{-\frac{1}{slope}} - 1$$

giving a scale from 0, no amplification of product per cycle, to 1, perfect doubling each cycle. The efficiency has been calculated as a percentage as for each primer used as detailed in Table 2.9 as a percentage.

Gene	Forward Sequence	Reverse Sequence	Efficiency
RPLP0	GCGACCTGGAAGTCCAACTA	GGATCTGCTGCATCTGCTTG	100 %
AHNAK	CGAGCCGGAGTTACAAGAGC	CATCATCCCCGCTCAGAACC	82 %
BASP1	GCCAGCCGAGAACTCCAA	TCCCTCCCTTGATGGGACAA	95 %
EMP1	TATAACCTCGGGAGGCAGGT	GGAAACCAACCAGACATTGGC	96 %
FADS1	GTGAGTTGCCCAAGACCCAC	TGTTTCCCAAGCTCCACAGAG	106 %
KLF9	AGAGTGCATACAGGTGAACGG	TGATCATGCTGGGGTGGAAC	109 %
NEDD4L	TCATCAACTGTCACGGGTGG	GTGTAGTTGTCCGTGGCAGA	90 %
NRCAM	GTCAATGGGAAAGGGGAGGG	GCCATCGCTTCATCCACAGT	103 %
PKIA	CGGGGAAGTCCCTGCTATGT	AAGCAATCAGAGAAGGGGGC	100 %
PREX1	CTCAACGAGATCTTGGGCAC	CTGGAACTGTAAGAGGAGGC	92 %
SH3BGRL	ATCTCGCGGTGCTATTCGAG	GAAGGCATCATAGTCCCCGC	96 %
SOCS2	TCATCAACTGTCACGGGTGG	GTGTAGTTGTCCGTGGCAGA	91 %
STC2	AATACAGCGGAGATCCAGCAC	CGAGGTGCAGAAGCTCAAGA	92 %

Table 2.9: SYBR Green Primer Sequences used for Validation of the Gene Expression Array.

Reagent	Volume (µL)
2x SYBR Green PCR Master Mix	5.00
Forward Primer (10 mM)	0.05 to 0.50
Reverse Primer	0.10 to 0.50
cDNA (1 ng·µL^{-1})	1.00 to 2.00
RNase Free H_2O	2.00 to 3.85
Total Reaction Volume	10.00

Table 2.10: Sybr Green RT-qPCR Reaction.

2.2.3 RNA Samples for miRNA Study

Cells to be used for total RNA extractions are washed in PBS before being stored at -20 °C until total RNA is extracted using either the mirVana miRNA Isolation kit (Ambion by Thermo Fisher Scientific) as per the manufacturer's instructions, or a column-free adaptation of the protocol detailed below.

The column free miRNA extraction uses reagents from the mirVana miRNA Isolation kit. The cells are disrupted in 600 µL of Lysis/Binding Buffer and miRNA Homogenate Additive is added to each sample at a 1:10 ratio. This solution is vortexed for 10 seconds and incubated on ice for 10 minutes. One volume of Acid-Phenol:Chloroform is added to the tubes and the samples are vortexed for 30 seconds before being centrifuged at 12000 RPM for 5 minutes. The upper aqueous phase is transferred to a new tube whilst the organic phase

Gene	Primer Concentration (nM)	
	Forward	**Reverse**
RPLP0	0.50	0.50
AHNAK	0.05	0.10
BASP1	0.10	0.10
EMP1	0.05	0.10
FADS1	0.10	0.10
KLF9	0.30	0.30
NEDD4L	0.10	0.10
NRCAM	0.05	0.10
PKIA	0.10	0.10
PREX1	0.50	0.50
SH3BGRL	0.10	0.10
SOCS2	0.10	0.10
STC2	0.10	0.10

Table 2.11: Final SYBR Green Primer Concentrations used per Reaction for RT-qPCR Gene Expression Analysis.

Step		Temperature (°C)	Time
Enzyme Activation	Hold	95	10 minutes
40 cycles	Denature	95	15 seconds
	Anneal/Extend	60	60 seconds

Table 2.12: Sybr Green RT-qPCR Cycling Conditions.

is discarded. One volume of propan-2-ol is added to the aqueous phase to precipitate the RNA. This solution is vortexed for 10 seconds and incubated at room temperature for 10 minutes before being centrifuged at 12000 RPM for 8 minutes. The supernatant is removed without dislodging the RNA pellet and impurities are cleared with a 75 % ethanol wash centrifuged at 7500 RPM for 5 minutes. The supernatant is removed and the pellet is air dried prior to being re-suspended in RNase free H_2O. The RNA is then quantified using either the NanoDrop 1000 or NanoDrop 2000 spectrophotometer.

The TaqMan miRNA Reverse Transcription Kit (Applied Biosystems) is used according to the manufacturer's instructions, with predesigned TaqMan primers (Applied Biosystems) for the selected mature miRNA and small nucleolar RNA, C/D box 44 (SNORD44 or RNU44), used as the housekeeping control, detailed

in Table 2.15. 10 ng of RNA is added to each reaction as detailed in Table 2.13, and is incubated in the Veriti Thermal Cycler with the steps detailed in Table 2.14.

Reagent	**Volume (µL)**
dNTPs with dTTP (100 mM)	0.15
MultiScribe RT (50 U·µL^{-1})	1.00
10x RT Buffer	1.50
RNase Inhibitor (20 U·µL^{-1})	0.19
RNase Free H_2O	4.16
5x RT Primer (miRNA specific)	3.00
RNA (2 ng·µL^{-1})	5.00
Total Reaction Volume	15.00

Table 2.13: cDNA Reverse Transcription Reaction for miRNA using the TaqMan miRNA Reverse Transcription Kit.

Step	**Temperature (°C)**	**Time (minutes)**
1	16	30
2	42	30
3	85	5
4	4	∞

Table 2.14: cDNA Reverse Transcription Thermal Cycler Conditions for miRNA using the TaqMan miRNA Reverse Transcription Kit.

2.2.4 TaqMan Real Time Quantitative Polymerase Chain Reaction (RT-qPCR) and Quantification

cDNA previously generated using miRNA specific primers is used as template in the RT-qPCR reactions. The TaqMan Universal Master Mix II (Applied Biosystems) is used in 20 µL reactions as detailed in Table 2.16. Default TaqMan setting are used on the ABi 7500 thermal cycler or on the QuantStudio 5 (Applied Biosystems).

miRNA	Assay Name	Assay ID
RNU44	NR_002750	001094
miR127	hsa-miR-127	000452
miR409	hsa-miR-409-3p	002332
miR411	hsa-miR-411	001610
miR433	hsa-miR-433	001028
miR495	mmu-miR-495	001663
miR539	hsa-miR-539	001286

Table 2.15: TaqMan RNU44 MicroRNA Control Assay and MicroRNA Assays used for miRNA RT-qPCR Analysis of Expression Levels.

Reagent	Volume (µL)
2x TaqMan Master Mix	10.0
20x TaqMan miRNA Assay	1.0
cDNA ($2\ ng \cdot \mu L^{-1}$)	2.0
RNase Free H_2O	7.0
Total Reaction Volume	20.0

Table 2.16: TaqMan RT-qPCR Reaction.

Step		Temperature (°C)	Time
Enzyme Activation	Hold	95	10 minutes
40 cycles	Denature	95	15 seconds
	Anneal/Extend	60	60 seconds

Table 2.17: TaqMan RT-qPCR Cycling Conditions.

2.2.5 RT-qPCR Analysis using the ΔΔCt Method

For every experiment, a threshold of 0.1 is set for determining the threshold cycle (Ct) values generated from RT-qPCR runs and technical duplicates are averaged. A comparative Ct analysis is performed using the ΔΔCt method. Ct values for the reference gene (Ct_{Ref}), either RPLP0 for mRNA experiments, or RNU44 for miRNA expression, are subtracted from those of the gene of interest (Ct_{GoI}) giving the ΔCt value (2.1). The ΔCt values for each biological replicate are then averaged. Next, the ΔCt average value of the reference sample ($\Delta Ct_{Control}$) is subtracted to each ΔCt average ($\Delta Ct_{Treatment}$), giving the ΔΔCt average (2.2). This value is then utilised to calculate the fold change (F_{ch}) giving the expression of the gene of interest relative to the control for each sample (2.3).

$$Ct_{GoI} - Ct_{Ref} = \Delta Ct \tag{2.1}$$

$$\Delta Ct_{Treatment} - \Delta Ct_{Control} = \Delta\Delta Ct \tag{2.2}$$

$$F_{ch} = 2^{-\Delta\Delta Ct} \tag{2.3}$$

2.2.6 miRNA Array and Analysis

cDNA, prepared using the Megaplex Primer Pools (Applied Biosystems) as per manufacturer's instructions, is loaded onto the TaqMan low density miRNA Human A and B Array cards as per the manufacturers instructions and run on the ViiA 7 Real-Time PCR System (Applied Biosystems). The data is analysed using the ΔΔCt method and fold change analysis with DataAssist Software (*235*). A 10-fold cut-off is selected to obtain values in top quartile of upregulation for the BT-474 vs BT-474/L array. This cut-off was conserved for analysis of the other miRNA array.

2.2.7 Gene Expression Array and Analysis

Two independent array experiments (one with technical duplicates and another with triplicate), were completed with the Illumina Human HT12 v4.0 array on the lapatinib sensitive BT-474 and corresponding resistant cell line (BT-474/L). The arrays were combined in order to make the data more robust,

and were analysed to compare genes differentially expressed between the sensitive and resistant cells. To cross-reference these results, they were combined with the DMSO control conditions from the array used in the original publication of the BT-474/L cell line (*1*) using the Affymetrix Human Genome U133 Plus 2.0 Array platform (GEO accession number: GSE16179). Using this extra data set increase the number of replicates analysed, which should contribute to making the analysis more robust.

The bioinformatic analysis was performed by members of the Chelela group, Ai Nagano and Natasha Saghal. Normalisation and quality control of the expression data are performed on the upgraded version of o-miner transcriptomics analysis platform (*236*), adapting LUMI (*237–239*) in the R statistical environment via Bioconductor packages (*240*). Expression data is analysed using LIMMA (*241*) to fit a linear model to the expression data for each gene in order to detect differentially expressed genes between two groups. Differentially expressed genes are gauged using LIMMA empirical Bayes statistics module. The adjusted p-values (false discovery rate) are estimated by Benjamini and Hochberg procedure (*242*). The differentially expressed genes are selected when the adjusted p-value is less than 0.05 and the absolute value of log fold change is more than 1. Unsupervised hierarchical clustering (method: Ward, distance: Pearson correlation) is performed on the heat map to assess the reproducibility of the groupings. Once data from the different platforms have been analysed independently, the results are combined, comparing the differently expressed genes in both arrays.

2.3 Epigenetic Analysis

2.3.1 DNA Methylation and Histone Modification Reversal

The cells are grown until they are 60 % confluent. They are then treated with 5 µM 5-aza-2′-deoxycytidine (Aza) (Sigma-Aldrich) for 5 days. For the final 16 hours before collection of the cells, some samples are treated with 0.3 nM Trichostatin A (TSA) (Sigma-Aldrich). On day 5 the cells are trypsinised and washed with PBS before being pelleted and stored at -20 °C for use in further experiments.

Aza is a chemical analogue of cytidine (C) (Figure 2.1a) that can be integrated into the DNA of proliferating cells instead of C (*243*). The Azacytosine-Guanine dinucleotide is recognised by the methyltransferase and the nucleophilic attack for the methylation process occurs. This causes the formation of a covalent bond between the Azacytosine base and the enzyme (*244*). However, due to the presence of the nitrogen group in position 5 in the cytosine base, the reaction cannot proceed and the methylation mark is lost during replication causing hypomethylation of DNA (*245*). TSA (Figure 2.1b) is an anti-fungal antibiotic that inhibits class I and II mammalian HDACs (*246*, *247*). It prevents the removal of acetyl groups from core histone tails leading to the accumulation of hyperacetylated histones which causes the DNA to become de-condensed.

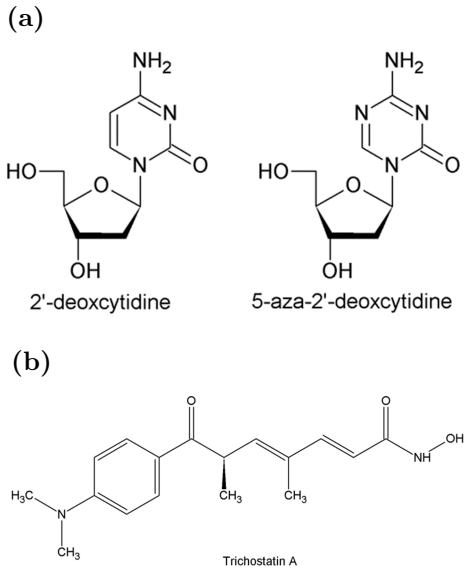

Figure 2.1: Chemical Structure of Aza and TSA. (a) Chemical structure of 2′-deoxycytidine and 5-aza-2′-deoxycytidine. Aza is a chemical analogue of cytidine that can get integrated into the DNA of proliferating cells. However the aza analogue contains a nitrogen in position 5 in the cytosine base leading to the methylation mark being lost during replication, leading to hypomethylation of DNA. (b) inhibits class I and II mammalian HDACs leading to the accumulation of hyperacetylated histones and to DNA becoming de-condensed

2.3.2 Bisulphite Conversion and Next Generation Sequencing

Multiplex bisulphite PCR assays was completed in Darren Korbie's laboratory as described by Korbie *et al.* (*248*). The regions selected for analysis are detailed

in Table 2.18. Aligned sequences were computationally analysed by the BCI Bioinformatics Core Team.

Region	Start Position	Stop Position	Length (bp)
IG-DMR	101276905	101277735	830
MEG3-DMR	101293428	101294433	1005
CpG 1	101348386	101348698	312
CpG 2	101349373	101349860	487

Table 2.18: CpG Regions Selected for Methylation Analysis. The regions are located on chromosome 14 using coordinates from the GRCh37/hg19 genome assembly.

2.4 Protein Assays

2.4.1 Protein Quantification

Samples are lysed from a 24 well plate in 100 µL radioimmunoprecipitation assay (RIPA) buffer and cell pellets collected after trypsinisation are washed in PBS and lysed in up to 1.5 mL of RIPA buffer. The samples are centrifuged for 10 minutes at 12500 RPM at 4 °C and boiled for 5 minutes at 98 °C in laemmli buffer.

2.4.2 Western Blotting

10 µg of protein are loaded onto either a 4-20 % gradient minigel (Bio-Rad, Hercules, CA, USA), a 10 %, or 12 % acrylamide gel depending on the size of the protein of interest. Lysates are separated by gel electrophoresis in tris-glycine SDS running buffer and the samples are transferred to a polyvinylidene difluoride (PVDF) membrane (GE Healthcare, Little Chalfont, Buckinghamshire, UK) in tris-glycine buffer. Running and transfer conditions are described in Table 2.19. The membrane is blocked for 45 minutes in the same buffer used for the primary antibody. Primary antibodies and their details are listed in Table 2.20.

The primary antibody is incubated at 4 °C overnight, washed prior to secondary anti-rabbit antibody (Cell Signalling Technology, 7074) incubation for 45 minutes at room temperature. After a final wash, the membrane is incub-

Running		Transfer	
Voltage (V)	Time (minutes)	Amperage (mA)	Time (minutes)
110	10	300	60
140	60		

Table 2.19: Running and Transfer Conditions Used for Western Blotting.

Protein	Host Species	Dilution	Buffer	Antibody
GAPDH	Rabbit	1:5000	5 % milk in TBST	CST2118
NEDD4L	Rabbit	1:1000	5 % milk in PBST	CST4013
PREX1	Rabbit	1:1000	5 % milk in PBST	ab102739
SH3BGRL	Rabbit	1:1000	5 % milk in PBST	ab80865

Table 2.20: Antibody Dilutions and Species used for Secondary Antibody. CST: Cell Signaling Technology, ab: abcam.

ated for 5 minutes with enhanced chemiluminescence (ECL) buffer. Detection is carried out by using the G:BOX Chemi XT system (Syngene, Cambridge, UK).

2.5 Statistical Analysis

Analysis was performed using GraphPad Prism version 5.03 for Windows (GraphPad Software, La Jolla, CA, USA, www.graphpad.com) normalised non-linear regression protocol for dose-response curves from IC50 data. Statistical significance was determined using a one-way ANOVA with a Dunnett's post-test comparing all conditions to the control condition. RT-qPCR data was analysed using the $\Delta\Delta$Ct relative quantification method with normalisation to RNU44 expression and scb control. Statistical significance was determined either using a one-way ANOVA with a Dunnett's post-test comparing all conditions to the control condition or a student's t-test. For all tests, $p \leq 0.05$ was considered statistically significant.

3 Mature miRNAs from the 14q32 Region are Upregulated in Acquired Resistance to Lapatinib

3.1 Sensitivity of HER2+ Cell Lines to Lapatinib

A panel of HER2+ breast cancer cell lines (Table 3.1) was screened to determine the sensitivity of their response to lapatinib (Figure 3.1). The average IC_{50} values for the cell lines are listed in Table 3.2, cell lines with an IC_{50} greater than 1 µM were considered resistant. Determination of IC_{50} values confirmed lapatinib sensitivity of BT-474, SKBR-3, and HCC1954 cells as well as intrinsic resistance of JIMT-1 and MDA-MB-36.

Cell Line	**Site**	**Morphology**	**Receptor Status**		
			ER	PR	HER2
BT-474	Primary	Epithelial	+	+	+
HCC1954	Primary	Epithelial	-	-	+
SKBR-3	Metastasis: pleural effusion	Epithelial	-	-	+
JIMT-1	Metastasis: pleural effusion	Epithelial	-	-	+
MDA-MB-361	Metastasis: brain	Epithelial	+	-	+

Table 3.1: Cell Line Characteristics (*249–252*). These cell lines are all derived from female breast cancers. ER: Œstrogen Receptor, PR: Progesterone Receptor, HER2: Human Epidermal Growth Factor Receptor 2.

In order to examine the mechanism driving acquired resistance to lapatinib the sensitive cell lines were made resistant to the drug through continuous exposure to increasing concentrations of lapatinib. BT-474/L resistant cells have been previously published (*1*) and SKBR-3/L and HCC1954/L cells were generated during the course of this research. IC_{50} determination showed a clear shift, with over a 20-fold increase in IC_{50} value for SKBR-3/L compared to SKBR-3, and

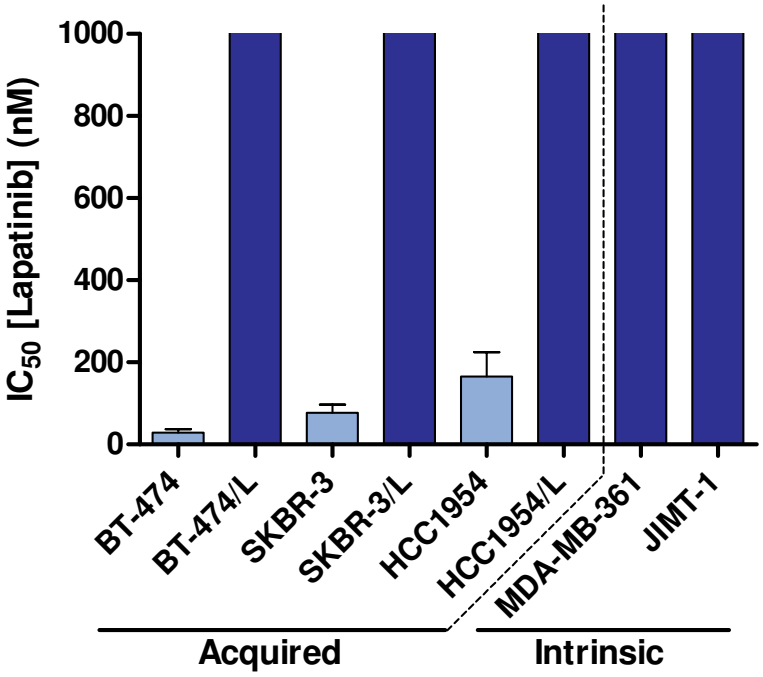

Figure 3.1: Lapatinib IC_{50} values for a Panel of HER2+ Breast Cancer Cell Lines. Three lapatinib sensitive cell lines were cultured in increasing concentrations of lapatinib to generate cell lines with acquired resistance to the drug; BT-474/L, SKBR-3/L, and HCC1954/L. Cell lines with an IC_{50} value greater than 1 µM are considered resistant. This value was used as the cut-off for the y-axis of the graph as the assay was designed to obtain IC_{50} values for the sensitive cell lines and mainly uses drug concentrations $< 1\ \mu M$ (Table 2.4). Higher IC_{50} values are, therefore, not accurate as they are extrapolated from the data. The IC_{50} values are obtained from non-linear regression analysis of cytotoxicity experiments, average of at least four experiments. MDA-MB-361 and JIMT-1 display intrinsic resistance to the drug with an IC_{50} greater than 1 µM; they were not grown in presence of the drug to develop resistance.

more than a 50-fold increase for HCC1954/L relative to HCC1954, confirming the cell lines have acquired resistance to lapatinib (Figure 3.1).

3.2 Cross-Resistance to Other Targeted Therapies

Having identified the lapatinib sensitive and resistant cells we decided to investigate how the cell's response to lapatinib affected cross-resistance with other HER targeting agents (Table 3.2) as other targeted therapies can be used to overcome resistance to a prior treatment as they may work via different pathways.

Cell Line	**Lapatinib** EGFR, HER2 (nM)	**Trastuzumab** HER2 ($mg \cdot L^{-1}$)	**Neratinib** pan-HER (nM)	**Dacomitinib** pan-HER (nM)	**Gefitinib** EGFR (µM)
BT-474	28	0.4	4	68	5
BT-474/L	17938	89	11996	16364	26
SKBR-3	77	0.2	21	151	13
SKBR-3/L	1567	0.4	78	205	16
HCC1954	165	39	21	246	15
HCC1954/L	8599	27	2049	551	5
MDA-MB-361	2652	-	21	536	59
JIMT-1	2270	-	344	14311	224

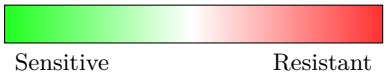

Table 3.2: Average IC_{50} Values for a Panel of HER2+ Breast Cancer Cell Lines to Various HER-Targeting Agents. The IC_{50} values are obtained from non-linear regression analysis of cytotoxicity experiments, average of at least three biological replicates. Sensitivity to the drug is shown in green and resistance in red.

3.2.1 Trastuzumab

BT-474 is sensitive to the HER2-targeting monoclonal antibody, trastuzumab; BT-474/L, however, is resistant to this treatment as it does not respond to doses under 10 $mg \cdot L^{-1}$. This threshold value was selected based on previously published data, as concentrations ranging from 4 $mg \cdot L^{-1}$ to 15 $mg \cdot L^{-1}$ are used to generate trastuzumab resistant cell lines (*253–257*). SKBR-3 is also sensitive to trastuzumab and, although the SKBR-3/L cells are still sensitive to the drug, they are less so than their parental line. HCC1954 cells are intrinsically resistant

to trastuzumab and this is conserved in the lapatinib resistant HCC1954/L (Figure 3.2a). MDA-MB-361 and JIMT-1 have been previously reported to be resistant to trastuzumab and they were not tested here (*66*, *77*).

3.2.2 Neratinib

Neratinib is a pan-HER inhibitor therefore it targets all the members of the HER family preventing compensation signalling through other HER receptors. Hence its effectiveness as a treatment on the sensitive and *de novo* resistant lines as their IC_{50}s are all brought under the 1 µM threshold. The lapatinib sensitive cells and SKBR-3/L also have low IC_{50} values with neratinib. The other two acquired resistant lines, BT-474/L and HCC1954/L, are resistant to this drug (Figure 3.2b).

3.2.3 Dacomitinib

Dacomitinib, another pan-HER inhibitor, on the other hand seems to be more effective on the acquired resistant lines as both IC_{50} values for SKBR-3/L and HCC1954/L are under the 1 µM resistance threshold. MDA-MB-361 is also sensitive to the inhibitor as are the lapatinib sensitive lines; BT-474/L and JIMT-1 however are not (Figure 3.2c).

3.2.4 Gefitinib

Since lapatinib targets both HER2 and EGFR, to confirm the sensitivity observed in the cell lines was due to the HER2 targeting, rather than blocking EGFR, the cells were also treated with an EGFR inhibitor, gefitinib. None of the cell lines responded to gefitinib treatment (Figure 3.2d) and all the cell lines have IC_{50} values greater than 1 µM. This confirms their dependence on HER2 signalling for survival and proliferation.

3.2.5 Summary

These results show there is some cross-resistance occurring with other HER2-targeting therapies as the lapatinib resistant cells are less responsive to other

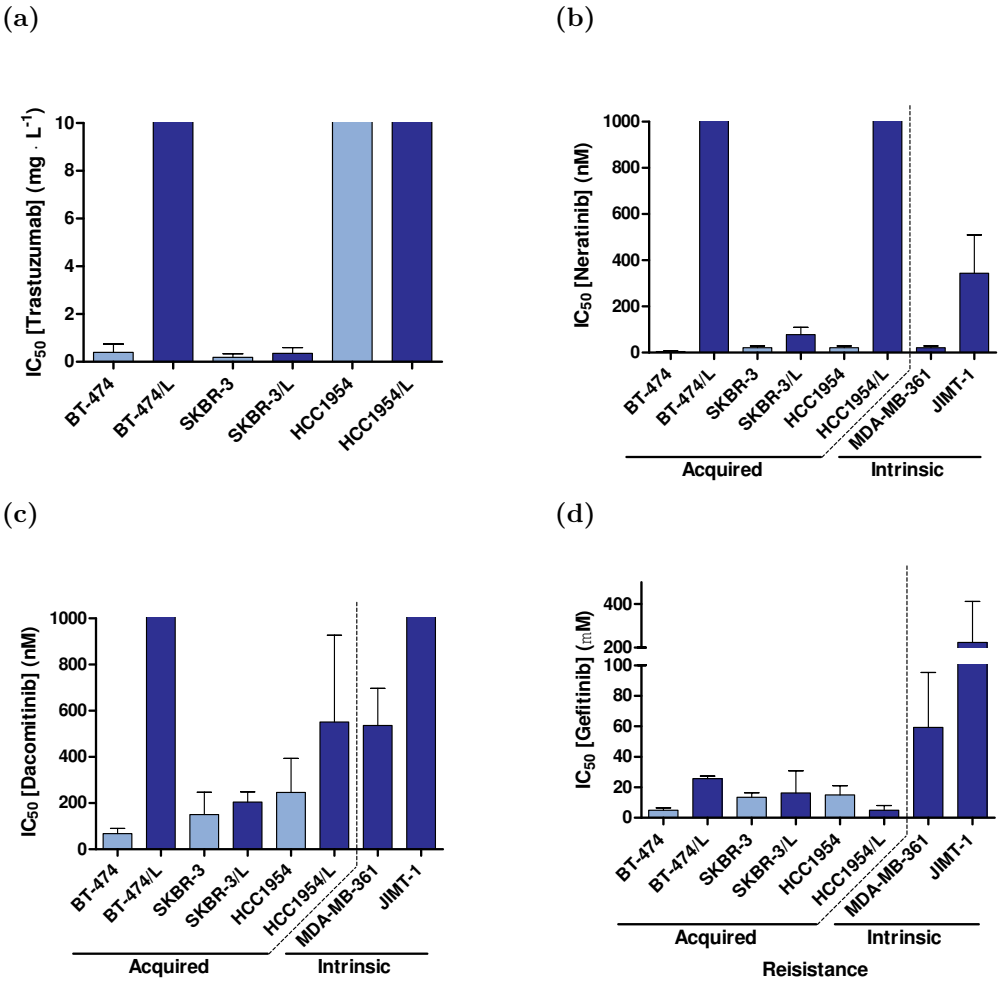

Figure 3.2: IC_{50} Values for a Panel of HER2+ Breast Cancer Cell Lines to Various HER-Targeting Agents. The IC_{50} values are obtained from non-linear regression analysis of cytotoxicity experiments, average of at least three experiments. (a) IC_{50} values for trastuzumab treatment in the paired sensitive and resistant cells. The y-axis is cut off at 10 mg·L^{-1}. (b) IC_{50} values for neratinib, and (c) IC_{50} values for dacomitinib in the paired cell lines as well as two lines intrinsically resistant to lapatinib. The y-axis is cut off at 1000 nM. (d) IC_{50} values for gefitinib in the paired cell lines as well as two lines intrinsically resistant to lapatinib. For (a, b, and c) the y-axis is cut off at the generally accepted threshold for resistance. This value was used as the cut-off for the y-axis of the graph as the assay was designed to obtain IC_{50} values for the sensitive cell lines and mainly uses drug concentrations $< 1\ \mu M$ (Table 2.4). Higher IC_{50} values are, therefore, not accurate as they are extrapolated from the data.

HER2-targeting treatments than the parental lines. Only BT-474/L cells were resistant to all the HER2 inhibitors tested, HCC1954/L is only sensitive to Dacomitinib while SKBR-3/L is sensitive to all the other HER2-targeting agents tested, although it is always less sensitive to the drug than SKBR-3, its parental line.

Similarly the *de novo* resistant lines behave differently, with MDA-MB-361 being sensitive to both pan-HER inhibitors, whilst JIMT-1 is only sensitive to neratinib.

3.3 Phenotypic Differences Between the Paired Cell Lines

3.3.1 Resistant Cells can Have More Filopodia and a Greater Surface Area than Sensitive Lines

To investigate phenotypic changes observed between the sensitive and resistant cells, the paired lines were stained with Hoechst and Phalloidin for immunofluorescence (Figure 3.3a). The resistant cells have more stress fibres visible in the cytoplasm, the cells also have a more irregular appearance with many lamellipodia and filopodia (white arrows in Figure 3.3a). This demonstrates that the resistant lines are phenotypically divergent to the sensitive line they are derived from; with the resistant lines appearing more motile and invasive.

Additionally, both BT-474/L and HCC1954/L cells are significantly bigger than their sensitive counterpart. BT-474 cells have a mean area of 300 μm^2 whilst BT-474/L cells are on average 1930 μm^2. HCC1954 cells are generally 634 μm^2 and the resistant HCC1954/L are 846 μm^2. SKBR-3 and SKBR-3/L cells are of a similar size, on average 357 and 325 μm^2 (Figure 3.3b). BT-474/L has a slightly bigger nucleus than its paired BT-474 line. The other two isogenic pairs have a similar nucleus size between sensitive and resistant (Supplementary Figure 7.8).

(a)

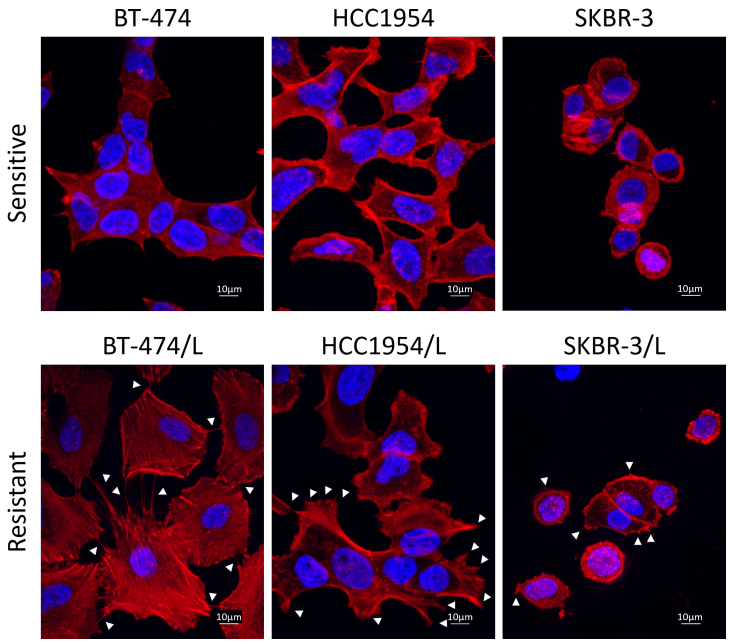

(b)

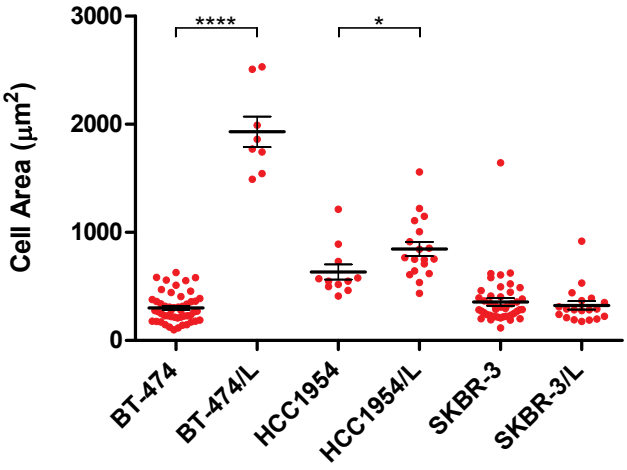

Figure 3.3: Comparison of Paired Lapatinib Sensitive and Acquired Resistant HER2+ Breast Cancer Cell Lines. (a) Hoechst (blue) and Phalloidin (red) staining of the paired sensitive and resistant lines. The resistant lines appear to have more stress fibres and filopodia, indicated by white arrows. This suggest resistant cells could be more motile and invasive. (b) Cell area measured for two to four frames per cell line. BT-474/L and HCC1954/L have a bigger cell area than their sensitive counterparts. Mean and standard error are shown, statistical significance is obtained from a one-way ANOVA with Bonferroni's Multiple Comparison post-test. Where results are statistically significant p-values are shown on the graph, with $\star$ for $p \leq 0.05$, and $\star\star\star\star$ for $p \leq 0.0001$.

3.3.2 Lapatinib Sensitive and Acquired Resistant Cells do not Have the Same Population Doubling Rate Rate

After showing the acquired resistant cells were might be invasive, although invasion assays would be needed to confirm this, we investigated whether there may also be a difference in the growth rate of the sensitive and resistant cells. To determine how acquired resistance influenced cell growth, population doubling studies were carried out. These showed BT-474 sensitive and BT-474/L resistant lines grew very differently, with the resistant cells growing almost three times faster than the sensitive ones. This, however, was not observed in the other two acquired resistant lines, which grew slower compared to their paired parental line. HCC1954 cells showed the most difference with a two fold decrease in doubling rate in the HCC1954/L (Figure 3.4).

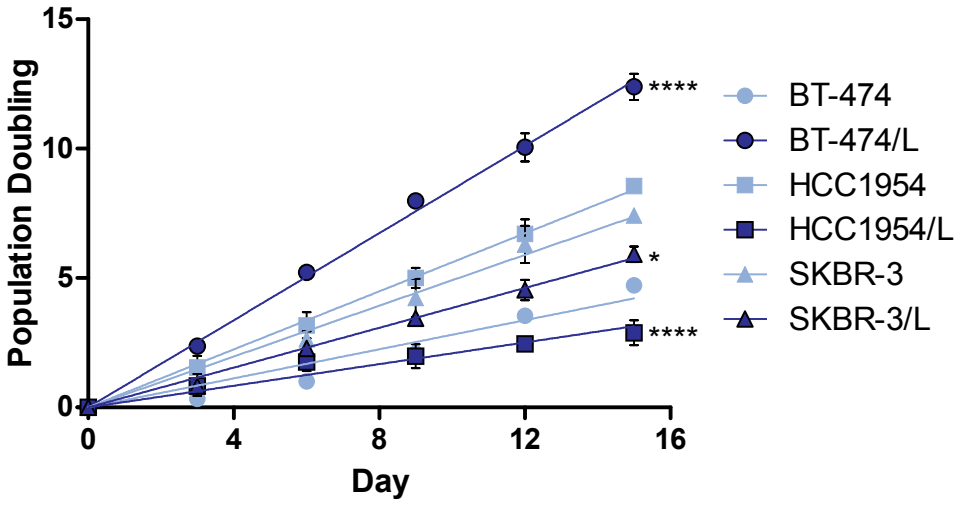

Figure 3.4: Comparison of the Population Doubling Rate of Paired Lapatinib Sensitive and Acquired Resistant HER2+ Breast Cancer Cell Lines without Lapatinib. BT-474/L cells are the fastest growing cell line with a doubling rate almost three times higher than its paired parental line. HCC1954 cells have a faster doubling rate than the paired HCC1954/L line. SKBR-3 and SKBR-3/L lines have similar population doubling rates with the sensitive cells growing slightly faster than the resistant ones. The population doubling was carried out over 15 days and cells were counted and re-plated every three days, an average of 3 biological replicates is shown. Statistical significance is displayed for each pair of cell lines at day 15 and obtained from a one-way ANOVA with Bonferroni's Multiple Comparison post-test, with $\star$ for $p \leq 0.05$, and $\star\star\star\star$ for $p \leq 0.0001$.

3.4 miRNA Expression Across HER2+ Breast Cancer Cell Lines

miRNAs have increasingly been linked to cancer and, in patients, changes in miRNA expression profiles have been found to occur with resistance to therapies. To identify the role of miRNAs in resistance to lapatinib, we investigated miRNA levels in our panel of HER2+ breast cancer cell lines.

3.4.1 miRNA Expression in BT-474 Sensitive vs BT-474/L Resistant Cells

In order to determine which miRNAs are involved in acquired resistance to lapatinib, we compared changes in expression between sensitive and resistant cell lines using a miRNA array. This showed many changes in miRNA expression levels between the two cell lines.

Numerous miRNAs were significantly upregulated in the resistant cells, with 164 miRNAs having over a 2-fold upregulation in the BT-474/L cells compared to the BT-474. The data was analysed using the $\Delta\Delta$Ct method and fold change analysis with DataAssist Software (*235*). Using a 10-fold change cut-off, 43 miRNAs were found to be upregulated in the resistant cells (Figure 3.5a). Fewer miRNAs were downregulated in BT-474/L, with only 12 targets displaying over a 10-fold downregulation compared to BT-474 (Figure 3.5b).

Of the most upregulated miRNAs, 44 % occupy the same genomic region: the 14q32, this region contains two miRNA clusters: the 14q32.2 and the 14q32.31. This was the most represented genomic region, the second most represented region with 8 upregulated miRNAs was the 19q13.42. There are nine other regions represented in the upregulated miRNAs which have on average 1.8 upregulated miRNAs (Figure 3.6a). As miRNAs from a same genomic locus have been shown to be involved in regulating similar pathways, we decided to investigate the 14q32 miRNAs.

The 19q13.42 is the second most upregulated miRNA region, with 8 miRNAs overexpressed in the resistant compared to the sensitive line. The 19q13.42 contains 34 known coding genes and a miRNA cluster of 50 miRNAs (*258*) There are few reports of this region's role in cancer. miRNAs in the 19q13.42 region

(a)

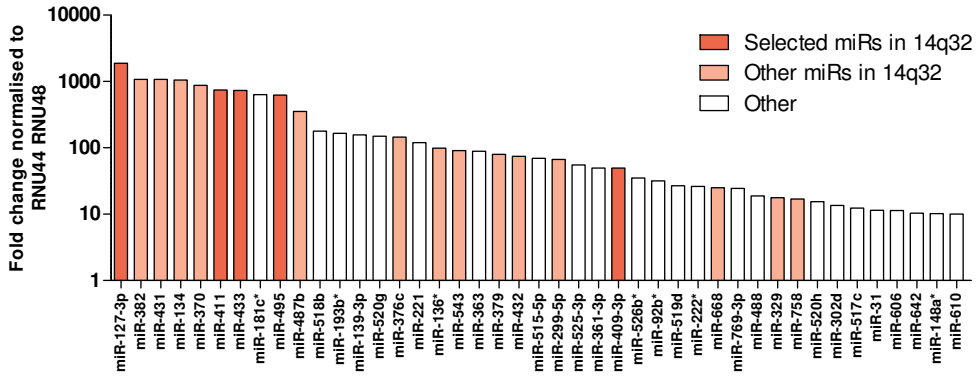

(b)

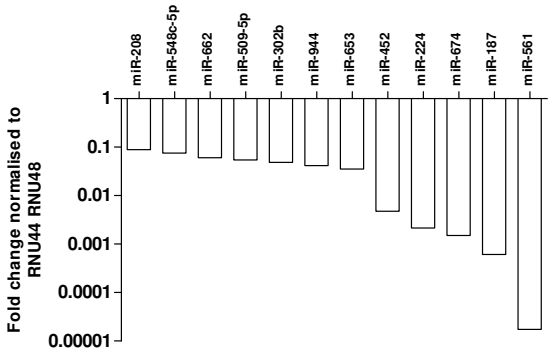

Figure 3.5: miRNA Expression in BT-474/L Relative to BT-474 Cells Measured by miRNA Array. miRNA profiling using the Human TaqMan Array Card for the lapatinib sensitive HER2+ BT-474 cell line and the paired lapatinib resistant cells BT-474/L, results are averaged for two replicates. This array identified a panel of differentially expressed miRNAs in the resistant compared to the sensitive cells. After fold change analysis a cut-off of 10-fold was selected. (a) 43 miRNAs were found to be significantly upregulated of which 44 % are located in the 14q32 locus (pink and red). miR127, miR409, miR411, miR433, and miR495 (red) were selected for further validation of their role in resistance; miR539 was also added to this list as it was upregulated in the resistant cells, with an 8-fold increase in expression. (b) 12 miRNAs were significantly downregulated with over a 10-fold decrease in expression.

(a)

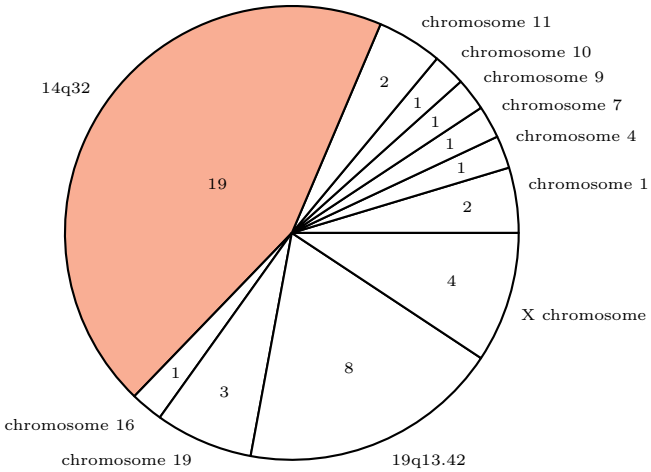

(b)

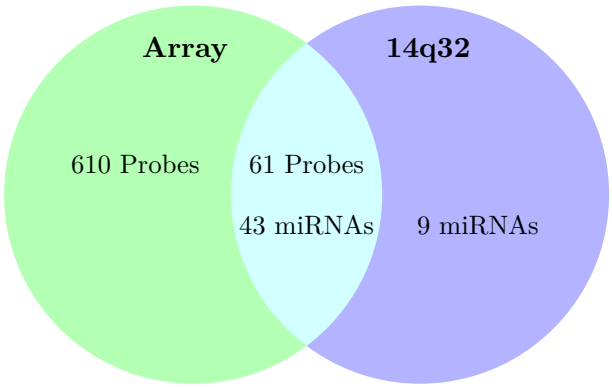

Figure 3.6: Analysis of the miRNA Array (a) Chromosomal location of miRNAs upregulated in the array. The 14q32 region is the most represented region, the second region is the 19q13.42 with less than half as many miRs as the 14q32 upregulated over 10-fold. (b) Comparison of the probes present in the array to miRNAs in 14q32 Region. Out of the individual 671 probes in the TaqMan miRNA array, 61 corresponded to 43 out of 52 miRNA genes found in the 14q32 miRNA clusters.

14q32.2			14q32.31			
miR-493	miR-337	miR-665	miR-379	miR-411	miR-299	miR-380
miR-431	miR-433	miR-127	miR-1197	miR-323a	miR-758	miR-329-1
miR-432	miR-136	miR-370	miR-329-2	miR-494	miR-1193	miR-543
			miR-495	miR-376c	miR-376a-2	miR-654
			miR-376b	miR-376a-1	miR-300	miR-1185-1
			miR-1185-2	miR-381	miR-487b	miR-539
			miR-889	miR-544a	miR-655	miR-487a
			miR-382	miR-134	miR-668	miR-485
			miR-323b	miR-154	miR-496	miR-377
			miR-541	miR-409	miR-412	miR-369
			miR-410	miR-656	miR-1274	

Table 3.3: miRNAs from the 14q32.2 and 14q32.31 Clusters. The miRNAs are listed in the order they are encoded in the genome within each cluster. The miRNAs selected for further validation are highlighted, two are in the 14q32.2 and four in the 14q32.31 cluster.

have been suggested to be oncogenes (*259*). The 19q13.42 miRNAs have been found to be upregulated in 10 % of pancreatic cancers and high expression of the miRNAs correlates to poor survival (*260*). Mainly, amplifications in this region have been linked to embryonal tumours with ependymoblastic rosettes (*261*). In these cancers amplification of the region can be used a diagnostic maker (*262*). The 19q13.42 region was not selected for further investigation due to the lack evidence of a role in either breast cancer or resistance to therapies. Moreover, even though both the 14q32 and 19q13.42 regions contain similar numbers of miRNAs, there are more than double the number of miRNAs upregulated in the 14q32 than in the 19q13.42 (Figure 3.6a).

There are 52 annotated miRNA genes in the 14q32 region (Table 3.3), not all of which were represented in the array (Figure 3.6b), and two protein coding genes. Expression levels of the genes was not significantly altered between the sensitive and resistant lines. This will be discussed further in Chapters 4 and 5. Six miRNAs from the 14q32 region were selected for further validation of their role in resistance: miR-127-3p (miR127), miR-409-3p (miR409), miR-411 (miR411), miR-433 (miR433), miR-495 (miR495), and miR-539 (miR539). Their sequence and miRBase accession number are listed in Table 3.4. The first five miRNAs have a fold change greater than 10 in the resistant cells compared to BT-474.

There are 9 miRNAs in the14q32.2 cluster, 5 of these, miR127, miR-431, miR-

miRNA	Sequence	miRBase Accession	Name
hsa-miR-127-3p	UCGGAUCCGUCUGAGCUUGGCU	MIMAT0000446	miR127
hsa-miR-409-3p	GAAUGUUGCUCGGUGAACCCCU	MIMAT0001639	miR409
hsa-miR-411-5p	UAGUAGACCGUAUAGCGUACG	MIMAT0003329	miR411
hsa-miR-433-3p	AUCAUGAUGGGCUCCUCGGUGU	MIMAT0001627	miR433
hsa-miR-495-3p	AAACAAACAUGGUGCACUUCUU	MIMAT0002817	miR495
hsa-miR-539-5p	GGAGAAAUUAUCCUUGGUGUGU	MIMAT0003163	miR539

Table 3.4: Mature miRNA Sequences and miRBase Accession Numbers for the Selected miRNAs and abbreviation used.

370, miR433, and miR-432 are upregulated over 10-fold. miR127 is the most upregulated miRNA from the array so it was selected for further analysis. It has been shown to be epigenetically regulated in prostate, bladder, and colon tumours (*263*) and can be silenced by CpG hypermethylation. In many cancer types miR127 has been found to be a tumour suppressor miRNA as it is often downregulated in tumours. miR127 expression can lead to inhibition of cell cycle progression, proliferation, and migration (*264*). miR127 has been seen to inhibit B-Cell chronic lymphocytic leukaemia (CLL)/Lymphoma 6 (BCL6) translation and lead to senescence (*265*). In breast cancer, miR127 is generally expressed at low levels, probably because of its tumour suppressive role. Indeed, low levels of the miR127 have been associated with poor prognosis and lymph node metastasis (*266*). Contrastingly, higher levels of miR127 have also been observed in patients with breast cancer compared to healthy (*267*). Most of the studies listed here haven't established differences in the breast cancer subtypes, thus it is impossible to confirm whether the affirmations made about miR127 are applicable to all subtypes equally. Due to these opposing findings, it is necessary to study miR127 more in detail to conclude on its role in resistance.

The average expression of the remaining 4 miRNAs from the 14q32.2 cluster is closest to levels of miR433. This miRNA was, therefore, selected as representative for this region. miR433 has been reported to be downregulated in breast cancer cell lines where it can inhibit AKT (*268*), and lead to inactivation of MAPK signalling causing apoptosis (*269*). These studies, however, did not look at variation of miR433 between different subtypes and no HER2+ cell lines were included in their work. The miRNA has also been shown to regulate the AKT β-catenin pathway in cervical cancer (*270*) and reduce EMT in bladder cancer by inhibiting AKT, GSK3, and Snail signalling (*271*). miR433 has been

shown to inhibit Notch signalling in retinoblastoma (*272*) and in ovarian cancer where the miRNA was linked to inhibition of invasion (*273*). In colorectal cancer, miR433 can suppress migration and proliferation (*274*) and reduce viability through Metastasis-Associated In Colon Cancer Protein 1 (MACC1) regulation (*275*). The microRNA has also been found to inhibit proliferation in oesophageal squamous cell carcinoma by targeting GRB2 (*276*). These results point towards miR433 acting as a tumour suppressive miRNA, however, this miRNA was also shown to be upregulated in resistance to certain cancer therapies. In ovarian cancer, miR433 was overexpressed in paclitaxel resistance, where it inhibits Cyclin Dependent Kinase 6 (CDK6) leading to a senescent phenotype (*277*). The miRNA was also found to be upregulated in gemcitabine acquired resistance in patients with gallbladder cancer, where increased serum levels of miR433 were observed in patients with drug resistant tumours (*278*). Due to the disparate roles identified for miR433 and the lack of data about its function in HER2+ breast cancer, it is necessary to further study this miRNA.

The other four miRNAs selected are encoded in the 14q32.31, this regions contains more miRNAs than the 14q32.2 which is why more miRNAs were selected from the 14q32.31 region.

miR409 functions in a context dependant manner acting either as a tumour suppressive or an oncogenic miRNA. In colorectal, gastric, and lung cancers, miR409 expression is generally reduced, backing its role as a tumour suppressor in those settings. Indeed, the miRNA is a negative regulator of cell migration, invasion, and metastasis in colorectal cancer (*279*) where it targets GRB2 Associated Binding Protein 1 (GAB1) leading to reduced levels of the protein (*280*). In gastric cancers, miR409 exerts it function as a tumour suppressor by binding the pro-metastatic gene Radixin (RDX) (*281*) as well as causing apoptosis by targeting the transcriptional regulator Plant homeodomain (PHD) Finger Protein 10 (PHF10) (*282*). This prevents PHF10 from binding to the Caspase 3, Apoptosis-Related Cysteine Peptidase (CASP3) promoter region leading to activation of the apoptosis caspase cascade. In lung adenocarcinoma miR409 is also involved in CASP3 dependant apoptosis, as the miRNA represses expression of the Mesenchymal Epithelial Transition Proto-Oncogene, Receptor Tyrosine Kinase (MET) which leads to a decrease in AKT phosphorylation, in turn causing the downregulation of B-Cell CLL/Lymphoma 2 (BCL2) and an increase in BCL2 Associated X, Apoptosis Regulator (BAX) levels eventually

leading to apoptosis (*283*). Similarly, in breast cancer, the miRNA was found to target AKT Serine/Threonine Kinase 1 (AKT1). This leads to inhibition of cancer cell growth and metastasis (*284*). This work was carried out in triple negative and luminal A cell lines, which are all HER2 negative. miR409 has also been suggested to reduce cell growth and invasion by targeting Zinc Finger E-Box Binding Homeobox 1 (ZEB1) (*285*). This work was done in a triple negative cell line and might thus not be relevant in HER2+ breast cancer. miR409 levels were also seen to be lower in breast cancer compared to healthy tissue (*286*), however, this study did not look at levels in the individual subtypes nor how this influenced survival. Conversely, in prostate cancer, miR409 was found to act as oncogenic miRNA by promoting metastasis and EMT (*287*). Indeed high levels of miR409 in patients has been associated with poor prognosis and reduced progression-free survival. The miRNA has been found to target tumour suppressor genes such as RAS Suppressor Protein 1 (RSU1) which is involved in inhibition of the RAS/MAPK pathway (*288*). Due to the dual role of miR409 depending on the context and the lack of evidence in HER2+ breast cancer, further validation is necessary to conclude on its role in resistance.

miR411 has been reported to be a tumour suppressive miRNA in renal cell cancer (*289*), in ovarian cancer (*290*), and in gastric adenocarcinoma (*291*) as its expression downregulated. In breast cancer it has also been suggested to act as a tumour suppressor as it was found to be downregulated in patients (*292*), however, this study did not correlate levels of the miRNA with the different subtypes so it is not possible to say whether this data is relevant to HER2+ breast cancers. miR411 was reported to prevent proliferation and migration of cells by inhibiting Specificity Protein 1 (SP1) (*293*) as well as GRB2, and therefore RAS, signalling (*292*). Again, none of these papers specifically investigated how miR411 expression was altered in HER2+ breast cancer compared to other subtypes. miR411 was found to be expressed at lower levels in drug resistant malignant pleural mesothelioma when compared to sensitive (*294*). In lung cancer however, miR411 was found to act as an oncogenic miRNA as it targets Sprouty Receptor Tyrosine Kinase Signalling Antagonist 4 (SPRY4) and Thioredoxin Interacting Protein (TXNIP) (*295*) as well as the tumour suppressor Forkhead Box O1 (FOXO1) which leads to increased proliferation of the cancer (*296*). In hepatocellular carcinoma the miRNA targets Itchy E3 Ubiquitin Protein Ligase (ITCH) which leads to upregulation of CCND and c-

MYC which promotes proliferation (*297*). As there is no conclusive evidence for the role of miR411 in resistance in HER2+ breast cancer, further investigation of the miRNA is necessary.

miR495 has a context dependant role; it can act as both a tumour suppressor or an oncogene. The miRNA has been reported to be downregulated in mixed lineage leukaemia (MLL) (*298*) suggesting it acts as a tumour suppressor in this cancer. miR495 has been shown to target CDK6 in glioblastoma (*299*), and inhibit migration by downregulating Protein Tyrosine Phosphatase Type IVA, Member 3 (PTP4A3) in gastric cancer (*300*, *301*). It also leads to downregulation of Metastasis Associated 1 Family, Member 3 (MTA3) in non-small cell lung carcinoma (NSCLC) (*302*). In cisplatin (DDP) resistant NSCLC upregulation of the miRNA has been shown to lead to downregulation of anti-drug genes ATP Binding Cassette Subfamily G Member 2 (Junior Blood Group) (ABCG2) and Excision Repair Cross-Complementing 1, Endonuclease Non-Catalytic Subunit (ERCC1) (*303*). miR495 has been found to be downregulated in breast cancer cells after induced EMT (*304*). Contrastingly, miR495 has also been found to act as an oncogenic miRNA in hepatocellular carcinoma where it is upregulated leading to increased proliferation. By artificially decreasing levels of the miRNA, miR495 was found to target Menage A Trois Cyclin Dependent Kinase-Activating Kinase Assembly Factor 1 (MNAT1) leading to decreased tumour growth (*305*). The miRNA has been found to be significantly upregulated in breast cancer compared to normal tissue. It also promotes cell mobility and migration through inhibition of the junctional adhesion molecule F11 Receptor (F11R) and is associated with increased breast cancer progression (*306*). miR495 has been found to be upregulated in breast cancer stem cell populations as well as to promote oncogenesis and hypoxia resistance (*307*). Due to the available data on miR495, it appears to be a promising target to investigate resistance in HER2+ breast cancers.

miR539 is expressed approximately eight times higher in BT-474/L compared to BT-474 and is therefore not represented in Firgure 3.5a. It was selected to represent the other 14q32 miRNAs, the ones that are not upregulated more than 10-fold but are still expressed at higher levels in the resistant cells compared to the sensitive ones. miR539 has been found to act as a tumour suppressor. In colorectal cancer, miR539 targets the oncogene Runt Related Transcription Factor 2 (RUNX2) thus low levels of the miRNA have been found to correl-

ate with a more advanced stage and lymph node metastasis (*308*). High levels of miR539 have been shown to reduce tumour growth in xenograft models, where the miRNA was found to inhibit SRY (Sex Determining Region Y)-Box 4 (SOX4). This miRNA has been linked to reduced proliferation and invasion in glioma cells where it targets DIX Domain Containing 1 (DIXDC1) which is a positive regulator of Wingless-Type MMTV Integration Site (Wnt) signalling (*309*). In prostate cancer, miR539 also inhibits progression by targeting the oncogene Sperm Associated Antigen 5 (SPAG5), which is required for progression into anaphase (*310*). miR539 has also been found to inhibit thyroid cancer metastasis by targeting Caspase Recruitment Domain Family Member 11 (CARD11) thus preventing activation of Nuclear Factor Kappa B Subunit (NF-κB) signalling and of the Inhibitor Of Nuclear Factor Kappa B Kinase (IKK) complex (*311*). Breast cancer tissue was identified as having lower levels of miR539 than normal tissue, where low levels of the miRNA correlated with lymph node metastasis. miR539 was found to lead to a decrease in EGFR levels in luminal and triple negative cell lines (*312*). In triple negative breast cancers, the miRNA was found to lead to downregulation of Laminin Subunit Alpha 4 (LAMA4) which appears to be involved in proliferation and migration (*313*). In melanoma, mi539 has been observed to be upregulated by the Androgen Receptor (AR) which causes increased Melanocyte Inducing Transcription Factor (MITF) protein degradation leading to increased invasiveness (*314*). miR539 has been reported to be involved in resistance to therapy where it was reported to be both down- and upregulated. miR539 was downregulated in DDP resistant compared to sensitive NSCLC where loss of the miRNA leads to increased levels of Doublecortin Like Kinase 1 (DCLK1) as it is no longer repressed by miR539. This upregulation allows for increased pro-survival PI3K/AKT/mTOR signalling (*315*). miR539 was also found to overcome arsenic trioxide resistance in hepatocellular carcinoma, where overexpression of the miRNA leads to decreased expression of the anit-apoptotic factors BCL2 and BCL2 Like 1 (BCL2L1), leading to cell death (*316*). None of these studies investigated the role of miR539 in HER2+ breast cancer therefore further investigation of the miRNA would be necessary.

Due to the conflicting reports on these miRNAs, and the lack of evidence in HER2+ breast cancer, the 14q32 region necessitates further investigation to conclude on the role of these miRNAs in resistance to therapy.

3.4.2 Baseline miRNA Expression in Other HER2+ Breast Cancer Cell Lines

The changes in miRNA expression observed in BT-474 paired cell lines were validated by stem-loop RT-qPCR on the HER2+ breast cancer panel with paired lapatinib sensitive and acquired resistant cell lines as well as intrinsically resistant lines (Figure 3.7). miRNA levels in all the cell lines represented in Figure 3.7 are shown relative to BT-474, to allow comparison between all the different cell lines.

In the sensitive cell lines, we compared the expression of the miRNA to the sensitive BT-474 cell line in order to determine the variability of miRNA expression across our panel. SKBR-3 sensitive cells have similar levels of miRNA expression than BT-474, HCC1954 cells also express miR127 and miR539 at similar levels to BT-474. However, in the HCC1954 line, the other miRNAs are present at higher levels with miR409 and miR495 having approximately a 2-fold overexpression, and miR411 and miR433 about a 14- and 10-fold increase respectively when compared to BT-474 expression levels (Figure 3.7a).

The *de novo* resistant lines MDA-MB-361 and JIMT-1 show quite different miRNA expression patterns, with MDA-MB-361 having high miRNA expression with levels very similar to those of BT-474/L. Conversely, JIMT-1 has very low levels of miRNAs (Figure 3.7b). Further investigating gene targets and signalling pathways altered between these cells lines could highlight similarities between them.

3.4.3 Baseline miRNA Expression in Lapatinib Acquired Resistant HER2+ Breast Cancer Cell Lines

In the acquired resistant lines, a greater than ten-fold upregulation for all six of the miRNAs was confirmed in the BT-474/L cells compared to the BT-474.

SKBR-3/L cells showed a slight increase in miR127 and miR539 expression compared to SKBR-3. The other four miRNAs have at least a ten-fold upregulation, with miR409 having the greatest increase in expression in the acquired resistant line.

In HCC1954/L there is an upregulation in all miRNA expression compared

(a)

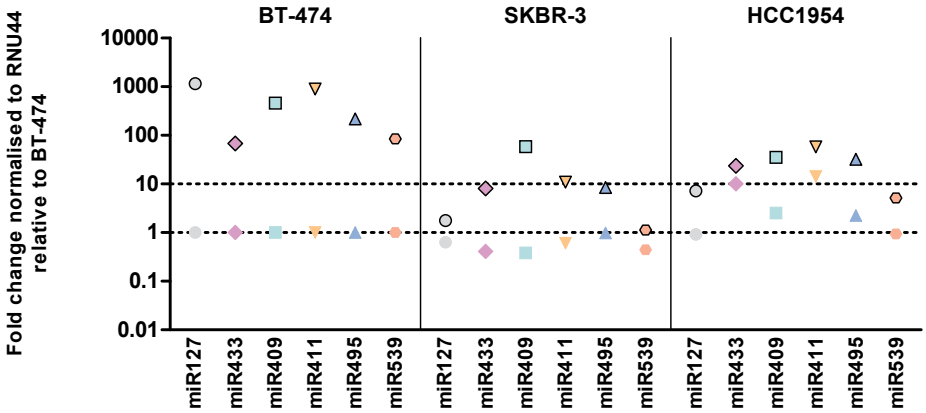

(b)

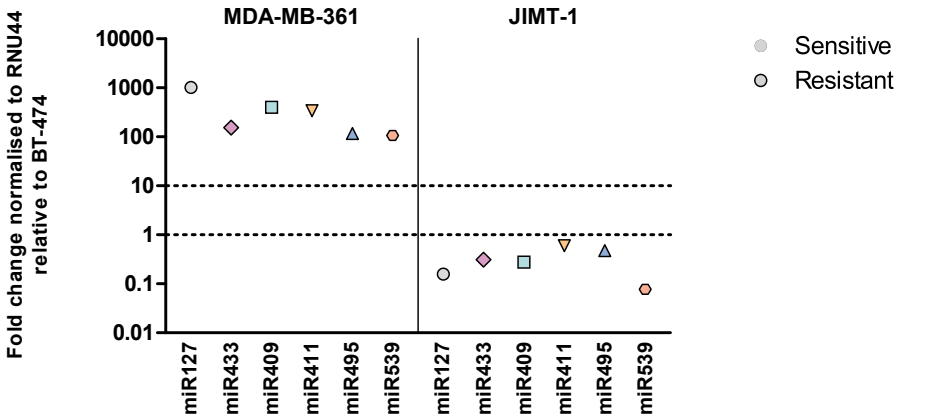

Figure 3.7: Baseline miRNA Expression in Sensitive and Resistant HER2+ Breast Cancer Cell Lines. Results are obtained by stem-loop RT-qPCR, are analysed by fold change analysis, and are averaged for at least three replicates. Expression for all cell lines is relative to BT-474 cells. (a) Overlay of miRNA expression in paired sensitive and acquired resistance lines relative to BT-474. (b) miRNA expression in cells intrinsically resistant to lapatinib relative to BT-474. Endogenous levels of miRNA expression were obtained by RT-qPCR and results analysed using the $\Delta\Delta$Ct relative quantification method, miRNA expression was normalised to RNU44 for each cell line. Baseline miRNA expression is similar between BT-474, SKBR-3, and JIMT-1 cell lines.

to the sensitive HCC1954 line. miR433 has the smallest change with only a 2.3-fold increase in the resistant cells, with levels ranging from approximately 10 to 23. miR409 and miR495 have the highest upregulation in HCC1954/L cells with a 14-fold increase in expression (Figure 3.7a).

3.5 Summary

These results indicate that the adaptive mechanisms of non-isogenic cells differ. Lapatinib resistance was found to decrease sensitivity to other HER2-targeting agents, however the cells do not all exhibit the same cross-resistance patterns suggesting they may have adapted to lapatinib in different ways. SKBR-3/L is the only cell line to show decreased sensitivity to other HER2-targeting agents without it being resistant to any of them. The other lapatinib acquired resistant cell lines display varying patterns of resistance to the HER2-targeting agents. Some cross-resistance was also observed in the intrinsically resistant HER2+ cells.

We also showed the acquired resistant lines had a different appearance, with both BT-474/L and HCC1954/L cells having a significantly bigger surface area than their parental line, with BT-474/L also displaying an enlargement in nucleus size. The resistant cell lines also have an increase in stress fibres as well as protrusions and filopodia, suggesting these cells could be more motile and invasive. Additionally, the acquired resistant cells do not have the same growth pattern, with the BT-474/L cells having the fastest population doubling rate, SKBR-3/L a similar rate to its parental line, and HCC1954/L cells growing slower than the HCC1954 line. Again, these differences suggest the cells have developed different mechanisms of adaptation to lapatinib.

miRNAs have been found to play an important role in resistance to therapies, with expression profiles being altered over time leading to differing levels of individual miRNAs in resistant cells compared to sensitive cells. To get insight into the changes occurring in the resistant cells we decided to investigate shifts in miRNA expression. Levels of many miRNAs were changed in the BT-474/L cells, with the majority of the most significantly upregulated targets located in the 14q32 region which contains two miRNA clusters. A similar pattern of miRNA overexpression in the other acquired resistance lines was observed.

Resistance is multi-factorial, thus it is not surprising that cells intrisically resistant to lapatinib do not have the same miRNA changes. Intrinsic resistance to lapatinib may not rely on changes in miRNA expression since JIMT-1 and MDA-MB-361 have opposing miRNA expression patterns. However, although the acquired resistant lines behave differently, they all have miRNA upregulation as a common finding of acquired resistance to lapatinib.

4 Epigenetic Regulation of 14q32 miRNAs

4.1 The 14q32 Cluster

4.1.1 Imprinting

The 14q32 region is located on chromosome 14 at band 32 and is an imprinted region which is highly conserved in mammals. It contains paternally expressed genes (PEGs), Delta, drosophila like homologue 1 (*DLK1*) and Retrotransposon-like gene 1 (*RTL1*), which are protein coding, and maternally expressed genes (MEGs), *MEG3*, or *Gtl2* in mice, *RTL1as*, and *MEG8*, which are non coding genes (*317*, *318*) (Figure 4.1). The function of MEG3 is not clear, however, it produces a long non-coding RNA (lnRNA) (*319*). DLK1 is a member of the delta-notch family of proteins (*320*) involved in cellular differentiation signalling (*321*, *322*) and is important in early embryonic development, postnatal growth, and fat deposition (*323*).

Imprinting of this region is thought to be controlled by three differentially methylated regions (DMRs) (*324*, *325*) with the intergenic-differentially methylated region (IG-DMR) (*325*, *326*) acting as the imprinting control region. Two secondary DMRs also contribute to regulate the imprinted genes; the *DLK1*-DMR (*327*) and the *MEG3*-DMR which overlaps the *MEG3* promoter region as well as the *MEG3* gene body (*326*, *328*, *329*). Contrary to imprinted methylation on the IG-DMR, which is inherited from the gametes (*330*), methylation on the *MEG3*-DMR appears post-fertilisation. This region contains seven putative CCCTC-binding factor (CTCF) binding sites (*324*, *331*), CTCF is an enhancer blocking protein which has been implicated in transcriptional activation or repression and imprinting, this protein binds to unmethylated DNA in an allele specific manner preventing target gene expression (*332*, *333*).

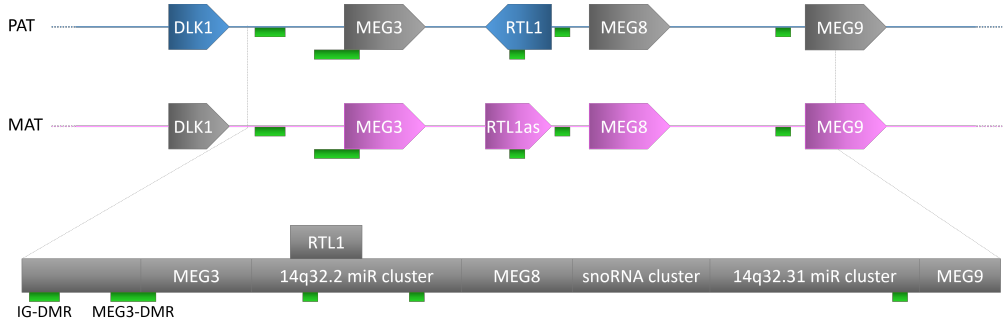

Figure 4.1: Schematic of the 14q32 Locus. miRNAs in the 14q32 domain are maternally imprinted. The intergenic-differentially methylated region (IG-DMR) is methylated on the paternal chromosome preventing expression of the maternally expressed genes (*MEG*) as well as the miRNA clusters. miR127 is located in the 14q32.2 miRNA cluster, while miR409 and miR495 are in the 14q32.31 miR cluster. miRNAs in both clusters are polycistronic however it is unclear whether both clusters are regulated by the same promoter region or if their transcription is regulated individually.

4.1.2 miRNA Regulation

The 14q32 region contains one of the largest polycistronic miRNA clusters identified, with 52 miRNAs in humans (*334*). It is syntenic to the distal region of the mouse chromosome 12 which contains 61 miRNAs (*318*).

This region is separated into two different miRNA clusters: 14q32.2 and 14q32.31 (Figure 4.1); it is unclear whether both miRNA clusters are transcribed as one long polycistronic RNA or as two separate smaller polycistronic RNAs (*334*). These miRNAs could be processed as long transcripts originating form the *MEG3* promoter, thus they would be controlled by both the *MEG3*- and IG-DMRs. If the miRNA clusters are transcribed separately, it has been speculated that the 14q32.2 miRNAs could be controlled by a separate promoter region (*334*, *335*).

Expression of the miRNAs is negatively correlated to methylation of the IG-DMR, thus on the paternal allele where the IG-DMR is methylated, the miRNAs are not expressed (*326*). The role of the *MEG3*-DMR on the other hand is not as straight forward; it has a bivalent pattern where methylation of the *MEG3* promoter region positively correlates with miRNA expression, and methylation of the gene body region is predominantly negatively correlated to miRNA expression (*327*).

4.1.3 Role of the 14q32

The primary role of this region has been found to be regulation of neovascularisation after injury (*336*) with most miRNAs silenced in healthy adult tissue (*327*). Other genes expressed in early developmental stages are expressed from the paternal allele (*337*, *338*). miRNAs from this region have also been involved in oncogenesis and malignant growth through increased proliferation and cell survival signalling (*339*, *340*). Loss of imprinting, leading to increased miRNA signalling has been identified in leukaemia (*327*) and has been found to promote metastasis in lung adenocarcinoma (*341*).

This region is involved in disease in the form of maternal and paternal uniparental disomies (UPDs), respectively upd(14)mat and upd(14)pat. Both UPDs have distinct phenotypes with various congenital anomalies and with deleterious phenotypes resulting from loss or overexpression of imprinted genes, suggesting that, here, gene copy number is a factor in regulating gene function (*342*, *343*). upd(14)mat, also known as Temple Syndrome, is the most common UPD of the two, with affected individuals having two maternal copies of the region (*344*, *345*), upd(14)pat, or Kagami-Ogata Syndrome, has a more severe phenotype and occurs less frequently (*344*, *346*, *347*). This suggests that genes expressed from the maternal allele play an important role in development.

4.2 14q32 miRNA Expression is Controlled by DNA Methylation and Histone Acetylation

The miRNA array showed that the region with the highest number of differentially expressed miRNAs in the acquired resistant BT-474/L line the 14q32 region. The miRNA are all expressed from the maternal allele. The paternal allele expresses the PEGs DLK1 and RTL1, which are the only coding genes of this chromosomal section. Their expression was not significantly altered between the sensitive and resistant lines (discussed in Chapter 5). Due to the substantial role of epigenetics in controlling gene expression in this region, and that only expression of the MEGs was altered, we investigated how epigenetic modifiers were involved in the difference of miRNA expression observed between the sensitive and resistant cell lines.

4.2.1 miRNA Expression is Increased in 5-Aza-2′-deoxycytidine (Aza) Treated Cells

To study how miRNAs are affected by methylation, BT-474 cells were treated with the global demethylating agent 5-Aza-2′-deoxycytidine (Aza). Altered levels of miRNA expression were measured by miRNA array and compared to untreated BT-474 cells.

Aza is a chemical analogue of C that can be integrated into the DNA of proliferating cells instead of C. The chemical structure of the analogue prevents methylation resulting in the hypomethylation of DNA. If promoter regions controlling the expression of the miRNAs are methylated, then treatment with a demethylating agent should lead to an increase in target expression.

When comparing the hypomethylated BT-474 Aza to the untreated BT-474 samples, there are 45 miRNAs with more than a 10-fold increase (Figure 4.2) and 13 with between 5 and 10-fold increase (data not shown) in the Aza compared to untreated sample.

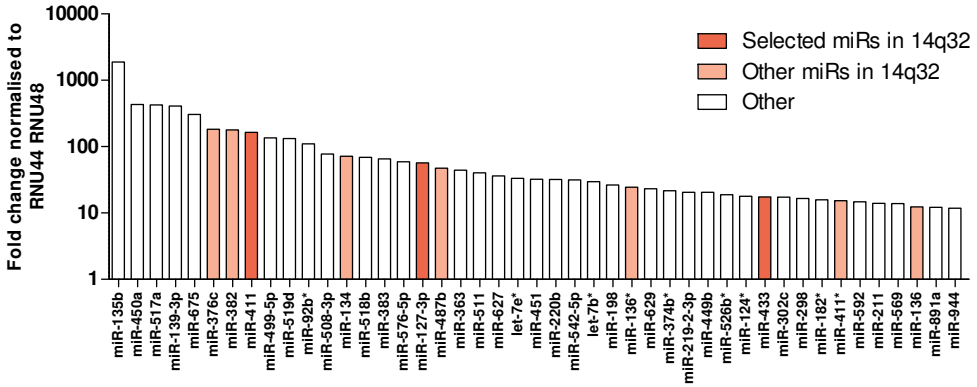

Figure 4.2: miRNA Expression in BT-474 Cells Treated with 5-Aza-2′-deoxycytidine (Aza) Relative to Untreated BT-474. miRNA profiling using the Human TaqMan Array Card for a single replicate of Aza treated and untreated BT-474 cells. This screen highlights the vast number of miRNAs affected by DNA demethylation. After fold change analysis a cut-off of 10 fold was selected.

4.2.2 14q32 miRNA Expression Changes in Aza and Trichostatin A (TSA) Treated Cell Lines

The results from the array suggests that expression of the miRNAs in the imprinted region can be altered by changes in methylation levels. To determine how epigenetic changes are involved in regulating miRNA expression in the lapatinib sensitive and acquired resistant lines, the samples were treated with the global demethylating agent Aza, the Histone deacetylase inhibitor Trichostatin A (TSA), or a combination of both agents.

Aza treatment should only lead to demethylation and increased expression of previously methylated genes. Histone acetylation is involved in chromatin structure, therefore by adding the HDAC inhibitor, the DNA is maintained in an open configuration. Nonetheless if the DNA is methylated, the open configuration will not affect gene expression. Thus the combination of both demethylation and an open chromatin structure, should lead to even higher levels of target gene expression than the single agent conditions. Due to the nature of these agents, the changes caused by both Aza and TSA are random. This leads to high variability between replicates. For this reason, the results shown in Figure 4.3 are of one representative experiment. Additional experiments are shown in Supplementary Figures 7.9 and 7.10.

In BT-474 cells treated with Aza, an increase in miRNA expression is observed relative to untreated BT-474 cells. This increase in miRNA is not observed in the BT-474/L cell line where there is less than a 3-fold increase in miRNA expression in the Aza treated cells compared to untreated BT-474/L cells. When the cells are treated with TSA alone, there is little variability in miRNA expression for miR127 and miR409 both in BT-474 and BT-474/L cells. A 10-fold increase is observed for miR495 in BT-474 cells, however, this is not the case in BT-474/L. The combination of Aza and TSA appears to have a synergistic effect in the sensitive BT-474 cells for miR127 and an additive effect for the other miRNAs (Figure 4.3a).

In HCC1954 and HCC1954/L cells, there is not much change in miR127 expression irrespective of the treatment, although an increase is observed in the Aza and TSA combination in the resistant cell line. For miR409 and miR495 and increase in miRNA expression is detected after Aza treatment and a synergistic effect is obtained after addition of both Aza and TSA, with little effect

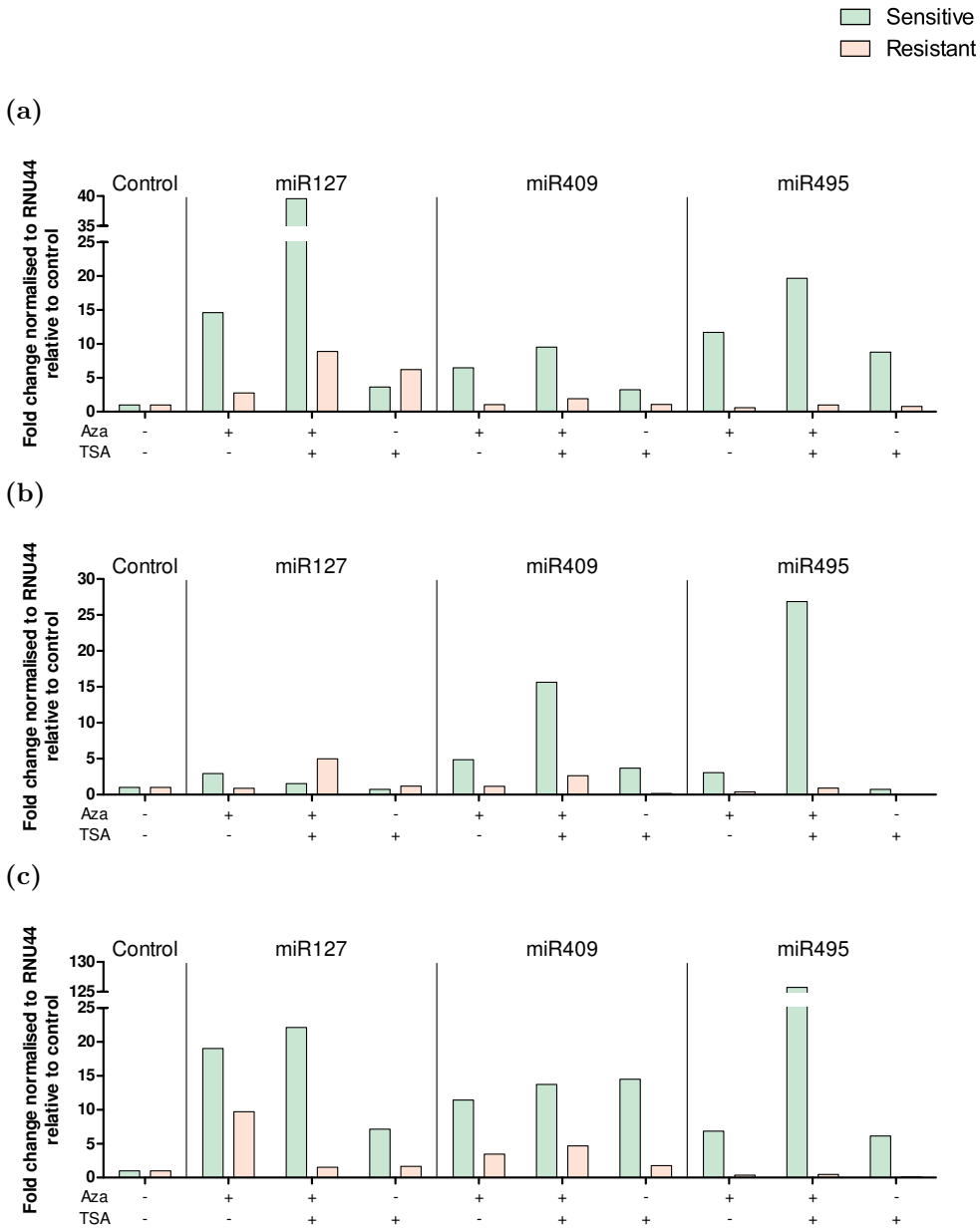

Figure 4.3: miRNA Expression after 5-Aza-2′-deoxycytidine (Aza) and Trichostatin A (TSA) Treatment. The data shown here is for one representative experiment of at least two replicates. Stem-loop RT-qPCR is expressed as fold change relative to RNU44 and normalised to the untreated condition for each cell line. This does not permit direct comparison of miRNA levels between the sensitive and resistant cells but shows the effect of each treatment on miRNA expression levels. (a) In BT-474 cells, after Aza treatment there is an upregulation of all three miRNAs compared to BT-474/L cells. This increase is greater when Aza and TSA are combined. (b) In HCC1954 cells there is some upregulation of the miRNAs in the sensitive cells after treatment with Aza, a further upregulation is observed when both Aza and TSA are combined. There is little change in HCC1954/L. (c) In SKBR-3 cells there is upregulation of the miRNAs in the Aza samples.

seen in the TSA single treatment in HCC1954. For these two miRNAs, there is little increase in expression with any of the treatments for HCC1954/L cells. A decrease in miRNA levels is even observed for the Aza or TSA alone conditions going up to a 90 % decrease for miR495 when treated with TSA (Figure 4.3b).

SKBR-3 cells respond to Aza treatment with an increase in expression of all three miRNAs, and the combination of Aza and TSA has a synergistic effect as greater miRNA overexpression of miR495 is observed. In this cell line TSA treatment alone also causes upregulation of the miRNAs. In the SKBR-3/L cell line, some upregulation of miR127 is detected after addition of Aza. Negligible changes in miRNA expression are observed in the other conditions (Figure 4.3c). These results suggest that for all the cell lines, the expression of the 14q32 miRNAs is regulated by epigenetic marks which are lost in the resistant cells, leading to increased expression of the miRNAs.

4.3 Methylation Levels are Altered in the 14q32 Region

The alterations in miRNA levels following methylation reversal indicated a role for methylation in controlling the expression of these miRNAs. To further investigate the role of methylation we examined the methylation levels in lapatinib sensitive and resistant cell lines.

4.3.1 Demethylation of the 14q32 Region Occurs after Aza Treatment in the Sensitive Cell Lines

To validate that Aza treatment led to the demethylation of the 14q32 region, bisulphite conversion followed by DNA re-sequencing was performed in the isogenic cells. During bisulphite conversion, unmethylated C residues are chemically modified to uracil (U) whilst m^5C remains unchanged. Through subsequent PCR the U is replaced with Tymidine (T) and m^5C with C; analysis of the sequencing data will identify the sites where C has remained unchanged and where it has been replaced by T, giving the methylation pattern of the region. Four different CpG regions; the IG-DMR, the *MEG3*-DMR, CpG region 1, and CpG region 2 (Figure 4.1) were interrogated.

The differences in methylation levels observed between the treated and un-

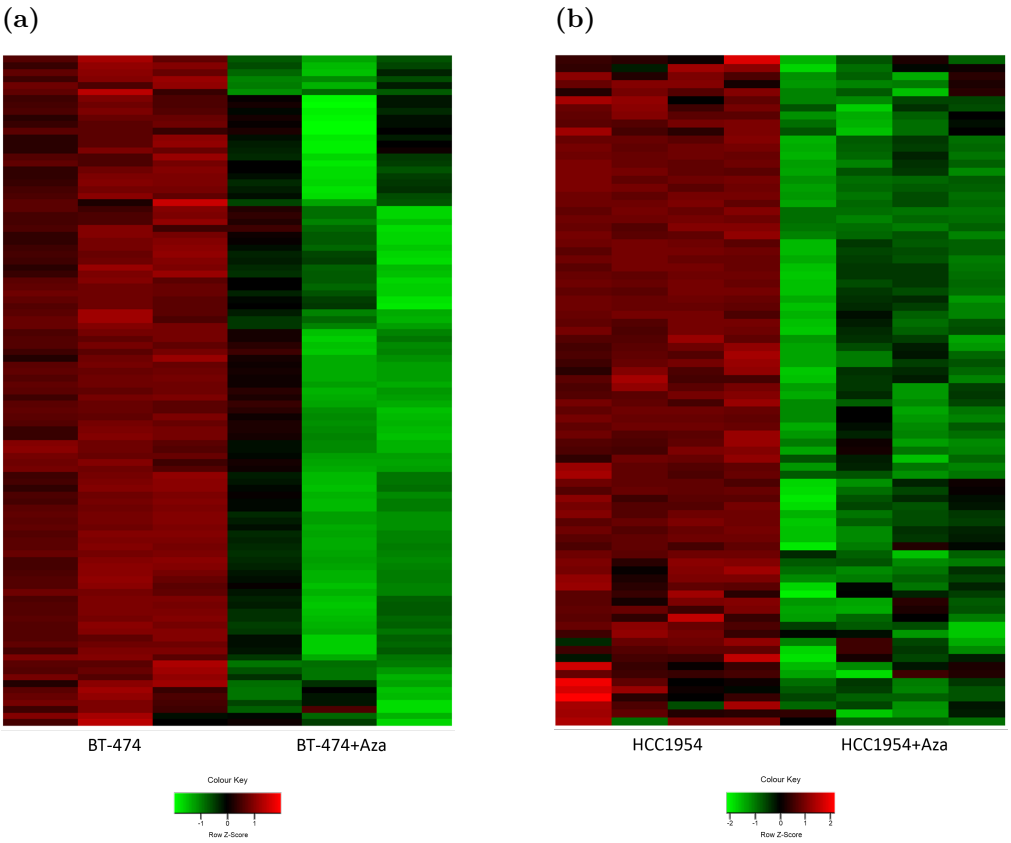

Figure 4.4: Methylation Changes in the 14q32 Region after Aza Treatment Measured by Methylation Resequencing. Each column of the heatmap represents one replicate, and each line a CpG site. (a) Heatmap of BT-474 and BT-474 with Aza treatment, (b) heatmap of HCC1954 and HCC1954 with Aza treatment. Both experiments show high levels of demethylation in the Aza treated samples.

treated samples reflects the changes in miRNA expression observed previously in the treated samples. Indeed, the Aza treated samples have lost most methylation marks at these sites (Figure 4.4). Methylation levels for each individual CpG site shown here is significantly changed in 3 to 4 replicates.

4.3.2 Lapatinib Resistant Cell Lines with Increased miRNA Expression Display Demethylation of the 14q32 Region

Since the use of a demethylating agent in the sensitive cells led to an increase in miRNA expression; differential methylation of this region could lead to the increase in miRNA levels observed in the resistant cells. To directly validate the control of methylation for the 14q32 region, bisulphite conversion and DNA re-sequencing was undertaken.

Globally, changes in the methylation patterns were observed between the sensitive and resistant pairs: BT-474 and BT-474/L, and HCC1954 and HCC1954/L cells (Figure 4.5). The CpG sites shown here were significantly changed between the lines in the 3 to 4 replicates used for analysis.

In BT-474 cells, the IG-DMR is methylated at levels higher than 75 %, these methylation marks are lost in the BT-474/L cells with levels reducing to 50 % or less. In the HCC1954 cell line, baseline levels of methylation are lower than 10 % on average, and in HCC1954/L cells methylation levels are increased to 50 %. There were no significant alterations between SKBR-3 and SKBR-3/L cells where methylation levels were altered more than 20 % (Figure 4.6a). The sites shown here were significantly changed between 3 or 4 replicates and displayed methylation level changes greater than 20 %.

In the *MEG3*-DMR methylation levels are altered in the distal region of the CpG island, changes in this region are observed in all three cell line pairs (Figure 4.6b and Table 4.1). Decreases in methylation levels are observed in both the CpG1 (Figure 4.6c) and CpG2 (Figure 4.6d) region between BT-474 and BT-474/L cell lines. Between HCC1954 and HCC1954/L lines there are few statistically significant decreases in methylation.

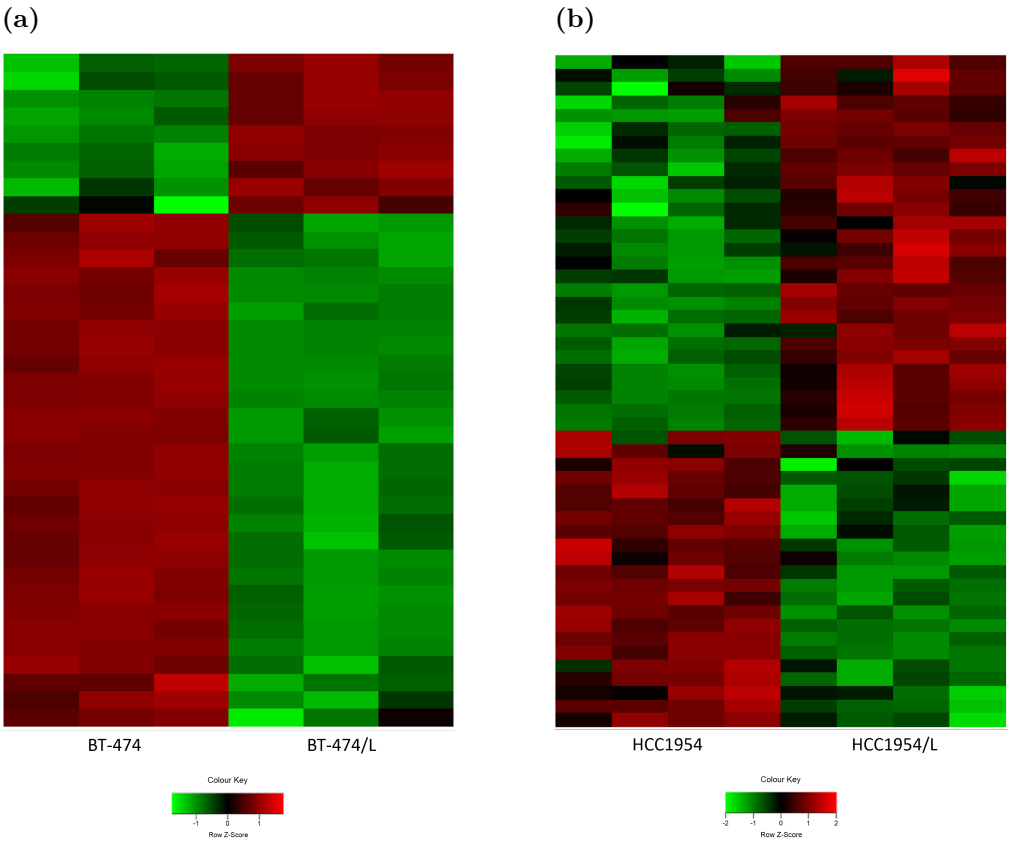

Figure 4.5: Methylation Changes in the 14q32 Region in Paired Sensitive and Resistant Cell Lines Measured by Methylation Resequencing. Each column of the heatmap represents one replicate, and each line a CpG site. (a) Heatmap of BT-474 and BT-47/L, (b) heatmap of HCC1954 and HCC1954/L. Both experiments show changes in methylation levels in the paired cell lines.

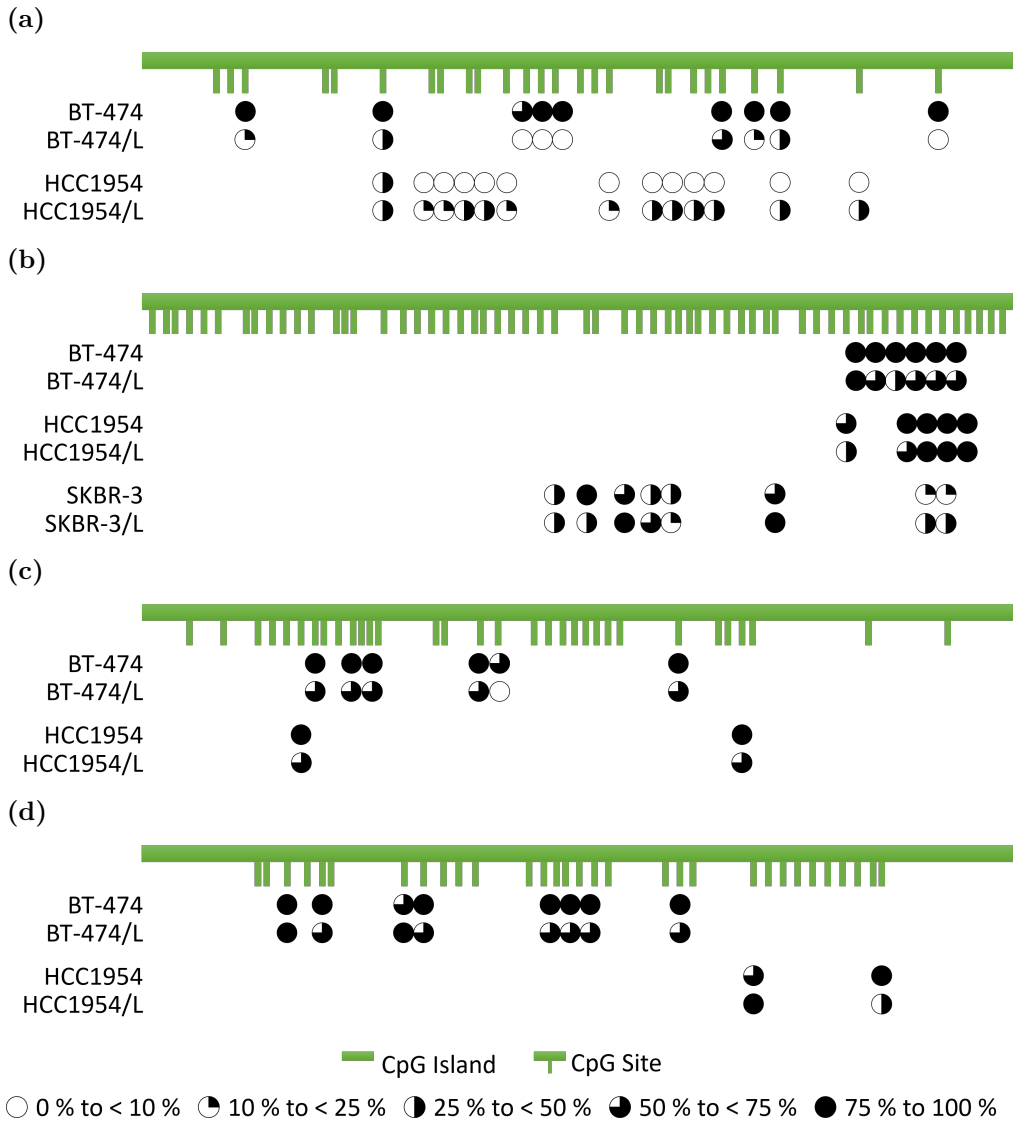

Figure 4.6: Significant Methylation Changes in the 14q32 Region Measured by Methylation Resequencing. Statistically significant changes, greater than 20 %, are represented here along with the neighbouring sites that are also significant but might have less than a 20 % change. (a) The intergenic-differentially methylated region (IG-DMR) is methylated in the BT-474 cells and demethylated in the BT-474/L cells, whereas it is mostly demethylated in HCC1954 cells and more methylated in the HCC1954/L line. (b) The differentially methylated region located on the *MEG3* gene (*MEG3*-DMR) is mostly methylated in both BT-474 and HCC1954 and is demethylated in the resistant BT-474/L and HCC1954/L cells. In SKBR-3 and SKBR-3/L cells, methylation levels vary across the region. (c) The first CpG island located in the 14q32.2 cluster is shown here, for both sensitive cell lines the region is methylated and it is less methylated in the resistant cells. (d) The second CpG island located in the 14q32.2 cluster is shown here, it is mostly methylated in BT-474 cells and less in the BT-474/L cells. There are few significant changes in methylation in the HCC1954 cells.

Cytosine Position	BT-474 (%)	BT-474/L (%)	HCC1954 (%)	HCC1954/L (%)	SKBR-3 (%)	SKBR-3/L (%)
823			62	39		
826	96	81				
844	95	69				
887	93	41				
900	96	69	90	70		
909	95	65	97	79	12	40
918	97	67	97	91	23	37
922			99	95		

Table 4.1: Percentage of Methylation in the *MEG3*-DMR. Results are shown for the individual CpG sites of the distal *MEG3*-DMR represented in Figure 4.6b. The cytosine position is given in reference to the starting position of the *MEG3*-DMR, listed in Table 2.18, which uses coordinates from the GRCh37/hg19 genome assembly.

4.4 Summary

Expression of genes in the 14q32 region is highly controlled by epigenetic changes. Through demethylation experiments we have identified DNA methylation as a mechanism controlling miRNA expression in this region. HDAC inhibition had a synergistic effect suggesting that histone acetylation is also involved in regulation of gene expression in this region. Methylation resequencing revealed demethylation with Aza treatment lead to the significant loss of methyl groups in the 14q32 region which resulted in an increase in miRNA expression.

Methylation changes were also observed between the isogenic sensitive and resistant cells, with different patterns reported within the pairs of cell lines. BT-474/L and HCC1954/L both displayed methylation levels in the IG-DMR lower than 50 %. This suggests that imprinted methylation levels are lost in these cells. HCC1954 also has low levels of methylation in this region. Moreover, both BT-474/L and HCC1954/L also displayed a decrease in methylation marks in the distal region of the *MEG3*-DMR; methylation changes in this region have been inversely correlated to alterations in miRNA expression (*327*). This indicates the decreased methylation in these regions could lead to the increased miRNA expression observed in the lapatinib resistant lines.

5 Putative Targets of 14q32 miRNAs and Their Role in Resistance

5.1 Target Selection from Gene Expression Array Comparing BT-474/L to BT-474 Cells

Having shown the miRNAs were upregulated by epigenetic changes in acquired resistance to lapatinib, we wanted to investigate whether the increase in miRNA was leading to resistance. Since miRNAs target the 3′UTR of mRNAs we therefore decided to study how gene expression between lapatinib sensitive and resistant BT-474 cells had changed. A combination of genome wide and *in silico* analysis was used to identify differentially expressed genes that were targets of the miRNAs.

5.1.1 Gene Expression Array Analysis

A first set of gene expression arrays was analysed identifying 261 significantly differentially expressed genes in BT-474/L compared to BT-474, with 142 up- and 119 downregulated (Figure 5.1). To increase the significance of these hits, the results were combined with the analysis of the gene expression array published by Liu *et al.* (*1*) (GSE16179). As there were no untreated controls in this data set, the DMSO controls were analysed instead. The samples were treated with a small amount of DMSO. DMSO is used as a vehicle to dissolve lapaintib for use in the IC_{50} experiments. There should, therefore, be very little change between the untreated and DMSO treated conditions. This comparison generated a list of 87 genes that were significantly differentially expressed in BT-474/L compared to BT-474 (Figure 5.2), with 41 up- and 46 downregulated genes. It is interesting to note that none of the 14q32 PEGs were found to be

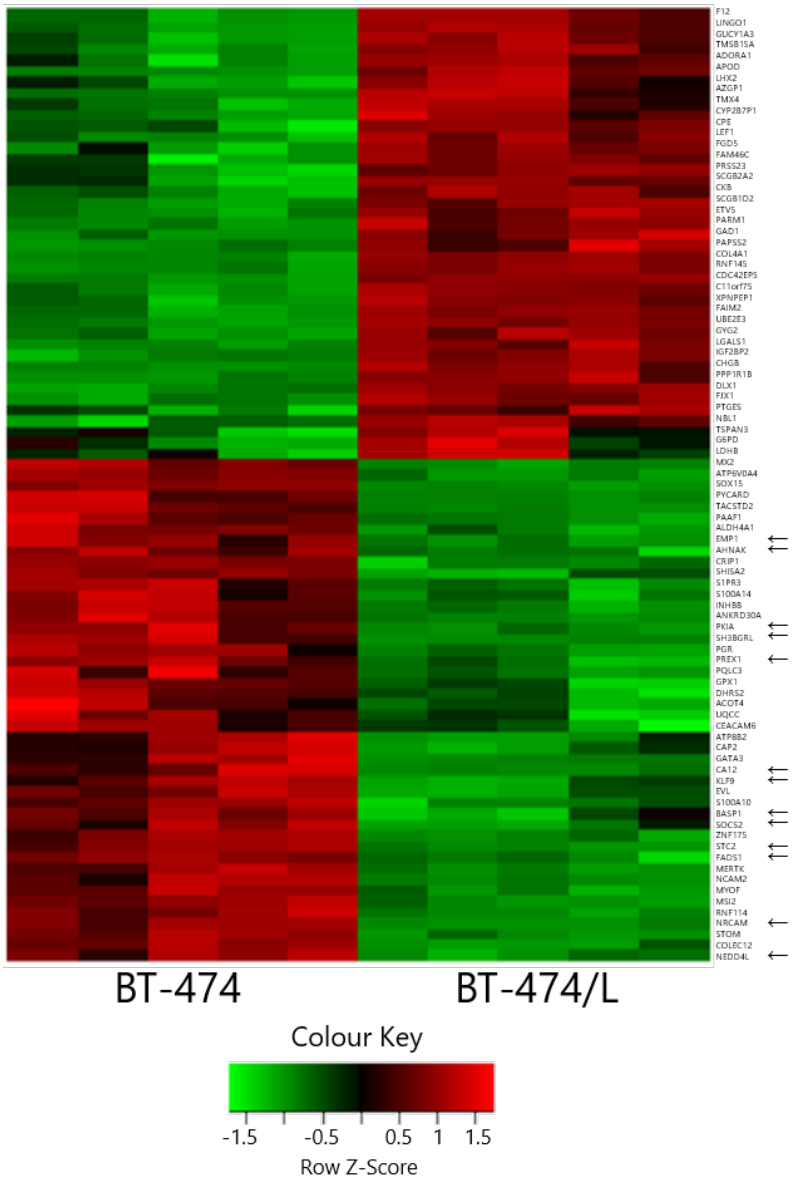

Figure 5.1: Heat Map of a Gene Expression Array Comparing BT-474 and BT-474/L cells. Cells were analysed using the Illumina Human HT12 v4.0 array, each column of the heatmap represents one replicate, and each line a gene. 261 genes (142 up- and 119 downregulated), with an adjusted p-value <0.05, were found to be differentially expressed between BT-474/L and BT-474 cells. Two independent arrays batch 1 and batch 2 were combined for this analysis.

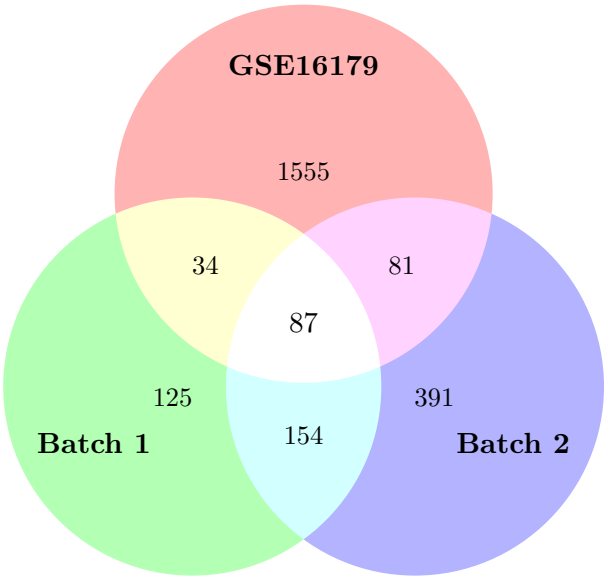

Figure 5.2: Comparison of the Number of Differentially Expressed Genes Between Array Batches 1, 2, and GSE16179. 87 genes were found to be significantly differentially expressed in BT-474/L cells compared to BT-474 which were common to all three arrays. The individual arrays were performed on different dates which could explain some of the difference between the arrays. The main difference is between the arrays performed on different platforms, this could be caused by the different arrays used as they don't have the same probes or be due to the fact that the experiments on the different platforms were performed in different laboratories. These factors introduce variation between the arrays which could cause variation in the results.

differentially expressed between the cell lines.

As there were more miRNAs that were highly upregulated than downregulated and here there were more downregulated genes compared to upregulated, we investigated downregulated genes as this could be caused by repression due to the increase in miRNA expression. However, it could also be interesting to look at upregulated genes as this could be caused by loss of repression due to a decrease in miRNA levels.

5.1.2 In Silico Analysis

In order to determine direct mRNA targets of the miRNAs upregulated in the resistant BT-474/L cells, only the downregulated genes were selected from the list of differentially expressed genes. This data was then compared to *in silico* predictions of putative miRNA targets obtained from miRWalk (*348*), TargetScan (*110*), RNA22 (*349*), and miRanda (*350*). These four databases were used to reduce the number of false negatives obtained. This identified 27 genes as being putative miR127, miR409, or miR495 targets, with 2 hits for miR127, 17 for miR409, and 23 for miR495 (Figure 5.3). The analysis found few miR127 targets but those identified were common to either two, miR127 and miR495, or all three miRNAs. miR409 and miR495 had the most overlap, with 12 genes being common to both miRNAs, 4 were miR409 targets only and another 9 were miR495 targets only.

miR495 was selected as it had the most downregulated putative targets in the gene set. Following mechanistic considerations, 13 targets, highlighted in Table 5.1, out of the 23 miR495 downregulated targets were selected for expression level validation by RT-qPCR in BT-474 and BT-474/L.

5.1.3 Gene Expression Array Validation

The miR495 target genes selected were validated by RT-qPCR (Figure 5.4). Of the 13 selected targets, AHNAK was not found to be significantly downregulated in BT-474/L compared to BT-474. FADS1 and EMP1 expression is decreased by less than 50 % in BT-474/L. Of the other genes, seven were selected for further functional validation, these are highlighted in Figure 5.4 and will

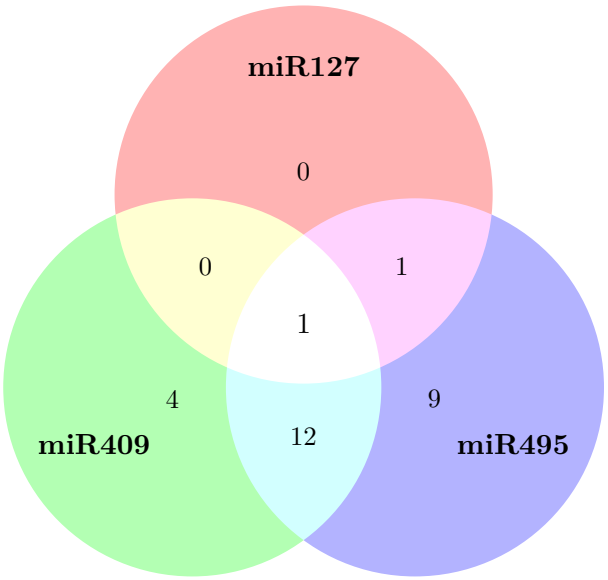

Figure 5.3: miRNA Seed Site Presence in Significantly Downregulated Genes in BT-474/L Cells Compared to BT-474. There are only two genes that have miR127 seed sites, one also has as site for miR495, and the other has sites for all three miRNAs. 12 targets have sites for both miR409 and miR495, 4 only have sites for miR409 and 9 only for miR495. Therefore miR495 has the most putative targets downregulated in BT-474/L cells compared to BT-474.

Symbol	Gene Name	miRWalk	miRanda	RNA22	TargetScan	Sum
AHNAK	AHNAK Nucleoprotein	1	0	0	1	2
ATP8B2	ATPase, Aminophospholipid Transporter, Class I, Type 8B, Member 2	1	0	0	0	1
BASP1	Brain Abundant, Membrane Attached Signal Protein 1	0	0	1	0	1
CA12	Carbonic Anhydrase XII	1	1	0	1	3
EMP1	Epithelial Membrane Protein 1	0	0	0	1	1
FADS1	Fatty Acid Desaturase 1	1	0	0	1	2
GATA3	GATA Binding Protein 3	1	1	0	1	3
INHBB	Inhibin Beta B	1	0	0	0	1
KLF9	Krüppel Like Factor 9	1	1	0	1	3
MSI2	Mushashi RNA-Binding Protein 2	1	1	1	1	4
MX2	MX Dynamin-Like GTPase 2	1	0	0	0	1
NEDD4L	Neural Precursor Cell Expressed, Developmentally Down-Regulated 4-Like	1	1	0	1	3
NRCAM	Neuronal Cell Adhesion Molecule	1	0	0	0	1
PAAF1	Proteosomal ATPase-Associated Factor 1	1	1	0	1	3
PGR	Progesterone Receptor	1	1	0	1	3
PKIA	Protein Kinase (cAMP-Dependant, Catalytic) Inhibitor Alpha	1	0	0	1	2
PQLC3	PQ Loop Repeat Containing 3	0	0	0	1	1
PREX1	Phosphatidylinositol-3,4,5-Triphosphate-Dependant Rac Exchange Factor 1	1	1	1	1	4
SH3BGRL	SH3 Domain Binding Glutamate-Rich Protein Like	1	1	0	1	3
SOCS2	Suppressor of Cytokine Signalling 2	0	0	0	1	1
STC2	Stanniocalcin	1	0	0	0	1
TACSTD2	Tumor-Associated Calcium Signal Transducer 2	1	1	0	1	3
UQCC	Ubiquinol-Cytochrome C Reductase Complex Chaperone	1	0	0	0	1

Table 5.1: miR495 Target Genes Downregulated in BT-474/L Lapatinib Resistant Cells Compared to Sensitive BT-474. Genes highlighted in grey were selected for further validation based on functional and mechanistic considerations. miRNA interaction prediction databases are listed on the right: miRWalk, miRanda, RNA22, and TargetScan, along with whether they predicted at least one hit for the target gene, marked as 1, or none, marked as 0. The number of databases that predicted the presence of a miRNA seed site in the 3′UTR of the gene is totalled in the column on the far right labelled Sum.

be discussed further. A list of putative mRNA targets for the miRNAs upregulated in the resistant cells was generated using the databases listed previously and the thirteen downregulated gene targets were compared to it. The presence of miRNA seed sites in their 3′UTR is shown in Figure 5.4.

All these targets have seed sites for at least two of the miRNAs selected (Figure 5.4). These genes are downregulated in the resistant cells, therefore to model resistance and investigate the role of the gene targets in acquired resistance to lapatinib, we used knock-down assays in the sensitive lines followed by IC_{50} experiments. The potential targets will now be discussed in detail.

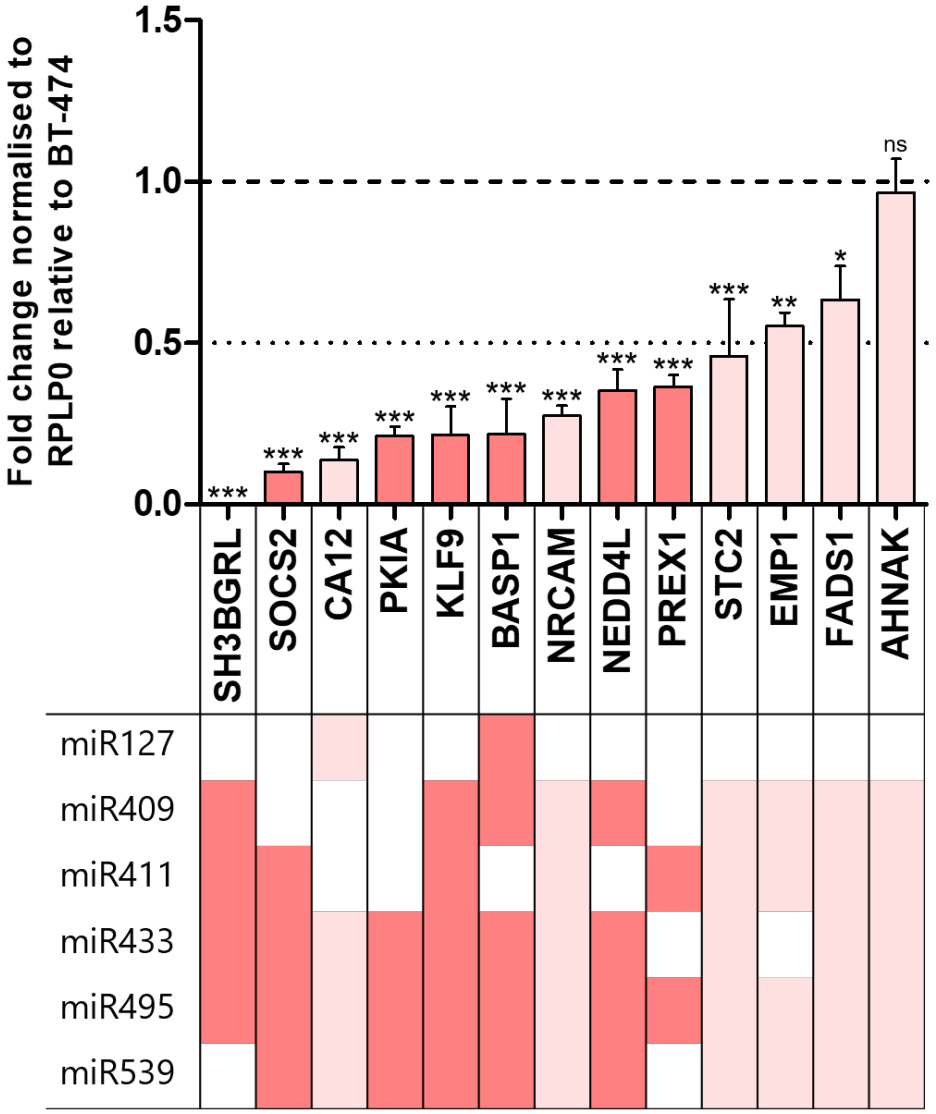

Figure 5.4: Downregulation of Targets in BT-474/L and miRNA Binding Sites. Targets selected for further validation are highlighted in a darker shade. mRNA expression values were obtained by RT-qPCR and results were analysed using the $\Delta\Delta$Ct relative quantification method and averaged for biological triplicates. mRNA expression was normalised to RPLP0 expression, relative to BT-474. Statistical significance is determined by one-way ANOVA with Dunnett's Multiple Comparison post-test. Where results are statistically significant p-values are shown on the graph, with $\star$ for $p \leq 0.05$, $\star\star$ for $p \leq 0.01$, $\star\star\star$ for $p \leq 0.001$, and ns for not significant. The presence of miRNA seed sites in each target is represented as a filled box in the column under the target name.

5.2 miRNA Target Genes Downregulated in BT-474/L are Involved in Resistance to HER2-Targeted Therapy

5.2.1 Suppressor of Cytokine Signalling 2

Suppressor of Cytokine Signalling 2 (SOCS2) has been suggested as a prognostic marker in ER+ breast cancers as high expression levels have been correlated with good prognosis (*351*). Loss of SOCS2 has been linked to increased cell proliferation and tumour growth (*352*); cancers that have lost SOCS2 have been found to be less differentiated. As such, it would be interesting to see if loss of SOCS2 affects response to HER2-targeting therapies.

SOCS2 was found to contain one putative miR495 seed site (Figure 5.5a), as well as sites for miR411, miR433, and miR539 (Figure 5.4).

Levels of *SOCS2* were found to be lower in HCC1954 and SKBR-3 cells compared to BT-474 (Figure 5.5b). In the resistant cells however it was only decreased in the BT-474 isogenic lines, BT-474/L and BT-474/T, a trastuzumab acquired resistance line (Figure 5.5c). BT-474/T was included in this analysis to compare the response of both of the BT-474 lines with acquired resistance to HER2-targeting therapy. There was an increase in SOCS2 expression in HCC1954/L and SKBR-3/L compared to their parental cell line (Figure 5.5d, e).

To replicate the miRNA targeted downregulation of SOCS2 and determine if loss of expression affects sensitivity to HER2-targeted therapy, IC_{50} values were determined following treatment with SOCS2 targeting siRNA. The experiments resulted in the downregulation of *SOCS2* in all three of the sensitive cell lines (Figures 5.6a, b, and c) which translated into a trend towards an increase in IC_{50} for both BT-474 and HCC1954 cells after siRNA knock-down (Figure 5.6d and e). These results, however, are not statistically significant. In SKBR-3 only siRNA 2 lead to a decrease in lapatinib sensitivity (Figure 5.6f). These results suggest that SOCS2 loss may contribute to lapatinib acquired resistance in BT-474/L cells.

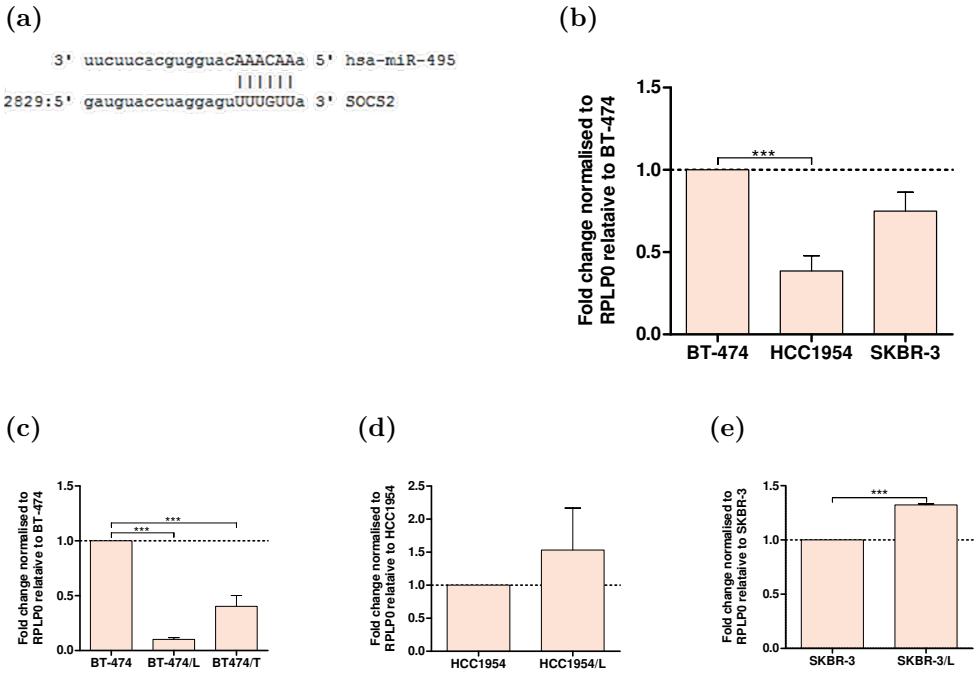

Figure 5.5: miRNA Seed Site and Baseline Expression Levels of *SOCS2*. (a) *SOCS2* contains a putative miRNA binding site for miR495. (b) Levels of *SOCS2* mRNA in all three sensitive cell lines compared to BT-474. mRNA levels in paired resistant and sensitive cell lines, normalised to the sensitive cell line for (c) BT-474, BT-474/L, and BT-474/T, (d) HCC1954 and HCC1954/L, and (e) SKBR-3 and SKBR-3/L. Statistical significance is obtained from a one-way ANOVA with Dunnett's Multiple Comparison post-test for (b) and (c), and Student's T-test for (d) and (e). Where results are statistically significant p-values are shown on the graph, with $\star\star\star$ for $p \leq 0.001$.

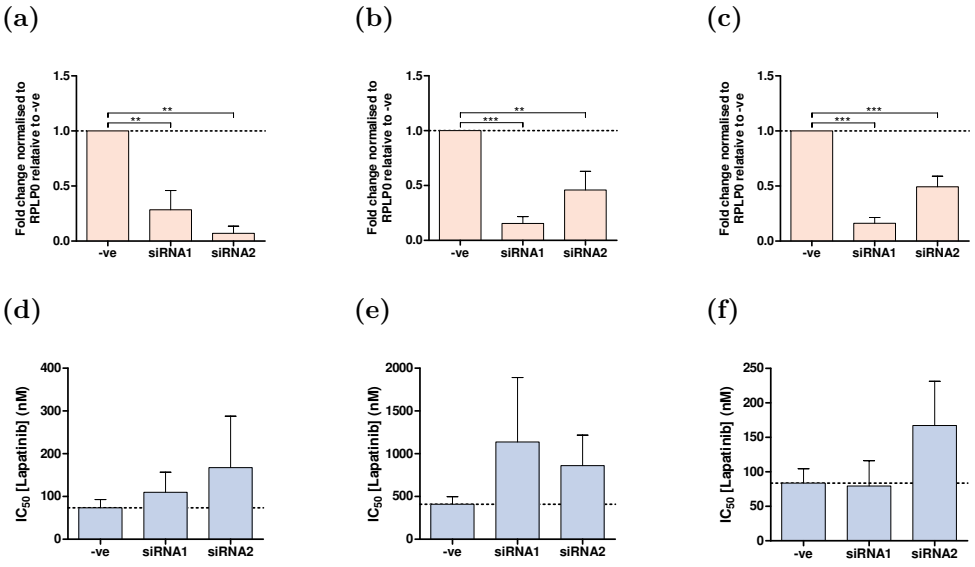

Figure 5.6: Effect of *SOCS2* Knock-down on Lapatinib Resistance. *SOCS2* mRNA expression after treatment with two different siRNAs normalised to the non-targeting control siRNA (-ve) in (a) BT-474, (b) HCC1954, and (c) SKBR-3. Lapatinib IC_{50} value after siRNA treatment in (d) BT-474, (e) HCC1954, and (f) SKBR-3. The IC_{50} values are obtained from non-linear regression analysis of cytotoxicity experiments and are averaged for at least three replicates. Statistical significance is obtained from a one-way ANOVA with Dunnett's Multiple Comparison post-test. Where results are statistically significant p-values are shown on the graph, with $\star\star$ for $p \leq 0.01$, and $\star\star\star$ for $p \leq 0.001$.

5.2.2 Protein Kinase (cAMP-Dependant, Catalytic) Inhibitor Alpha

Protein Kinase (cAMP-Dependant, Catalytic) Inhibitor Alpha (PKIA) inhibits the Cα and Cβ subunits of cAMP-dependent Protein Kinase (PKA) (*353*, *354*). PKA signalling has been found to be activated in trastuzumab resistant cell lines (*82*) and has also been identified as a driver of tumourigenesis in breast cancers through Proto-oncogene tyrosine-protein kinase Src (Src) (*355*). The latter has previously been shown to be important in the development and progression of breast cancer (*356*) as well as in trastuzumab resistance (*357*, *358*). Hence, downregulation of PKIA could be linked to resistance to HER2-targeting therapies.

PKIA was found to have three miRNA seed sites for miR495 (Figure 5.7a, b, and c) as well as sites for miR433 and miR539 (Figure 5.4).

Both HCC1954 and SKBR-3 express less *PKIA* mRNA than BT-474 (Figure 5.7d). In both BT-474 resistant cells, mRNA levels for *PKIA* are lower than in BT-474 sensitive cells (Figure 5.7e). This is also the case for the other two paired lapatinib sensitive and resistant cell lines, where the acquired resistant cells express less *PKIA* than their parental line (Figure 5.7f and g).

siRNA knock-down in the sensitive cell lines resulted in a significant decrease in *PKIA* expression for both siRNAs (Figure 5.8a, b, and c). Loss of PKIA expression led to shift in IC_{50} in both BT-474 (Figure 5.8d) and in HCC1954 (Figure 5.8e) which suggest a trend towards an increase in IC_{50}. These results, however, are not statistically significant. In SKBR-3 cells, only one siRNA, siRNA 2, appeared to lead to an increase in IC_{50} value.

This decrease in sensitivity to lapatinib observed after reduction of PKIA expression suggests that this target may be involved in acquired resistance to lapatinib in both BT-474/L and HCC1954/L cells.

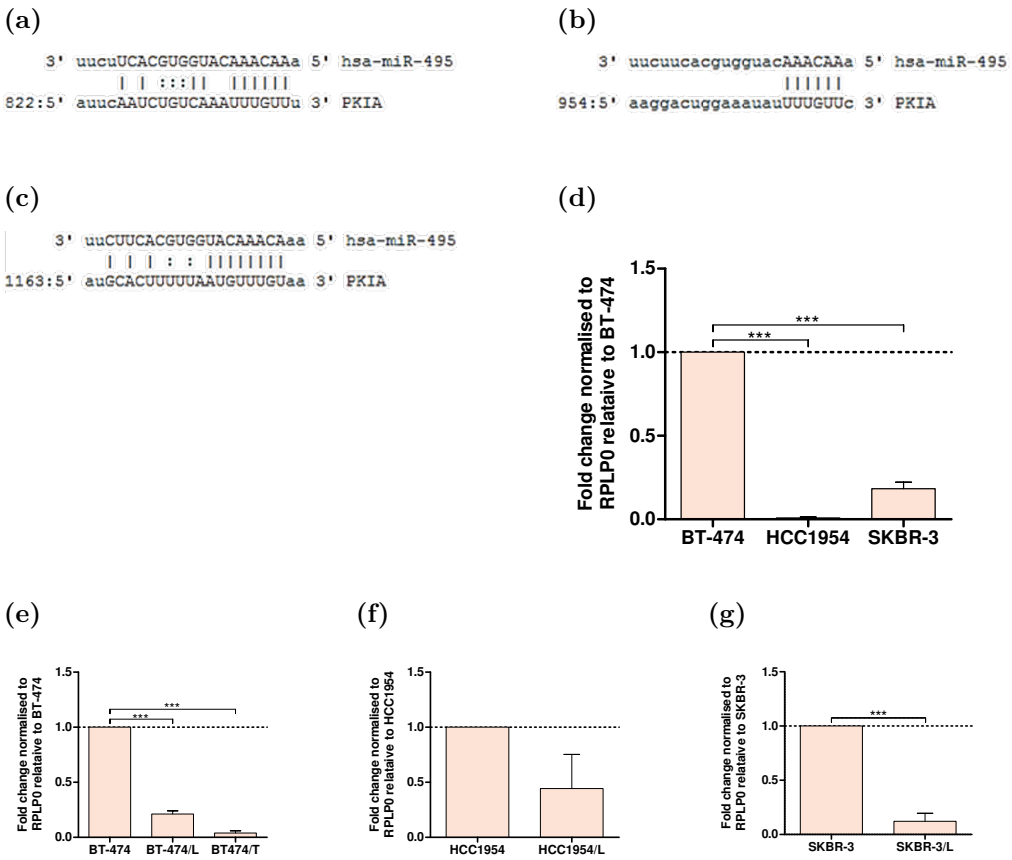

Figure 5.7: miRNA Seed Sites and Baseline Expression of *PKIA*. (a, b, c) *PKIA* contains three putative miRNA binding sites for miR495. (d) Levels of *PKIA* mRNA in all three sensitive cell lines compared to BT-474. mRNA levels in paired resistant and sensitive cell lines, normalised to the sensitive cell line for (e) BT-474, BT-474/L, and BT-474/T, (f) HCC1954 and HCC1954/L, and (g) SKBR-3 and SKBR-3/L. Statistical significance is obtained from a one-way ANOVA with Dunnett's Multiple Comparison post-test for (d) and (e), and Student's T-test for (f) and (g). Where results are statistically significant p-values are shown on the graph, with $\star\star\star$ for $p \leq 0.001$.

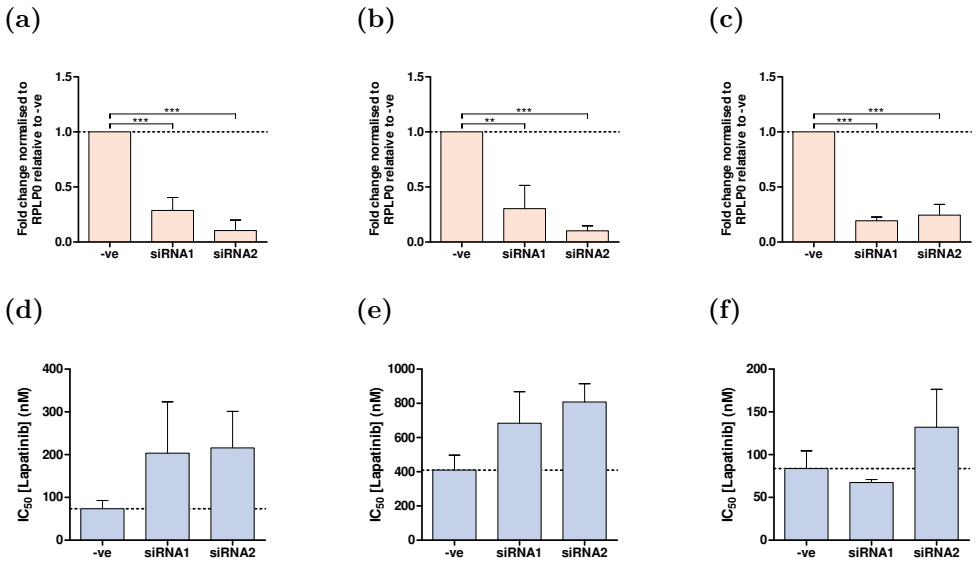

Figure 5.8: Effect of *PKIA* Knock-down on Lapatinib Resistance. mRNA expression after treatment with two different siRNAs normalised to the non-targeting control siRNA (-ve) in (a) BT-474, (b) HCC1954, and (c) SKBR-3. Lapatinib IC_{50} value after siRNA treatment in (d) BT-474, (e) HCC1954, and (f) SKBR-3. The IC_{50} values are obtained from non-linear regression analysis of cytotoxicity experiments and are averaged for at least three replicates. Statistical significance is obtained from a one-way ANOVA with Dunnett's Multiple Comparison post-test, where results are significant p-values are shown on the graph, with $\star\star$ for $p \leq 0.01$, and $\star\star\star$ for $p \leq 0.001$.

5.2.3 Brain Abundant Specific Protein 1

Brain Abundant Specific Protein 1 (BASP1) has been identified as a negative regulator of c-MYC as it inhibits *MYC* transcription (*359*). Low levels of BASP1 have been correlated to an upregulation in MYC, which leads to increased cell growth and proliferation (*360*). Additionally, MYC expression has been reported to be induced by Forkhead Box Protein O (FOXO) transcription factors in cells with reduced sensitivity to the lapatinib (*361*). This suggests that downregulation of BASP1 by upregulated miRNAs could be involved in upregulation of MYC in lapatinib resistance.

BASP1 was identified as a putative miR127 (Figure 5.9a), miR409 (Figure 5.9b) and miR495 (Figure 5.9c) target. BASP1 is also a miR433 and miR539 target (Figure 5.4).

BASP1 mRNA expression is lower in both HCC1954 and SKBR-3 cells compared to BT-474 (Figure 5.9d). In both of the BT-474 resistant lines, BT-474/L and BT-474/T, *BASP1* mRNA was decreased compared to BT-474 (Figure 5.10a). In the other resistant lines, HCC1954/L and SKBR-3/L, expression of *BASP1* was increased (Figure 5.10b and c).

siRNA knock-down was efficient in all three of the cell lines (Figure 5.10a, b, and c). This trended towards an increase in lapatinib IC_{50} for BT-474 (Figure 5.10d). There was only a trend towards an increase in IC_{50} value for one of the siRNAs in the other two cell lines, with siRNA 1 in HCC1954 cells (Figure 5.10e) and siRNA 2 in SKBR-3 cells (Figure 5.10f). These results, however, are not statistically significant.

After siRNA knock-down of *BASP1* (Figure 5.10g) BT-474 cells had an increase in IC_{50} for one of the siRNAs only (Figure 5.10h). This suggests that loss of BASP1 may be important for lapatinib resistance in BT-474/L cells.

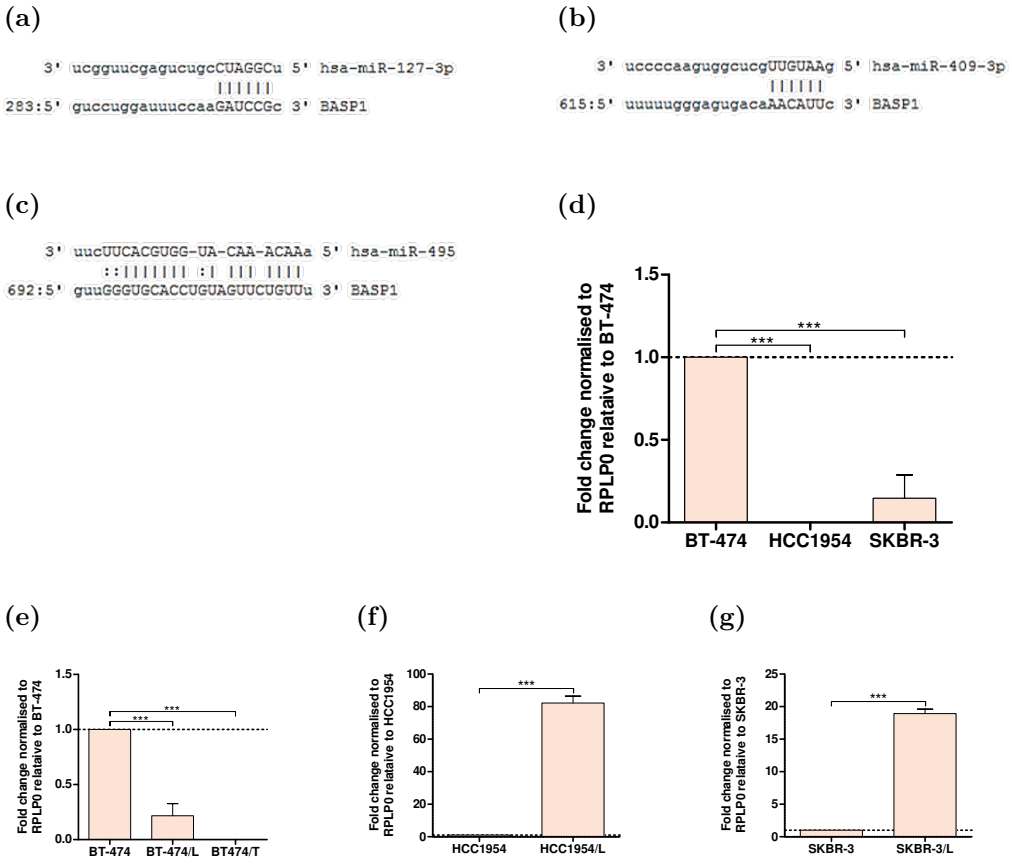

Figure 5.9: miRNA Seed Sites and Baseline Expression Levels of *BASP1*. *BASP1* contains putative miRNA binding sites for(a) miR127, (b) miR409, and (c) miR495. (d) Levels of *BASP1* mRNA in all three sensitive cell lines compared to BT-474. mRNA levels in paired resistant and sensitive cell lines, normalised to the sensitive cell line for (e) BT-474, BT-474/L, and BT-474/T, (f) HCC1954 and HCC1954/L, and (g) SKBR-3 and SKBR-3/L. Statistical significance is obtained from a one-way ANOVA with Dunnett's Multiple Comparison post-test for (d) and (e), and Student's T-test for (f) and (g). Where results are statistically significant p-values are shown on the graph, with $\star\star\star$ for $p \leq 0.001$.

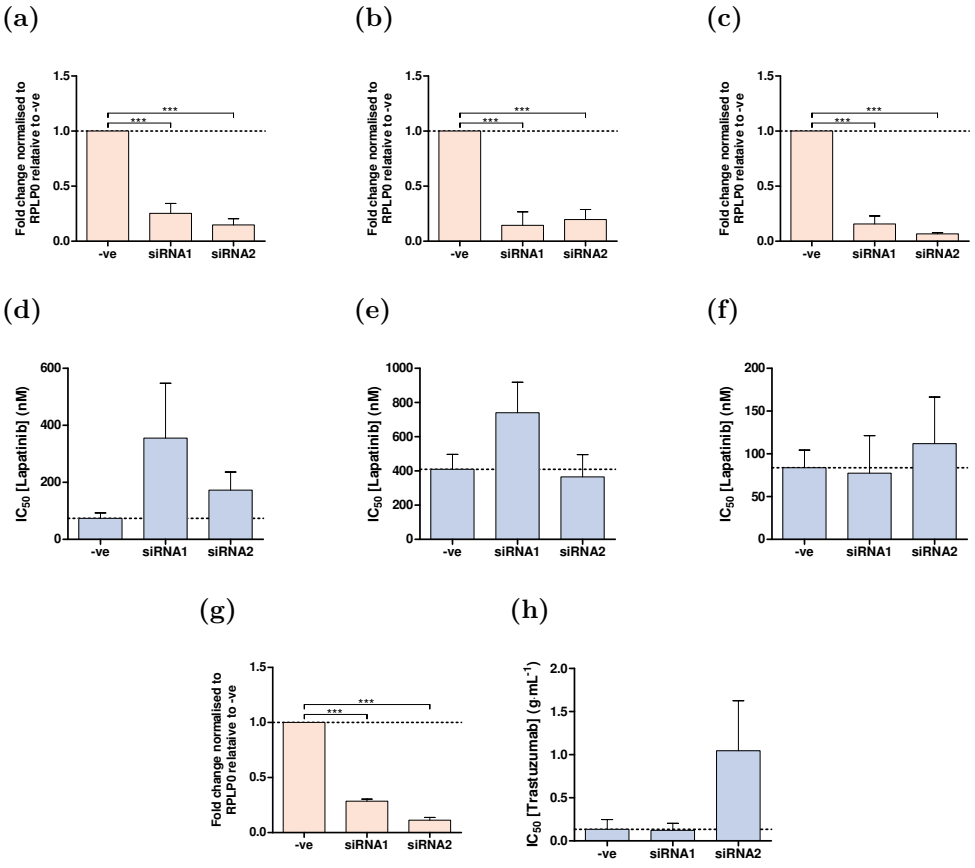

Figure 5.10: Effect of BASP1 Knock-down on Lapatinib and Trastuzumab Resistance. mRNA expression after treatment with two different siRNAs normalised to the non-targeting control siRNA (-ve) in (a) BT-474, (b) HCC1954, and (c) SKBR-3. Lapatinib IC_{50} value after siRNA treatment in (d) BT-474, (e) HCC1954, and (f) SKBR-3. Trastuzumab treatment was also used to confirm whether the effect observed in the cells was specific to lapatinib or could be applied to other HER2-targeting therapies. (g) mRNA changes in BT-474 cells after siRNA transfection for trastuzumab treatment. (h) BT-474 trastuzumab IC_{50}s after siRNA treatment. Statistical significance is obtained from a one-way ANOVA with Dunnett's Multiple Comparison post-test, where results are significant, p-values are shown on the graph with $\star\star\star$ for $p \leq 0.001$.

5.2.4 Neural Precursor Cell Expressed, Developmentally Down-Regulated 4-Like

Neural Precursor Cell Expressed, Developmentally Down-Regulated 4-Like (NEDD4L) is a ubiquitin ligase involved in negative regulation of the Dishevelled receptor (*362*). It has been reported to inhibit canonical Wnt signalling and downregulation of NEDD4L has been found to correlate with poor prognosis in colorectal cancers (*363*). Indeed, low levels of NEDD4L lead to increased canonical Wnt signalling, which means the cells are receiving more survival and proliferation signals. Additionally NEDD4L is also responsible for regulating Transforming Growth Factor Beta (TGF-β) (*364*) as well as its induced Smad complexes, thus moderating the extent of TGF-β downstream response (*365–367*). Furthermore, loss of NEDD4L and its inhibitory effect on TGF-β signalling has been linked to a poor prognosis in gastric cancers (*368*). Elevated TGF-β expression itself has been linked to poor prognosis in breast cancers (*369*).

NEDD4L was found to be a miR409 (Figure 5.11a) and a miR495 (Figure 5.11b, and c) putative target by three algorithms, miRWalk, miRanda, and TargetScan (Figure 5.1). It is also a target of miR433 and miR539 (Figure 5.4).

RT-qPCR showed NEDD4L mRNA is expressed at different levels between the three sensitive cell lines with BT-474 being the highest expresser. On the protein level HCC1954 appears to have the lowest levels of NEDD4L (Figure 5.11f). In the acquired resistant lines, the target mRNA was found to be downregulated in all three cell lines compared to their parental line (Figure 5.11g and h, and i). This result was validated by western blot for BT-474 and SKBR-3 lines, however, this did not appear to be true for HCC1954 and HCC1954/L.

BT-474/T, a trastuzumab acquired resistance line was also tested to identify whether the effect observed was specific to lapatinib or translated to HER2-targeted therapy in general. BT-474/T was found to have lost NEDD4L expression (Figure 5.11g).

To model the change observed in the acquired resistance lines, we used siRNA knock-down experiments to silence *NEDD4L* expression. In BT-474 cells, both siRNAs lead to efficient knock-down of the target on both the mRNA (Figure 5.12a) and protein levels (Figure 5.12d). This resulted in approximately a two

fold increase in IC_{50} to lapatinib for both siRNAs (Figure 5.12g).

HCC1954 cells displayed siRNA silencing of *NEDD4L* (Figure 5.12b), however, on the protein level siRNA 1 treated cells displayed better silencing of NEDD4L than siRNA 2 (Figure 5.12e). These results were reflected in the IC_{50} values as siRNA 1 resulted in a increase in IC_{50} and siRNA 2 did not (Figure 5.12h).

In SKBR-3 cells siRNA 1 lead to a 3-fold decrease in *NEDD4L*, siRNA 2 did not significantly affect expression (Figure 5.12c). Both siRNAs, however, even without much decrease in mRNA levels, resulted in loss of NEDD4L protein expression (Figure 5.12e) which lead to a trend suggesting an increase in lapatinib IC_{50} in the siRNA treated samples (Figure 5.12i). These results, however, are not statistically significant.

When BT-474 cells with reduced levels of *NEDD4L* (Figure 5.12j) were treated with trastuzumab there was a trend towards an increase in IC_{50} for one of the siRNAs (Figure 5.12k). These results, however, are not statistically significant.

These results suggest that an increase in miRNA levels which leads to the downregulation of NEDD4L may play a role in acquired resistance to lapatinib in both BT-474/L and SKBR-3/L.

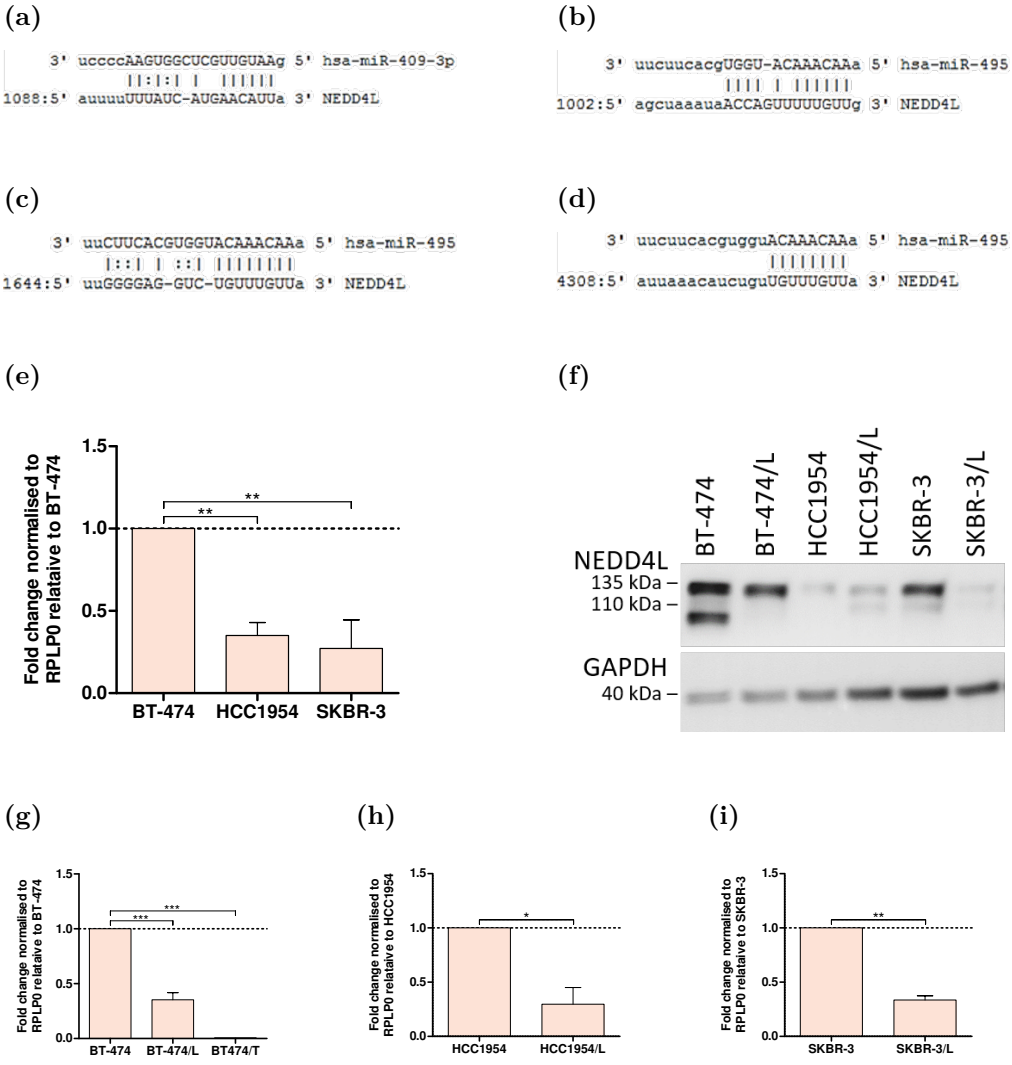

Figure 5.11: miRNA Seed Sites and Baseline Expression of NEDD4L. *NEDD4L* contains putative miRNA binding sites for (a) miR409, and (b,c,d) miR495. (e) Levels of *NEDD4L* mRNA in all three sensitive cell lines compared to BT-474. (f) Protein levels in paired resistant and sensitive cell lines. mRNA levels in paired resistant and sensitive cell lines, normalised to the sensitive cell line for (g) BT-474, BT-474/L, and BT-474/T, (h) HCC1954 and HCC1954/L, and (i) SKBR-3 and SKBR-3/L. Statistical significance is obtained from a one-way ANOVA with Dunnett's Multiple Comparison post-test for (e) and (g), and Student's T-test for (h) and (i). Where results are statistically significant p-values are shown on the graph, with $\star$ for $p \leq 0.05$, $\star\star$ for $p \leq 0.01$, and $\star\star\star$ for $p \leq 0.001$.

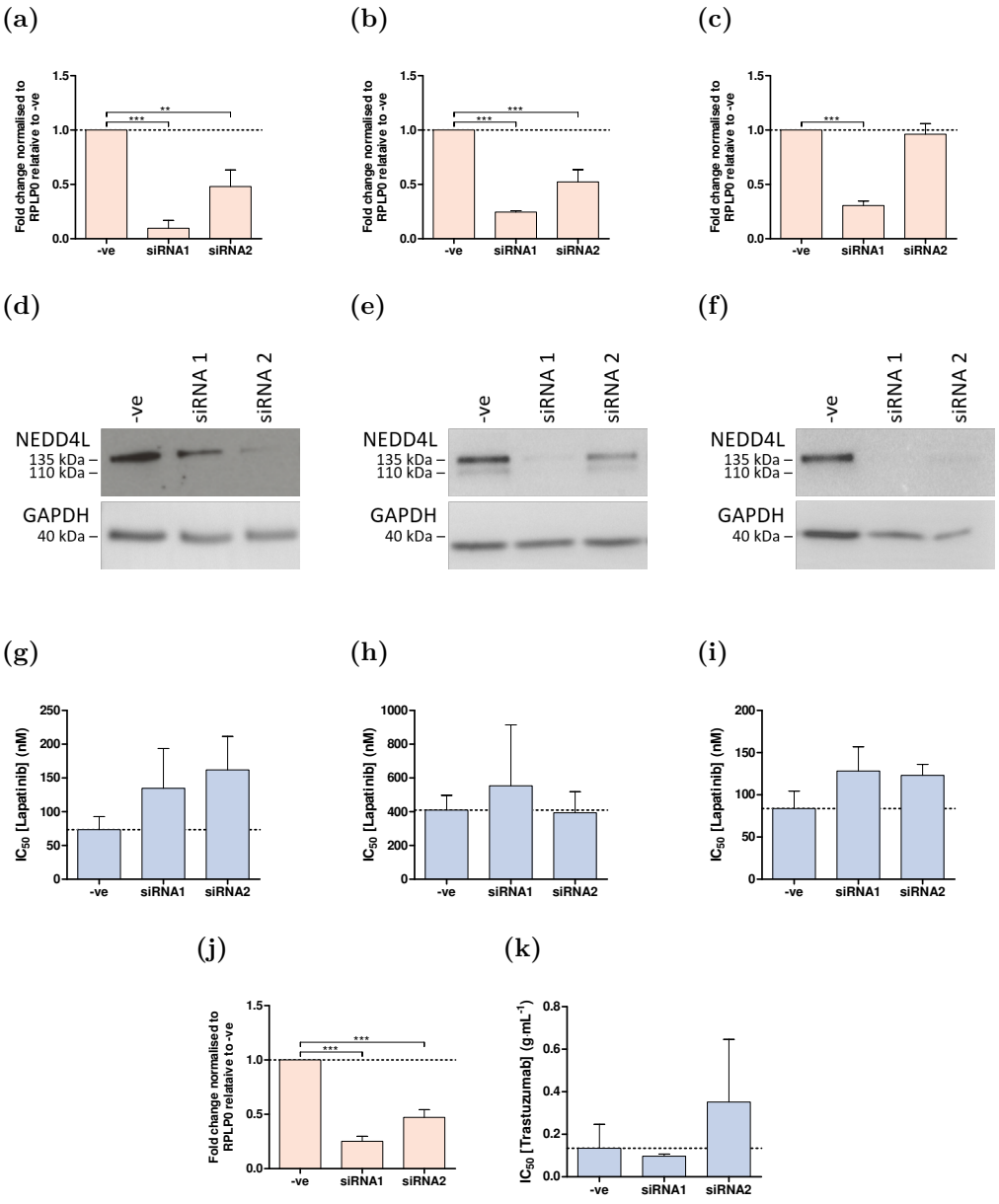

Figure 5.12: Effect of NEDD4L Knock-down on Lapatinib and Trastuzumab Resistance. mRNA expression after treatment with two different siRNAs normalised to the non-targeting control siRNA (-ve) in (a) BT-474, (b) HCC1954, and (c) SKBR-3. Protein knock-down in (d) BT-474, (e) HCC1954, and (f) SKBR-3. Lapatinib IC_{50} value after siRNA treatment in (g) BT-474, (h) HCC1954, and (i) SKBR-3. (j) mRNA changes in BT-474 cells after siRNA transfection. (k) BT-474 trastuzumab IC_{50}s after siRNA treatment. The IC_{50} values are obtained from non-linear regression analysis of cytotoxicity experiments and are averaged for at least three replicates. Where results are statistically significant, as determined by one-way ANOVA with Dunnett's Multiple Comparison post-test, p-values are shown on the graph, with $\star\star$ for $p \leq 0.01$, and $\star\star\star$ for $p \leq 0.001$.

5.2.5 SH3 Domain Containing Protein Ligand

The SH3 Domain Containing Protein Ligand (SH3BGRL) has been previously identified as a tumour suppressor in humans (*370*). Loss of SH3BGRL has been found to lead to v-Rel-mediated transformation of cells via activation of TGF-β/Sma- and Mad-Related Protein (SMAD) signalling (*371*). Additionally, elevated TGF-β signalling, along with EMT, have been observed in trastuzumab resistant cells (*372*).

SH3BGRL was found to have a miRNA binding site for miR409 (Figure 5.13a) and one for miR495 (Figure 5.13b). It also has miR411 and miR433 seed sites in its 3′UTR (Figure 5.4).

SH3BGRL is expressed at lower levels in the other two sensitive cell lines compared to BT-474 (Figure 5.13c), on the protein levels, these cell lines appear to have similar levels of SH3BGRL (Figure 5.13d); and was decreased in all three of the acquired resistant lines, both on the RNA and protein level (Figure 5.13d, e, f, and g). Additionally, *SH3BGRL* mRNA expression was decreased in BT-474/T cells (Figure 5.13e).

siRNA knock-down experiments resulted in good mRNA knock-down in all three cell lines (Figure 5.14a, b, and c). Yet in BT-474 and HCC1954, only one of the siRNAs led to a trend towards an increase in IC_{50} (Figure 5.14d and e) and none in SKBR-3 cells (Figure 5.14f). These results, however, are not statistically significant.

In the BT-474 cells with reduced *SH3BGRL* (Figure 5.14g) an increase in trastuzumab IC_{50} was observed (Figure 5.14h). This data suggests that, although loss of SH3BGRL does not appear to be involved in lapatinib acquired resistance, it seems to be important in trastuzumab resistance.

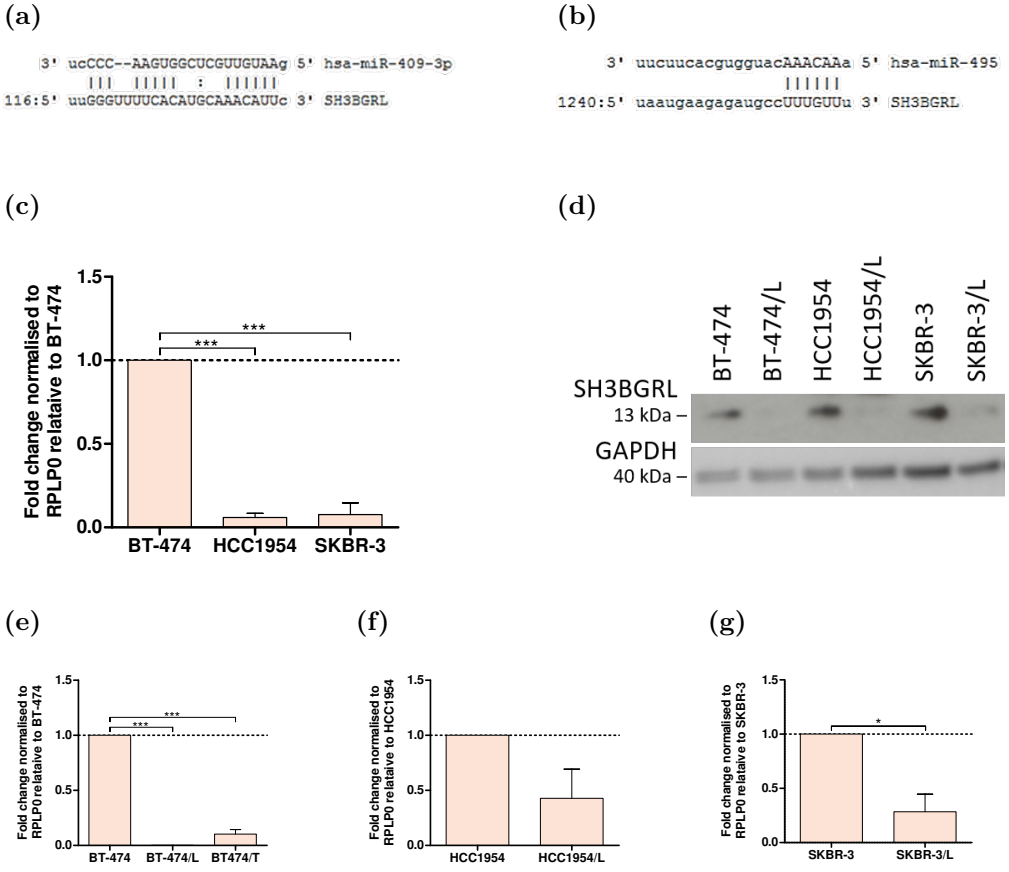

Figure 5.13: miRNA Seed Sites and SH3BGRL Baseline Expression. *SH3BGRL* contains putative miRNA binding sites for (a) miR409, and (b) miR495. (c) Levels of *SH3BGRL* mRNA in all three sensitive cell lines compared to BT-474. (d) Protein levels of paired resistant and sensitive cell lines. mRNA levels in paired resistant and sensitive cell lines, normalised to the sensitive cell line for (e) BT-474, BT-474/L, and BT-474/T, (f) HCC1954 and HCC1954/L, and (g) SKBR-3 and SKBR-3/L.Statistical significance is obtained from a one-way ANOVA with Dunnett's Multiple Comparison post-test for (c) and (e), and Student's T-test for (f) and (g). Where results are statistically significant p-values are shown on the graph, with $\star\star\star$ for $p \leq 0.001$.

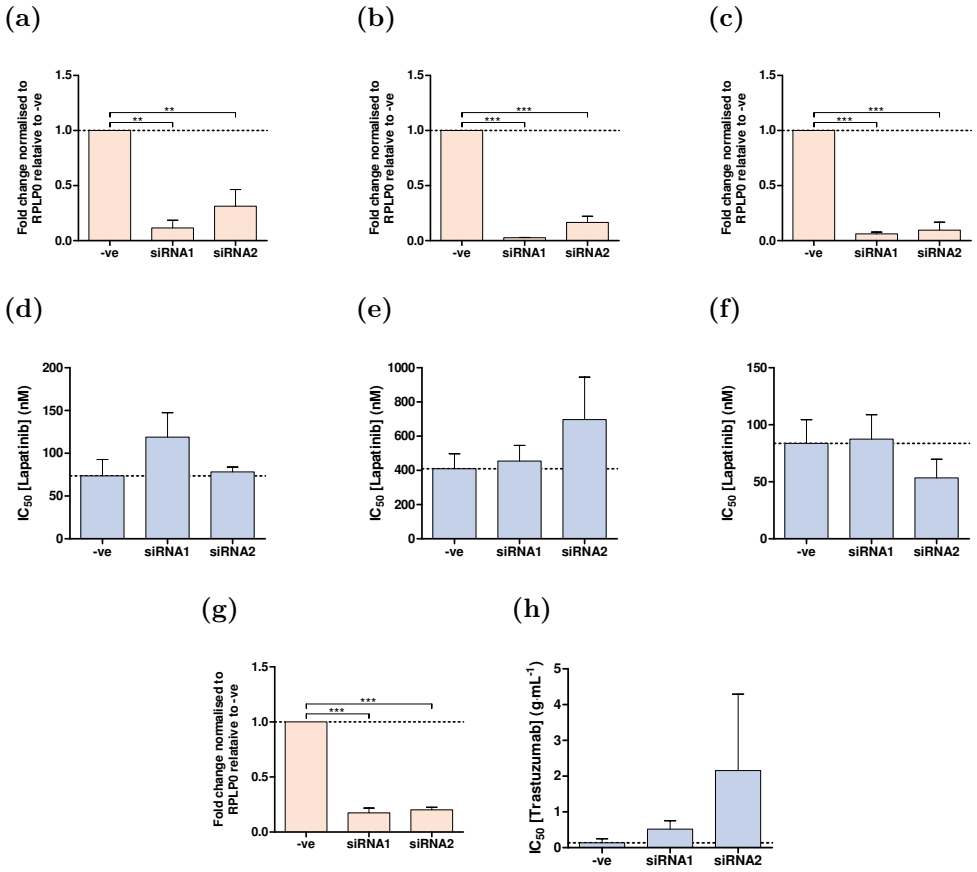

Figure 5.14: Effect of SH3BGRL Knock-down on Lapatinib and Trastuzumab Resistance. mRNA expression after treatment with two different siRNAs normalised to the non-targeting control siRNA (-ve) in (a) BT-474, (b) HCC1954, and (c) SKBR-3. Lapatinib IC_{50} value after siRNA treatment in (d) BT-474, (e) HCC1954, and (f) SKBR-3. Trastuzumab treatment was also used to confirm whether the effect observed in the cells was specific to lapatinib. (g) Target mRNA changes in BT-474 cells after siRNA transfection for trastuzumab treatment. (h) BT-474 trastuzumab IC_{50}s after siRNA treatment. The IC_{50} values are obtained from non-linear regression analysis of cytotoxicity experiments and are averaged for at least three replicates. Statistical significance is obtained from a one-way ANOVA with Dunnett's Multiple Comparison post-test. Where results are statistically significant p-values are shown on the graph, with $\star$ for $p \leq 0.05$, $\star\star$ for $p \leq 0.01$, and $\star\star\star$ for $p \leq 0.001$.

5.3 SOCS2, BASP1, NEDD4L, and SH3BGRL Appear to be Clinically Relevant to HER2-Targeting Treatment Outcome

To confirm these results and investigate how expression levels of these genes affect patient outcome we used data obtained from the NeoALTTO trial (ClinicalTrials.gov Identifier: NCT00553358). This trial looked at dual blockade of HER2 in the neoadjuvant setting for HER2+ early breast cancer, the study design is depicted in Figure 5.15. Patients were randomly assigned to treatment with either lapatinib alone, trastuzumab alone, or a combination of both HER2-targeting agents. Paclitaxel was also added to the treatments after six weeks. The patients then underwent surgery and received adjuvant chemotherapy in combination with their previous HER2-targeting regime (*373*). The primary endpoint is the rate of pathological complete response (pCR), defined in this study as ypT0/is ypN0, meaning the absence of disease in both breast and lymph node tissue regardless of the presence of DCIS (*374*).

Baseline frozen core needle tumour biopsies were collected and 135 were available for gene expression analysis (*375*). Due to this low number of patient data available, the treatment groups were combined for analysis. RNA expression data was used to calculate the pCR odds ratio for each of the target genes. NEDD4L, FADS1, STC2, and NRCAM all had significant p-values when the whole cohort was analysed. Of these, NEDD4L was the most downregulated in the gene expression array validation, results from this cohort do not show the other targets significantly affecting the outcome (Table 5.2).

We hypothesise that high expression of the target genes would lead to better survival for the patients. The top quartile of gene expression values was used to represent the high expressers for each target as the gene expression data had a positive skew in distribution. There was data for 135 patients, thus each quartile contained either 33 or 34 patients. After calculating the odds ratio for this subgroup, more than 70 % decrease in odds ratio was observed for BASP1 and SOCS2 between the whole cohort analysis and the top quartile result (Table 5.2). This suggests that patients with high expression of these genes are more likely to reach pCR.

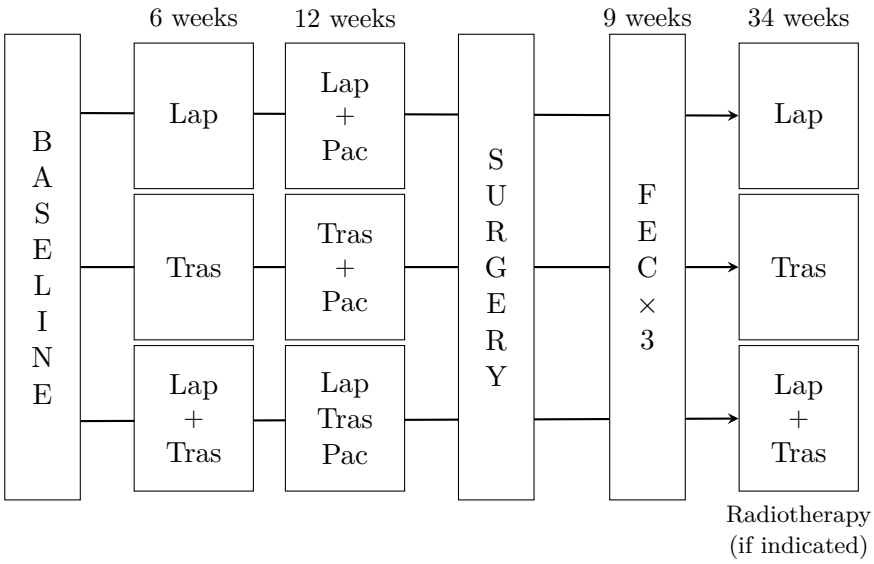

Figure 5.15: NeoALTTO Study Design (*373*). Baseline core needle tumour biopsy were collected and used for the gene expression analysis presented in Table 5.2. Lap: Lapatinib, Tras: Trastuzumab, Pac: Paclitaxel, FEC: Fluorouracil, epirubicin, and cyclophosphamide.

Gene	**Whole Cohort**				**Top Quartile**				Decrease in $OR_{(\%)}$
	OR	5 % CI	95 % CI	p-value	OR	5 % CI	95 % CI	p-value	
AHNAK	0.849	0.511	1.416	0.595	0.151	0.001	6.537	0.404	82
BASP1	0.865	0.742	1.008	0.117	0.196	0.008	2.019	0.225	77
SOCS2	0.778	0.557	1.061	0.196	0.207	0.024	1.000	0.089	73
CA12	0.939	0.776	1.136	0.585	0.269	0.006	2.982	0.389	71
NEDD4L	0.608	0.401	0.906	0.044	0.540	0.015	7.406	0.679	11
SH3BGRL	1.129	0.892	1.458	0.412	0.584	0.080	3.102	0.551	48
FADS1	1.463	1.057	2.045	0.056	0.720	0.216	2.191	0.567	51
STC2	0.733	0.569	0.929	0.036	0.871	0.289	2.018	0.766	-19
EMP1	1.112	0.883	1.402	0.450	0.875	0.163	3.673	0.861	21
PREX1	0.794	0.539	1.154	0.318	1.244	0.211	5.611	0.778	-57
NRCAM	0.695	0.511	0.918	0.040	1.374	0.625	3.221	0.432	-98
PKIA	0.962	0.771	1.194	0.771	1.776	0.717	4.752	0.219	-85
KLF9	1.225	0.695	2.173	0.556	6.479	0.643	90.507	0.128	-425

Table 5.2: Data Analysis of Gene Expression and pCR from the NeoALTTO Clinical Trail. Due to the small number of patients, the odds ratio for pCR was calculated for either the whole cohort or the top quartile of expressers for each gene. The targets that appear to be involve in either lapatinib or trastuzumab resistance are highlighted in the table. CI: confidence interval, OR: odds ratio.

The odds ratio for NEDD4L and SH3BGRL also decreased in the analysis of the high expressers, however the value only decreased by 10 and 48 % respectively. For PKIA on the other hand, there was almost a doubling in odds ratio (Table 5.2). This appears to suggest that high expression of PKIA is not beneficial to pCR. These results, however, are not statistically significant due to the low number of patients in the group analysed.

This trial is not the ideal setting to study the role of these genes in acquired resistance to HER2-targeting therapies as the RNA analysis was performed on baseline biopsies. This doesn't permit to take into account any changes in gene expression that might occur during the treatment course of the patients. In the case of acquired resistance this is the period of time when we would expect to see the most changes in miRNA expression and therefore in target gene expression. In this setting the data obtained might be more appropriate to study *de novo* resistance. Another consideration to be noted is that all patients are also receiving chemotherapy, which might influence the mechanism of resistance as this is putting additional pressure on the cells. Obtaining biopsies at different time points would allow the study of mRNA expression at baseline and after treatment generating results more relevant to acquired resistance. Looking at miRNA expression levels at these times would also permit a better understanding of the clinical relevance of the proposed miRNA role in acquired resistance. Another interesting experiment to do, would be to look at what targets these miRNAs are bound to within the cancer tissue after treatment. This can be done through biochemical isolation of the miRNA RISC with methods such as high-throughput sequencing of RNA isolated by crosslinking immunoprecipitation (HITS-CLIP). In this technique, the RNA bound proteins are cross linked through UV irradiation before undergoing immunoprecipitation. The RNAs are then be sequenced allowing the identification of mRNA targets for the miRNAs (*376*).

5.4 Summary

We previously identified miRNAs that were upregulated in acquired resistance to lapatinib. These will in turn affect gene expression in the acquired resistance lines. To identify miRNA gene targets affected by the changes we focused on a list of downregulated genes in BT-474/L compared to BT-474 obtained from

a gene expression array. This was compared to a list of mRNAs with putative miRNA binding sites predicted by various databases. This highlighted 23 miR495 target genes, these all have at least one other predicted miRNA seed site. 13 genes were then chosen for validation, of which one was found not to be downregulated in BT-474/L cells by RT-qPCR. From the downregulated genes, seven were selected for functional validation.

These results showed that, although none of the changes in IC_{50} are statistically significant, a trend is observed suggesting that NEDD4L, BASP1, SOCS2, and PKIA loss is involved in acquired resistance to lapatinib. When expression of these genes is lost the cells lose sensitivity to lapatinib.

SH3BGRL, appears to be exclusive to BT-474 cells. The last two targets tested, KLF9 and PREX1, did not appear to be involved in acquired resistance to lapatinib as their loss did not affect sensitivity to lapatinib in the cells tested.

The experimental data confirmed that the reduction in expression levels of BASP1, SOCS2, NEDD4L, or SH3BGRL was sufficient to increase the IC_{50} value of the cell lines to either lapatinib or trastuzumab. The NeoALTTO data, suggests that these targets could be involved resistance to HER2-targeting therapies, as high expressers of the genes appeared to have better pCR. However, as mentioned previously, this is linked to intrinsic resistance rather than acquired resistance as the mRNA samples were extracted from baseline biopsies. Altogether this suggests that these genes could be involved in resistance to HER2-targeting therapies. Thus these proteins, or other downstream proteins, could be targeted to overcome resistance to HER2 therapies.

6 Discussion

6.1 Overview

HER2+ breast cancer remains a significant clinical challenge, despite improved outcome of patients following targeted therapy. Few patients respond to the treatment (*77*) and a significant portion display primary resistance (*50*). To improve the outcome, it is important to study the process of acquired resistance and identify new therapeutic targets to overcome refractory disease progression.

Here, through demethylation assays and methylation resequencing, we have shown that demethylation of key sections in the 14q32 domain causes to increased expression of miRNAs coded in this region which are involved in acquired resistance to lapatinib. Subsequently, this leads to downregulation of certain target genes of the upregulated miRNAs, identified by gene expression array and *in silico* analysis. Therefore, we propose a novel mechanism of acquired resistance to HER2-targeted therapy initiated by epigenetic changes in the 14q32 region leading to an increase in expression levels of miRNAs in this region. In turn these miRNAs will repress the expression of gene targets. We have identified four downregulated targets, with the potential to be involved in resistance, SOCS2, BASP1, NEDD4L, and SH3BGRL (Figure 6.1).

6.2 Cells with Intrinsic Resistance to Lapatinib Adapt Through Different Resistance Mechanisms

JIMT-1 and MDA-MB-361 are both intrinsically resistant to lapatinib and do not respond to the drug. Both cell lines are also resistant to trastuzumab (*66*, *77*) but are sensitive to neratinib. This is likely to be due to the difference in mechanisms of drug action, as neratinib exposure leads to G1/S phase ar-

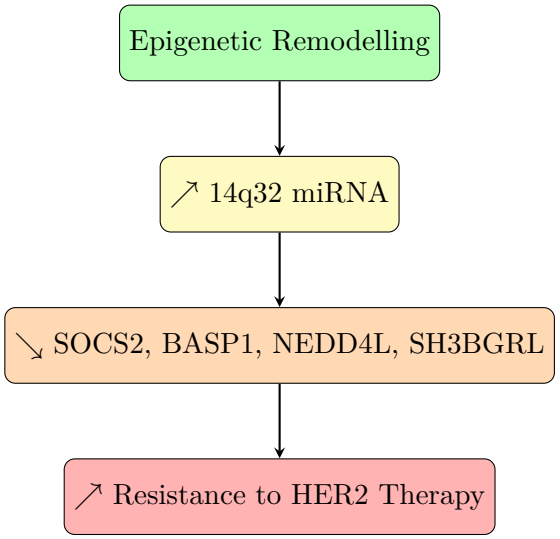

Figure 6.1: Proposed Mechanism for Acquired Resistance to Lapatinib. Epigenetic remodelling in the 14q32 region of HER2+ breast cancer cells sensitive to targeted therapy leads to an increase expression of miRNAs from these clusters. This in turn causes downregulation of target genes such as SOCS2, BASP1, NEDD4L, or SH3BGRL leading to an increase in resistance to HER2-targeting therapy.

rest (*377*) whilst lapatinib has been found to induce G0/G1 phase arrest (*378*, *379*). Additionally, these cells display differing cross-resistance patterns for dacomitinib. JIMT-1 is resistant to the drug, which, like lapatinib, leads to G0/G1 phase arrest (*68*), however, as dacomitinib is a pan-HER inhibitor this could account for the sensitivity of MDA-MB-361 cells to this treatment. Therefore, the intrinsically resistant lines might still be dependent on signalling through other HER receptors. The different response of the cells to dacomitinib could also originate from differences between the two cell lines: they are derived from metastatic site in different patients. JIMT-1 originates from a pleural effusion and MDA-MB-361 the brain. Additionally MDA-MB-361 expresses ER which JIMT-1 does not.

miRNA levels in these cell lines are quite different, with MDA-MB-361 displaying high levels of miRNAs, similar to those in BT-474/L, and JIMT-1 having low levels of 14q32 miRNAs similar to those in the sensitive BT-474. There is, therefore, a heterogeneity in response to different types of therapies across genetically diverse, yet classed as the same subtype, cancers. It might, however be interesting to study the selected gene targets in the MDA-MB-361 cells in order

Cell Line	Trastuzumab	Neratinib	Dacomitinib
BT-474/L			
HCC1954/L			
SKBR-3/L			

Table 6.1: Summary of Lapatinib Acquired Resistant Cell Line Cross-Resistance. Sensitivity to the drug is shown in green and resistance in red. These results are detailed in Figure 3.2. BT-474/L is resistant to all the other drugs tested, whilst SKBR-3/L is sensitive to all. HCC1954/L shows a more nuanced cross resistance pattern.

to identify whether these targets are involved in both acquired and intrinsic lapatinib resistance when there is increased 14q32 miRNA signalling.

These results confirm that miRNA changes leading to the development of acquired resistance do not mimic intrinsic resistance.

6.3 Lapatinib Acquired Resistant Lines Display Different Phenotypes Suggesting Adaptation Through Different Mechanisms

6.3.1 Lapatinib Acquired Resistant Cells Display Different Cross-Resistance Patterns to Other HER2-Targeting Agents

It appears that all three cell lines have adapted differently to develop acquired resistance to lapatinib. This is evidenced in the different cross-resistance patterns observed, as previously described in the results (Figure 6.1). Trastuzumab is the least effective drug as can be expected since it is a reversible HER2 inhibitor; the cells treated here have already become resistant to lapatinib which also targets HER2. They could therefore have accumulated HER2 receptor mutations (*78*) as well as switched to signalling through different RTKs (*1*) to overcome HER2 inhibition. Although SKBR-3/L can still be treated with trastuzumab, its sensitivity has halved.

It is important to note that neither lapatinib, neratinib, nor dacomitinib are routinely used in treatment of advanced breast cancer although they are involved in optimisation studies. The two pan-HER inhibitors, neratinib and dacomitinib, do not have the same effect on the cell lines. These are two irreversible small molecule inhibitors therefore they covalently bind the receptor active site and permanently block its activity. Dacomitinib has not been used in clinical trials for HER2+ breast cancers whilst neratinib is licenced and has been used in a phase III trial (*380*). The drug has been shown to slightly improve patient survival even after trastuzumab or lapatinib treatment (*380*, *381*), however in a previous phase II trial it was also shown to bring no benefit or disadvantage when compared to lapatinib treatment (*382*).

In the cell lines tested here, BT-474/L is resistant to both neratinib and dacomitinib, whereas HCC1954/L is only resistant to neratinib, and HCC1954/L and SKBR-3/L are sensitive to dacomitinib. The various resistance patterns observed between the cells suggest they have adapted to lapatinib exposure differently. They could also be due to the differences between the cell lines. BT-474 and HCC1954 are both derived from primary ductal carcinomas, but BT-474 is ER+ and PR+ whilst HCC1954 is negative for both. SKBR-3, which is also ER- and PR- is derived from a metastatic pleural effusion site. These difference between the cells could contribute to the differing cross-resistance observed.

The varying degree of response to the pan-HER therapies could also be due to the disparate binding affinities the two compounds have to the individual HER-family receptors and the difference in their mode of action; while neratinib treatment leads to G1-S phase arrest (*377*), dacomitinib exerts its anti-proliferative effect through G0/G1 arrest and induction of apoptosis (*68*). These mechanisms could be a reason HCC1954/L responds to dacomitinib but is resistant to neratinib.

Both these agents have previously been shown to be effective against lapatinib or trastuzumab resistance *in vitro* (*68*, *383*, *384*), however, here we have shown that they cannot reliably be used to treat lapatinib resistant lines. Therefore, in clinical trials where patients have been previously treated with other HER2-targeting agents, it might be necessary to further stratify patients in order to derive optimal benefit from neratinib once they have progressed through their treatment.

6.3.2 Lapatinib Acquired Resistant Cells Display a Different Behaviour and Appearance Compared to their Parental Line

Another difference observed between the three cell lines comes from their growth speed. BT-474/L was found to proliferate at a much faster rate than both the other resistant lines as well as its isogenic pair; the other two resistant lines divide at slower rates. These results further confirm the cells have adapted differently. The faster growing cell line could have become more invasive, as suggested by the increase in stress fibres in the cytoplasm of the cells as well as their irregular appearance with many lamellipodia and filopodia. The other two lines could be developing more stem cell-like features, such as quiescence, explaining their slower population doubling rate. A gel invasion assay would, however, be necessary to confirm the invasiveness of the cells.

Moreover, both BT-474/L and HCC1954/L were shown to, on average, have a larger cytoplasmic area than their paired sensitive line, with the difference not only caused by an increase in nucleus size. This could be due to TGF-β induced EMT which has been found to lead to an increase in cell size (*385*). This is also accompanied by an increase of invasive behaviour such as the development of lamellipodia, filopodia, and stress fibres, necessary for migration (*386*, *387*) and consistent with EMT (*388*, *389*).

Overall this suggests that certain of the lapatinib resistant cells have undergone EMT, which could have contributed to their resistant phenotype. Indeed, EMT has previously been associated with reduced drug sensitivity in cancer (*390–393*). Additionally, TGF-β induced EMT can be promoted by miRNAs located in the 14q32 region: miR487a (*394*), miR134, miR487b, and miR655 (*395*); and artificial overexpression of 14q32 miRNAs has been shown to lead to more migratory and invasive cells (*341*).

HCC1954/L, however, shows a large spread in individual cell size suggesting not all cells have an enlarged cytoplasm. SKBR-3/L cells do not appear to be significantly bigger than the sensitive line, which would be consistent with these cells becoming more stem cell-like rather than becoming more invasive. Cells with stem cell features have been found to be resistant to chemotherapy (*396*, *397*). Cancer stem cells can also arise as a result of EMT (*398–400*), and can have high TGF-β expression (*401*, *402*). Furthermore, increased levels of miRNAs from the 14q32 have been linked to cells developing more stem cell-

like features in hepatocellular carcinoma (*403*) and miR495 was shown to be involved in breast cancer stem cell formation (*307*).

In order to confirm this hypothesis, further validation would be required; 5-bromo-2′-deoxyuridine (BrdU) incorporation assays could be carried out to asses the stemness of the cell population (*404*) as well as flow cytometry analysis using expression of know cancer stem cell markers, such as $CD44^{+}$ and $CD24^{-/low}$ (*307*), to quantify the stem cell population. Invasion assays could also be carried out to measure the invasiveness of the cell populations, additionally, levels of known markers of EMT, such as loss of CDH1 or upregulation of Snail Family Transcriptional Repressors 1 (SNAI1) and 2 (SNAI2) (*405–407*) could be investigated. In the Illumina arrays, 34.5 % average decrease of CDH1 was observed in BT-474/L compared to sensitive BT-474. These results were not statistically significant, therefore, RT-qPCR or western blot assays would be necessary to confirm the loss of CDH1 in BT-474/L resistant cells. A 4.5 % and 2 % decrease was observed for SNAI1 and SNAI2 respectively. As these changes are so small and results were also not statistically significant, further experimental validation would be necessary to conclude on the expression status of these genes in the resistant lines.

6.4 Epigenetic Changes Lead to Increased Expression of miRNAs from the 14q32 in Acquired Resistance to Lapatinib

6.4.1 14q32 miRNA Expression is Upregulated in Acquired Resistance to Lapatinib

All of the lapatinib acquired resistant cell lines studied here display an increase in expression of miRNAs from the 14q32 region compared to their isogenic parental line. Interestingly, the paternally expressed coding genes found in this region were not found to be differentially expressed between the cell lines by the gene expression array. The maternal allele contains only non-coding genes.

miRNAs from the 14q32 region have previously been found to be important in many different cancers and have been attributed disparate roles as both tumour suppressing or oncogenic depending on the setting. Indeed, decreased levels of

the miRNAs were shown to be important in glioma progression (*408*), melanoma (*409*), neuroblastoma (*410*), osteocarcinoma (*411*), and ovarian carcinoma (*412*). In these examples the miRNAs are functioning as tumour suppressors. In other cases they are oncogenic: increased expression of the miRNAs has been correlated to a decreased time until relapse in ependymoma (*413*); in hepatocellular carcinoma to stem cell-like phenotypes and increased invasion (*403*), and in lung adenocarcinoma to a decrease in disease free survival time (*341*). For these latter examples, the apparent correlation between increased levels of 14q32 miRNAs and metastatic progression and relapse suggests a role for these miRNAs in resistance to therapy.

In prostate cancer these miRNAs can either be downregulated, suggesting a tumour suppressive role (*414*) or upregulated promoting cell proliferation and invasion, indicating an oncogenic role (*287*). These two studies, however, did not investigate the same individual 14q32 miRNAs. In the former, ten miRNAs were found to be decreased in tumour compared to normal samples whereas in the latter only miR409 was investigated. As the experiments were not carried out in the same cell lines and did not investigate the same miRNAs, the results are hard to interpret. This highlights the importance of context specificity of miRNAs. 14q32 miRNAs have been attributed different roles depending on the cancer type and cell lines used in the studies.

To directly confirm the correlation between miRNA levels and resistance, here, miRNA mimics and inhibitors were transfected into the cells prior to cytotoxicity assays with lapatinib or neratinib. These experiments measured the IC_{50} values for each condition (Supplementary Figures 7.3 and 7.6) and were also used for viability studies (Supplementary Figures 7.5 and 7.7). However, none of the conditions used displayed the anticipated increase or decrease in resistance.

The experiments were designed with miRNA mimics or inhibitors being transfected into the cells on day 0, the drug was then added at day 1 and left until day 7 where the MTT assay was performed. While miRNA mimics have been shown to be effective in the cells on average 3 days (*415*), in our experiments, high levels of miRNA were still measured at day 7, the end day of the experiment. This could, however, be the stem-loop RT-qPCR assay picking up the unprocessed miRNA mimic in the cell. Although the stem-loop primer should be specific to the mature form of the miRNA, it has previously been shown that some assays can detect unprocessed mimic (*416*). Preliminary stem-loop RT-qPCR results,

with mimic addition before and after cells were collected for miRNA extraction, showed this was probably the case for our experiment as well. Therefore it is possible that the miRNA levels obtained by RT-qPCR after mimic transfection really include the original levels of mimic transfected and thus do not reflect levels of mature and active miRNA in these experiments.

This is not the case for inhibitors as their sequence is complementary to the mature miRNA and cannot bind to the stem-loop primer, allowing for the detection of the actual amount of mature miRNA present in the cells after transfection. There was a time discordance with the IC_{50} measurements, optimised at day 7, and the maximum effect of the inhibitors, observed at 48 hours. Therefore, a different end point assay may have been better suited to determine the sensitivity of the cells to lapatinib following mimic or inhibitor transfection. For instance, measuring an event that occurred faster in lapatinib response such as upregulation of Forkhead Box O1 (FOXO3A), CDKN1B, Cyclin D1 (CCND1), RB1 Inducible Coiled-Coil 1 (RB1CC1), and Nuclear Receptor Subfamily 3 Group C Member 1 (NR3C1) which can be measured by RT-qPCR from as early as 12 hours after drug exposure (*417*).

Although there was no direct confirmation of the link between miRNA upregulation and resistance through our experiments, a clear increase in expression of the miRNAs from both 14q32 clusters was observed in acquired resistance to lapatinib compared to the low native levels of these miRNAs in the sensitive cell lines (Figure 3.7a).

6.4.2 miRNAs from the 14q32 Region are Epigenetically Regulated and Demethylated in Acquired Resistance to Lapatinib

The 14q32 region has been shown to be tightly regulated by both DNA methylation and histone modification (*418*). Very little research has been done to confirm that the changes in miRNA expression observed in cancers are due to epigenetic changes in the 14q32 region. This is the first report of its' kind. In lung adenocarcinoma the increase in miRNA was found not to be due to loss of imprinting in the region, but due to a gradual hypomethylation from healthy cells to lymph node metastasis which correlated to miRNA expression levels (*341*). In uterine carcinosarcoma no decrease in methylation was observed in the IG-DMR (*419*), however, the other DMRs in the region were not studied. In

hepatocellular carcinoma loss of imprinting has been suggested to be the cause of increased 14q32 miRNA expression (*403*), although no experimental validation has been carried out. In this study, epigenetic changes were shown to occur in acquired lapatinib resistant breast cancer lines.

Here, we investigated the influence of epigenetic markers on miRNA expression using DNA demethylation and inhibition of histone deacetylation. Due to the random nature of this experiment, with Aza and TSA affecting each individual cell differently, there was some variation between the results. Thus a representative biological repeat was displayed in Figure 4.3. There are two miRNA clusters in the 14q32, which will be discussed separately by examining the different miRNA expression patterns.

In the 14q32.31 region, these experiments showed that miR495 was the most consistently altered miRNA between all the cell lines. It displayed an increase in expression in the sensitive cell lines with both Aza and TSA treatments and little to no change in the acquired resistant lines. miR409 also presented this pattern apart from in SKBR-3 cells. This suggests that the regions controlling the expression of the miRNAs are already demethylated in the resistant cells, whereas they are not in the sensitive lines. Additionally in the sensitive lines, the methylated DNA seems to be in a closed state as TSA in addition to Aza treatment further increased miRNA upregulation. Thus, in the sensitive cells, the DNA is not in an open configuration as the genes are not normally expressed in adult tissues. In the resistant cells, the chromatin, which could have been decondensed through acetylation of key histones, is now in an open state allowing for the newly demethylated genes to be expressed. This suggests that the chromatin, in a facultative heterochromatic state in the sensitive cell lines, transitions to a euchromatic configuration.

In SKBR-3, these results show that HDAC inhibition, on top of demethylation, does not lead to much variation in miR409 expression compared to demethylation alone suggesting that here DNA demethylation might be more important for miRNA expression than histone acetylation. The chromatin could already be in an open configuration with the DNA methylated in the sensitive lines.

miR127, located in the 14q32.2, varied the most between all the cell lines, with BT-474 displaying the previous pattern of upregulation in the Aza and Aza with

TSA treated samples. Interestingly, miR127 levels also increased in BT-474/L, however in this case there was little increase in the Aza only condition and a bigger upregulation for the TSA conditions. This implies that, here, the promoter DNA is already demethylated and the inhibition is occurring from the acetylation levels and thus the histone configuration. In HCC1954 and HCC1954/L cells, there is almost no change in any condition suggesting the promoter region is demethylated and in an open configuration. As the epigenetic control taking place on this gene is neither dependant on DNA methylation, nor histone acetylation, other regulators could be more important. For instance, activating histone methylation marks, such as trimethylation of lysine 4 on H3 (H3K4me3) in the *MEG3*-DMR (*420*), could be more frequent in the resistant cells leading to the 10-fold increase in miRNA expression observed between HCC1954 and HCC1954/L (Figure 3.7). To measure changes in histone methylation further experiments, such as chromatin immunoprecipitation (ChIP) followed by a DNA microarray (*421*), also called ChIP on chip, could be carried out. In the SKBR-3 line, a big increase in miRNA expression is observed for the Aza treated conditions highlighting the role of methylation, more than histone acetylation, in controlling miR127 expression in this cell line. In the resistant SKBR-3/L there is also an increase in miRNA expression in the Aza treatment alone. This suggests that, here, not all methylation is lost in resistance. This could explain why SKBR-3/L cells have the lowest 14q32 miRNA expression out of the three resistant lines (Figure 3.7a).

These results show that the subtle differences in variation of expression observed between miR127 and the other two miRNAs is controlled by different promoter regions which do not respond the same to DNA methylation and histone acetylation patterns, and are probably dependant on other epigenetic regulators as has previously been hypothesised (*334*).

Methylation resequencing experiments were carried out to confirm the location of DNA demethylation leading to the changes in miRNA expression observed previously. In BT-474/L cells the IG-DMR was found to be relatively demethylated compared to BT-474 where the region was highly methylated. In HCC1954 cells the IG-DMR was already demethylated and in HCC1954/L some sites increased in methylation levels but they remained under 50 % methylation. In the SKBR-3 lines there were no significant changes in methylation levels in this region. Similar result have previously been observed in uterine carcinosarcoma

where no change in IG-DMR methylation was observed although there was increased miRNA expression in the cancer compared to healthy tissue (*419*). In both SKBR-3 and SKBR-3/L, overall methylation levels of the region were of approximately 5 %. Altogether, these results suggest that imprinting of the IG-DMR is lost in most of the cell lines and other mechanisms are also involved in controlling the expression of the miRNAs. This was observed in the previous experiments where in most cases the combination of Aza and TSA lead to the biggest changes in miRNA expression, suggesting histone acetylation could be a key regulator in controlling expression of the miRNAs.

The *MEG3*-DMR appears to be a key regulator of the miRNA expression as it is the only region significantly changed in all three cell lines. Demethylation is occurring in the distal region of the DMR confirming that methylation levels in this region are essential in controlling expression of the miRNAs (*327*).

CpG islands 1 and 2 have undergone the most demethylation in BT-474/L compared to its sensitive parental cell line. The amount of demethylation observed could hypothetically explain the extent of the changes in miRNA expression levels between BT-474 and BT-474/L. Indeed, this resistant cell line displays the biggest increase in miRNA expression levels which could result from the demethylation observed across all four CpG regions tested. HCC1954/L has undergone more modest changes, but it still displays low levels of methylation overall which, when combined with changes in histone modifications, could lead to the increase in miRNA expression levels observed between the sensitive and resistant cells. In SKBR-3 and SKBR-3/L cells these regions are generally mostly demethylated with on average less than 3 % methylation. This implies that methylation in these regions are not key in controlling 14q32 miRNA upregulation for this cell line, with histone modfication maybe driving the change in miRNA expression between the sensitive and resistant lines.

Overall SKBR-3 and SKBR-3/L have the lowest levels of miRNA expression in their respective categories as lapatinib sensitive or acquired resistant cells. These cell lines also displayed the least changes in cross-resistance patterns for SKBR-3/L. All these factors could be explained by the methylation changes observed here, where the only significantly altered region is the *MEG3*-DMR. Therefore, out of the isogenic pairs, SKBR-3 and SKBR-3/L have undergone the least epigenetic changes.

6.5 Key miRNA Target Genes are Downregulated in the Resistant Cells and Appear to be Involved in Resistance

6.5.1 Differences in miRNA Expression Occur with Changes in Gene Expression in Acquired Resistance

miRNA therapy has not yet been widely investigated and there are no successful clinical trials. The first phase I trial, MRX34, used a miR34a mimic to reduce metastasis in hepatocellular carcinoma, however, the trial had to be ended prematurely due to serious adverse effects in patents (*422*). Moreover, it has been suggested that unexpected effects of miRNA therapies could be caused by the context dependant role of miRNAs (*423*), as illustrated by miR34a which was found to be both inhibiting metastasis (*424–426*) and promoting it (*427*).

Although a number of miRNA based therapeutics have been trialled with more successful results than the MRX34 trial, none of the ongoing cancer trials have published successful results (*168*), however, certain patients might benefit from miRNA therapy. Cancers, compared to other diseases, are constantly mutating and changing. This makes cancer cells very adaptable, as demonstrated by the therapeutic resistance phenomenon. This characteristic of the cells combined with the ambiguous role many miRNAs play which is very context dependant, suggest that tumours are likely to hijack a miRNA therapy to its advantage. Additionally, in many cancers, it is not just a single miRNA that is alter but a whole cluster or family which is deregulated, as is the case here with the 14q32 cluster. Removing a single drop of contaminated water from a glass of muddy water will not clean the contents of the entire glass. Similarly, targeting one or two miRNAs out of the whole cluster will probably not induce a significant change in downstream targets as these are most likely also regulated by many other miRNAs deregulated in the cancer (Figure 6.2a). Identifying a different level of where an action could have a vaster impact is essential. Here, acting on downstream effectors of the miRNAs, with clear defined roles appears to be the better treatment option (Figure 6.2b). This is the same reasoning for the widely accepted conclusion that transcription factors are difficult cancer therapeutic targets.

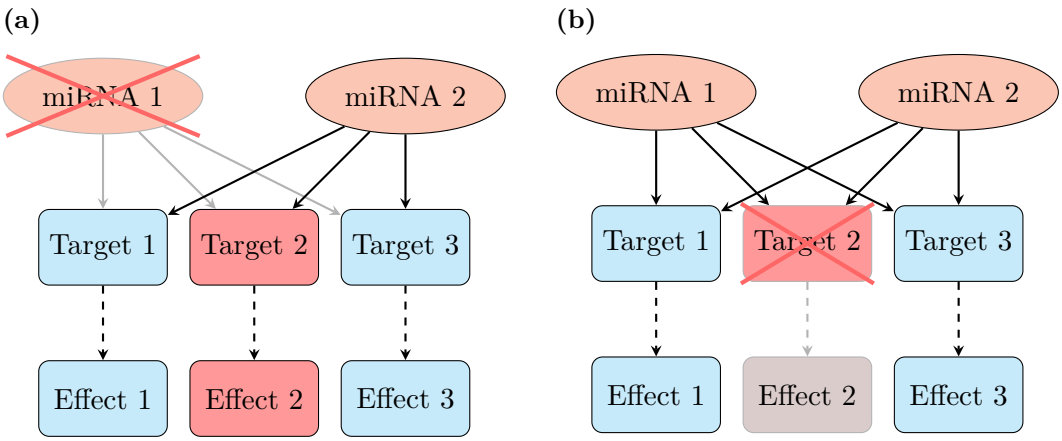

Figure 6.2: Differences Between Targeting miRNAs or Downstream Targets. In cancers where whole miRNA clusters are deregulated, miRNAs will likely affect similar targets. Here only two miRNAs and three downstream effectors are considered, however in the case of the 14q32 miRNAs and resistance investigated in this work, 52 miRNAs from a single genomic cluster are deregulated. These miRNAs affect hundreds of mRNA targets. In this schematic the therapeutic target is shown by a red cross on the digram and impaired downstream effects are greyed out. Targets and effects that play a key role in cancer are highlighted in red. (a) miRNA 1 is targeted in this scenario. This prevents the miRNA from affecting its downstream targets, however, these are also regulated by miRNA 2 which can compensate for the loss of miRNA 1. Therefore, in this situation, targeting miRNA 1 is not significantly affecting downstream effects and not resulting in clinical benefit. (b) In this situation, Target 2 is selected as the therapeutic target. In this case, selecting a downstream effector of the miRNAs overcomes the redundant nature of miRNA targeting. This leads to impaired signalling downstream of Target 2 leading to therapeutic benefit.

As previously mentioned, many different and contradictory roles have been identified for 14q32 miRNAs with evidence hinting that they can act as both oncogenic or tumour suppressor miRNAs depending on the context. This, and the results from the MRX34 trial, advise against targeting miRNAs as it could lead to unwanted effects. Thus determining how the miRNAs are affecting downstream genes will help to identify therapeutic targets. Therefore promising therapeutic pathways should be downregulated in the resistant cells and targeted by multiple miRNAs from the 14q32 cluster as miRNAs from a same genomic cluster tend to have similar effects in cancer (*414*).

In the experiment here, genes were selected from a gene expression array comparing BT-474/L expression to BT-474. This identified 27 genes that were differentially expressed and miR127, miR409 or miR495 targets. From these, 13 genes were selected which had sites for at least two of the six validated miRNAs. Seven of these targets were validated in siRNA experiments. Each target was studied individually to assess their role in resistance. Therefore in these experiments the IC_{50} values for the cell lines was not expected to go from sensitive to resistant, yet if a gene is important in acquired resistance, the value is anticipated to increase making the cell more resistant to the drug than the untreated sensitive sample. Following knock-down of a single target, we do not expect to see a complete shift in IC_{50} from sensitive to resistant, but, if a gene is important in acquired resistance, we anticipate some loss in sensitivity when compared to the control.

Having identified targets with the potential to be involved in resistance to HER2-targeted therapy further experiments could be carried out to confirm their importance through the reciprocal experiment: re-expressing the targets in resistant cell lines through plasmid transfection with the aim of reducing the IC_{50} value for these cells.

Furthermore, to confirm the miRNAs directly target the mRNAs of the chosen genes, luciferase assays could be carried out (*428*). The target mRNA 3′UTR sequence would be cloned into the luciferase vector and then transfected into the paired cell line, this should lead to lower levels of the luciferase protein in the resistant lines where the higher levels of miRNA are binding to the seed site in the 3′UTR and inhibiting luciferase translation. This was attempted, however due to problems in the cloning process these assays were not successful. After numerous attempts varying PCR conditions, it was found that the seed sequences

used as templates were too palindromic and GC rich for successful cloning. If this had worked, the luciferase could have been transfected into sensitive cells at the same time as miRNA mimics to validate the inhibition of each selected miRNA on each target gene. Another method to identify miRNA-mRNA interaction would be to use photoactivatable-ribonucleoside-enhanced crosslinking and immunoprecipitation (PAR-CLIP) to identify miRNA-containing ribonucleoprotein complexes (*429*).

6.5.2 Three Putative miRNA Targets, SOCS2, BASP1, and NEDD4L, Appear to be Involved in Acquired Resistance to Lapatinib

SOCS2 is a putative target of four out of the six investigated 14q32 miRNAs. Loss of SOCS2 has been found to lead to an increase in cell proliferation and less differentiated, thus more stem-like, tumours. In the resistant cell lines there was little upregulation in SOCS2 levels in HCC1954/L and SKBR-3/L compared to their isogenic pair, however in both the BT-474/L and BT-474/T cell lines there was a decrease in SOCS2 expression. This difference is a reminder of the individual adaptation each cell line has undergone in the process of acquired resistance. Only one acquired lapatinib resistant line was tested for each sensitive line. To obtain more robust results would require clonal selection and the repetition of these experiments on multiple clones. Cancer is a clonal disease and individual clones might adapt differently to the drug, multiple adaptations can originate from a sensitive cell population where one mutation can dominate until it is targeted and eliminated, allowing for another to take its place (*430*, *431*).

Here, siRNA knock-down leads to a decrease in *SOCS2* mRNA expression in all the sensitive lines and the upregulation in IC_{50} was observed in both BT-474 and HCC1954 after treatment with lapatinib. No consistent effect was observed in SKBR-3 cells, however, as identified in previous experiments, this cell line has adapted the most differently to lapatinib compared to the other two lines. Consistently, this results for this cell line do not match the other two cell line pairs studied. This could explain why SOCS2 knock-down only lead to the increase in resistance in HCC1954 and BT-474. SOCS2 appears to have a potential role in resistance to lapatinib, and possibly HER2-targeting therapies

more generally, although more IC_{50} experiments with other HER2-targeting agents would be necessary to confirm this.

BASP1 was found to be a putative target for five out of the six miRNAs investigated. Its expression was lower in HCC1954 and SKBR-3 than in BT-474. In both HCC1954/L and SKBR-3/L there was an increase in BASP1 compared to their paired sensitive line. As expected, due to these results, an increase in IC_{50} was only observed for the lapatinib treated BT-474 cells after siRNA transfection. BASP1 is involved in inhibition of MYC signalling, therefore loss of BASP1 could lead to increased cell proliferation; this characteristic was only observed in the BT-474/L cells compared to BT-474 and not in the other pairs. This could be explained by the levels of BASP1 measured in the resistant cells. It could also be a reason why HCC1954 and SKBR-3 cells did not respond to the siRNA experiment in the same way as BT-474 cells did. Surprisingly, no consistent effect was observed in the cells treated with trastuzumab. An explanation could be that lapatinib and trastuzumab are quite different as lapatinib is a small molecule inhibitor targeting the ATP-binding domain on the intracellular part of the receptor (*378*), whilst trastuzumab is a monoclonal antibody that binds the HER2 ectodomain, on the extracellular side of the receptor (*36*). These distinctions lead to different cellular responses (*432*), which could clarify why BASP1 knock-down leads to an increase in resistance to lapatinib but not trastuzumab in BT-474 cells.

NEDD4L is a putative target of four 14q32 miRNAs tested, and its mRNA expression was lower in both HCC1954 and SKBR-3 cells compared to BT-474. The resistant cells also had lower *NEDD4L* expression than their sensitive pair. On the protein level both HCC1954 appeared to have NEDD4L levels considerably lower than the other sensitive cell lines, with the protein being expressed at a similar degree than HCC1954/L. Discrepancies between observed levels of mRNA and protein can be caused by differences in either transcription, translation, or degradation rates as well as by inhibition of the mRNA transcription by RNA interference (*433*). In the siRNA treated samples where protein knock-down was measured, an increase in IC_{50} was observed The effect is consistent for both BT-474 and SKBR-3 cell lines. In HCC1954 cells, the baseline levels of NEDD4L were already low thus the siRNA knock-down might not have affected the sensitivity of the cell line for lapatinib.

These targets, therefore, appear to be involved in acquired resistance to lapat-

inib for at least one of the cell lines tested. Although none of the changes in IC_{50} are statistically significant, a trend is observed. The lack of statistical significance could be a reflection of miRNA processes, upregultation of the 14q32 miRNAs leads to the downregulation of many target genes which in turn affect multiple signalling pathways. Here, in the experiments, we targeted individual genes. This causes a more modest downstream effect which leads to a smaller increase in resistance. Additionally, three of these genes, SOCS2, BASP1, and NEDD4L, seem to have some clinical relevance as high expression of these increase the probability of pCR, however, due to the low number of patients, these results are not statistically significant.

PKIA, a putative target for three of the tested 14q32 miRNAs, was downregulated in all the acquired resistant lines compared to their isogenic sensitive line. This target was already expressed at lower levels in HCC1954 and SKBR-3 compared to BT-474. Similarly to the results observed for SOCS2, there was only an increase in lapatinib resistance for BT-474 and HCC1954 cells after siRNA transfection. As previously stated, SKBR-3 cells adapted to lapatinib resistance in the most different way. SKBR-3/L cells have the lowest miRNA expression and have the least change in methylation levels out of the acquired resistant cells. The clinical data for this target is inconclusive as the odds ratio for the top quartile of PKIA expressers is greater than 1. This suggest that high levels of this target might not be beneficial for pCR, although the data set used for this analysis is very small and a larger cohort would improve the statistical relevance of this result.

6.5.3 SH3BGRL, a Putative miRNA Target Appears to be Involved in Acquired Resistance to Trastuzumab

SH3BGRL is expressed at lower levels in both HCC1954 and SKBR-3 compared to BT-474 cells. In all the acquired resistant cells, expression is also lessened compared to their isogenic sensitive cell line. In the lapatinib treated siRNA knock-down experiments no consistent changes in IC_{50} values was observed across the panel of cell lines. In the BT-474 cells treated with trastuzumab an increase in IC_{50} was measured. As mentioned previously, these two drugs do not inhibit HER2 signalling in the same fashion, which could lead to the differences observed here, where loss of SH3BGRL seems to be involved in

trastuzumab but not lapatinib acquired resistance.

6.5.4 Reduced Expression of SOCS2, BASP1, NEDD4L, and SH3BGRL Could Lead to Upregulated MYC and TGF-β Signalling

The combination of the IC_{50} results and the clinical data discussed above, seems to suggest that these targets are important in resistance to HER2 therapies and patient outcome as, in patients, high expression of the genes is associated with better pCR. Both NEDD4L and SH3BGRL are involved in negative regulation of TGF-β signalling, BASP1 is a MYC inhibitor, and SOCS2 inhibits JAK/STAT signalling (Figure 6.3). These pathways are involved in defining characteristics of resistant cells: cell growth and EMT. BT-474 was the cell line where loss of all these genes appeared to be implicated in resistance, therefore preliminary validation experiments were performed in BT-474 and BT-474/L to investigate how levels of *MYC* and *TGFBI* were affected in the resistant cells (Figure 6.4). This would suggest the resistant cells have upregulated signalling through these pathways, enabling the cells to compensate for the block of HER2 signalling promoting cell proliferation.

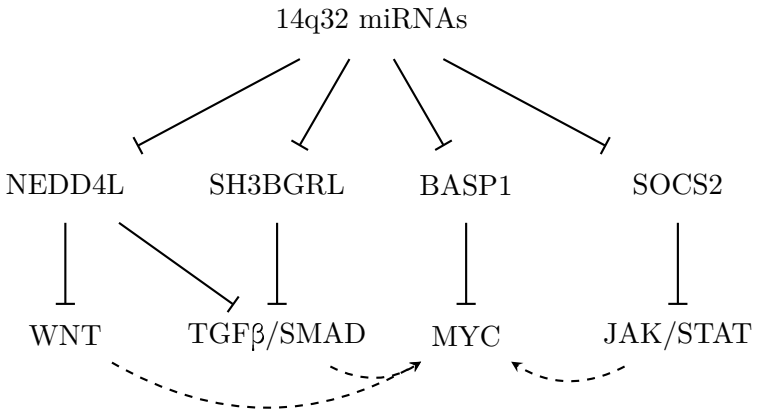

Figure 6.3: 14q32 miRNA Inhibition of Target Genes and Effect on Downstream Pathways. 14q32 miRNAs inhibit target genes such as NEDD4L, SH3BGRL, BASP1, or SOCS2. These genes are involved in inhibition of WNT, TGFβ/SMAD, MYC, and JAK/STAT signalling. Additiannally, the WNT, TGFβ/SMAD, and JAK/STAT pathways are involved in promoting MYC signalling. Therefore an increase in miRNA levels leads to higher inhibition of NEDD4L, SH3BGRL, BASP1, or SOCS2. This will remove inhibition on the downstream pathways promoting WNT, TGFβ/SMAD, and JAK/STAT signalling. Ultimately leading to increased proliferation and cell survival.

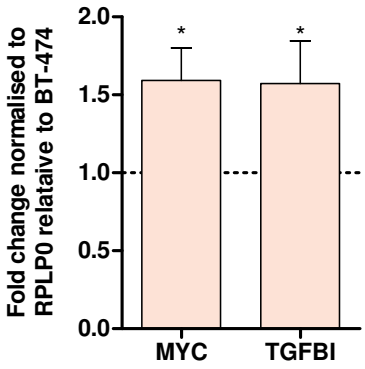

Figure 6.4: Preliminary Validation of MYC and TGF-β Activation in the Lapatinib Resistant BT-474/L. RT-qPCR measuring levels of *MYC* and *TGF-βI* mRNA in BT-474/L cells normalised to levels in BT-474. Statistical significance is obtained from a one-way ANOVA with Dunnett's Multiple Comparison post-test, significance is shown on the graph, with $\star$ for $p \leq 0.05$.

6.6 Concluding Remarks

At the end of this research, the main conclusions are that upregulation of 14q32 miRNAs, caused by epigenetic alterations, such as methylation loss and altered histone acetylation, was identified as a driver of lapatinib acquired resistance in HER2+ breast cancer cell lines. This lead to downregulation of key genes that are putative targets of the upregulated miRNAs and also appear to be involved in resistance to HER2-targeting therapy. These genes have previously been shown to be involved in regulation of signalling pathways which can lead to EMT and stemness and in turn, these can affect resistance. Additionally SOCS2, BASP1, NEDD4L, and SH3BGRL appear to be relevant in patients since high levels of these gene targets seem to correlate with a better probability of pCR.

Expression levels of 14q32 miRNAs could thus be a relevant prognostic biomarker, after first round of HER2-targeted therapy, to identify patients that are likely to relapse and develop refractory disease. Gene expression of the targets could also be used as a predictive biomarker to identify patients who will respond favourably to HER2-targeted therapy.

7 Supplementary Data

7.1 Other miRNA Putative Gene Targets

7.1.1 Krüppel-Like Factor 9

Krüppel-Like Factor 9 (KLF9) is a member of the Krüppel-Like super family. Its expression has been found to suppress invasive growth in breast cancer by transcriptionally repressing matrix metalloproteinases, thus preventing remodelling of the extracellular matrix (*434*, *435*).

There is one putative miR409 seed site in *KLF9* (Figure 7.1a) and three miR495 sites (Figure 7.1b, c, and d). *KLF9* is also predicted to have sites for miR411, miR433 and miR539 (Figure 5.4).

KLF9 mRNA levels were down in HCC1954 cells and up in SKBR-3 cells when compared to BT-474 (Figure 7.1e). In all the lapatinib resistant lines as well as in BT-474/T, the trastuzumab resistance line, mRNA levels of KLF9 were lower than in the paired sensitive line (Figure 7.1f, g, and h).

siRNA transfection in the sensitive cell lines resulted in a decrease of over 50 % in mRNA expression for all three cell lines (Figure 7.1i, j, and k). The knock-down, however only resulted in an increase in IC_{50} for siRNA 2 in the BT-474 and HCC1954 cells (Figure 7.1l and m). In SKBR-3 only the siRNA 1 treated sample had an increase in IC_{50} (Figure 7.1n). The effect observed in these cells suggest the IC_{50} changes are caused by off target effects of the siRNA, indicating that KLF9 loss is not essential in acquired resistance to lapatinib.

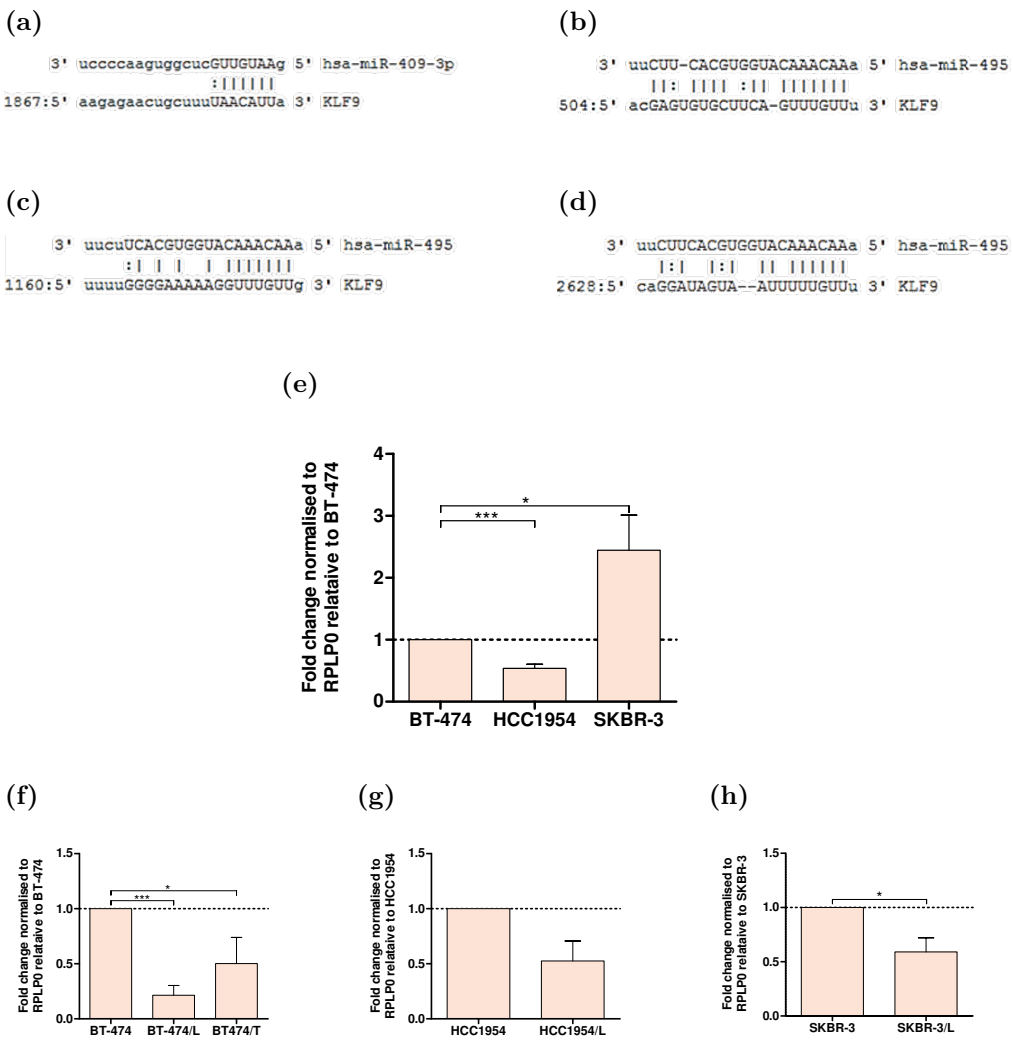

Figure 7.1: miRNA Seed Sites and Baseline Expression of *KLF9*. *KLF9* contains putative miRNA binding sites for (a) miR409, and (b, c, d) miR495. (e) Levels of *KLF9* mRNA in all three sensitive cell lines compared to BT-474. mRNA levels in paired resistant and sensitive cell lines, normalised to the sensitive cell line for (f) BT-474, BT-474/L, and BT-474/T, (g) HCC1954 and HCC1954/L, and (h) SKBR-3 and SKBR-3/L. Statistical significance is obtained from a one-way ANOVA with Dunnett's Multiple Comparison post-test for (e) and (f), and Student's T-test for (g) and (h). Where results are statistically significant p-values are shown on the graph, with $\star$ for $p \leq 0.05$, and $\star\star\star$ for $p \leq 0.001$.

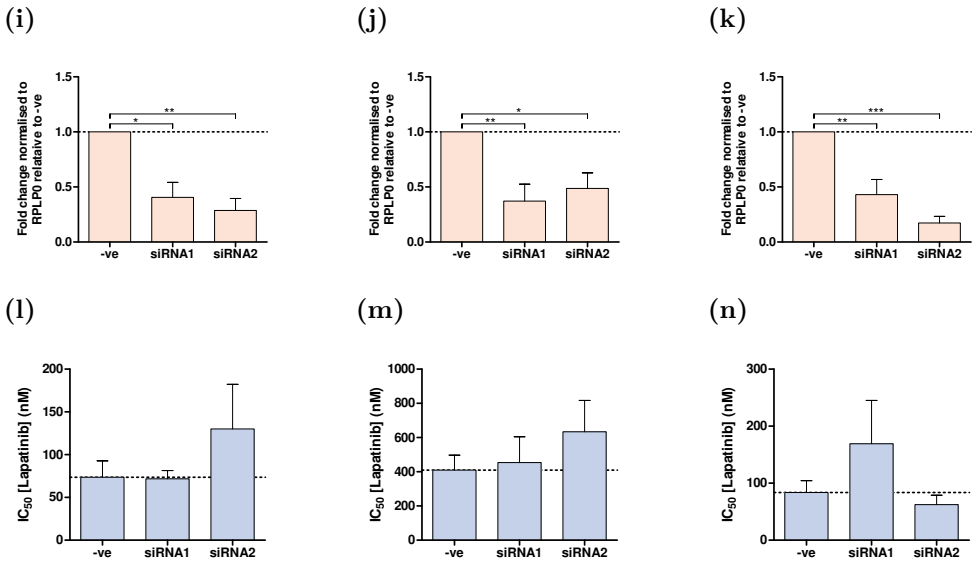

Figure 7.1: Effect of KLF9 Knock-down on Lapatinib Resistance. mRNA expression after treatment with two different siRNAs in (i) BT-474, (j) HCC1954, and (k) SKBR-3. Lapatinib IC_{50} value after siRNA treatment in (l) BT-474, (m) HCC1954, and (n) SKBR-3. The IC_{50} values are obtained from non-linear regression analysis of cytotoxicity experiments and are averaged for at least three replicates. Where results are statistically significant, as determined by one-way ANOVA with Dunnett's Multiple Comparison post-test, p-values are shown on the graph, with $\star$ for $p \leq 0.05$, $\star\star$ for $p \leq 0.01$, and $\star\star\star$ for $p \leq 0.001$.

7.1.2 Phosphatidylinositol-3,4,5-Trisphosphate-Dependent Rac Exchange Factor 1

Phosphatidylinositol-3,4,5-Trisphosphate-Dependent Rac Exchange Factor 1 (PREX1) is a Rac1 GEF that exchanges Rac bound GDP for GTP activating Rac and allowing for downstream signalling through the MAP kinase pathway (*436–438*).

PREX1 was found to have two miR495 seed sites (Figure 7.2a and b) as well as being a miR411 target (Figure 5.4).

mRNA levels of *PREX1* were found to lower in BT-474/L cells compared to be BT-474 (Figure 7.2c) this was confirmed on the protein level, with BT-474/L appearing to have lost PREX1 expression (Figure 7.2d).

To investigate the functional role of PREX1 in lapatinib resistance, a knock-down experiment using siRNAs was performed in BT-474 cells. With two individual siRNAs, knock-down of PREX1 protein expression was observed (Figure 7.2e). This did not, however, affect the sensitivity of the cells to lapatinib as all conditions have similar IC_{50} values (Figure 7.2f). These results suggest that PREX1 is not causal in lapatinib acquired resistance.

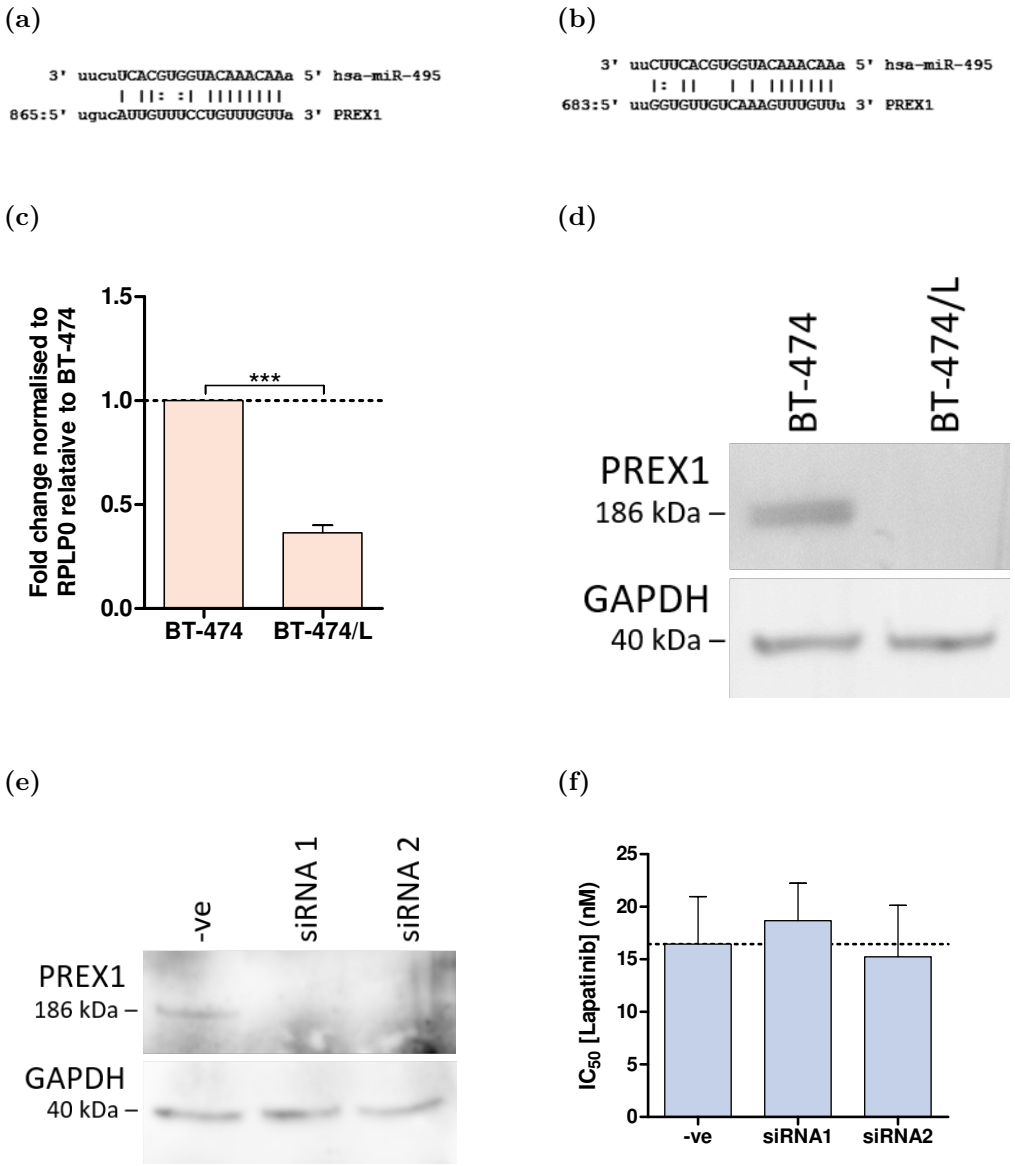

Figure 7.2: PREX1 Baseline Expression and Effect of Knock-down on Lapatinib Resistance. (a, b) *PREX1* contains two putative miRNA binding sites for miR495. (c) Levels of *PREX1* mRNA in BT-474/L cells compared to BT-474. (d) PREX1 protein levels in BT-474 and BT-474/L. (e) Protein knock-down after siRNA treatment in BT-474 cells. (f) Lapatinib IC_{50} value after siRNA treatment in BT-474. The IC_{50} values are obtained from non-linear regression analysis of cytotoxicity experiments and are averaged for at least three replicates. Statistical significance is determined by a Student's T-test, where results are significant p-values are shown on the graph, with $\star\star\star$ for $p \leq 0.001$.

7.2 Modulating miRNA Levels in Vitro to Affect Lapatinib Sensitivity

To directly link miRNAs and acquired resistance to HER2-targeting therapy, we decided to modulate miRNA expression using miRNA mimics or inhibitors. This was combined with drug treatment to investigate how the induced changes in miRNA expression affect resistance.

7.2.1 miRNA Mimic Transfection in Sensitive Cell Lines with Lapatinib Treatment for IC_{50} Studies

As we found elevated levels of miR127, miR409 and miR495 in BT-474/L cells relative to BT-474, miRNA mimics were used to increase the levels of these mature miRNAs in the lapatinib sensitive cell lines in an attempt to make them more resistant to the drug. miRNA mimics are synthetic oligonucleotides that form small double-stranded RNA molecules imitating endogenous pri-miRNAs. When they are transfected into cells they are be processed by the miRNA machinery and loaded onto the RISC complex thus increasing the proportion of RISCs containing the selected miRNA.

For all three cell lines different seeding densities and mimic concentrations were used for IC_{50} assays (Figure 7.3). In BT-474, for all three conditions, no effect was observed on the IC_{50} values in mimic transfected samples (Figure 7.3a) even though over a thousand fold increase in miRNA expression was was achieved after mimic treatment (Figure 7.4). The only effect observed was an overall decrease in IC_{50} value when cell numbers were decreased.

In HCC1954 cells, a significant decrease in IC_{50} was obtained when the highest concentration of miR409 mimic was used with a seeding density of $6.0{\cdot}10^4$ cells$\cdot$mL^{-1} (Figure 7.3b). In the other conditions tested, no significant change was observed between the treatments though miRNA levels were increased as measured by RT-qPCR (Figure 7.4).

SKBR-3 cells were only tested at a seeding density of $6.0{\cdot}10^4$ cells$\cdot$mL^{-1} and 2.5 nM mimic (Figure 7.3c). No change was observed during the experiment albeit the 100-fold increase in miRNA levels achieved after transfection (Figure 7.4).

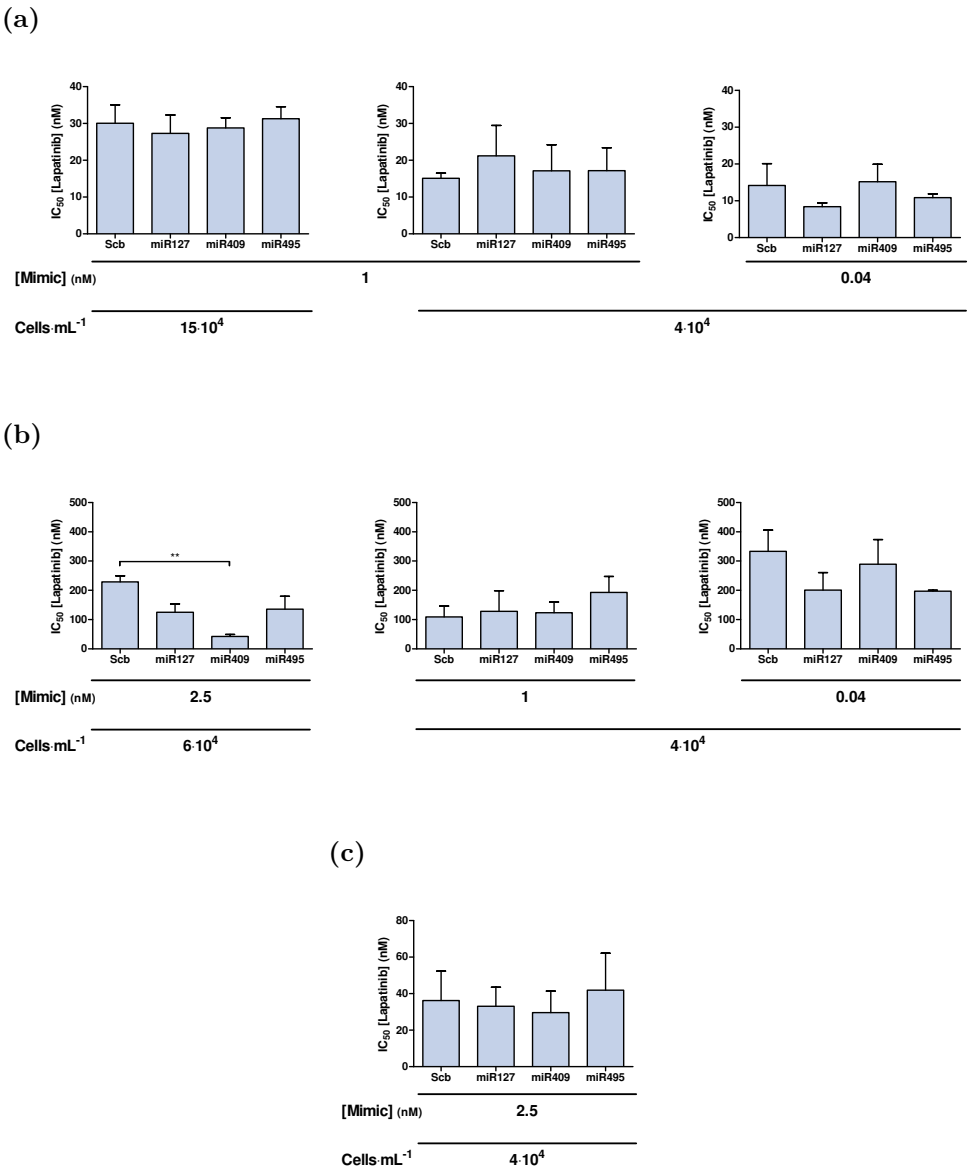

Figure 7.3: Cell Line Sensitivity to Lapatinib after Modulation of miRNA Levels by Mimic Transfection (a) in BT-474 cells, (b) in HCC1954 cells, (c) in SKBR-3 cells. For all three cell lines irrespective of the different experimental conditions used there was no significant increase in resistance to lapatinib. The IC_{50} values are obtained from non-linear regression analysis of cytotoxicity experiments, average for three replicates. Where results are statistically significant, as determined by one-way ANOVA with Dunnett's Multiple Comparison post-test, p-values are shown on the graph, with $\star\star$ for $p \leq 0.01$.

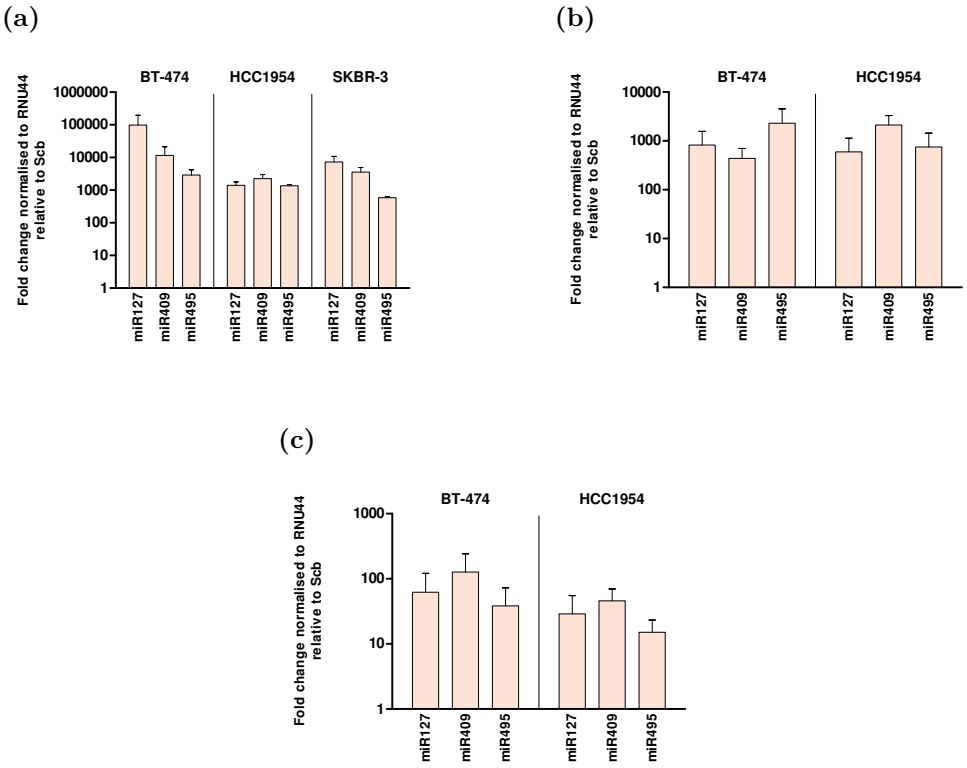

Figure 7.4: miRNA Expression Levels Measured by Stem-Loop RT-qPCR after Mimic Transfection. Results are analysed using the $\Delta\Delta$Ct method and averaged for three different biological replicates. (a) 2.5 nM, (b) 1.0 nM, and (c) 0.04 nM of mimic. In all cases a high upregulation of the mature miRNAs was observed after transfection with the mimics.

7.2.2 miRNA Mimic Transfection in Sensitive Cell Lines with Lapatinib Single Dose Treatment

The sensitive cell lines were transfected with different concentration of mimic, ranging from 50 nM to 40 pM. Cells were plated at a density of $4.0 \cdot 10^4$ cells·mL^{-1}. The cells were treated with a single dose of lapatinib for three days, rather than for seven days as used for previous IC_{50} experiments. The lapatinib dose chosen was close to the cell lines IC_{50} value for the drug. Within the treatment groups, no difference in miRNA mimic compared to scb negative control was observed (Figure 7.5).

When the cells were treated with 50 nM mimic, approximately 50 % death was observed for all conditions in BT-474 and SKBR-3 cell lines (Figure 7.5a and c). In HCC1954 cells for this condition, 30 to 40 % cell death was observed (Figure 7.5b). The other mimic transfection conditions, 1 nM and 40 pM, had between 70 and 80 % cell death. Again, no increase in resistance was obtained in the mimic transfected samples compared to Scb (Figure 7.5).

7.2.3 miRNA Mimic Transfection in Sensitive Cell Lines with Neratinib Treatment for IC_{50} Studies

As BT-474/L and HCC1954/L showed the biggest change in sensitivity to Neratinib, when compared to their paired sensitive line, we decided to study how transfection with the mimics affected resistance to this drug in the sensitive cell lines.

All three paired sensitive cell lines were transfected with the individual mimics and treated with a range of Neratinib doses to obtain IC_{50} values. For all three cell lines this yielded similar results to the lapatinib treatment where the only significant change observed was for the miR409 mimic treatment in HCC1954 cells (Figure 7.6).

Although the experiments technically worked and miRNA upregulation was present, we were not able to detect an increase in IC_{50} value after transfection with miRNA mimic in the lapatinib sensitive cells.

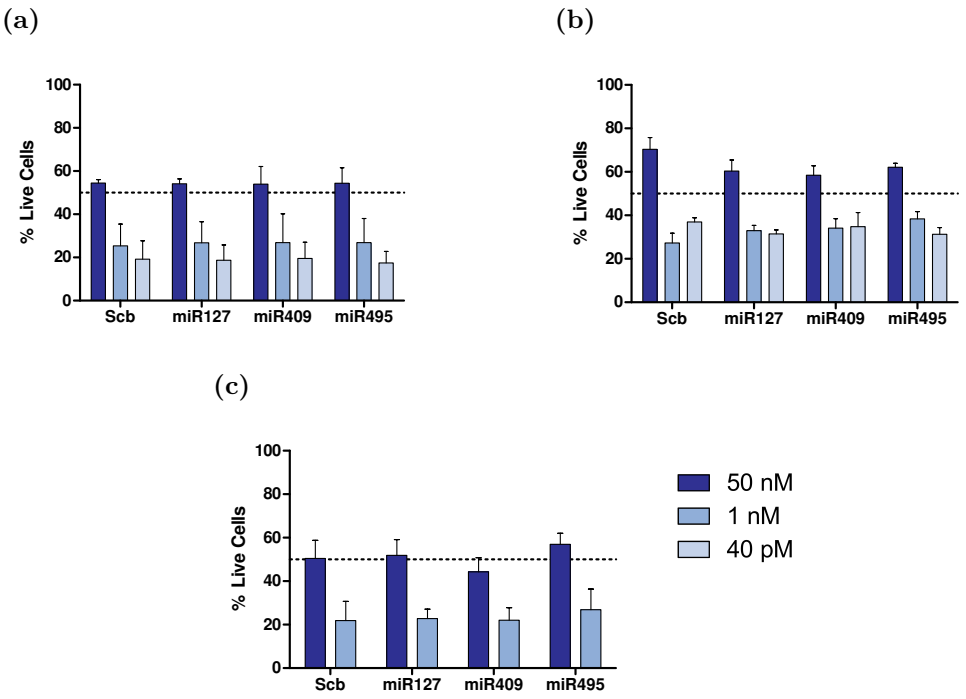

Figure 7.5: Lapatinib IC_{50} Dose Treatment after Mimic Transfection (a) in BT-474 with 50 nM of lapatinib, (b) in HCC1954 with 200 nM of lapatinib, and (c) in SKBR-3 with 100 nM of lapatinib. Optical density of the samples is normalised to the untreated control for each condition and is averaged for three replicates.

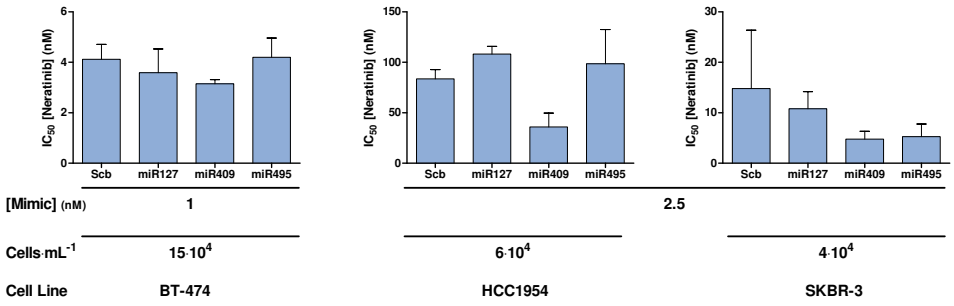

Figure 7.6: Cell Line Sensitivity to Neratinib after Modulation of miRNA Levels by Mimic Transfection. For all three cell lines there was no increase in resistance to neratinib after mimic treatment of the cells. The IC_{50} values are obtained from non-linear regression analysis of cytotoxicity experiments, average for three replicates.

7.2.4 miRNA Inhibitor Transfection in Resistant Cell Lines with Lapatinib Dose Treatment

To model the change in miRNA expression that occurs in the acquired resistant cells, BT-474/L cells were transfected with 25 nM miRNA inhibitor. miRNA inhibitors are short synthetic oligonucleotides with complimentary sequences to the mRNAs they inhibit, therefore they will bind to them with high specificity and prevent the miRNA from binding to the 3′UTR region of mRNA targets. The decrease in miRNA levels in the resistant cells should make the resistant cells more similar to the paired sensitive cell line. To see if the decrease in miRNA had an effect on resistance, the cells were treated with 500 nM or 1 µM of lapatinib for either 5 or 7 days.

In all the BT-474/L conditions cell survival was close to 100 % after 5 and 7 days with both 500 nM (Figure 7.7a) or 1 µM of lapatinib (Figure 7.7b) whereas survival in the control BT-474 cells was between 10 and 1 % after treatment with the drug (Figure 7.7).

Although a 60 to 80 % decrease in miRNA levels was observed (Figure 7.7c), the cells did not appear to become more sensitive when they were treated with the miRNA inhibitors.

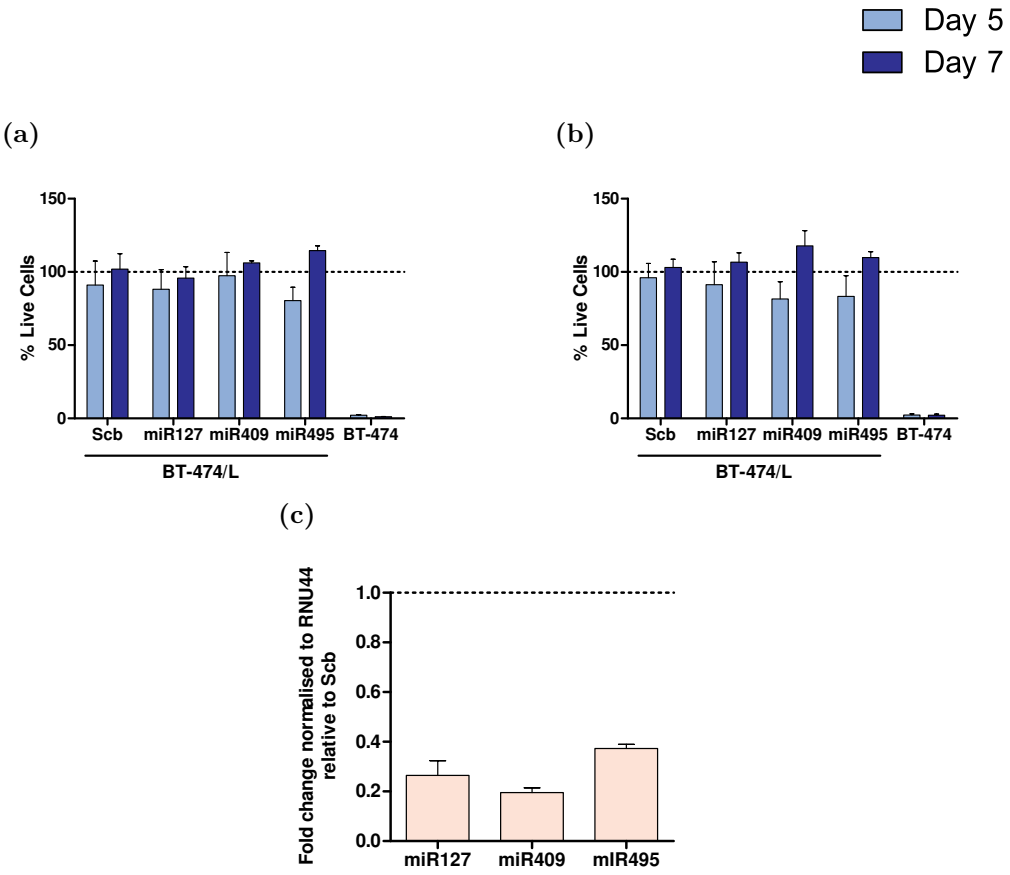

Figure 7.7: Cell Line Sensitivity to Lapatinib after Modulation of miRNA Levels by Inhibitor Transfection. BT-474/L, lapatinib resistant cells were transfected with 5 nM of mimic and treated (a) with 500 nM and (b) with 1 µM of lapatinib. For each experiment, BT-474 sensitive cells were used as a positive control. Optical density of the samples is normalised to the untreated control for each condition and is averaged for replicates. (c) miRNA expression levels measured by stem-loop RT-qPCR 48 hours after inhibitor transfection normalised to RNU44 relative to the scb treated sample. Over 60 % downregulation of all three miRNAs was observed in the BT-474/L cells after transfection. Results were averaged for two replicates.

7.3 Supplementary Figures

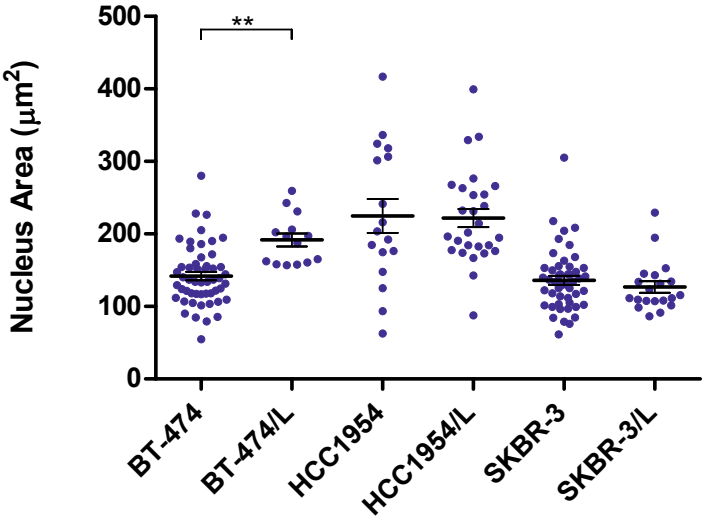

Figure 7.8: Comparison of Nucleus Area in Paired Lapatinib Sensitive and Resistant HER2+ Breast Cancer Cell Lines. Nucleus area measured for two to four frames per cell line. Both HCC1954 and SKBR-3 sensitive and resistant pairs on average appear to have similar nucleus size. The mean nucleus size for BT-474/L cells is greater than that of BT-474 cells. Overall, HCC1954 and HCC1954/L have the biggest nucleus. Statistical significance is obtained from a one-way ANOVA with Bonferroni's Multiple Comparison post-test. Where results are statistically significant p-values are shown on the graph, with $\star\star$ for $p \leq 0.01$.

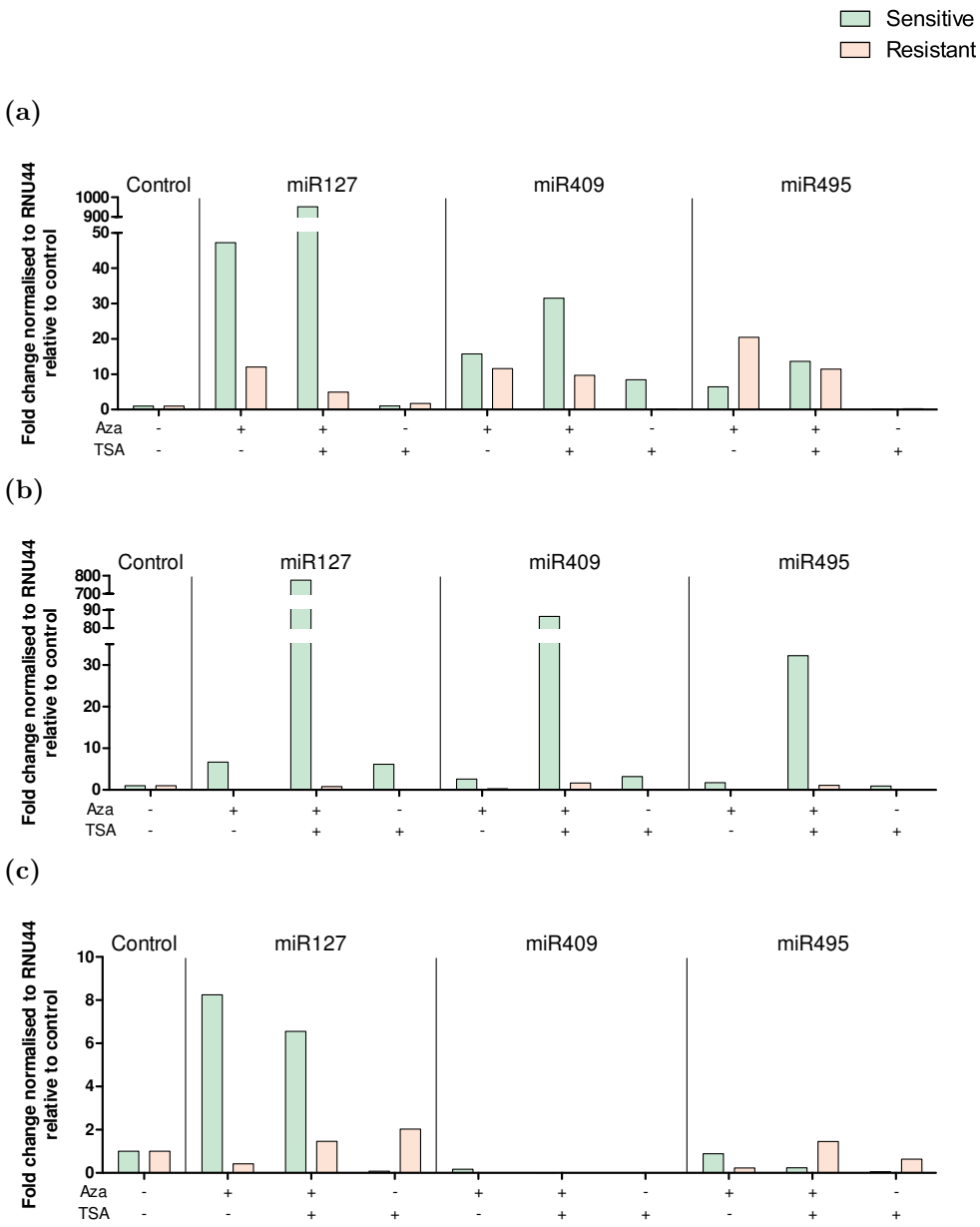

Figure 7.9: miRNA Expression after 5-Aza-2′-deoxycytidine (Aza) and Trichostatin A (TSA) Treatment. Replicate two of the experiment. The experiments are shown separately due to the high variability of the experiment. Stem-loop RT-qPCR is expressed as fold change relative to RNU44 and normalised to the untreated condition for each cell line. This does not permit direct comparison of miRNA levels between the sensitive and resistant cells but shows the effect of each treatment on miRNA expression levels. (a) In BT-474 cells, (b) in HCC1954 cells, and (c) in SKBR-3 cells.

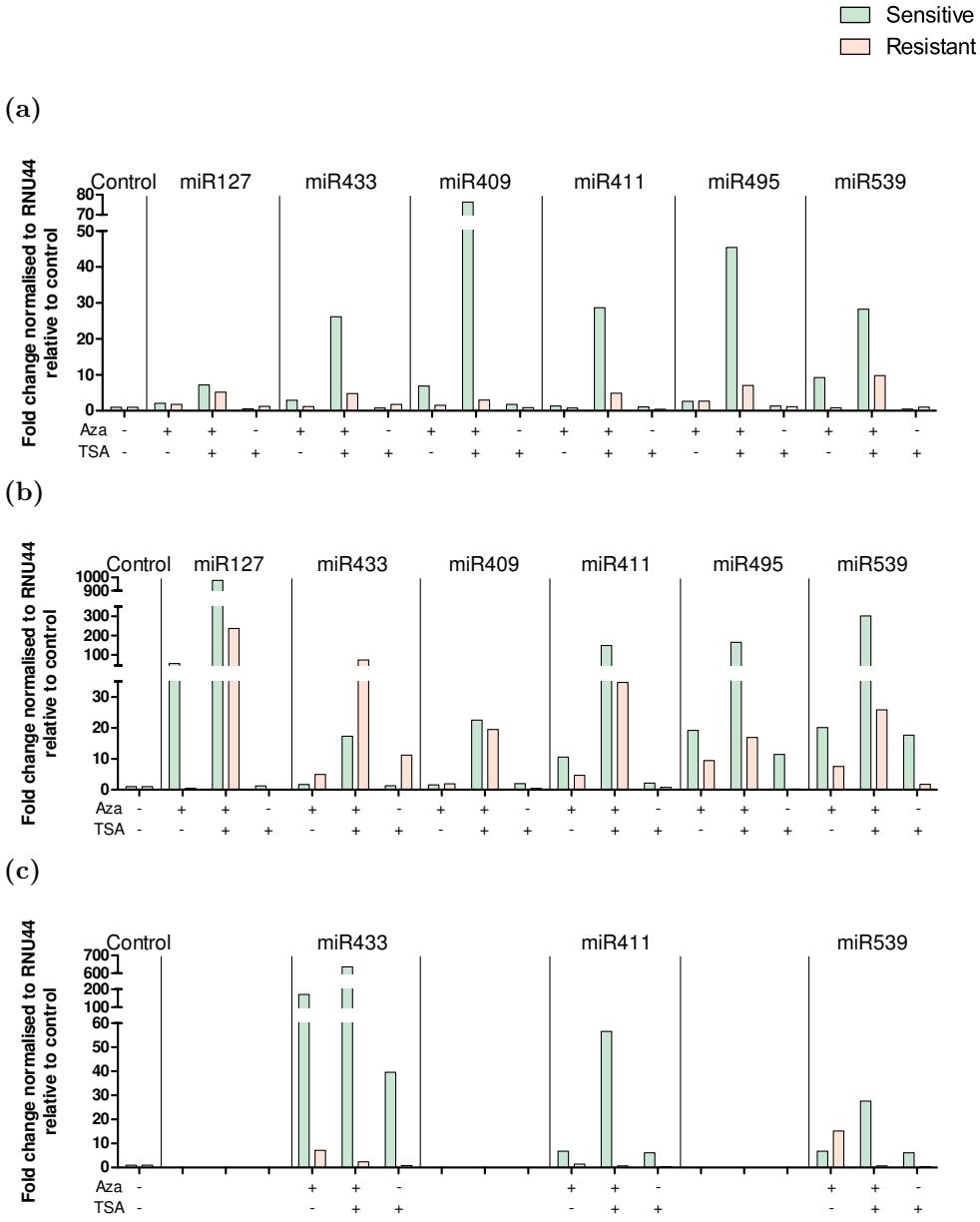

Figure 7.10: miRNA Expression after 5-Aza-2′-deoxycytidine (Aza) and Trichostatin A (TSA) Treatment. Replicate three of the experiment, miR433, miR411, and miR539 were only performed on this replicate. The experiments are shown separately due to the high variability of the experiment. Stem-loop RT-qPCR is expressed as fold change relative to RNU44 and normalised to the untreated condition for each cell line. This does not permit direct comparison of miRNA levels between the sensitive and resistant cells but shows the effect of each treatment on miRNA expression levels. (a) In BT-474 cells, (b) in HCC1954 cells, and (c) in SKBR-3 cells.

References

(*1*) Liu, L., Greger, J., Shi, H., Liu, Y., Greshock, J., Annan, R., Halsey, W., Sathe, G. M., Martin, A.-M. and Gilmer, T. M. (2009). Novel mechanism of lapatinib resistance in HER2-positive breast tumor cells: activation of AXL. *Cancer Research 69*, 6871–6878.

(*2*) Althuis, M. D., Dozier, J. M., Anderson, W. F., Devesa, S. S. and Brinton, L. A. (2005). Global trends in breast cancer incidence and mortality 1973-1997. *International Journal of Epidemiology 34*, 405–412.

(*3*) Shapiro, S, Coleman, E. a., Broeders, M, Codd, M, de Koning, H, Fracheboud, J, Moss, S, Paci, E, Stachenko, S and Ballard-Barbash, R (1998). Breast cancer screening programmes in 22 countries: current policies, administration and guidelines. International Breast Cancer Screening Network (IBSN) and the European Network of Pilot Projects for Breast Cancer Screening. *International Journal of Epidemiology 27*, 735–742.

(*4*) Jemal, A., Bray, F. and Center, M. (2011). Global cancer statistics. *CA: A Cancer Journal for Clinicians 61*, 69–90.

(*5*) Ozsoy, A., Barca, N., Akdal Dolek, B., Aktas, H., Elverici, E., Araz, L. and Ozkaraoglu, O. (2017). The Relationship Between Breast Cancer and Risk Factors: A Single-Center Study. *European Journal of Breast Health 13*, 145–149.

(*6*) Allred, D. C. (2010). Ductal carcinoma in situ: Terminology, classification, and natural history. *Journal of the National Cancer Institute - Monographs 41*, 134–138.

(*7*) Van Cleef, A, Altintas, S, Huizing, M, Papadimitriou, K, Van Dam, P and Tjalma, W (2014). Current view on ductal carcinoma in situ and importance of the margin thresholds: A review. *Facts Views Vis Obgyn 6*, 210–218.

(*8*) Place, A. E., Jin Huh, S. and Polyak, K. (2011). The microenvironment in breast cancer progression: Biology and implications for treatment. *Breast Cancer Research 13*, 227.

(*9*) Wellings, S. R., Jensen, H. M. and Marcum, R. G. (1975). An Atlas of Subgross Pathology of the Human Breast With Special Reference to Possible Precancerous Lesions. *Journal of the National Cancer Institute 55*, 231–273.

(*10*) Hu, M. et al. (2008). Regulation of In Situ to Invasive Breast Carcinoma Transition. *Cancer Cell 13*, 394–406.

(*11*) Mego, M., Mani, S. A. and Cristofanilli, M. (2010). Molecular mechanisms of metastasis in breast cancer–clinical applications. *Nature reviews. Clinical oncology 7*, 693–701.

(*12*) Cowell, C. F., Weigelt, B., Sakr, R. A., Ng, C. K. Y., Hicks, J., King, T. A. and Reis-Filho, J. S. (2013). Progression from ductal carcinoma in situ to invasive breast cancer: revisited. *Molecular Oncologyl 7*, 859–869.

(*13*) Virnig, B. A., Tuttle, T. M., Shamliyan, T. and Kane, R. L. (2010). Ductal carcinoma in Situ of the breast: A systematic review of incidence, treatment, and outcomes. *Journal of the National Cancer Institute 102*, 170–178.

(*14*) Lakhani, S. R., Audretsch, W., Cleton-Jensen, A.-M., Cutuli, B., Ellis, I., Eusebi, V., Greco, M., Houslton, R. S., Kuhl, C. K., Kurtz, J., Palacios, J., Peterse, H., Rochard, F. and Rutgers, E. (2006). The management of lobular carcinoma in situ (LCIS). Is LCIS the same as ductal carcinoma in situ (DCIS)? *European Journal of Cancer 42*, 2205–2211.

(*15*) Cole, K., Tabernero, M. and Anderson, K. S. (2010). Biologic characteristics of premalignant breast disease. *Cancer Biomarkers 9*, 177–192.

(*16*) Schnitt, S. J. (2010). Classification and prognosis of invasive breast cancer: from morphology to molecular taxonomy. *Modern Pathology 23 Suppl 2*, S60–S64.

(*17*) Warnberg, F, Casalini, P, Nordgren, H, Bergkvist, L, Holmberg, L and Menard, S (2002). Ductal carcinoma in situ of the breast: a new phenotype classification system and its relation to prognosis. *Breast cancer research and treatment 73*, 215–221.

(*18*) Stasik, C. J., Davis, M., Kimler, B. F., Fan, F., Damjanov, I., Thomas, P. and Tawfik, O. W. (2011). Grading Ductal Carcinoma in Situ of the Breast Using an Automated Proliferation Index. *Annals of Clinical and Laboratory Science 41*, 122–130.

(*19*) Yersal, O. and Barutca, S. (2014). Biological subtypes of breast cancer: Prognostic and therapeutic implications. *World Journal of Clinical Oncology 5*, 412–425.

(*20*) Guedj, M, Marisa, L, Reynies, A. D., Orsetti, B, Schiappa, R, Bibeau, F and Macgrogan, G (2012). A refined molecular taxonomy of breast cancer. *Oncogene 31*, 1196–1206.

(*21*) Chivukula, I. V., *Dysregulated notch signaling in breast cancer and liver disease*; Karolinska Institutet: Stockholm, Sweden, 2015.

(*22*) The Cancer Genome Atlas Genome Network (2012). Comprehensive molecular portraits of human breast tumours. *Nature 490*, 61–70.

(*23*) Sorlie, T. et al. (2003). Repeated observation of breast tumor subtypes in independent gene expression data sets. *Proceedings of the National Academy of Sciences 100*, 8418–8423.

(*24*) Kittaneh, M., Montero, A. J. and Glück, S. (2013). Molecular Profiling for Breast Cancer: A Comprehensive Review. *Biomarkers in Cancer 5*, 61–70.

(*25*) Metzger-Filho, O., Sun, Z., Viale, G., Price, K. N., Crivellari, D., Snyder, R. D., Gelber, R. D., Castiglione-Gertsch, M., Coates, A. S., Goldhirsch, A. and Cardoso, F. (2013). Patterns of recurrence and outcome according to breast cancer subtypes in lymph node-negative disease: Results from international breast cancer study group trials VIII and IX. *Journal of Clinical Oncology 31*, 3083–3090.

(*26*) Voduc, K. D., Cheang, M. C. U., Tyldesley, S., Gelmon, K., Nielsen, T. O. and Kennecke, H. (2010). Breast cancer subtypes and the risk of local and regional relapse. *Journal of Clinical Oncology 28*, 1684–1691.

(*27*) Li, Z.-h., Hu, P.-h., Tu, J.-h. and Yu, N.-s. (2016). Luminal B breast cancer: patterns of recurrence and clinical outcome. *Oncotarget 7*, 65024–65033.

(*28*) Ignatiadis, M. and Sotiriou, C. (2013). Luminal breast cancer: from biology to treatment. *Nature reviews. Clinical oncology 10*, 494–506.

(*29*) Sorlie, T et al. (2001). Gene expression patterns of breast carcinomas distinguish tumor subclasses with clinical implications. *Proceedings of the National Academy of Sciences 98*, 10869–10874.

(*30*) Sinn, H. P. and Kreipe, H. (2013). A brief overview of the WHO classification of breast tumors, 4th edition, focusing on issues and updates from the 3rd edition. *Breast Care 8*, 149–154.

(*31*) Viale, G (2012). The current state of breast cancer classification. *Annals of Oncology 23*, x207–x210.

(*32*) Sotiriou, C. and Pusztai, L. (2009). Gene-Expression Signatures in Breast Cancer. *New England Journal of Medicine 360*, 790–800.

(*33*) Dawson, S. J., Rueda, O. M., Aparicio, S. and Caldas, C. (2013). A new genome-driven integrated classification of breast cancer and its implications. *EMBO Journal 32*, 617–628.

(*34*) Cardiff, R. D. and Borowsky, A. D. (2014). At last: Classification of human mammary cells elucidates breast cancer origins. *Journal of Clinical Investigation 124*, 478–480.

(*35*) Santagata, S. et al. (2014). Taxonomy of breast cancer based on normal cell phenotype predicts outcome. *Journal of Clinical Investigation 124*, 859–870.

(*36*) Hynes, N. E. and Lane, H. a. (2005). ERBB receptors and cancer: the complexity of targeted inhibitors. *Nature Reviews Cancer 5*, 341–354.

(*37*) Olayioye, M. A., Neve, R. M., Lane, H. A. and Hynes, N. E. (2000). The ErbB signaling network: receptor heterodimerization in development and cancer. *The EMBO Journal 19*, 3159–3167.

(*38*) Yarden, Y. and Sliwkowski, M. X. (2001). Untangling the ErbB Signalling Network. *Nature Reviews Molecular Cell Biology 2*, 127–137.

(*39*) Olayioye, M. A. (2001). Update on HER-2 as a target for cancer therapy: intracellular signaling pathways of ErbB2/HER-2 and family members. *Breast Cancer Research 3*, 385–389.

(*40*) Baselga, J. and Swain, S. M. (2009). Novel anticancer targets: revisiting ERBB2 and discovering ERBB3. *Nature Reviews Cancer 9*, 463–475.

(*41*) Engelman, J. A., Luo, J. and Cantley, L. C. (2006). The evolution of phosphatidylinositol 3-kinases as regulators of growth and metabolism. *Nature Reviews Genetics 7*, 606–619.

(*42*) Vanhaesebroeck, B., Guibert, J. G. and Graupera, M. (2010). The emerging mechanisms of isoform-specific PI3K signalling. *Nature Reviews Molecular Cell Biology 11*, 329–341.

(*43*) Cantley, L. C. (2002). The Phosphoinositide 3-Kinase Pathway. *Science 296*, 1655–1657.

(*44*) Sun, H., Lesche, R., Li, D.-M., Liliental, J., Zhang, H., Gao, J., Gavrilova, N., Mueller, B., Lui, X. and Wu, H. (1999). PTEN modulates cell cycle progression and cell survival by regulating phosphatidylinositol 3, 4, 5-trisphosphate and Akt/protein kinase B signaling pathway. *Cell Biology 96*, 6199–6204.

(*45*) Song, M. S., Salmena, L. and Pandolfi, P. P. (2012). The functions and regulation of the PTEN tumour suppressor. *Nature Reviews Molecular Cell Biology 13*, 283–296.

(*46*) Stambolic, V., Suzuki, A., Pompa, L. D., Brothers, G. M., Mirtsos, C., Sasaki, T., Ruland, J. and Penninger, J. M. (1998). Negative Regulation of PKB / Akt-Dependent Cell Survival by the Tumor Suppressor PTEN. *Cell 95*, 29–39.

(*47*) Vivanco, I. and Sawyers, C. L. (2002). The Phosphatidylinositol 3-Kinase-AKT Pathway in Human Cancer. *Nature Reviews Cancer 2*, 489–501.

(*48*) Ménard, S., Tagliabue, E., Campiglio, M. and Pupa, S. M. (2000). Role of HER2 gene overexpression in breast carcinoma. *Journal of Cellular Physiology 182*, 150–162.

(*49*) Wolff, A. C., Hammond, M. E. H., Allison, K. H., Harvey, B. E., McShane, L. M. and Dowsett, M. (2018). HER2 Testing in Breast Cancer: American Society of Clinical Oncology/College of American Pathologists Clinical Practice Guideline Focused Update Summary. *Journal of Oncology Practice 14*, 437–441.

(*50*) Wolff, A. C. et al. (2007). American Society of Clinical Oncology/College of American Pathologists guideline recommendations for human epidermal growth factor receptor 2 testing in breast cancer. *Archives of Pathology & Laboratory Medicine 131*, 18–43.

(*51*) Roskoski, R. (2014). The ErbB/HER family of protein-tyrosine kinases and cancer. *Pharmacological Research 79*, 34–74.

(*52*) Dawood, S., Broglio, K., Buzdar, A. U., Hortobagyi, G. N. and Giordano, S. H. (2010). Prognosis of women with metastatic breast cancer by HER2 status and trastuzumab treatment: An institutional-based review. *Journal of Clinical Oncology 28*, 92–98.

(*53*) Klapper, L., Waterman, H., Sela, M. and Yarden, Y. (2000). Tumor-inhibitory antibodies to HER-2/ErbB-2 may act by recruiting c-Cbl and enhancing ubiquitination of HER-2. *Cancer Research 60*, 3384–3388.

(*54*) Nielsen, D. L., Kümler, I., Palshof, J. a. E. and Andersson, M. (2013). Efficacy of HER2-targeted therapy in metastatic breast cancer. Monoclonal antibodies and tyrosine kinase inhibitors. *The Breast 22*, 1–12.

(*55*) Fralick, M, Hilton, J. F., Bouganim, N, Clemons, M and Amir, E (2012). Dual blockade of HER2 - twice as good or twice as toxic? *Clinical Oncology 24*, 593–603.

(*56*) Xu, Z.-q., Zhang, Y., Li, N., Liu, P.-j., Gao, L., Gao, X. and Tie, X.-j. (2017). Efficacy and safety of lapatinib and trastuzumab for HER2-positive breast cancer: a systematic review and meta-analysis of randomised controlled trials. *BMJ Open 7*, e013053.

(*57*) Giordano, S. H., Temin, S., Chandarlapaty, S., Crews, J. R., Esteva, F. J., Kirshner, J. J., Krop, I. E., Levinson, J., Lin, N. U., Modi, S., Patt, D. A., Perlmutter, J., Ramakrishna, N., Winer, E. P. and Davidson, N. E. (2018). Systemic Therapy for Patients With Advanced Human Epidermal Growth Factor Receptor 2–Positive Breast Cancer. *Journal of Clinical Oncology 36*, 7.

(*58*) Baselga, J., Tripathy, D., Mendelsohn, J., Baughman, S., Benz, C. C., Dantis, L., Sklarin, N. T., Seidman, A. D., Hudis, C. A., Moore, J., Rosen, P. P., Twaddell, T., Henderson, I. C. and Norton, L. (1996). Phase II Study of Weekly Intravenous Recombinant Humanized Anti-p185 HER2 Monoclonal Antibody in Patients With HER2/neu-Overexpressing Metastatic Breast Cancer. *Journal of Clinical Oncology 14*, 737–744.

(*59*) Cobleigh, M. A., Vogel, C. L., Tripathy, D., Robert, N. J., Scholl, S., Fehrenbacher, L., Wolter, J. M., Paton, V., Shak, S., Lieberman, G. and Slamon, D. J. (1999). Multinational Study of the Efficacy and Safety of Humanized Anti-HER2 Monoclonal Antibody in Women Who Have HER2-Overexpressing Metastatic Breast Cancer That Has Progressed After Chemotherapy for Metastatic Disease. *Journal of Clinical Oncology 17*, 2639–2648.

(*60*) Metzger-Filho, O., Winer, E. P. and Krop, I. (2013). Pertuzumab: Optimizing HER2 blockade. *Clinical Cancer Research 19*, 5552–5556.

(*61*) Barthélémy, P., Leblanc, J., Goldbarg, V., Wendling, F. and Kurtz, J.-E. (2014). Pertuzumab: development beyond breast cancer. *Anticancer Research 34*, 1483–91.

(*62*) Verma, S., Miles, D., Gianni, L., Krop, I. E., Welslau, M., Baselga, J., Pegram, M., Oh, D.-Y., Diéras, V., Guardino, E., Fang, L., Lu, M. W., Olsen, S. and Blackwell, K. (2012). Trastuzumab Emtansine for HER2-Positive Advanced Breast Cancer. *New England Journal of Medicine 367*, 1783–1791.

(*63*) Doroshow, D. B. and LoRusso, P. M. (2018). Trastuzumab emtansine: determining its role in management of HER2+ breast cancer. *Future Oncology 14*, 589–602.

(*64*) Rusnak, D. W., Lackey, K., Affleck, K., Wood, E. R., Alligood, K. J., Rhodes, N, Keith, B. R., Murray, D. M., Knight, W. B., Mullin, R. J. and Gilmer, T. M. (2001). The effects of the novel, reversible epidermal growth factor receptor/ErbB-2 tyrosine kinase inhibitor, GW2016, on the growth of human normal and tumor-derived cell lines in vitro and in vivo. *Molecular Cancer Therapeutics 1*, 85–94.

(*65*) Tevaarwerk, A. J. and Kolesar, J. M. (2009). Lapatinib: a small-molecule inhibitor of epidermal growth factor receptor and human epidermal growth factor receptor-2 tyrosine kinases used in the treatment of breast cancer. *Clinical Therapeutics 31 Pt 2*, 2332–2348.

(*66*) Canonici, A. et al. (2013). Neratinib overcomes trastuzumab resistance in HER2 amplified breast cancer. *Oncotarget 4*, 1592–1605.

(*67*) López-Tarruella, S., Jerez, Y., Márquez-Rodas, I. and Martín, M. (2012). Neratinib (HKI-272) in the treatment of breast cancer. *Future Oncology 8*, 671–681.

(*68*) Kalous, O., Conklin, D., Desai, A. J., O'Brien, N. A., Ginther, C., Anderson, L., Cohen, D. J., Britten, C. D., Taylor, I., Christensen, J. G., Slamon, D. J. and Finn, R. S. (2012). Dacomitinib (PF-00299804), an irreversible Pan-HER inhibitor, inhibits proliferation of HER2-amplified breast cancer cell lines resistant to trastuzumab and lapatinib. *Molecular Cancer Therapeutics 11*, 1978–1987.

(*69*) Lee, I. H., Sohn, M, Lim, H. J., Yoon, S, Oh, H, Shin, S, Shin, J. H., Oh, S.-H., Kim, J, Lee, D. K., Noh, D. Y., Bae, D. S., Seong, J. K. and Bae, Y. S. (2014). Ahnak functions as a tumor suppressor via modulation of TGFβ/Smad signaling pathway. *Oncogene 33*, 4675–4684.

(*70*) Barker, A. J., Gibson, K. H., Grundy, W., Godfrey, A. A., Barlow, J. J., Healy, M. P., Woodburn, J. R., Ashton, S. E., Curry, B. J., Scarlett, L., Henthorn, L. and Richards, L. (2001). Studies Leading to the Identification of ZD1839 (Iressa): An Orally Active, Selective Epidermal Growth Factor Receptor Tyrosine Kinase Inhibitor Targeted to the Treatment of Cancer. *Bioorganic & Medicinal Chemistry Letters 11*, 1911–1914.

(*71*) Rahman, A. F.M. M., Korashy, H. M. and Kassem, M. G. (2014). Gefitinib. *Profiles of Drug Substances, Excipients and Related Methodology 39*, 239–264.

(*72*) Konecny, G. E., Pegram, M. D., Venkatesan, N., Finn, R., Yang, G., Rahmeh, M., Untch, M., Rusnak, D. W., Spehar, G., Mullin, R. J., Keith, B. R., Gilmer, T. M., Berger, M., Podratz, K. C. and Slamon, D. J. (2006). Activity of the dual kinase inhibitor lapatinib (GW572016) against HER-2-overexpressing and trastuzumab-treated breast cancer cells. *Cancer Research 66*, 1630–1639.

(*73*) Han, J. and Sun, P. (2007). The pathways to tumor suppression via route p38. *Trends in Biochemical Sciences 32*, 364–371.

(*74*) Abukhdeir, A. M. and Park, B. H. (2008). p21 and p27: Roles in carcinogenesis and drug resistance. *Expert Reviews in Molecular Medicine 10*, e19.

(*75*) Abbas, T. and Dutta, A. (2009). P21 in cancer: Intricate networks and multiple activities. *Nature Reviews Cancer 9*, 400–414.

(*76*) National Institute for Health and Care Excellence (2018). Managing advanced breast cancer. *NICE Pathways*, 1–22.

(*77*) Narayan, M., Wilken, J. A., Harris, L. N., Baron, A. T., Kimbler, K. D. and Maihle, N. J. (2009). Trastuzumab-Induced HER Reprogramming in "Resistant" Breast Carcinoma Cells. *Cancer Research 69*, 2191–2194.

(*78*) Trowe, T. et al. (2008). EXEL-7647 inhibits mutant forms of ErbB2 associated with lapatinib resistance and neoplastic transformation. *Clinical Cancer Research 14*, 2465–2475.

(*79*) Pohlmann, P. R., Mayer, I. A. and Mernaugh, R. (2009). Resistance to trastuzumab in breast cancer. *Clinical Cancer Research 15*, 7479–7491.

(*80*) Fiszman, G. L. and Jasnis, M. A. (2011). Molecular Mechanisms of Trastuzumab Resistance in HER2 Overexpressing Breast Cancer. *International Journal of Breast Cancer 2011*, 352182.

(*81*) Cuello, M, Ettenberg, S. A., Clark, A. S., Keane, M. M., Posner, R. H., Nau, M. M., Dennis, P. A. and Lipkowitz, S (2001). Down-regulation of the erbB-2 receptor by trastuzumab (herceptin) enhances tumor necrosis factor-related apoptosis-inducing ligand-mediated apoptosis in breast and ovarian cancer cell lines that overexpress erbB-2. *Cancer Research 61*, 4892–4900.

(*82*) Gu, L., Lau, S. K., Loera, S., Somlo, G. and Kane, S. E. (2009). Protein kinase A activation confers resistance to trastuzumab in human breast cancer cell lines. *Clinical Cancer Research 15*, 7196–7206.

(*83*) Berns, K., Horlings, H. M., Hennessy, B. T., Madiredjo, M., Hijmans, E. M., Beelen, K., Linn, S. C., Gonzalez-Angulo, A. M., Stemke-Hale, K., Hauptmann, M., Beijersbergen, R. L., Mills, G. B., van de Vijver, M. J. and Bernards, R. (2007). A Functional Genetic Approach Identifies the PI3K Pathway as a Major Determinant of Trastuzumab Resistance in Breast Cancer. *Cancer Cell 12*, 395–402.

(*84*) Junttila, T. T., Akita, R. W., Parsons, K., Fields, C., Lewis Phillips, G. D., Friedman, L. S., Sampath, D. and Sliwkowski, M. X. (2009). Ligand-Independent HER2/HER3/PI3K Complex Is Disrupted by Trastuzumab and Is Effectively Inhibited by the PI3K Inhibitor GDC-0941. *Cancer Cell 15*, 429–440.

(*85*) Garrett, J. T., Olivares, M. G., Rinehart, C., Granja-Ingram, N. D., Sanchez, V., Chakrabarty, A., Dave, B., Cook, R. S., Pao, W., McKinely, E., Manning, H. C., Chang, J. and Arteaga, C. L. (2011). Transcriptional and posttranslational up-regulation of HER3 (ErbB3) compensates for inhibition of the HER2 tyrosine kinase. *Proceedings of the National Academy of Sciences 108*, 5021–5026.

(*86*) Lee-Hoeflich, S. T., Crocker, L., Yao, E., Pham, T., Munroe, X., Hoeflich, K. P., Sliwkowski, M. X. and Stern, H. M. (2008). A central role for HER3 in HER2-amplified breast cancer: Implications for targeted therapy. *Cancer Research 68*, 5878–5887.

(*87*) Lu, Y., Zi, X., Zhao, Y., Mascarenhas, D. and Pollak, M. (2001). Insulin-Like Growth Factor-I Receptor Signaling and Resistance to Trastuzumab (Herceptin). *Journal of the National Cancer Institute 93*, 1852–1857.

(*88*) Nahta, R., Yuan, L. X. H., Zhang, B., Kobayashi, R. and Esteva, F. J. (2005). Insulin-like growth factor-I receptor/human epidermal growth factor receptor 2 heterodimerization contributes to trastuzumab resistance of breast cancer cells. *Cancer Research 65*, 11118–11128.

(*89*) O'Brien, N. A., Browne, B. C., Chow, L., Wang, Y., Ginther, C., Arboleda, J., Duffy, M. J., Crown, J., O'Donovan, N. and Slamon, D. J. (2010). Activated Phosphoinositide 3-Kinase/AKT Signaling Confers Resistance to Trastuzumab but not Lapatinib. *Molecular Cancer Therapeutics 9*, 1489–1502.

(*90*) Ritter, C. A., Perez-Torres, M., Rinehart, C., Guix, M., Dugger, T., Engelman, J. A. and Arteaga, C. L. (2007). Human breast cancer cells selected for resistance to trastuzumab in vivo overexpress epidermal growth factor receptor and ErbB ligands and remain dependent on the ErbB receptor network. *Clinical Cancer Research 13*, 4909–4919.

(*91*) Motoyama, A. B., Hynes, N. E. and Lane, H. A. (2002). The efficacy of ErbB receptor targeted anti-cancer therapeutics is influenced by the availability of EGF-related peptides. *Cancer Research 62*, 3151–3158.

(*92*) Wood, E. R., Truesdale, A. T., McDonald, O. B., Yuan, D., Hassell, A., Dickerson, S. H., Ellis, B., Pennisi, C., Horne, E., Lackey, K., Alligood, K. J., Rusnak, D. W., Gilmer, T. M. and Shewchuk, L. (2004). A Unique Structure for Epidermal Growth Factor Receptor Bound to GW572016 (Lapatinib). *Cancer Research 64*, 6652–6659.

(*93*) Baselga, J. (2006). Targeting tyrosine kinases in cancer: The second wave. *Science 312*, 1175–1178.

(*94*) Xia, W., Petricoin, E. F., Zhao, S., Liu, L., Osada, T., Cheng, Q., Wulfkuhle, J. D., Gwin, W. R., Yang, X., Gallagher, R. I., Bacus, S., Lyerly, H. K. and Spector, N. L. (2013). An heregulin-EGFR-HER3 autocrine signaling axis can mediate acquired lapatinib resistance in HER2+ breast cancer models. *Breast Cancer Research 15*, DOI: `10.1186/bcr3480`.

(*95*) Nagata, Y., Lan, K. H., Zhou, X., Tan, M., Esteva, F. J., Sahin, A. A., Klos, K. S., Li, P., Monia, B. P., Nguyen, N. T., Hortobagyi, G. N., Hung, M. C. and Yu, D. (2004). PTEN activation contributes to tumor inhibition by trastuzumab, and loss of PTEN predicts trastuzumab resistance in patients. *Cancer Cell 6*, 117–127.

(*96*) Xia, W., Husain, I., Liu, L., Bacus, S., Saini, S., Spohn, J., Pry, K., Westlund, R., Stein, S. H. and Spector, N. L. (2007). Lapatinib antitumor activity is not dependent upon phosphatase and tensin homologue deleted on chromosome 10 in ErbB2-overexpressing breast cancers. *Cancer Research 67*, 1170–1175.

(*97*) Vazquez-Martin, A., Oliveras-Ferraros, C. and Menendez, J. A. (2009). Autophagy facilitates the development of breast cancer resistance to the anti-HER2 monoclonal antibody trastuzumab. *PLoS ONE 4*, DOI: `10.1371/journal.pone.0006251`.

(*98*) Chen, S., Li, X., Feng, J., Chang, Y., Wang, Z. and Wen, A. (2011). Autophagy facilitates the Lapatinib resistance of HER2 positive breast cancer cells. *Medical Hypotheses 77*, 206–208.

(*99*) Karakashev, S. V. and Reginato, M. J. (2015). Hypoxia/HIF1alpha induces lapatinib resistance in ERBB2-positive breast cancer cells via regulation of DUSP2. *Oncotarget 6*, 1967–1980.

(*100*) Bartel, D. P. (2004). MicroRNAs: Genomics, Biogenesis, Mechanism, and Function. *Cell 116*, 281–297.

(*101*) Winter, J., Jung, S., Keller, S., Gregory, R. I. and Diederichs, S. (2009). Many roads to maturity: microRNA biogenesis pathways and their regulation. *Nature Cell Biology 11*, 228–234.

(*102*) Hutvagner, G. and Zamore, P. D. (2002). A microRNA in a Multiple-Turnover RNAi Enzyme Complex. *Science 297*, 2056–2060.

(*103*) Zhang, P. Y. et al. (2016). Dicer interacts with SIRT7 and regulates H3K18 deacetylation in response to DNA damaging agents. *Nucleic Acids Research 44*, 3629–3642.

(*104*) Wilson, R. C., Tambe, A., Kidwell, M. A., Noland, C. L., Schneider, C. P. and Doudna, J. A. (2015). Dicer-TRBP complex formation ensures accurate mammalian MicroRNA biogenesis. *Molecular Cell 57*, 397–408.

(*105*) Abdelfattah, A. M., Park, C. and Choi, M. Y. (2014). Update on non-canonical microRNAs. *Biomolecular Concepts 5*, 275–287.

(*106*) Havens, M. A., Reich, A. A., Duelli, D. M. and Hastings, M. L. (2012). Biogenesis of mammalian microRNAs by a non-canonical processing pathway. *Nucleic Acids Research 40*, 4626–4640.

(*107*) Bartel, D. P. (2009). MicroRNAs: target recognition and regulatory functions. *Cell 136*, 215–233.

(*108*) Liu, J., Carmell, M. A., Rivas, F. V., Marsden, C. G., Thompson, J. M., Song, J.-J., Hammond, S. M., Joshua-Tor, L. and Hannon, G. J. (2004). Argonaute2 Is the Catalytic Engine of Mammalian RNAi. *Science 305*, 1437–1441.

(*109*) Meister, G., Landthaler, M., Patkaniowska, A., Dorsett, Y., Teng, G. and Tuschl, T. (2004). Human Argonaute2 mediates RNA cleavage targeted by miRNAs and siRNAs. *Molecular Cell 15*, 185–197.

(*110*) Grimson, A., Farh, K. K.-H., Johnston, W. K., Garrett-Engele, P., Lim, L. P. and Bartel, D. P. (2007). MicroRNA targeting specificity in mammals: determinants beyond seed pairing. *Molecular Cell 27*, 91–105.

(*111*) Wilczynska, A and Bushell, M (2014). The complexity of miRNA-mediated repression. *Cell Death and Differentiation 22*, 22–33.

(*112*) Lewis, B. P., Burge, C. B. and Bartel, D. P. (2005). Conserved Seed Pairing, Often Flanked by Adenosines, Indicates that Thousands of Human Genes are MicroRNA Targets. *Cell 120*, 15–20.

(*113*) Friedman, R. C., Farh, K. K.-H.K.-H., Burge, C. B. and Bartel, D. P. (2009). Most mammalian mRNAs are conserved targets of microRNAs. *Genome Research 19*, 92–105.

(*114*) Suzuki, H., Maruyama, R., Yamamoto, E. and Kai, M. (2012). DNA methylation and microRNA dysregulation in cancer. *Molecular Oncology 6*, 567–578.

(*115*) De Cola, A et al. (2015). MIR-205-5p-mediated downregulation of ERBB/HER receptors in breast cancer stem cells results in targeted therapy resistance. *Cell Death and Disease 6*, e1823.

(*116*) Calin, G. a. and Croce, C. M. (2006). MicroRNA signatures in human cancers. *Nature Reviews Cancer 6*, 857–866.

(*117*) Lu, J., Getz, G., Miska, E. a., Alvarez-Saavedra, E., Lamb, J., Peck, D., Sweet-Cordero, A., Ebert, B. L., Mak, R. H., Ferrando, A. a., Downing, J. R., Jacks, T., Horvitz, H. R. and Golub, T. R. (2005). MicroRNA expression profiles classify human cancers. *Nature 435*, 834–838.

(*118*) Calin, G. A., Sevignani, C., Dumitru, C. D., Hyslop, T., Noch, E., Yendamuri, S., Shimizu, M., Rattan, S., Bullrich, F., Negrini, M. and Croce, C. M. (2004). Human microRNA genes are frequently located at fragile sites and genomic regions involved in cancers. *Proceedings of the National Academy of Sciences 101*, 2999–3004.

(*119*) Vincent, K., Pichler, M., Lee, G. W. and Ling, H. (2014). MicroRNAs, genomic instability and cancer. *International Journal of Molecular Sciences 15*, 14475–14491.

(*120*) Yu, S. L. et al. (2008). MicroRNA Signature Predicts Survival and Relapse in Lung Cancer. *Cancer Cell 13*, 48–57.

(*121*) Landi, M. T. et al. (2010). MicroRNA expression differentiates histology and predicts survival of lung cancer. *Clinical Cancer Research 16*, 430–441.

(*122*) Yanaihara, N., Caplen, N., Bowman, E., Seike, M., Kumamoto, K., Yi, M., Stephens, R. M., Okamoto, A., Yokota, J., Tanaka, T., Calin, G. A., Liu, C. G., Croce, C. M. and Harris, C. C. (2006). Unique microRNA molecular profiles in lung cancer diagnosis and prognosis. *Cancer Cell 9*, 189–198.

(*123*) Zhang, L. et al. (2006). microRNAs exhibit high frequency genomic alterations in human cancer. *Proceedings of the National Academy of Sciences 103*, 9136–9141.

(*124*) Iorio, M. V. et al. (2005). MicroRNA gene expression deregulation in human breast cancer. *Cancer Research 65*, 7065–7070.

(*125*) Tsang, J. Y., Ni, Y. B., Ng, E. K., Shin, V. Y., Mak, K. F., Go, E. M. L., Tawasil, J., Chan, S. K., Ko, C. W., Kwong, A. and Tse, G. M. (2015). MicroRNAs are differentially deregulated in mammary malignant phyllodes tumour. *Histopathology 67*, 294–305.

(*126*) Teoh, S. L. and Das, S. (2017). The Role of MicroRNAs in Diagnosis, Prognosis, Metastasis and Resistant Cases in Breast Cancer. *Current Pharmaceutical Design 23*, 1845–1859.

(*127*) Halvorsen, A. R., Helland, Å., Gromov, P., Wielenga, V. T., Talman, M. L. M., Brunner, N., Sandhu, V., Børresen-Dale, A. L., Gromova, I. and Haakensen, V. D. (2017). Profiling of microRNAs in tumor interstitial fluid of breast tumors – A novel resource to identify biomarkers for prognostic classification and detection of cancer. *Molecular Oncology 11*, 220–234.

(*128*) Bravatà, V., Cammarata, F. P., Forte, G. I. and Minafra, L. (2013). "Omics" of HER2-Positive Breast Cancer. *OMICS: A Journal of Integrative Biology 17*, 119–129.

(*129*) Croce, C. M. (2009). Causes and consequences of microRNA dysregulation in cancer. *Nature Reviews Genetics 10*, 704–714.

(*130*) Fang, L., Du, W. W., Yang, W., Rutnam, Z. J., Peng, C., Li, H., O'Malley, Y. Q., Askeland, R. W., Sugg, S., Liu, M., Mehta, T., Deng, Z. and Yang, B. B. (2012). MiR-93 enhances angiogenesis and metastasis by targeting LATS2. *Cell Cycle 11*, 4352–4365.

(*131*) Li, H. and Yang, B. B. (2013). Friend or foe: the role of microRNA in chemotherapy resistance. *Acta Pharmacologica Sinica 34*, 870–879.

(*132*) Siragam, V., Rutnam, Z. J., Yang, W., Fang, L., Luo, L., Yang, X., Li, M., Deng, Z., Qian, J., Peng, C. and Yang, B. B. (2012). MicroRNA miR-98 inhibits tumor angiogenesis and invasion by targeting activin receptor-like kinase-4 and matrix metalloproteinase-11. *Oncotarget 3*, 1370–1385.

(*133*) Ye, G., Fu, G., Cui, S., Zhao, S., Bernaudo, S., Bai, Y., Ding, Y., Zhang, Y., Yang, B. B. and Peng, C. (2011). MicroRNA 376c enhances ovarian cancer cell survival by targeting activin receptor-like kinase 7: implications for chemoresistance. *Journal of Cell Science 124*, 359–368.

(*134*) Si, M. L., Zhu, S, Wu, H., Lu, Z, Wu, F and Mo, Y. Y. (2007). miR-21-mediated tumor growth. *Oncogene 26*, 2799–2803.

(*135*) Scott, G. K., Goga, A., Bhaumik, D., Berger, C. E., Sullivan, C. S. and Benz, C. C. (2007). Coordinate suppression of ERBB2 and ERBB3 by enforced expression of micro-RNA miR-125a or miR-125b. *The Journal of Biological Chemistry 282*, 1479–1486.

(*136*) Yu, Z., Wang, C., Wang, M., Li, Z., Casimiro, M. C., Liu, M., Wu, K., Whittle, J., Ju, X., Hyslop, T., McCue, P. and Pestell, R. G. (2008). A cyclin D1/microRNA 17/20 regulatory feedback loop in control of breast cancer cell proliferation. *Journal of Cell Biology 182*, 509–517.

(*137*) Zhu, S., Si, M. L., Wu, H. and Mo, Y. Y. (2007). MicroRNA-21 targets the tumor suppressor gene tropomyosin 1 (TPM1). *Journal of Biological Chemistry 282*, 14328–14336.

(*138*) Mertens-Talcott, S. U., Chintharlapalli, S., Li, X. and Safe, S. (2007). The oncogenic microRNA-27a targets genes that regulate specificity protein transcription factors and the G2-M checkpoint in MDA-MB-231 breast cancer cells. *Cancer Research 67*, 11001–11011.

(*139*) Mattie, M. D., Benz, C. C., Bowers, J., Sensinger, K., Wong, L., Scott, G. K., Fedele, V., Ginzinger, D., Getts, R. and Haqq, C. (2006). Optimized high-throughput microRNA expression profiling provides novel biomarker assessment of clinical prostate and breast cancer biopsies. *Molecular Cancer 5*, 24.

(*140*) Yu, F., Yao, H., Zhu, P., Zhang, X., Pan, Q., Gong, C., Huang, Y., Hu, X., Su, F., Lieberman, J. and Song, E. (2007). let-7 Regulates Self Renewal and Tumorigenicity of Breast Cancer Cells. *Cell 131*, 1109–1123.

(*141*) Jones, R., Watson, K., Bruce, A., Nersesian, S., Kitz, J. and Moorehead, R. (2017). Re-expression of miR-200c suppresses proliferation, colony formation and in vivo tumor growth of murine claudin-low mammary tumor cells. *Oncotarget 8*, 23727–23749.

(*142*) Tavanafar, F., Safaralizadeh, R., Hosseinpour-Feizi, M. A., Mansoori, B., Shanehbandi, D., Mohammadi, A. and Baradaran, B. (2017). Restoration of miR-143 expression could inhibit migration and growth of MDA-MB-468 cells through down-regulating the expression of invasion-related factors. *Biomedicine and Pharmacotherapy 91*, 920–924.

(*143*) Dentelli, P., Traversa, M., Rosso, A., Togliatto, G., Olgasi, C., Marchiò, C., Provero, P., Lembo, A., Bon, G., Annaratone, L., Sapino, A., Falcioni, R. and Brizzi, M. F. (2014). miR-221/222 control luminal breast cancer tumor progression by regulating different targets. *Cell Cycle 13*, 1811–1826.

(*144*) Pan, Y., Li, J., Zhang, Y., Wang, N., Liang, H., Liu, Y., Zhang, C. Y., Zen, K. and Gu, H. (2016). Slug-upregulated MIR-221 promotes breast cancer progression through suppressing E-cadherin expression. *Scientific Reports 6*, 25798.

(*145*) Huang, Q. et al. (2008). The microRNAs miR-373 and miR-520c promote tumour invasion and metastasis. *Nature Cell Biology 10*, 202–210.

(*146*) Zhu, S., Wu, H., Wu, F., Nie, D., Sheng, S. and Mo, Y. Y. (2008). MicroRNA-21 targets tumor suppressor genes in invasion and metastasis. *Cell Research 18*, 350–359.

(*147*) McGuire, A., Brown, J. A. L. and Kerin, M. J. (2015). Metastatic breast cancer: the potential of miRNA for diagnosis and treatment monitoring. *Cancer and Metastasis Reviews 34*, 145–155.

(*148*) Cummins, J. M. and Velculescu, V. E. (2006). Implications of micro-RNA profiling for cancer diagnosis. *Oncogene 25*, 6220–6227.

(*149*) Camps, C., Buffa, F. M., Colella, S., Moore, J., Sotiriou, C., Sheldon, H., Harris, A. L., Gleadle, J. M. and Ragoussis, J. (2008). Hsa-miR-210 is induced by hypoxia and is an independent prognostic factor in breast cancer. *Clinical Cancer Research 14*, 1340–1348.

(*150*) Fkih M'hamed, I., Privat, M., Trimeche, M., Penault-Llorca, F., Bignon, Y. J. and Kenani, A. (2017). miR-10b, miR-26a, miR-146a And miR-153 Expression in Triple Negative Vs Non Triple Negative Breast Cancer: Potential Biomarkers. *Pathology and Oncology Research 23*, 815–827.

(*151*) Zhu, W., Qin, W., Atasoy, U. and Sauter, E. R. (2009). Circulating microRNAs in breast cancer and healthy subjects. *BMC Research Notes 2*, 89.

(*152*) Heneghan, H. M., Miller, N., Lowery, A. J., Sweeney, K. J. and Kerin, M. J. (2010). MicroRNAs as Novel Biomarkers for Breast Cancer. *Journal of Oncology 2010*, 950201.

(*153*) Lowery, A. J., Miller, N., McNeill, R. E. and Kerin, M. J. (2008). MicroRNAs as prognostic indicators and therapeutic targets: Potential effect on breast cancer management. *Clinical Cancer Research 14*, 360–365.

(*154*) Castilla, M. Á., Díaz-Martín, J., Sarrió, D., Romero-Pérez, L., López-García, M. Á., Vieites, B., Biscuola, M., Ramiro-Fuentes, S., Isacke, C. M. and Palacios, J. (2012). MicroRNA-200 Family Modulation in Distinct Breast Cancer Phenotypes. *PLoS ONE 7*, e47709.

(*155*) Chen, J., Tian, W., Cai, H., He, H. and Deng, Y. (2012). Down-regulation of microRNA-200c is associated with drug resistance in human breast cancer. *Medical Oncology 29*, 2527–2534.

(*156*) García-Becerra, R., Santos, N., Díaz, L. and Camacho, J. (2012). Mechanisms of Resistance to Endocrine Therapy in Breast Cancer: Focus on Signaling Pathways, miRNAs and Genetically Based Resistance. *International Journal of Molecular Sciences 14*, 108–145.

(*157*) Kastl, L, Brown, I and Schofield, A. C. (2012). miRNA-34a is associated with docetaxel resistance in human breast cancer cells. *Breast Cancer Research and Treatment 131*, 445–454.

(*158*) Meng, F., Henson, R., Lang, M., Wehbe, H., Maheshwari, S., Mendell, J. T., Jiang, J., Schmittgen, T. D. and Patel, T. (2006). Involvement of human micro-RNA in growth and response to chemotherapy in human cholangiocarcinoma cell lines. *Gastroenterology 130*, 2113–2129.

(*159*) Liu, B., Su, F., Chen, M., Li, Y., Qi, X., Xiao, J., Li, X., Liu, X., Liang, W., Zhang, Y. and Zhang, J. (2017). Serum miR-21 and miR-125b as markers predicting neoadjuvant chemotherapy response and prognosis in stage II/III breast cancer. *Human Pathology 64*, 44–52.

(*160*) Raychaudhuri, M., Bronger, H., Buchner, T., Kiechle, M., Weichert, W. and Avril, S. (2017). MicroRNAs miR-7 and miR-340 predict response to neoadjuvant chemotherapy in breast cancer. *Breast Cancer Research and Treatment 162*, 511–521.

(*161*) Liu, B., Su, F., Li, Y., Qi, X., Liu, X., Liang, W., You, K., Zhang, Y. and Zhang, J. (2017). Changes of serum miR34a expression during neoadjuvant chemotherapy predict the treatment response and prognosis in stage II/III breast cancer. *Biomedicine and Pharmacotherapy 88*, 911–917.

(*162*) Ye, X., Bai, W., Zhu, H., Zhang, X., Chen, Y., Wang, L., Yang, A., Zhao, J. and Jia, L. (2014). Mir-221 promotes trastuzumab-resistance and metastasis in her2-positive breast cancers by targeting PTEN. *BMB Reports 47*, 268–273.

(*163*) Jung, E. J., Santarpia, L., Kim, J., Esteva, F. J., Moretti, E., Buzdar, A. U., Di Leo, A., Le, X. F., Bast, R. C., Park, S. T., Pusztai, L. and Calin, G. A. (2012). Plasma microRNA 210 levels correlate with sensitivity to trastuzumab and tumor presence in breast cancer patients. *Cancer 118*, 2603–2614.

(*164*) Gong, C., Yao, Y., Wang, Y., Liu, B., Wu, W., Chen, J., Su, F., Yao, H. and Song, E. (2011). Up-regulation of miR-21 mediates resistance to trastuzumab therapy for breast cancer. *Journal of Biological Chemistry 286*, 19127–19137.

(*165*) Corcoran, C., Rani, S., Breslin, S., Gogarty, M., Ghobrial, I. M., Crown, J. and O'Driscoll, L. (2014). MiR-630 targets IGF1R to regulate response to HER-targeting drugs and overall cancer cell progression in HER2 over-expressing breast cancer. *Molecular Cancer 13*, 71.

(*166*) Mulrane, L., McGee, S. F., Gallagher, W. M. and O'Connor, D. P. (2013). miRNA dysregulation in breast cancer. *Cancer Research 73*, 6554–6562.

(*167*) Mandujano-Tinoco, E. A., García-Venzor, A., Melendez-Zajgla, J. and Maldonado, V. (2018). New emerging roles of microRNAs in breast cancer. *Breast Cancer Research and Treatment 171*, 247–259.

(*168*) Rupaimoole, R. and Slack, F. J. (2017). MicroRNA therapeutics: Towards a new era for the management of cancer and other diseases. *Nature Reviews Drug Discovery 16*, 203–221.

(*169*) Turner, B. M. (2007). Defining an epigenetic code. *Nature Cell Biology 9*, 2–6.

(*170*) Cheng, X. (1995). Structure and Function of DNA Methyltransferases. *Annual Review of Biophysics and Biomolecular Structure 24*, 293–318.

(*171*) Denis, H., Ndlovu, M. N. and Fuks, F. (2011). Regulation of mammalian DNA methyltransferases: a route to new mechanisms. *EMBO Reports 12*, 647–656.

(*172*) Esteller, M. (2007). Cancer epigenomics : DNA methylomes and histone-modification maps. *Nature Reviews Genetics 8*, 286–298.

(*173*) Smith, Z. D. and Meissner, A. (2013). DNA methylation : roles in mammalian development. *Nature Reviews Genetics 14*, 204–220.

(*174*) Ehrlich, M., A.Gama-Sosa, M., Huang, L.-H., Midgett, R. M., Kuo, K. C., A.McCune, R. and Gehrke, C. (1982). Amount and distribution of 5-methylcytosine in human DNA from different types of tissues or cells. *Nucleic Acids Research 10*, 2709–2721.

(*175*) Du, Q., Wang, Z. and Schramm, V. L. (2016). Human DNMT1 transition state structure. *Proceedings of the National Academy of Sciences 113*, 2916–2921.

(*176*) Klimasauskas, S., Kumar, S., Roberts, R. J. and Cheng, X. (1994). Hhal methyltransferase flips its target base out of the DNA helix. *Cell 76*, 357–369.

(*177*) Bird, A. (2002). DNA methylation patterns and epigenetic memory. *Genes and Development 16*, 6–21.

(*178*) Vinson, C. and Chatterjee, R. (2012). CG methylation. *Epigenomics 4*, 655–663.

(*179*) Song, J., Teplova, M., Ishibe-Murakami, S. and Patel, D. J. (2012). Structure-based mechanistic insights into DNMT1-mediated maintenance DNA methylation. *Science 335*, 709–712.

(*180*) Bashtrykov, P., Jankevicius, G., Smarandache, A., Jurkowska, R. Z., Ragozin, S. and Jeltsch, A. (2012). Specificity of dnmt1 for methylation of hemimethylated CpG sites resides in its catalytic domain. *Chemistry and Biology 19*, 572–578.

(*181*) Li, E., Bestor, T. H. and Jaenisch, R. (1992). Targeted mutation of the DNA methyltransferase gene results in embryonic lethality. *Cell 69*, 915–926.

(*182*) Tada, M., Tada, T., Lefebvre, L., Barton, S. C. and Surani, M. A. (1997). Embryonic germ cells induce epigenetic reprogramming of somatic nucleus in hybrid cells. *The EMBO Journal 16*, 6510–6520.

(*183*) Monk, M., Boubelik, M. and Lehnert, S. (1987). Temporal and regional changes in DNA methylation in the embryonic, extraembryonic and germ cell lineages during mouse embryo development. *Development 99*, 371–382.

(*184*) Kafri, T., Ariel, M., Brandeis, M., Shemer, R., Urven, L., McCarrey, J., Cedar, H. and Razin, A. (1992). Developmental pattern of gene-specific DNA methylation in the mouse embryo and germ line. *Genes and Development 6*, 705–714.

(*185*) Jurkowska, R. Z., Jurkowski, T. P. and Jeltsch, A. (2011). Structure and Function of Mammalian DNA Methyltransferases. *ChemBioChem 12*, 206–222.

(*186*) Barlow, D. P. and Bartolomei, M. S. (2014). Genomic Imprinting in Mammals. *Cold Spring Harbor Perspectives in Biology 6*, a018382.

(*187*) Plasschaert, R. N. and Bartolomei, M. S. (2014). Genomic imprinting in development, growth, behavior and stem cells. *Development 141*, 1805–1813.

(*188*) Kaneda, M., Okano, M., Hata, K. and Sado, T. (2004). Essential role for de novo DNA methyltransferase Dnmt3a in paternal and maternal imprinting. *Nature 429*, 900–903.

(*189*) Reik, W., Dean, W. and Walter, J. (2001). Epigenetic Reprogramming in Mammalian Development. *Science 293*, 1089–1094.

(*190*) Angulo, M. A., Butler, M. G. and Cataletto, M. E. (2015). Prader-Willi syndrome: A review of clinical, genetic, and endocrine findings. *Journal of Endocrinological Investigation 38*, 1249–1263.

(*191*) Cassidy, S. B., Schwartz, S., Miller, J. L. and Driscoll, D. J. (2012). Prader-Willi syndrome. *Genetics in Medicine 14*, 10–26.

(*192*) Margolis, S. S., Sell, G. L., Zbinden, M. A. and Bird, L. M. (2015). Angelman Syndrome. *Neurotherapeutics 12*, 641–650.

(*193*) Kalsner, L. and Chamberlain, S. J. (2015). Prader-Willi, Angelman, and 15q11-q13 Duplication Syndromes. *Pediatric Clinics of North America 62*, 587–606.

(*194*) Jones, P. A. and Baylin, S. B. (2002). The fundamental role of epigenetic events in cancer. *Nature Reviews Genetics 3*, 415–428.

(*195*) Fletcher, T. M. and Hansen, J. C. (1996). The nucleosomal array: structure/function relationships. *Critical Reviews in Eukaryotic Gene Expression 6*, 149–88.

(*196*) Kornberg, R. D. (1974). Chromatin Structure : A Repeating Unit of Histones and DNA. *Science 184*, 868–871.

(*197*) Thomas, J. O. (1984). The higher order structure of chromatin and histone H1. *Journal of cell science. Supplement 1*, 1–20.

(*198*) Bannister, A. J. and Kouzarides, T. (2011). Regulation of chromatin by histone modifications. *Cell Research 21*, 381–395.

(*199*) Strålfors, A. and Ekwall, K. In *Encyclopedia of Molecular Cell Biology and Molecular Medicine*; Wiley-VCH Verlag GmbH & Co. KGaA: Weinheim, Germany, 2006.

(*200*) Bártová, E., Krejčí, J., Harničarová, A., Galiová, G. and Kozubek, S. (2008). Histone modifications and nuclear architecture: A review. *Journal of Histochemistry and Cytochemistry 56*, 711–721.

(*201*) Biterge, B. (2016). A Mini Review on Post-Translational Histone Modifications. *MOJ Cell Science & Report 3*, 00047.

(*202*) Trojer, P. and Reinberg, D. (2007). Facultative Heterochromatin: Is There a Distinctive Molecular Signature? *Molecular Cell 28*, 1–13.

(*203*) Saksouk, N., Simboeck, E. and Déjardin, J. (2015). Constitutive heterochromatin formation and transcription in mammals. *Epigenetics and Chromatin 8*, 3.

(*204*) Luger, K., Mäder, A. W., Richmond, R. K., Sargent, D. F. and Richmond, T. J. (1997). Crystal structure of the nucleosome core particle at 2.8 A resolution. *Nature 389*, 251–260.

(*205*) Uberbacher, E. C. and Bunick, G. J. (1989). Structure of the nucleosome core particle at 8 Å resolution. *Journal of Biomolecular Structure and Dynamics 7*, 1–18.

(*206*) Henikoff, S. (2008). Nucleosome destabilization in the epigenetic regulation of gene expression. *Nature Reviews Genetics 9*, 15–26.

(*207*) Yang, Z., Zheng, C., Thiriet, C. and Hayes, J. J. (2005). The core histone N-terminal tail domains negatively regulate binding of transcription factor IIIA to a nucleosome containing a 5S RNA gene via a novel mechanism. *Molecular and cellular biology 25*, 241–249.

(*208*) Quina, A. S., Buschbeck, M. and Di Croce, L. (2006). Chromatin structure and epigenetics. *Biochemical Pharmacology 72*, 1563–1569.

(*209*) Venkatesh, S. and Workman, J. L. (2015). Histone exchange, chromatin structure and the regulation of transcription. *Nature Reviews Molecular Cell Biology 16*, 178–189.

(*210*) Bassett, S. A. and Barnett, M. P. (2014). The role of dietary histone deacetylases (HDACs) inhibitors in health and disease. *Nutrients 6*, 4273–4301.

(*211*) Gong, F. and Miller, K. M. (2013). Mammalian DNA repair: HATs and HDACs make their mark through histone acetylation. *Mutation Research - Fundamental and Molecular Mechanisms of Mutagenesis 750*, 23–30.

(*212*) Struhl, K. (1998). Histone acetylation and transcriptional regulatory mechanisms. *Genes and Development 12*, 599–606.

(*213*) Eberharter, A. and Becker, P. B. (2002). Histone acetylation : a switch between repressive and permissive chromatin Second in review series on chromatin dynamics. *EMBO Reports 3*, 224–229.

(*214*) Forsberg, E. C. and Bresnick, E. H. (2001). Histone acetylation beyond promoters: Long-range acetylation patterns in the chromatin world. *BioEssays 23*, 820–830.

(*215*) Barneda-Zahonero, B. and Parra, M. (2012). Histone deacetylases and cancer. *Molecular Oncology 6*, 579–589.

(*216*) Parra, M. (2015). Class IIa HDACs - New insights into their functions in physiology and pathology. *FEBS Journal 282*, 1736–1744.

(*217*) Stengel, K. R. and Hiebert, S. W. (2015). Class I HDACs Affect DNA Replication, Repair, and Chromatin Structure: Implications for Cancer Therapy. *Antioxidants & Redox Signaling 23*, 51–65.

(*218*) Aksoy, P., Escande, C., White, T. A., Thompson, M., Soares, S., Benech, J. C. and Chini, E. N. (2006). Regulation of SIRT 1 mediated NAD dependent deacetylation: A novel role for the multifunctional enzyme CD38. *Biochemical and Biophysical Research Communications 349*, 353–359.

(*219*) Borradaile, N. M. and Pickering, J. G. (2009). NAD(+), sirtuins, and cardiovascular disease. *Current pharmaceutical design 15*, 110–117.

(*220*) Parbin, S., Kar, S., Shilpi, A., Sengupta, D., Deb, M., Rath, S. K. and Patra, S. K. (2014). Histone Deacetylases: A Saga of Perturbed Acetylation Homeostasis in Cancer. *Journal of Histochemistry and Cytochemistry 62*, 11–33.

(*221*) Saha, R. N. and Pahan, K (2006). HATs and HDACs in neurodegeneration: A tale of disconcerted acetylation homeostasis. *Cell Death and Differentiation 13*, 539–550.

(*222*) Chevallier, N., Corcoran, C. M., Lennon, C., Hyjek, E., Chadburn, A., Bardwell, V. J., Licht, J. D. and Melnick, A. (2004). ETO protein of t(8;21) AML is a corepressor for Bcl-6 B-cell lymphoma oncoprotein. *Blood 103*, 1454–1463.

(*223*) Huang, B. H., Laban, M, Leung, C. H.-W., Lee, L, Lee, C. K., Salto-Tellez, M, Raju, G. C. and Hooi, S. C. (2005). Inhibition of histone deacetylase 2 increases apoptosis and p21Cip1/WAF1 expression, independent of histone deacetylase 1. *Cell Death and Differentiation 12*, 395–404.

(*224*) Mottet, D, Pirotte, S, Lamour, V, Hagedorn, M, Javerzat, S, Bikfalvi, A, Bellahcène, A, Verdin, E and Castronovo, V (2009). HDAC4 represses p21WAF1/Cip1 expression in human cancer cells through a Sp1- dependent, p53-independent mechanism. *Oncogene 28*, 243–256.

(*225*) Patra, S. K., Patra, A. and Dahiya, R. (2001). Histone deacetylase and DNA methyltransferase in human prostate cancer. *Biochemical and Biophysical Research Communications 287*, 705–713.

(*226*) Yasui, W., Oue, N., Ono, S., Mitani, Y., Ito, R. and Nakayama, H. (2003). Histone acetylation and gastrointestinal carcinogenesis. *Annals of the New York Academy of Sciences 983*, 220–231.

(*227*) Fraga, M. F. et al. (2005). Loss of acetylation at Lys16 and trimethylation at Lys20 of histone H4 is a common hallmark of human cancer. *Nature Genetics 37*, 391–400.

(*228*) Khan, O. and La Thangue, N. B. (2012). HDAC inhibitors in cancer biology: Emerging mechanisms and clinical applications. *Immunology and Cell Biology 90*, 85–94.

(*229*) Sato, S., Yoshida, W., Soejima, H., Nakabayashi, K. and Hata, K. (2011). Methylation dynamics of IG-DMR and Gtl2-DMR during murine embryonic and placental development. *Genomics 98*, 120–127.

(*230*) Kunej, T., Godnic, I., Ferdin, J., Horvat, S., Dovc, P. and Calin, G. A. (2011). Epigenetic regulation of microRNAs in cancer: An integrated review of literature. *Mutation Research/Fundamental and Molecular Mechanisms of Mutagenesis 717*, 77–84.

(*231*) Fabbri, M. et al. (2007). MicroRNA-29 family reverts aberrant methylation in lung cancer by targeting DNA methyltransferases 3A and 3B. *Proceedings of the National Academy of Sciences 104*, 15805–15810.

(*232*) Noonan, E. J., Place, R. F., Pookot, D, Basak, S, Whitson, J. M., Hirata, H, Giardina, C and Dahiya, R (2009). miR-449a targets HDAC-1 and induces growth arrest in prostate cancer. *Oncogene 28*, 1714–1724.

(*233*) Untergasser, A., Cutcutache, I., Koressaar, T., Ye, J., Faircloth, B. C., Remm, M. and Rozen, S. G. (2012). Primer3-new capabilities and interfaces. *Nucleic Acids Research 40*, e115.

(*234*) Koressaar, T. and Remm, M. (2007). Enhancements and modifications of primer design program Primer3. *Bioinformatics 23*, 1289–1291.

(*235*) Xia, M., Sherlock, J., Hegerich, P. and You, X. (2010). DataAssist™–Data Analysis Software for TaqMan® Real-Time PCR Data. *Proceedings of the International MultiConference of Engineers and Computer Scientists I*, 17–19.

(*236*) Cutts, R. J., Ullah, A. Z. D., Sangaralingam, A., Gadaleta, E., Lemoine, N. R. and Chelala, C. (2012). O-miner : an integrative platform for automated analysis and mining of -omics data. *Nucleic Acids Research 40*, 560–568.

(*237*) Du, P., Kibbe, W. A. and Lin, S. M. (2008). lumi: A pipeline for processing Illumina microarray. *Bioinformatics 24*, 1547–1548.

(*238*) Du, P., Zhang, X., Huang, C.-c., Jafari, N., Kibbe, W. A., Hou, L. and Lin, S. M. (2010). Comparison of Beta-value and M-value methods for quantifying methylation levels by microarray analysis. *BMC Bioinformatics 11*, 587.

(*239*) Lin, S. M., Du, P., Huber, W. and Kibbe, W. A. (2008). Model-based variance-stabilizing transformation for Illumina microarray data. *Nucleic Acids Research 36*, e11.

(*240*) Gentleman, R. C. et al. (2004). Bioconductor: open software development for computational biology and bioinformatics. *Genome Biology 5*, R80.

(*241*) Ritchie, M. E., Phipson, B., Wu, D., Hu, Y., Law, C. W., Shi, W. and Smyth, G. K. (2015). limma powers differential expression analyses for RNA-sequencing and microarray studies. *Nucleic Acids Research 43*, e47.

(*242*) Benjamini, Y. and Hochberg, Y. (1995). Controlling the False Discovery Rate : A Practical and Powerful Approach to Multiple Testing. *Journal of the Royal Statistical Society. Series B (Methodological) 57*, 289–300.

(*243*) Chen, L., MacMillan, A. M., Chang, W., Ezaz-Nikpay, K., Lane, W. S. and Verdine, G. L. (1991). Direct identification of the active-site nucleophile in a DNA (cytosine-5)-methyltransferase. *Biochemistry 30*, 11018–11025.

(*244*) Santi, D. V., Norment, A. and Garrett, C. E. (1984). Covalent bond formation between a DNA-cytosine methyltransferase and DNA containing 5-azacytosine. *Proceedings of the National Academy of Sciences 81*, 6993–6997.

(*245*) Stresemann, C. and Lyko, F. (2008). Modes of action of the DNA methyltransferase inhibitors azacytidine and decitabine. *International Journal of Cancer 123*, 8–13.

(*246*) Tsuji, N., Kobayashi, M., Nagashima, K., Wakisaka, Y. and Koizumi, K. (1976). A New Antifungal Antibiotic, Trichostatin*. *The Journal of Antibiotics 29*, 1–6.

(*247*) Yoshida, M., Kijima, M., Akita, M. and Beppu, T. (1990). Potent and Specific Inhibition of Mammalian Histone Deacetylase Both in Vivo and in Vitro by Trichostatin A *. *The Journal of Bological Chemistry 265*, 17174–17179.

(*248*) Korbie, D., Lin, E., Wall, D., Nair, S. S., Stirzaker, C., Clark, S. J. and Trau, M. (2015). Multiplex bisulfite PCR resequencing of clinical FFPE DNA. *Clinical Epigenetics 7*, 28.

(*249*) Dai, X., Cheng, H., Bai, Z. and Li, J. (2017). Breast cancer cell line classification and Its relevance with breast tumor subtyping. *Journal of Cancer 8*, 3131–3141.

(*250*) Subik, K., Lee, J. F., Baxter, L., Strzepek, T., Costello, D., Crowley, P., Xing, L., Hung, M. C., Bonfiglio, T., Hicks, D. G. and Tang, P. (2010). The expression patterns of ER, PR, HER2, CK5/6, EGFR, KI-67 and AR by immunohistochemical analysis in breast cancer cell lines. *Breast Cancer: Basic and Clinical Research 4*, 35–41.

(*251*) Neve, R. M. et al. (2006). A collection of breast cancer cell lines for the study of functionally distinct cancer subtypes. *Cancer Cell 10*, 515–527.

(*252*) Tanner, M., Kapanen, A. I., Junttila, T., Raheem, O., Grenman, S., Elo, J., Elenius, K. and Isola, J. (2004). Characterization of a novel cell line established from a patient with Herceptin-resistant breast cancer. *Molecular Cancer Therapeutics 3*, 1585–1592.

(*253*) Eichhorn, P. J. A., Gili, M., Scaltriti, M., Serra, V., Guzman, M., Nijkamp, W., Beijersbergen, R. L., Valero, V., Seoane, J., Bernards, R. and Baselga, J. (2008). Phosphatidylinositol 3-kinase hyperactivation results in lapatinib resistance that is reversed by the mTOR/phosphatidylinositol 3-kinase inhibitor NVP-BEZ235. *Cancer Research 68*, 9221–9230.

(*254*) Nahta, R., Takahashi, T. and Ueno, N. T. (2004). P27 kip1 Down-Regulation Is Associated with Trastuzumab Resistance in Breast Cancer Cells P27 kip1 Down-Regulation Is Associated with Trastuzumab Resistance in Breast Cancer Cells. *Cancer Research 64*, 3981–3986.

(*255*) Chen, X., Wang, H., Ou-Yang, X.-N., Xie, F.-W. and Wu, J.-J. (2013). Research on drug resistance mechanism of trastuzumab caused by activation of the PI3K/Akt signaling pathway. *Contemporary Oncology (Pozn) 17*, 363–369.

(*256*) Wang, C., Wang, L., Yu, X., Zhang, Y., Meng, Y., Wang, H., Yang, Y., Gao, J., Wei, H., Zhao, J., Lu, C., Chen, H., Sun, Y. and Li, B. (2017). Combating acquired resistance to trastuzumab by an anti-ErbB2 fully human antibody. *Oncotarget 8*, 42742–42751.

(*257*) Zazo, S., González-Alonso, P., Martín-Aparicio, E., Chamizo, C., Cristóbal, I., Arpí, O., Rovira, A., Albanell, J., Eroles, P., Lluch, A., Madoz-Gúrpide, J. and Rojo, F. (2016). Generation, characterization, and maintenance of trastuzumab-resistant HER2+ breast cancer cell lines. *American Journal of Cancer Research 6*, 2661–2678.

(*258*) Petre, G. et al. (2018). Genomic duplication in the 19q13.42 imprinted region identified as a new genetic cause of intrauterine growth restriction. *Clinical Genetics 94*, 575–580.

(*259*) Pfister, S., Remke, M., Castoldi, M., Bai, A. H., Muckenthaler, M. U., Kulozik, A., von Deimling, A., Pscherer, A., Lichter, P. and Korshunov, A. (2009). Novel genomic amplification targeting the microRNA cluster at 19q13.42 in a pediatric embryonal tumor with abundant neuropil and true rosettes. *Acta neuropathologica 117*, 457–464.

(*260*) Kuuselo, R., Simon, R., Karhu, R., Tennstedt, P., Marx, A. H., Izbicki, J. R., Yekebas, E., Sauter, G. and Kallioniemi, A. (2010). NIH Public Access. *Genes Chromosomes and Cancer 49*, 569–575.

(*261*) Nobusawa, S. et al. (2012). Analysis of chromosome 19q13.42 amplification in embryonal brain tumors with ependymoblastic multilayered rosettes. *Brain Pathology 22*, 689–697.

(*262*) Korshunov, A. et al. (2010). Focal genomic amplification at 19q13.42 comprises a powerful diagnostic marker for embryonal tumors with ependymoblastic rosettes. *Acta Neuropathologica 120*, 253–260.

(*263*) Saito, Y., Liang, G., Egger, G., Friedman, J. M., Chuang, J. C., Coetzee, G. a. and Jones, P. a. (2006). Specific activation of microRNA-127 with downregulation of the proto-oncogene BCL6 by chromatin-modifying drugs in human cancer cells. *Cancer Cell 9*, 435–443.

(*264*) Zhao, X., Duan, Z., Liu, X., Wang, B., Wang, X., He, J., Yao, Z. and Yang, J. (2013). MicroRNA-127 is downregulated by Tudor-SN protein and contributes to metastasis and proliferation in breast cancer cell line MDA-MB-231. *The Anatomical Record 296*, 1842–1849.

(*265*) Chen, J., Wang, M., Guo, M., Xie, Y. and Cong, Y.-S. (2013). miR-127 regulates cell proliferation and senescence by targeting BCL6. *PLoS ONE 8*, e80266.

(*266*) Wang, S., Li, H., Wang, J., Wang, D., Yao, A. and Li, Q. (2014). Prognostic and biological significance of microRNA-127 expression in human breast cancer. *Disease Markers 2014*, 401986.

(*267*) Cuk, K., Zucknick, M., Madhavan, D., Schott, S., Golatta, M., Heil, J., Marmé, F., Turchinovich, A., Sinn, P., Sohn, C., Junkermann, H., Schneeweiss, A. and Burwinkel, B. (2013). Plasma microRNA panel for minimally invasive detection of breast cancer. *PLoS ONE 8*, e76729.

(*268*) Hu, X., Wang, J., He, W., Zhao, P. and Ye, C. (2018). MicroRNA-433 targets AKT3 and inhibits cell proliferation and viability in breast cancer. *Oncology Letters 15*, 3998–4004.

(*269*) Zhang, T., Jiang, K., Zhu, X., Zhao, G., Wu, H., Deng, G. and Qiu, C. (2018). miR-433 inhibits breast cancer cell growth via the MAPK signaling pathway by targeting Rap1a. *International Journal of Biological Sciences 14*, 622–632.

(*270*) Liang, C., Ding, J., Yang, Y., Deng, L. and Li, X. (2017). MicroRNA-433 inhibits cervical cancer progression by directly targeting metadherin to regulate the AKT and β-catenin signalling pathways. *Oncology Reports 38*, 3639–3649.

(*271*) Xu, G., Zhang, Y., Huang, Z., Wang, H., Luo, Q., Ye, Y., Fan, C., Cai, H., Zhang, C., Liu, G. and Xiao, R. (2016). miR-411-5p inhibits proliferation and metastasis of breast cancer cell via targeting GRB2. *Biochemical and Biophysical Research Communications 476*, 607–613.

(*272*) Li, X., Yang, L., Shuai, T., Piao, T. and Wang, R. (2016). MiR-433 inhibits retinoblastoma malignancy by suppressing Notch1 and PAX6 expression. *Biomedicine and Pharmacotherapy 82*, 247–255.

(*273*) Liang, T., Guo, Q., Li, L., Cheng, Y., Ren, C. and Zhang, G. (2016). MicroRNA-433 inhibits migration and invasion of ovarian cancer cells via targeting Notch1. *Neoplasma 63*, 696–704.

(*274*) Zhang, J., Zhang, L., Zhang, T., Dong, X. M., Zhu, Y. and Chen, L. H. (2018). Reduced miR-433 expression is associated with advanced stages and early relapse of colorectal cancer and restored miR-433 expression suppresses the migration, invasion and proliferation of tumor cells in vitro and in nude mice. *Oncology Letters 15*, 7579–7588.

(*275*) Li, J., Mao, X., Wang, X., Miao, G. and Li, J. (2017). MiR-433 reduces cell viability and promotes cell apoptosis by regulating MACC1 in colorectal cancer. *Oncology Letters 13*, 81–88.

(*276*) Shi, Q., Wang, Y., Mu, Y., Wang, X. and Fan, Q. (2018). MiR-433-3p Inhibits Proliferation and Invasion of Esophageal Squamous Cell Carcinoma by Targeting GRB2. *Cellular Physiology and Biochemistry 46*, 2187–2196.

(*277*) Weiner-Gorzel, K. et al. (2015). Overexpression of the microRNA miR-433 promotes resistance to paclitaxel through the induction of cellular senescence in ovarian cancer cells. *Cancer Medicine 4*, 745–758.

(*278*) Yu, J., Zhang, W., Lu, B., Qian, H., Tang, H., Zhu, Z., Yuan, X. and Ren, P. (2017). miR-433 accelerates acquired chemoresistance of gallbladder cancer cells by targeting cyclin M. *Oncology Letters 15*, 3305–3312.

(*279*) Liu, M., Xu, A., Yuan, X., Zhang, Q., Fang, T., Wang, W. and Li, C. (2015). Downregulation of microRNA-409-3p promotes aggressiveness and metastasis in colorectal cancer: an indication for personalized medicine. *Journal of Translational Medicine 13*, 195.

(*280*) Bai, R., Weng, C., Dong, H., Li, S., Chen, G. and Xu, Z. (2015). MicroRNA-409-3p suppresses colorectal cancer invasion and metastasis partly by targeting GAB1 expression. *International Journal of Cancer 137*, 2310–2322.

(*281*) Zheng, B, Liang, L, Huang, S, Zha, R, Liu, L, Jia, D, Tian, Q, Wang, Q, Wang, C, Long, Z, Zhou, Y, Cao, X, Du, C, Shi, Y and He, X (2012). MicroRNA-409 suppresses tumour cell invasion and metastasis by directly targeting radixin in gastric cancers. *Oncogene 31*, 4509–4516.

(*282*) Li, C., Nie, H., Wang, M., Su, L., Li, J., Yu, B., Wei, M., Ju, J., Yu, Y., Yan, M., Gu, Q., Zhu, Z. and Liu, B. (2012). MicroRNA-409-3p regulates cell proliferation and apoptosis by targeting PHF10 in gastric cancer. *Cancer Letters 320*, 189–197.

(*283*) Wan, L., Zhu, L., Xu, J., Lu, B., Yang, Y., Liu, F. and Wang, Z. (2014). MicroRNA-409-3p functions as a tumor suppressor in human lung adenocarcinoma by targeting c-Met. *Cellular Physiology and Biochemistry 34*, 1273–1290.

(*284*) Zhang, G., Liu, Z., Xu, H. and Yang, Q. (2016). MIR-409-3p suppresses breast cancer cell growth and invasion by targeting Akt1. *Biochemical and Biophysical Research Communications 469*, 189–195.

(*285*) Ma, Z., Li, Y., Xu, J., Ren, Q., Yao, J. and Tian, X. (2016). MicroRNA-409-3p regulates cell invasion and metastasis by targeting ZEB1 in breast cancer. *IUBMB Life 68*, 394–402.

(*286*) Cao, G.-H., Sun, X.-L., Wu, F., Chen, W.-F. and Hu, J.-Q. (2016). Low expression of miR-409-3p is a prognostic marker for breast cancer. *European Review for Medical and Pharmacological Sciences 20*, 3825–3829.

(*287*) Josson, S. et al. (2014). miR-409-3p/-5p promotes tumorigenesis, epithelial to mesenchymal transition, and bone metastasis of human prostate cancer. *Clinical Cancer Research 20*, 4636–4646.

(*288*) Josson, S, Gururajan, M, Sung, S. Y., Hu, P, Shao, C, Zhau, H. E., Liu, C, Lichterman, J, Duan, P, Li, Q, Rogatko, A, Posadas, E. M., Haga, C. L. and Chung, L. W. K. (2015). Stromal fibroblast-derived miR-409 promotes epithelial to mesenchymal transition and prostate tumorigenesis. *Oncogene 34*, 2690–2699.

(*289*) Zhang, X., Zhang, M., Cheng, J., Lv, Z., Wang, F. and Cai, Z. (2017). MiR-411 functions as a tumor suppressor in renal cell cancer. *International Journal of Biological Markers 32*, e454–e460.

(*290*) Kim, Y. W., Kim, E. Y., Jeon, D., Liu, J. L., Kim, H. S., Choi, J. W. and Ahn, W. S. (2014). Differential microRNA expression signatures and cell type-specific association with Taxol resistance in ovarian cancer cells. *Drug Design, Development and Therapy 8*, 293–314.

(*291*) Azarbarzin, S., Feizi, M. A. H., Safaralizadeh, R., Ravanbakhsh, R., Karimi, N., Kazemzadeh, M., Fateh, A., Sadat, A. T. E. and Somi, M. H. (2016). Reduced expression of miR-411 in intestinal type of gastric adenocarcinoma. *Meta Gene 10*, 23–26.

(*292*) Zhang, J. E. (2016). microRNA : emerging biomarkers in human disease and profiling challenges. *Biochemist 38*, 26–29.

(*293*) Guo, L., Yuan, J., Xie, N., Wu, H., Chen, W., Song, S. and Wang, X. (2016). MiRNA-411 acts as a potential tumor suppressor miRNA via the downregulation of specificity protein 1 in breast cancer. *Molecular Medicine Reports 14*, 2975–2982.

(*294*) Yamamoto, K., Seike, M., Takeuchi, S., Soeno, C., Miyanaga, A., Noro, R., Minegishi, Y., Kubota, K. and Gemma, A. (2014). miR-379/411 cluster regulates IL-18 and contributes to drug resistance in malignant pleural mesothelioma. *Oncology Reports 32*, 2365–2372.

(*295*) Zhang, D., Lee, H., Zhu, Z., Minhas, J. K. and Jin, Y. (2017). Enrichment of selective miRNAs in exosomes and delivery of exosomal miRNAs in vitro and in vivo. *American Journal of Physiology - Lung Cellular and Molecular Physiology 312*, L110–L121.

(*296*) Zhao, Z., Qin, L. and Li, S. (2016). miR-411 contributes the cell proliferation of lung cancer by targeting FOXO1. *Tumor Biology 37*, 5551–5560.

(*297*) Xia, K., Zhang, Y., Cao, S., Wu, Y., Guo, W., Yuan, W. and Zhang, S. (2015). MiR-411 regulated ITCH expression and promoted cell proliferation in human hepatocellular carcinoma cells. *Biomedicine and Pharmacotherapy 70*, 158–163.

(*298*) Jiang, X., Huang, H., Li, Z and He, C. (2012). miR-495 is a tumor-suppressor microRNA down-regulated in MLL-rearranged leukemia. *Proceedings of the National Academy of Sciences 109*, 19397–19402.

(*299*) Chen, S.-m., Chen, H.-c., Chen, S.-j., Huang, C.-y., Chen, P.-y., Wu, T.-w. E., Feng, L.-y., Tsai, H.-c., Lui, T.-n., Hsueh, C. and Wei, K.-c. (2013). MicroRNA-495 inhibits proliferation of glioblastoma multiforme cells by downregulating cyclin-dependent kinase 6. *World Journal of Surgical Oncology 11*, 87.

(*300*) Li, Z., Cao, Y., Jie, Z., Liu, Y., Li, Y., Li, J., Zhu, G., Liu, Z., Tu, Y., Peng, G., Lee, D.-w. and Park, S.-s. (2012). miR-495 and miR-551a inhibit the migration and invasion of human gastric cancer cells by directly interacting with PRL-3. *Cancer Letters 323*, 41–47.

(*301*) Li, Z., Zhang, G., Li, D., Jie, Z., Chen, H., Xiong, J., Liu, Y., Cao, Y., Jiang, M., Le, Z. and Tan, S. (2015). Methylation-associated silencing of miR-495 inhibit the migration and invasion of human gastric cancer cells by directly targeting PRL-3. *Biochemical and Biophysical Research Communications 456*, 344–350.

(*302*) Chu, H., Chen, X., Wang, H., Du, Y., Wang, Y., Zang, W., Li, P., Li, J., Chang, J., Zhao, G. and Zhang, G. (2014). MiR-495 regulates proliferation and migration in NSCLC by targeting MTA3. *Tumor Biology 35*, 3487–3494.

(*303*) Guo, J., Jin, D., Wu, Y., Yang, L., Du, J., Gong, K., Chen, W., Dai, J., Miao, S. and Xi, S. (2018). The miR 495-UBE2C-ABCG2/ERCC1 axis reverses cisplatin resistance by downregulating drug resistance genes in cisplatin-resistant non-small cell lung cancer cells. *EBioMedicine 35*, 204–221.

(*304*) Haga, C. L. and Phinney, D. G. (2012). MicroRNAs in the imprinted DLK1-DIO3 region repress the epithelial-to-mesenchymal transition by targeting the TWIST1 protein signaling network. *Journal of Biological Chemistry 287*, 42695–42707.

(*305*) Yang, H., Cho, M. E., Li, T. W. H., Peng, H., Ko, K. S., Mato, J. M. and Lu, S. C. (2013). MicroRNAs regulate methionine adenosyltransferase 1A expression in hepatocellular carcinoma. *Journal of Clinical Investigation 123*, 285–298.

(*306*) Cao, M., Nie, W., Li, J., Zhang, Y., Yan, X., Guan, X., Chen, X., Zen, K., Zhang, C. Y., Jiang, X. and Hou, D. (2014). MicroRNA-495 induces breast cancer cell migration by targeting JAM-A. *Protein and Cell 5*, 862–872.

(*307*) Hwang-Verslues, W. W., Chang, P.-H., Wei, P.-C., Yang, C.-Y., Huang, C.-K., Kuo, W.-H., Shew, J.-Y., Chang, K.-J., Lee, E. Y.-H. P. and Lee, W.-H. (2011). miR-495 is upregulated by E12/E47 in breast cancer stem cells, and promotes oncogenesis and hypoxia resistance via downregulation of E-cadherin and REDD1. *Oncogene 30*, 2463–2474.

(*308*) Wen, D., Li, S., Jiang, W., Zhu, J., Liu, J. and Zhao, S. (2017). miR-539 inhibits human colorectal cancer progression by targeting RUNX2. *Biomedicine and Pharmacotherapy 95*, 1314–1320.

(*309*) Quan, J., Qu, J. and Zhou, L. (2017). MicroRNA-539 inhibits glioma cell proliferation and invasion by targeting DIXDC1. *Biomedicine and Pharmacotherapy 93*, 746–753.

(*310*) Zhang, H., Li, S., Yang, X., Qiao, B., Zhang, Z. and Xu, Y. (2016). MIR-539 inhibits prostate cancer progression by directly targeting SPAG5. *Journal of Experimental and Clinical Cancer Research 35*, 1–9.

(*311*) Gu, L. and Sun, W. (2015). MiR-539 inhibits thyroid cancer cell migration and invasion by directly targeting CARMA1. *Biochemical and Biophysical Research Communications 464*, 1128–1133.

(*312*) Guo, J., Gong, G. and Zhang, B. (2018). MiR-539 acts as a tumor suppressor by targeting epidermal growth factor receptor in breast cancer. *Scientific Reports 8*, 1–10.

(*313*) Yang, Z., Zhang, B., Wei, J., Jiang, G., Wu, Y., Leng, B. and Xing, C. (2018). MiR-539 inhibits proliferation and migration of triple-negative breast cancer cells by down-regulating LAMA4 expression. *Cancer Cell International 18*, 16.

(*314*) Wang, Y, Yeh, S, Ou, Z, Chang, C, Long, J, Wang, X and Sun, Y (2017). Androgen receptor promotes melanoma metastasis via altering the miRNA-539-3p/USP13/MITF/AXL signals. *Oncogene 36*, 1644–1654.

(*315*) Deng, H., Qianqian, G., Ting, J. and Aimin, Y. (2018). miR-539 enhances chemosensitivity to cisplatin in non-small cell lung cancer by targeting DCLK1. *Biomedicine and Pharmacotherapy 106*, 1072–1081.

(*316*) Zhu, C., Zhou, R., Zhou, Q., Chang, Y. and Jiang, M. (2016). microRNA-539 suppresses tumor growth and tumorigenesis and overcomes arsenic trioxide resistance in hepatocellular carcinoma. *Life Sciences 166*, 34–40.

(*317*) Charlier, C., Segers, K., Wagenaar, D., Karim, L., Berghmans, S., Jaillon, O., Shay, T., Weissenbach, J., Cockett, N., Gyapay, G. and Georges, M. (2001). Human-ovine comparative sequencing of a 250-kb imprinted domain encompassing the callipyge (clpg) locus and identification of six imprinted transcripts: DLK1, DAT, GTL2, PEG11, antiPEG11, and MEG8. *Genome Research 11*, 850–862.

(*318*) Cavaillé, J., Seitz, H., Paulsen, M., Ferguson-Smith, A. C. and Bachellerie, J.-P. (2002). Identification of tandemly-repeated C/D snoRNA genes at the imprinted human 14q32 domain reminiscent of those at the Prader-Willi/Angelman syndrome region. *Human Molecular Genetics 11*, 1527–1538.

(*319*) Schuster-Gossler, K., Bilinski, P., Sado, T., Ferguson-Smtth, A. and Gossler, A. (1998). The mouse Gtl2 gene is differentially expressed during embryonic development, encodes multiple alternatively spliced transcripts, and may act as an RNA. *Developmental Dynamics 212*, 214–228.

(*320*) Laborda, J. (1993). dlk, a Putative Mammalian Homeotic Gene Differentially Expressed in Small Cell Lung Carcinoma and Neuroendocrine Tumor Cell Line. *The Journal of Biological Chemistry 268*, 3817–3820.

(*321*) Laborda, J (2000). The role of the epidermal growth factor-like protein dlk in cell differentiation. *Histology and Histopathology 15*, 119–129.

(*322*) Ruiz-Hidalgo, M. J., Gubina, E., Tull, L., Baladrón, V. and Laborda, J. (2002). Dlk Modulates Mitogen-Activated Protein Kinase Signaling To Allow or Prevent Differentiation. *Experimental Cell Research 274*, 178–188.

(*323*) Moon, Y. S., Smas, C. M., Lee, K., Josep, A, Kim, K.-h., Yun, E. J., Sul, H. S. and Villena, J. A. (2002). Mice Lacking Paternally Expressed Pref-1 / Dlk1 Display Growth Retardation and Accelerated Adiposity Mice Lacking Paternally Expressed Pref-1 / Dlk1 Display Growth Retardation and Accelerated Adiposity. *Molecular and Cellular Biology 22*, 5585–5592.

(*324*) Wylie, A. A., Murphy, S. K., Orton, T. C. and Jirtle, R. L. (2000). Novel Imprinted DLK1/GTL2 Domain on Human Chromosome 14 Contains Motifs that Mimic Those Implicated in IGF2/H19 Regulation. *Genome Research 10*, 1711–1718.

(*325*) Kagami, M., O'Sullivan, M. J., Green, A. J., Watabe, Y., Arisaka, O., Masawa, N., Matsuoka, K., Fukami, M., Matsubara, K., Kato, F., Ferguson-Smith, A. C. and Ogata, T. (2010). The IG-DMR and the MEG3-DMR at human chromosome 14q32.2: Hierarchical interaction and distinct functional properties as imprinting control centers. *PLoS Genetics 6*, e1000992.

(*326*) Lin, S. P., Youngson, N, Takada, S, Seitz, H, Reik, W, Paulsen, M, Cavaille, J and Ferguson-Smith, A. C. (2003). Asymmetric regulation of imprinting on the maternal and paternal chromosomes at the Dlk1-Gtl2 imprinted cluster on mouse chromosome 12. *Nature Genetics 35*, 97–102.

(*327*) Manodoro, F., Marzec, J. and Chaplin, T. (2014). Loss of imprinting at the 14q32 domain is associated with microRNA overexpression in acute promyelocytic leukemia. *Blood 123*, 2066–2075.

(*328*) Murphy, S. K., Wylie, A. A., Coveler, K. J., Cotter, P. D., Papenhausen, P. R., Sutton, V. R., Shaffer, L. G. and Jirtle, R. L. (2003). Epigenetic detection of human chromosome 14 uniparental disomy. *Human Mutation 22*, 92–97.

(*329*) Paulsen, M., Takada, S., Youngson, N. a., Benchaib, M., Charlier, C., Segers, K., Georges, M. and Ferguson-smith, A. C. (2001). Comparative Sequence Analysis of the Imprinted Dlk1 − Gtl2 Locus in Three Mammalian Species Reveals Highly Conserved Genomic Elements and Refines Comparison with the Igf2 − H19 Region Comparative Sequence Analysis of the Imprinted Dlk1 – Gtl2 Locus in Thr. *Genome Research 11*, 2085–2094.

(*330*) Takada, S., Paulsen, M., Tevendale, M., Tsai, C.-E., Kelsey, G., Cattanach, B. M. and Ferguson-Smith, A. C. (2002). Epigenetic analysis of the Dlk1-Gtl2 imprinted domain on mouse chromosome 12: implications for imprinting control from comparison with Igf2-H19. *Human Molecular Genetics 11*, 77–86.

(*331*) Rosa, A. L., Wu, Y. Q., Kwabi-Addo, B., Coveler, K. J., Sutton, V. R. and Shaffer, L. G. (2005). Allele-specific methylation of a functional CTCF binding site upstream of MEG3 in the human imprinted domain of 14q32. *Chromosome Research 13*, 809–818.

(*332*) Bell, A. C., West, A. G. and Felsenfeld, G. (1999). The protein CTCF is required for the enhancer blocking activity of vertebrate insulators. *Cell 98*, 387–396.

(*333*) Szabó, P. E., Tang, S. H. E., Rentsendorj, A., Pfeifer, G. P. and Mann, J. R. (2000). Maternal-specific footprints at putative CTCF sites in the H19 imprinting control region give evidence for insulator function. *Current Biology 10*, 607–610.

(*334*) Seitz, H, Royo, H and Bortolin, M. (2004). A large imprinted microRNA gene cluster at the mouse Dlk1-Gtl2 domain. *Genome Research 14*, 1741–1748.

(*335*) Dimmeler, S. and Ylä-Herttuala, S. (2014). 14q32 miRNA cluster takes center stage in neovascularization. *Circulation Research 115*, 680–682.

(*336*) Welten, S. M., Bastiaansen, A. J., De Jong, R. C., De Vries, M. R., Peters, E. A., Boonstra, M. C., Sheikh, S. P., Monica, N. L., Kandimalla, E. R., Quax, P. H. and Yaël Nossent, A. (2014). Inhibition of 14q32 MicroRNAs miR-329, miR-487b, miR-494, and miR-495 increases neovascularization and blood flow recovery after ischemia. *Circulation Research 115*, 696–708.

(*337*) Kota, S. K., Llères, D., Bouschet, T., Hirasawa, R., Marchand, A., Begon-Pescia, C., Sanli, I., Arnaud, P., Journot, L., Girardot, M. and Feil, R. (2014). ICR noncoding RNA expression controls imprinting and DNA replication at the Dlk1-Dio3 domain. *Developmental Cell 31*, 19–33.

(*338*) Falix, F. A., Aronson, D. C., Lamers, W. H. and Gaemers, I. C. (2012). Possible roles of DLK1 in the Notch pathway during development and disease. *Biochimica et Biophysica Acta 1822*, 988–995.

(*339*) Benetatos, L., Hatzimichael, E., Londin, E., Vartholomatos, G., Loher, P., Rigoutsos, I. and Briasoulis, E. (2013). The microRNAs within the DLK1-DIO3 genomic region: involvement in disease pathogenesis. *Cellular and Molecular Life Sciences 70*, 795–814.

(*340*) Swarbrick, A. et al. (2010). MiR-380-5p represses p53 to control cellular survival and is associated with poor outcome in MYCN-amplified neuroblastoma. *Nature Medicine 16*, 1134–1140.

(*341*) González-Vallinas, M. et al. (2018). Epigenetically Regulated Chromosome 14q32 miRNA Cluster Induces Metastasis and Predicts Poor Prognosis in Lung Adenocarcinoma Patients. *Molecular Cancer Research 16*, 390–402.

(*342*) Kagami, M., Nishimura, G., Okuyama, T., Hayashidani, M., Takeuchi, T., Tanaka, S., Ishino, F., Kurosawa, K. and Ogata, T. (2005). Segmental and full paternal isodisomy for chromosome 14 in three patients: Narrowing the critical region and implication for the clinical features. *American Journal of Medical Genetics 138 A*, 127–132.

(*343*) Kotzot, D. (2004). Maternal uniparental disomy 14 dissection of the phenotype with respect to rare autosomal recessively inherited traits, trisomy mosaicism, and genomic imprinting. *Annales de Genetique 47*, 251–260.

(*344*) Reid Sutton, V. and Shaffer, L. G. (2000). Search for imprinted regions on chromosome 14: Comparison of maternal and paternal UPD cases with cases of chromosome 14 deletion. *American Journal of Medical Genetics 93*, 381–387.

(*345*) Kurosawa, K., Sasaki, H., Sato, Y., Yamanaka, M., Shimizu, M., Ito, Y., Okuyama, T., Matsuo, M., Imaizumi, K., Kuroki, Y. and Nishimura, G. (2002). Paternal UPD14 is responsible for a distinctive malformation complex. *American Journal of Medical Genetics 110*, 268–272.

(*346*) Kamnasaran, D. (2001). Epigenetic inheritance associated with human chromosome 14. *Clinical Investigative Medicine 24*, 138–146.

(*347*) Eggermann, T., Zerres, K., Eggermann, K., Moore, G. and Wollmann, H. A. (2002). Uniparental disomy: Clinical indications for testing in growth retardation. *European Journal of Pediatrics 161*, 305–312.

(*348*) Dweep, H., Sticht, C., Pandey, P. and Gretz, N. (2011). miRWalk–database: prediction of possible miRNA binding sites by "walking" the genes of three genomes. *Journal of Biomedical Informatics 44*, 839–847.

(*349*) Miranda, K. C., Huynh, T., Tay, Y., Ang, Y.-S., Tam, W.-L., Thomson, A. M., Lim, B. and Rigoutsos, I. (2006). A Pattern-Based Method for the Identification of MicroRNA Binding Sites and Their Corresponding Heteroduplexes. *Cell 126*, 1203–1217.

(*350*) Betel, D., Wilson, M., Gabow, A., Marks, D. S. and Sander, C. (2008). The microRNA.org resource: targets and expression. *Nucleic Acids Research 36*, D149–D153.

(*351*) Haffner, M. C., Petridou, B., Peyrat, J. P., Révillion, F., Müller-Holzner, E., Daxenbichler, G., Marth, C. and Doppler, W. (2007). Favorable prognostic value of SOCS2 and IGF-I in breast cancer. *BMC Cancer 7*, 136.

(*352*) Farabegoli, F., Ceccarelli, C., Santini, D. and Taffurelli, M. (2005). Suppressor of cytokine signalling 2 (SOCS-2) expression in breast carcinoma. *Journal of Clinical Pathology 58*, 1046–1050.

(*353*) Scott, J. D., Glaccum, M. B., Fischer, E. H. and Krebs, E. G. (1986). Primary-structure requirements for inhibition by the heat-stable inhibitor of the cAMP-dependent protein kinase. *Proceedings of the National Academy of Sciences of the United States of America 83*, 1613–1616.

(*354*) Olsen, S. R. and Uhler, M. D. (1991). Inhibition of protein kinase-A by overexpression of the cloned human protein kinase inhibitor. *Molecular Endocrinology 5*, 1246–1256.

(*355*) Beristain, A. G., Molyneux, S. D., Joshi, P. A., Pomroy, N. C., Di Grappa, M. A., Chang, M. C., Kirschner, L. S., Privé, G. G., Pujana, M. A. and Khokha, R. (2015). PKA signaling drives mammary tumorigenesis through Src. *Oncogene 34*, 1160–1173.

(*356*) Zou, D., Yoon, H. S., Anjomshoaa, A., Perez, D., Fukuzawa, R., Guilford, P. and Humar, B. (2009). Increased levels of active c-Src distinguish invasive from in situ lobular lesions. *Breast Cancer Research 11*, R45.

(*357*) Zhang, S., Huang, W. C., Li, P., Guo, H., Poh, S. B., Brady, S. W., Xiong, Y., Tseng, L. M., Li, S. H., Ding, Z., Sahin, A. A., Esteva, F. J., Hortobagyi, G. N. and Yu, D. (2011). Combating trastuzumab resistance by targeting SRC, a common node downstream of multiple resistance pathways. *Nature Medicine 17*, 461–469.

(*358*) Peiró, G., Ortiz-Martínez, F., Gallardo, A., Pérez-Balaguer, A., Sánchez-Payá, J., Ponce, J. J., Tibau, A., López-Vilaro, L., Escuin, D., Adrover, E., Barnadas, A. and Lerma, E. (2014). Src, a potential target for overcoming trastuzumab resistance in HER2-positive breast carcinoma. *British Journal of Cancer 111*, 689–695.

(*359*) Hartl, M., Nist, A., Khan, M. I., Valovka, T. and Bister, K. (2009). Inhibition of Myc-induced cell transformation by brain acid-soluble protein 1 (BASP1). *Proceedings of the National Academy of Sciences 106*, 5604–5609.

(*360*) Green, L. M., Wagner, K. J., Campbell, H. A., Addison, K. and Roberts, S. G. E. (2009). Dynamic interaction between WT1 and BASP1 in transcriptional regulation during differentiation. *Nucleic Acids Research 37*, 431–440.

(*361*) Matkar, S., Sharma, P., Gao, S., Gurung, B., Katona, B. W., Liao, J., Muhammad, A. B., Kong, X. C., Wang, L., Jin, G., Dang, C. V. and Hua, X. (2015). An Epigenetic Pathway Regulates Sensitivity of Breast Cancer Cells to HER2 Inhibition via FOXO/c-Myc Axis. *Cancer Cell 28*, 472–485.

(*362*) Ding, Y., Zhang, Y., Xu, C., Tao, Q. H. and Chen, Y. G. (2013). HECT domain-containing E3 ubiquitin ligase NEDD4L negatively regulates Wnt signaling by targeting dishevelled for proteasomal degradation. *The Journal of Biological Chemistry 288*, 8289–8298.

(*363*) Tanksley, J. P., Chen, X. and Coffey, R. J. (2013). NEDD4L is downregulated in colorectal cancer and inhibits canonical WNT signaling. *PLoS ONE 8*, e81514.

(*364*) Chen, Y. G. and Wang, X. F. (2009). Finale: The Last Minutes of Smads. *Cell 139*, 658–660.

(*365*) Morén, A., Imamura, T., Miyazono, K., Heldin, C. H. and Moustakas, A. (2005). Degradation of the tumor suppressor Smad4 by WW and HECT domain ubiquitin ligases. *The Journal of Biological Chemistry 280*, 22115–22123.

(*366*) Gao, S., Alarcón, C., Sapkota, G., Rahman, S., Chen, P.-Y., Goerner, N., Macias, M. J., Erdjument-Bromage, H., Tempst, P. and Massagué, J. (2009). Ubiquitin Ligase Nedd4L Targets Activated Smad2/3 to Limit TGF-β Signaling. *Molecular Cell 36*, 457–468.

(*367*) Piersma, B., Bank, R. A. and Boersema, M. (2015). Signaling in Fibrosis: TGF-β, WNT, and YAP/TAZ Converge. *Frontiers in Medicine 2*, 59.

(*368*) Gao, C., Pang, L., Ren, C. and Ma, T. (2012). Decreased expression of Nedd4L correlates with poor prognosis in gastric cancer patient. *Medical Oncology 29*, 1733–1738.

(*369*) Teicher, B. A. (2001). Malignant cells, directors of the malignant process: Role of transforming growth factor-beta. *Cancer and Metastasis Reviews 20*, 133–143.

(*370*) Wang, H., Liu, B., Al-Aidaroos, A. Q. O., Shi, H., Li, L., Guo, K., Li, J., Tan, B. C. P., Loo, J. M., Tang, J. P., Thura, M. and Zeng, Q. (2016). Dual-faced SH3BGRL: Oncogenic in mice, tumor suppressive in humans. *Oncogene 35*, 3303–3313.

(*371*) Majid, S. M., Liss, a. S., You, M and Bose, H. R. (2006). The suppression of SH3BGRL is important for v-Rel-mediated transformation. *Oncogene 25*, 756–768.

(*372*) Bai, W. D., Ye, X. M., Zhang, M. Y., Zhu, H. Y., Xi, W. J., Huang, X., Zhao, J., Gu, B., Zheng, G. X., Yang, A. G. and Jia, L. T. (2014). MiR-200c suppresses TGF-β signaling and counteracts trastuzumab resistance and metastasis by targeting ZNF217 and ZEB1 in breast cancer. *International Journal of Cancer 135*, 1356–1368.

(*373*) Baselga, J. et al. (2012). Lapatinib with trastuzumab for HER2-positive early breast cancer (NeoALTTO): A randomised, open-label, multicentre, phase 3 trial. *The Lancet 379*, 633–640.

(*374*) de Azambuja, E. et al. (2014). Lapatinib with trastuzumab for HER2-positive early breast cancer (NeoALTTO): survival outcomes of a randomised, open-label, multicentre, phase 3 trial and their association with pathological complete response. *The Lancet Oncology 15*, 1137–1146.

(*375*) Shi, W et al. (2016). Pathway level alterations rather than mutations in single genes predict response to HER2 targeted therapies in the neoALTTO trial. *Annals of Oncology 28*, 128–135.

(*376*) Darnell, R. B. (2010). HITS-CLIP: Panoramic views of protein-RNA regulation in living cells. *Wiley Interdisciplinary Reviews: RNA 1*, 266–286.

(*377*) Rabindran, S. K. et al. (2004). Antitumor Activity of HKI-272 , an Orally Active , Irreversible Inhibitor of the HER-2 Tyrosine Kinase. *Cancer Research*, 3958–3965.

(*378*) Segovia-Mendoza, M., González-González, M. E., Barrera, D., Díaz, L. and García-Becerra, R. (2015). Efficacy and mechanism of action of the tyrosine kinase inhibitors gefitinib, lapatinib and neratinib in the treatment of her2-positive breast cancer: Preclinical and clinical evidence. *American Journal of Cancer Research 5*, 2531–2561.

(*379*) Tang, L., Wang, Y., Strom, A., Gustafsson, J. A. and Guan, X. (2013). Lapatinib induces p27 Kip1-dependent G1 arrest through both transcriptional and post-translational mechanisms. *Cell Cycle 12*, 2665–2674.

(*380*) Martin, M. et al. (2017). Neratinib after trastuzumab-based adjuvant therapy in HER2-positive breast cancer (ExteNET): 5-year analysis of a randomised, double-blind, placebo-controlled, phase 3 trial. *The Lancet Oncology 18*, 1688–1700.

(*381*) Saura, C., Garcia-Saenz, J. A., Xu, B., Harb, W., Moroose, R., Pluard, T., Cortés, J., Kiger, C., Germa, C., Wang, K., Martin, M., Baselga, J. and Kim, S. B. (2014). Safety and efficacy of neratinib in combination with capecitabine in patients with metastatic human epidermal growth factor receptor 2-positive breast cancer. *Journal of Clinical Oncology 32*, 3626–3634.

(*382*) Martin, M., Bonneterre, J., Geyer, C. E. J., Ito, Y., Ro, J., Lang, I., Kim, S.-B., Germa, C., Vermette, J., Wang, K. K., Wang, K. K. and Awada, A. (2013). A phase two randomised trial of neratinib monotherapy versus lapatinib plus capecitabine combination therapy in patients with HER2+ advanced breast cancer. *European Journal of Cancer 49*, 3763–3772.

(*383*) Rexer, B. N. and Arteaga, C. L. (2012). Intrinsic and acquired resistance to HER2-targeted therapies in HER2 gene-amplified breast cancer: mechanisms and clinical implications. *Critical Reviews in Oncogenesis 17*, 1–16.

(*384*) Schroeder, R. L., Stevens, C. L. and Sridhar, J. (2014). Small Molecule Tyrosine Kinase Inhibitors of ErbB2/HER2/Neu in the Treatment of Aggressive Breast Cancer. *Molecules 19*, 15196–15212.

(*385*) Lamouille, S. and Derynck, R. (2007). Cell size and invasion in TGF-β-induced epithelial to mesenchymal transition is regulated by activation of the mTOR pathway. *Journal of Cell Biology 178*, 437–451.

(*386*) Nemethova, M., Auinger, S. and Small, J. V. (2008). Building the actin cytoskeleton: Filopodia contribute to the construction of contractile bundles in the lamella. *Journal of Cell Biology 180*, 1233–1244.

(*387*) Burridge, K. and Guilluy, C. (2016). Focal adhesions, stress fibers and mechanical tension. *Experimental Cell Research 343*, 14–20.

(*388*) Olson, M. F. and Sahai, E. (2009). The actin cytoskeleton in cancer cell motility. *Clinical and Experimental Metastasis 26*, 273–287.

(*389*) Sun, B., Fang, Y., Li, Z., Chen, Z. and Xiang, J. (2015). Role of cellular cytoskeleton in epithelial-mesenchymal transition process during cancer progression (Review). *Biomedical Reports 3*, 603–610.

(*390*) Yauch, R. L., Januario, T., Eberhard, D. A., Cavet, G., Zhu, W., Fu, L., Pham, T. Q., Soriano, R., Stinson, J., Seshagiri, S., Modrusan, Z., Lin, C. Y., O'Neill, V. and Amler, L. C. (2005). Epithelial versus mesenchymal phenotype determines in vitro sensitivity and predicts clinical activity of erlotinib in lung cancer patients. *Clinical Cancer Research 11*, 8686–8698.

(*391*) Thomson, S., Buck, E., Petti, F., Griffin, G., Brown, E., Ramnarine, N., Iwata, K. K., Gibson, N. and Haley, J. D. (2005). Epithelial to mesenchymal transition is a determinant of sensitivity of non-small-cell lung carcinoma cell lines and xenografts to epidermal growth factor receptor inhibition. *Cancer Research 65*, 9455–9462.

(*392*) Rho, J. K., Choi, Y. J., Lee, J. K., Ryoo, B. Y., Na, I. I., Yang, S. H., Kim, C. H. and Lee, J. C. (2009). Epithelial to mesenchymal transition derived from repeated exposure to gefitinib determines the sensitivity to EGFR inhibitors in A549, a non-small cell lung cancer cell line. *Lung Cancer 63*, 219–226.

(*393*) Thiery, J. P., Acloque, H., Huang, R. Y. and Nieto, M. A. (2009). Epithelial-Mesenchymal Transitions in Development and Disease. *Cell 139*, 871–890.

(*394*) Ma, M., He, M., Jiang, Q., Yan, Y., Guan, S., Zhang, J., Yu, Z., Chen, Q., Sun, M., Yao, W., Zhao, H., Jin, F. and Wei, M. (2016). Mir-487a promotes TGF-β1-induced EMT, the migration and invasion of breast cancer cells by directly targeting MAGI2. *International Journal of Biological Sciences 12*, 397–408.

(*395*) Kitamura, K., Seike, M., Okano, T., Matsuda, K., Miyanaga, A., Mizutani, H., Noro, R., Minegishi, Y., Kubota, K. and Gemma, A. (2014). MiR-134/487b/655 Cluster Regulates TGF-b Induced Epithelial Mesenchymal Transition and Drug Resistance to Gefitinib by Targeting MAGI2 in Lung Adenocarcinoma Cells. *Molecular Cancer Therapeutics 13*, 444–453.

(*396*) Li, X., Lewis, M. T., Huang, J., Gutierrez, C., Osborne, C. K., Wu, M. F., Hilsenbeck, S. G., Pavlick, A., Zhang, X., Chamness, G. C., Wong, H., Rosen, J. and Chang, J. C. (2008). Intrinsic resistance of tumorigenic breast cancer cells to chemotherapy. *Journal of the National Cancer Institute 100*, 672–679.

(*397*) Kotiyal, S. and Bhattacharya, S. (2014). Breast cancer stem cells, EMT and therapeutic targets. *Biochemical and Biophysical Research Communications 453*, 112–116.

(*398*) Mani, S. A., Guo, W., Liao, M. J., Eaton, E. N., Ayyanan, A., Zhou, A. Y., Brooks, M., Reinhard, F., Zhang, C. C., Shipitsin, M., Campbell, L. L., Polyak, K., Brisken, C., Yang, J. and Weinberg, R. A. (2008). The Epithelial-Mesenchymal Transition Generates Cells with Properties of Stem Cells. *Cell 133*, 704–715.

(*399*) Polyak, K. and Weinberg, R. A. (2009). Transitions between epithelial and mesenchymal states: Acquisition of malignant and stem cell traits. *Nature Reviews Cancer 9*, 265–273.

(*400*) Singh, A. and Settleman, J. (2010). EMT, cancer stem cells and drug resistance: An emerging axis of evil in the war on cancer. *Oncogene 29*, 4741–4751.

(*401*) Santisteban, M., Reiman, J. M., Asiedu, M. K., Behrens, M. D., Nassar, A., Kalli, K. R., Haluska, P., Ingle, J. N., Hartmann, L. C., Manjili, M. H., Radisky, D. C., Ferrone, S. and Knutson, K. L. (2009). Immune-induced epithelial to mesenchymal transition in vivo generates breast cancer stem cells. *Cancer Research 69*, 2887–2895.

(*402*) Shipitsin, M. et al. (2007). Molecular Definition of Breast Tumor Heterogeneity. *Cancer Cell 11*, 259–273.

(*403*) Luk, J. M. et al. (2011). DLK1-DIO3 genomic imprinted microRNA cluster at 14q32.2 defines a stemlike subtype of hepatocellular carcinoma associated with poor survival. *The Journal of Biological Chemistry 286*, 30706–30713.

(*404*) Nakamura-Ishizu, A., Takizawa, H. and Suda, T. (2014). The analysis, roles and regulation of quiescence in hematopoietic stem cells. *Development 141*, 4656–4666.

(*405*) Medici, D., Hay, E. D. and Olsen, B. R. (2008). Snail and Slug promote epithelial-mesenchymal transition through beta-catenin-T-cell factor-4-dependent expression of transforming growth factor-beta3. *Molecular Biology of the Cell 19*, 4875–4887.

(*406*) Wang, Y., Shi, J., Chai, K., Ying, X. and Zhou, B. (2013). The Role of Snail in EMT and Tumorigenesis. *Current Cancer Drug Targets 13*, 963–972.

(*407*) Lamouille, S., Xu, J. and Derynck, R. (2014). Molecular mechanisms of epithelial-mesenchymal transition. *National Review Molecular Cell Biology 15*, 178–196.

(*408*) Lavon, I. et al. (2010). Gliomas display a microRNA expression profile reminiscent of neural precursor cells. *Neuro-Oncology 12*, 422–433.

(*409*) Zehavi, L., Avraham, R., Barzilai, A., Bar-Ilan, D., Navon, R., Sidi, Y., Avni, D. and Leibowitz-Amit, R. (2012). Silencing of a large microRNA cluster on human chromosome 14q32 in melanoma: biological effects of mir-376a and mir-376c on insulin growth factor 1 receptor. *Molecular Cancer 11*, 44.

(*410*) Gattolliat, C. H., Thomas, L., Ciafrè, S. A., Meurice, G., Le Teuff, G., Job, B., Richon, C., Combaret, V., Dessen, P., Valteau-Couanet, D., May, E., Busson, P., Douc-Rasy, S. and Bénard, J. (2011). Expression of miR-487b and miR-410 encoded by 14q32.31 locus is a prognostic marker in neuroblastoma. *British Journal of Cancer 105*, 1352–1361.

(*411*) Thayanithy, V., Sarver, A. L., Kartha, R. V., Li, L., Angstadt, A. Y., Breen, M., Steer, C. J., Modiano, J. F. and Subramanian, S. (2012). Perturbation of 14q32 miRNAs-cMYC gene network in osteosarcoma. *Bone 50*, 171–181.

(*412*) Zhang, L et al. (2008). Genomic and epigenetic alterations deregulate microRNA expression in human epithelial ovarian cancer. *Proceedings of the National Academy of Sciences 105*, 7004–7009.

(*413*) Costa, F. F., Bischof, J. M., Vanin, E. F., Lulla, R. R., Wang, M., Sredni, S. T., Rajaram, V., de Fátima Bonaldo, M., Wang, D., Goldman, S., Tomita, T. and Soares, M. B. (2011). Identification of micrornas as potential prognostic markers in ependymoma. *PLoS ONE 6*, e25114.

(*414*) Formosa, A, Markert, E. K., Lena, A. M., Italiano, D, Finazzi-Agro', E, Levine, A. J., Bernardini, S, Garabadgiu, A. V., Melino, G and Candi, E (2014). MicroRNAs, miR-154, miR-299-5p, miR-376a, miR-376c, miR-377, miR-381, miR-487b, miR-485-3p, miR-495 and miR-654-3p, mapped to the 14q32.31 locus, regulate proliferation, apoptosis, migration and invasion in metastatic prostate cancer cells. *Oncogene 33*, 5173–5182.

(*415*) Jin, H. Y., Gonzalez-martin, A., Miletic, A. V., Lai, M., Knight, S., Sabouri-Ghomi, M., Head, S. R., Macauley, M. S., Rickert, R. C. and Xiao, C. (2015). Transfection of microRNA Mimics Should Be Used with Caution. *Frontiers in Genetics 6*, 340.

(*416*) Thomson, D. W., Bracken, C. P., Szubert, J. M. and Goodall, G. J. (2013). On Measuring miRNAs after Transient Transfection of Mimics or Antisense Inhibitors. *PLoS ONE 8*, e55214.

(*417*) O'Neill, F., Madden, S. F. S., Aherne, S. T. S., Clynes, M., Crown, J., Doolan, P. and O'Connor, R. (2012). Gene expression changes as markers of early lapatinib response in a panel of breast cancer cell lines. *Molecular Cancer 11*, 41.

(*418*) Ogata, T., Kagami, M. and Ferguson-Smith, A. C. (2008). Molecular mechanisms regulating phenotypic outcome in paternal and maternal uniparental disomy for chromosome 14. *Epigenetics 3*, 181–187.

(*419*) Devor, E. J., de Mik, J. N., Ramachandran, S., Goodheart, M. J. and Leslie, K. K. (2012). Global dysregulation of the chromosome 14q32 imprinted region in uterine carcinosarcoma. *Experimental and Therapeutic Medicine 3*, 677–682.

(*420*) Han, Z., Yu, C., Tian, Y., Zeng, T., Cui, W., Mager, J. and Wu, Q. (2015). Expression patterns of long noncoding RNAs from Dlk1-Dio3 imprinted region and the potential mechanisms of Gtl2 activation during blastocyst development. *Biochemical and Biophysical Research Communications 463*, 167–173.

(*421*) Milne, T. A., Zhao, K. and Hess, J. L. (2009). Chromatin Immunoprecipitation (ChIP) for Analysis of Histone Modifications and Chromatin-Associated Proteins. *Methods in Molecular Biology 538*, 409–423.

(*422*) Beg, M. S., Brenner, A. J., Sachdev, J., Borad, M., Kang, Y.-K., Stoudemire, J., Smith, S., Bader, A. G., Kim, S. and Hong, D. S. (2017). Phase I study of MRX34, a liposomal miR-34a mimic, administered twice weekly in patients with advanced solid tumors. *Investigational New Drugs 35*, 180–188.

(*423*) Park, J. H., Theodoratou, E., Calin, G. A. and Shin, J. I. (2016). From cell biology to immunology: Controlling metastatic progression of cancer via microRNA regulatory networks. *OncoImmunology 5*, e1230579.

(*424*) Yang, S., Li, Y., Gao, J., Zhang, T., Li, S., Luo, A., Chen, H., Ding, F., Wang, X. and Liu, Z. (2013). MicroRNA-34 suppresses breast cancer invasion and metastasis by directly targeting Fra-1. *Oncogene 32*, 4294–4303.

(*425*) Siemens, H., Jackstadt, R., Hünten, S., Kaller, M., Menssen, A., Götz, U. and Hermeking, H. (2011). miR-34 and SNAIL form a double-negative feedback loop to regulate epithelial-mesenchymal transitions. *Cell Cycle 10*, 4256–4271.

(*426*) Liu, C., Kelnar, K., Liu, B., Chen, X., Calhoun-davis, T., Li, H., Patrawala, L., Yan, H., Jeter, C., Honorio, S., Wiggins, J. F., Bader, G, Fagin, R., Brown, D. and Tang, D. G. (2011). Identification of miR-34a as a potent inhibitor of prostate cancer progenitor cells and metastasis by directly repressing CD44. *Nature Medicine 17*, 211–215.

(*427*) Heinemann, A., Zhao, F., Pechlivanis, S., Eberle, J., Steinle, A., Diederichs, S., Schadendorf, D. and Paschen, A. (2012). Tumor suppressive microRNAs miR-34a/c control cancer cell expression of ULBP2, a stress-induced ligand of the natural killer cell receptor NKG2D. *Cancer Research 72*, 460–471.

(*428*) Clancy, J. L., Nousch, M., Humphreys, D. T., Westman, B. J., Beilharz, T. H. and Preiss, T. In *Methods in Enzymology*; Methods in Enzymology, Vol. 431; Academic Press: 2007, pp 83–111.

(*429*) Thomas, M., Lieberman, J. and Lal, A. (2010). Desperately seeking microRNA targets. *Nature Structural and Molecular Biology 17*, 1169–1174.

(*430*) McGranahan, N. and Swanton, C. (2017). Clonal Heterogeneity and Tumor Evolution: Past, Present, and the Future. *Cell 168*, 613–628.

(*431*) Friedman, R. (2016). Drug resistance in cancer: molecular evolution and compensatory proliferation. *Oncotarget 7*, 11746–11755.

(*432*) Scaltriti, M., Verma, C., Guzman, M., Jimenez, J., Parra, J. L., Pedersen, K., Smith, D. J., Landolfi, S., Ramon Y Cajal, S., Arribas, J. and Baselga, J. (2009). Lapatinib, a HER2 tyrosine kinase inhibitor, induces stabilization and accumulation of HER2 and potentiates trastuzumab-dependent cell cytotoxicity. *Oncogene 28*, 803–814.

(*433*) Wang, D. (2008). Discrepancy between mRNA and protein abundance: Insight from information retrieval process in computers. *Computational Biological Chemistry 32*, 462–468.

(*434*) Bai, X.-Y., Li, S., Wang, M., Li, X., Yang, Y., Xu, Z., Li, B., Li, Y., Xia, K., Chen, H. and Wu, H. (2018). Krüppel-like factor 9 down-regulates matrix metalloproteinase 9 transcription and suppresses human breast cancer invasion. *Cancer Letters 412*, 224–235.

(*435*) Limame, R., de Beeck, K. O., Van Laere, S., Croes, L., De Wilde, A., Dirix, L., Van Camp, G., Peeters, M., De Wever, O., Lardon, F. and Pauwels, P. (2014). Expression profiling of migrated and invaded breast cancer cells predicts early metastatic relapse and reveals Kruppel-like factor 9 as a potential suppressor of invasive growth in breast cancer. *Oncoscience 1*, 69–81.

(*436*) Nie, B., Cheng, N., Dinauer, M. C. and Ye, R. D. (2010). Characterization of P-Rex1 for its role in fMet-Leu-Phe-induced superoxide production in reconstituted COS(phox) cells. *Cellular Signalling 22*, 770–782.

(*437*) Pandiella, A. and Montero, J. C. (2013). Molecular pathways: P-Rex in cancer. *Clinical Cancer Research 19*, 4564–4569.

(*438*) Montero, J. C., Seoane, S. and Pandiella, A. (2013). Phosphorylation of P-Rex1 at serine 1169 participates in IGF-1R signaling in breast cancer cells. *Cellular Signalling 25*, 2281–2289.